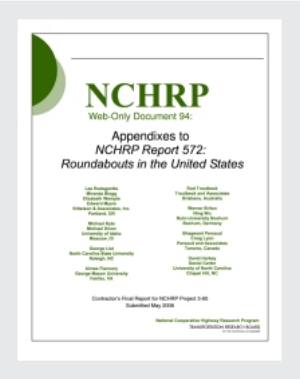

Appendixes to NCHRP Report 572: Roundabouts in the United States

DETAILS

0 pages | | PAPERBACK

ISBN 978-0-309-43172-9 | DOI 10.17226/21999

AUTHORS

NCHRP

Web-Only Document 94:

Appendixes to *NCHRP Report 572: Roundabouts in the United States*

Lee Rodegerdts
Miranda Blogg
Elizabeth Wemple
Edward Myers
Kittelson & Associates, Inc.
Portland, OR

Michael Kyte
Michael Dixon
University of Idaho
Moscow, ID

George List
North Carolina State University
Raleigh, NC

Aimee Flannery
George Mason University
Fairfax, VA

Rod Troutbeck
Troutbeck and Associates
Brisbane, Australia

Werner Brilon
Ning Wu
Ruhr-University Bochum
Bochum, Germany

Bhagwant Persaud
Craig Lyon
Persaud and Associates
Toronto, Canada

David Harkey
Daniel Carter
University of North Carolina
Chapel Hill, NC

Contractor's Final Report for NCHRP Project 3-65
Submitted May 2006

National Cooperative Highway Research Program
TRANSPORTATION RESEARCH BOARD
OF THE NATIONAL ACADEMIES

ACKNOWLEDGMENT

This work was sponsored by the American Association of State Highway and Transportation Officials (AASHTO), in cooperation with the Federal Highway Administration, and was conducted in the National Cooperative Highway Research Program (NCHRP), which is administered by the Transportation Research Board (TRB) of the National Academies.

THE NATIONAL ACADEMIES

Advisers to the Nation on Science, Engineering, and Medicine

The **National Academy of Sciences** is a private, nonprofit, self-perpetuating society of distinguished scholars engaged in scientific and engineering research, dedicated to the furtherance of science and technology and to their use for the general welfare. On the authority of the charter granted to it by the Congress in 1863, the Academy has a mandate that requires it to advise the federal government on scientific and technical matters. Dr. Ralph J. Cicerone is president of the National Academy of Sciences.

The **National Academy of Engineering** was established in 1964, under the charter of the National Academy of Sciences, as a parallel organization of outstanding engineers. It is autonomous in its administration and in the selection of its members, sharing with the National Academy of Sciences the responsibility for advising the federal government. The National Academy of Engineering also sponsors engineering programs aimed at meeting national needs, encourages education and research, and recognizes the superior achievements of engineers. Dr. William A. Wulf is president of the National Academy of Engineering.

The **Institute of Medicine** was established in 1970 by the National Academy of Sciences to secure the services of eminent members of appropriate professions in the examination of policy matters pertaining to the health of the public. The Institute acts under the responsibility given to the National Academy of Sciences by its congressional charter to be an adviser to the federal government and, on its own initiative, to identify issues of medical care, research, and education. Dr. Harvey V. Fineberg is president of the Institute of Medicine.

The **National Research Council** was organized by the National Academy of Sciences in 1916 to associate the broad community of science and technology with the Academy's purposes of furthering knowledge and advising the federal government. Functioning in accordance with general policies determined by the Academy, the Council has become the principal operating agency of both the National Academy of Sciences and the National Academy of Engineering in providing services to the government, the public, and the scientific and engineering communities. The Council is administered jointly by both the Academies and the Institute of Medicine. Dr. Ralph J. Cicerone and Dr. William A. Wulf are chair and vice chair, respectively, of the National Research Council.

The **Transportation Research Board** is a division of the National Research Council, which serves the National Academy of Sciences and the National Academy of Engineering. The Board's mission is to promote innovation and progress in transportation through research. In an objective and interdisciplinary setting, the Board facilitates the sharing of information on transportation practice and policy by researchers and practitioners; stimulates research and offers research management services that promote technical excellence; provides expert advice on transportation policy and programs; and disseminates research results broadly and encourages their implementation. The Board's varied activities annually engage more than 5,000 engineers, scientists, and other transportation researchers and practitioners from the public and private sectors and academia, all of whom contribute their expertise in the public interest. The program is supported by state transportation departments, federal agencies including the component administrations of the U.S. Department of Transportation, and other organizations and individuals interested in the development of transportation. **www.TRB.org**

www.national-academies.org

CONTENTS

APPENDIX A

LITERATURE REVIEW ON SAFETY PERFORMANCE

This appendix presents a detailed literature review of the safety models used in this project. A reference list for this appendix is included at the end.

Safety Prediction Models

The following contains a comprehensive review of each source, by country of origin followed by a summary indicating how useful the insights from this review were in guiding the current research effort.

United Kingdom

In the mid 1980's the Transportation Research Group of the University of Southampton conducted a study of accidents at four-arm roundabouts for the Transport and Road Research Laboratory on behalf of the UK Government Department of Transport *(A1)*. The researchers selected a cross-sectional sample of a pre-defined target type of roundabout (4-arm, single-grade, approximately circular central island, no unusual features, etc.) with specific sub-samples having particular characteristics (e.g., small or large central island, speed limit 30–40 mph or 50–70 mph). An extensive reconnaissance survey of possible sites was undertaken and the samples were selected to give the widest range of vehicle and pedestrian flows and geometry within each sub-group, while being as similar as possible in those characteristics that were not being measured (e.g. environment, congestion).

A sample of 84 four-arm roundabouts on main roads in the UK was used. At each site, traffic and pedestrian flow counts were obtained and detailed geometric measurements were made. Personal-injury accidents occurring over a six-year period (1974–1979) were also obtained. Each accident was classified by type and associated (by a convention) to a particular arm of the roundabout. The type of each road user involved was also linked to each of the vehicle or pedestrian movements defining the accident type.

The resulting accident type groups were:

- Entering-circulating accidents (between an entering vehicle and a circulating vehicle)
- Approaching accidents (mostly rear-ends, but also changing lane accidents)
- Single-vehicle accidents (a single vehicle colliding with some part of the intersection layout or furniture)
- Other accidents (variety of non-pedestrian accidents)
- Pedestrian accidents (any accident involving a pedestrian casualty).

The main statistical analysis used generalized linear modeling to investigate the relationships between the accident frequency and the traffic and pedestrian flows and geometry at the roundabout sites. The analyses were undertaken in two main stages:

- Analysis of total injury accidents at the roundabout as a whole, where each roundabout contributed one data unit to the analysis.
- Analyses of arm-specific accidents by type, where each roundabout contributed four data units (i.e. arms) to each accident type analysis.

The analysis was conducted for three categories of roundabouts:

- *Small roundabouts*. Small roundabouts were defined as those with central islands greater than 4 m (13.1 ft) in diameter with a relatively large ratio of inscribed circle diameter to central island size and often with widened entries and flared approaches.
- *Normal roundabouts with single carriageway (undivided roadway) arms*. As compared to small roundabouts, normal roundabouts have relatively large central islands and un-flared entries.
- Normal with one pair of dual carriageway (divided roadway) arms.

The basic model in each case was of the form given in Equations A-1a or A-1b as follows:

$$A = kQ^{\alpha}, \text{ or} \quad \text{(A-1a)}$$

$$A = kQ_a{}^{\alpha} Q_b{}^{\beta} \quad \text{(A-1b)}$$

where A = injury accidents per year;
Q or Q_a, Q_b = functions of the vehicle and pedestrian flow movements, respectively, at the roundabout (all 24-hour annual average flows in thousands); and
k, α, β = parameters to be estimated.

The analysis method used assumed that the dependent variable had a Poisson error distribution.

For the analysis of total injury accidents at the whole roundabout, the study tried three basic flow functions:

- Total inflow;
- Cross-product flow (product of total entering flows on one pair of opposite arms with the total entering flow on the other pair of opposite arms); and
- Entering-circulating flow (sum of the products of entering and circulating flow at each entry).

All three flow-functions fitted very well with few distinctions for choosing between them. For comparison with other types of intersections the cross-product flow function was preferred, yielding the models for total injury accidents as shown in Table A-1. The table shows a common value for the flow exponent (α), since there was no significant difference in its value between the roundabout categories. The models indicate that injury accidents are expected to be higher at small roundabouts than normal roundabouts (due presumably to their wider flared entries) and that higher speeds are generally associated with a higher accident frequency. Using the simplifying assumption of averaging the constant parameter for the semi-urban (30–40 mph, or 48–64 km/h) and rural (50–70 mph, or 80–112 km/h) models, the specific models used for this study (with model designations noted) as are follows:

$A = 0.062$ (Major AADT/1000 * Minor AADT/1000)$^{0.68}$ (A-1c, UK-INJ1)
$A = 0.0685$ (Major AADT/1000 * Minor AADT/1000)$^{0.68}$, single carriageway (A-1d, UK-INJ2)
$A = 0.059$ (Major AADT/1000 * Minor AADT/1000)$^{0.68}$, dual carriageway (A-1e, UK-INJ2)
$A = 0.04$ (Entering AADT)$^{1.256}$ (A-1f, UK-INJ3)

TABLE A-1: Models of Total Injury Accidents at UK Roundabouts

Speed Limit	Small	Normal – Single Carriageway arms	Normal - One pair of Dual-Carriageway arms
30-40 mph	$A = 0.101\ Q^{0.68}$ (25 sites)	$A = 0.057\ Q^{0.68}$ (11 sites)	$A = 0.057\ Q^{0.68}$ (14 sites)
50-70 mph	$A = 0.081\ Q^{0.68}$ (11 sites)	$A = 0.080\ Q^{0.68}$ (11 sites)	$A = 0.061\ Q^{0.68}$ (12 sites)
All mph	$A = 0.095\ Q^{0.68}$ (36 sites)	$A = 0.062\ Q^{0.68}$ (48 sites)	

Note: Q = cross-product flow function = (major AADT)/1000 * (minor AADT)/1000
SOURCE: *(A1)*

One of the objectives of the study was to try to relate the roundabout accidents to the geometry. In the first stage of the modeling described above, differences between types of layout are reflected only in the categories of the roundabout. However, each arm of a roundabout has a different geometry so in the second stage of the analysis, each arm (or more strictly each quadrant) of the roundabout was used as the basic unit of analysis. Full geometric data was available for 78 of the roundabouts, thus providing 312 data units for the analyses.

The arm level models included the geometric and other site variables through using a model of the form given in Equation A-2 as follows:

$$A = kQ_a^{\alpha} Q_b^{\beta} \exp\left(\sum \gamma_{ij} D_{ij} + \sum \varepsilon_i G_i\right) \qquad \text{(A-2)}$$

where
A = accident frequency, in accidents per year;
Q_a, Q_b = functions of the vehicle and pedestrian flow movements;
D_{ij} (j=2,n) = dummy variables representing the 2nd to nth level of each discrete factor;
G_i = continuous variables (e.g., flow proportions, geometric variables); and
k, α, β, γ_{ij}, ε_i = model parameters estimated from data.

The geometric and other variables and factors were added to the models in a stepwise procedure. At each step the most useful explanatory variable or factor was selected from the whole range of available variables and factors. These choices were made on the grounds of plausibility (i.e., whether the variable was sensible or not), design usefulness (whether the variable was acceptable in a design sense) and statistical validity. At some steps there was a difficult choice between very similar variables so several possible combinations of variable were investigated to inform the most appropriate choice of model.

The resulting full models are presented in linear form in Table A-2. Note that these models are found in the ARCADY software. These models were useful in informing the type and estimated magnitude of variables for consideration in this project's research.

TABLE A-2: Full Approach Models by Accident Type at UK Roundabouts

Accident Type	Model term	Parameter value	Standard Error
ENTERING-CIRCULATING ACCIDENTS			
L(Constant)	*Lk*	-3.09	0.47
L(entering flow)	LQ_e	0.65	0.12
L(circulating flow)	LQ_c	0.36	0.11
Entry path curvature	C_e	-40.3	9.6
Entry width	*e*	0.16	0.025
Approach width correction	*ev*	-0.009	0.0038
Ratio factor	*RF*	-1.0	0.23
Percentage of motorcycles	*Pm*	0.21	0.063
Angle between arms	*A*	-0.008	0.0025
Gradient category	*g*	0.09	0.038
APPROACHING ACCIDENTS			
L(Constant)	*Lk*	-4.71	0.52
L(entering flow)	LQ_e	1.76	0.15
Entry path curvature	C_e	20.7	7.6
Reciprocal sight distance	$1/V_r$	-43.9	13.4
Entry width	*E*	-0.093	0.038
Gradient category	*g*	-0.13	0.06
SINGLE VEHICLE ACCIDENTS			
L(Constant)	*Lk*	-4.71	0.40
L(entering flow)	LQ_e	0.82	0.16
Approach width	*v*	0.21	0.04
Entry path curvature	C_e	23.7	6.4
Approach curvature category	C_a	-0.17	0.05
Reciprocal sight distance	$1/V_r$	-33.0	13.1
OTHER (NON-PEDESTRIAN) ACCIDENTS			
L(constant)	*Lk*	-5.69	0.50
L(entering x circulating flow)	LQ_{ec}	0.73	0.10
Percentage of motorcycles	*Pm*	0.21	0.08
PEDESTRIAN ACCIDENTS			
L(constant)	*Lk*	-3.59	0.27
L((entering + exiting vehicle flow) x Pedestrian flow)	LQ_{exp}	0.53	0.13

- *Entry path curvature* - Equal to the inverse of the minimum radius of travel in the region of entry for a vehicle passing straight through the roundabout and taking the shortest possible path while staying on the curbside of the roadway. Signing convention is positive if deflection is to left and negative if the path deflects to the right. (m^{-1})
- *Entry width* - Perpendicular roadway width at the point of entry (m).
- *Approach width* - Width of the roadway on the approach (m)
- *Approach width correction* - Equal to the product of entry and approach width (m^2)
- *Approach curvature category* - Categories of -3, -2, -1, 0, 1, 2, 3. Negative values represent left-hand bends and positive values right-hand bends on the approach. An absolute value of 3 indicates a severe bend, 0 would indicate a straight alignment.
- *Ratio factor* - Ratio of inscribed circle diameter to central island diameter
- *Percentage of motorcycles* - Percentage of the relevant traffic volumes consisting of motorcycles
- *Angle between arms* - The angle in degrees between the approach arm and the next arm clockwise.
- *Gradient category* - The gradient on the approach, categories of -3, -2, -1, 0, 1, 2, 3,. This is a subjective category with -3 indicating a severe downhill grade towards the roundabout and +3 indicating a severe uphill grade towards the roundabout.
- *Reciprocal sight distance* - Reciprocal of the sight distance to the right, from 15m back from the give-way line (m^{-1}) using an object height of 1.05m

SOURCE: *(A1)*

Australia

Two documents authored by Arndt were reviewed. The first *(A2)* discusses in detail the collection of accident, traffic flow and geometric data for roundabouts constructed in Australia. Models for determining the vehicle paths of drivers through roundabouts and the 85th-percentile speed were developed. The output of these models was used as explanatory variables in a linear regression model developed to predict single vehicle accidents.

The second document *(A3)* follows upon the first by revisiting the single vehicle accident model and developing additional models for several more accident types. Both linear and non-linear Poisson-based regression models were developed, with the non-linear models recommended as being more accurate for predicting accident frequencies. The regression models were based on driver behavior. To predict an accident of a given type, the vehicle paths of the relevant vehicles and the 85th-percentile speeds are first predicted. This information is then fed into a regression model, along with other significant predictors of accidents, to estimate the annual accident frequency.

Table A-3 summarizes the accident data used to develop the accident prediction models. All injury severities were included. Not all of the accidents that occurred were used for specific accident type models due to their scarcity. In this case, these crashes were combined into an "other" model. Over eighty percent of accidents involved more than one vehicle and, of these, just over one half involved an entering vehicle colliding with a circulating vehicle. The author noted that detailed information for accidents could not be found for some accidents and subsequently multiplied the model equations by 1.209 to account for the missing data.

TABLE A-3 Summary of Accident Data used by Arndt

Accident Categories and Frequencies			
Total Accidents 492 (100%)	Single Vehicle Accidents 90 (18.3%)	Single Vehicle - Crashes involving only one vehicle. 90 (18.3%)	Approaching – 13 Entering – 13 Circulating – 51 Departing – 13
	Multiple Vehicle Accidents 402 (81.7%)	Rear End One vehicle collides into the rear of another vehicle. 90 (18.3%)	Approaching – 83 Circulating – 6 Departing – 1
		Entering/Circulating - An entering vehicle fails to yield and collides with a circulating vehicle. 250 (50.8%)	NA
		Exiting/Circulating A vehicle driving from the inner circulating lane to the departure leg collides with a vehicle circulating on the outer circulating lane. 32 (6.5%)	NA
		Side Swipe - Two vehicles side swipe while travelling on different paths in the same direction. 18 (3.7%)	Approaching – 2 Entering – 2 Circulating – 10 Exiting – 2 Departing – 2
		Low Frequency - Other infrequent crash types. 12 (2.4%)	

SOURCE: *(A3)*

Detailed instructions are provided for constructing vehicle paths through single and multi-lane roundabouts. The procedure is based on observations that vehicles traveling through roundabouts do so in a manner to obtain the largest possible radii, and thus speed, possible. Construction of the vehicle paths allows the distance traveled and the estimated 85th percentile speed on each geometric element to be determined.

On the approach and departure legs, assuming a 2-m-wide vehicle, the following distances from the center of the vehicle to the centerline and edge geometric features are assumed:

- 1.5 m from a road centerline
- 1.5 m from a concrete curb
- 1.0 m from a painted edge line or chevron

For movements within the roundabout, curves are drawn tangent to the centerline and the approach-departure path line that allow for the largest radii of movement.

A model for predicting the 85th-percentile speed as a function of the speed environment and the horizontal curve radius is presented in graphical form in Figure A-1. The predicted speed is plotted on the *y*-axis versus curve radius on the *x*-axis for a series of curves for various speed environments. This model has altered previous work on rural roads to allow the predicted 85th-percentile speed to equal the speed environment at large values of curve radius and to more accurately predict speeds at lower radii curves.

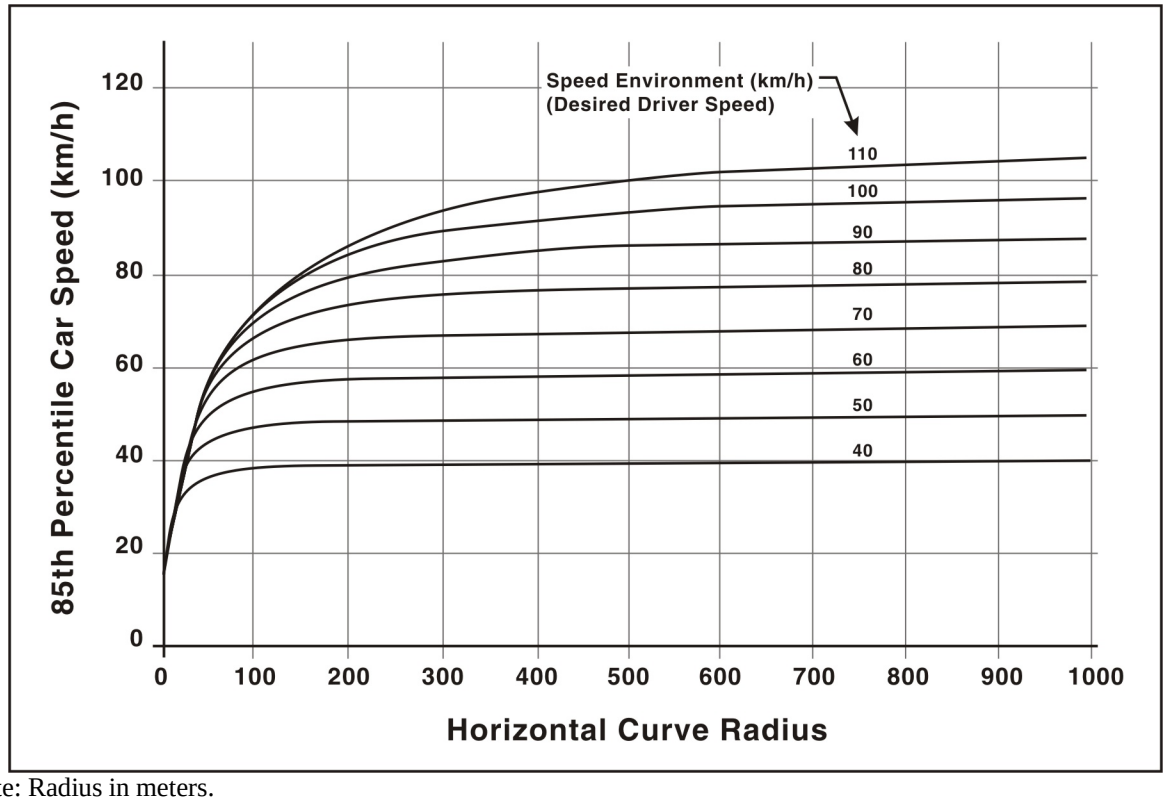

Note: Radius in meters.
SOURCE: *(A3)*

Figure A-1: Australian Method for Speed Estimation

Accident Model for Single Vehicles. This model applies only to vehicles making right turns (equivalent to left turns in the US); it does not apply to vehicles making left turns (equivalent to right turns in the US) or U-turns through the roundabout. The model, divided into two components, is given in Equations A-3a and A-3b as follows:

$$A_{sp} = \frac{1.64\times10^{-12} Q^{1.17} L(S+\Delta S)^{4.12}}{R^{1.91}}, \text{ and} \quad \text{(A-3a)}$$

$$A_{sa} = \frac{1.79\times10^{-9} Q^{0.91} L(S+\Delta S)^{1.93}}{R^{0.65}}; \quad \text{(A-3b)}$$

where
- A_{sp} = number of single vehicle accidents per year per leg for vehicle path segments *prior* to the giveway line;
- A_{sa} = number of single vehicle accidents per year per leg for vehicle path segments *after* the giveway line;
- Q = AADT in direction considered;
- L = length of vehicle path on the horizontal geometric element (m);
- S = 85th-percentile speed on the horizontal geometric element (km/h);
- ΔS = decrease in 85th-percentile speed at the start of the horizontal geometric element (km/h); and
- R = vehicle path radius on the horizontal geometric element (m).

Accident Model for Approaching Rear-End Vehicles. Only rear-end accidents occurring on the roundabout approach curves are considered. The model is given in Equation A-4 as follows:

$$A_r = 1.81\times10^{-18} Q_a^{1.39} \left(\sum Q_{ci}\right)^{0.65} S_a^{4.77} N_a^{2.31} \quad \text{(A-4)}$$

where
- A_r = number of approaching rear-end vehicle accidents per year per approach leg;
- Q_a = AADT on the approach;
- Q_{ci} = circulating vehicle AADTs from the other approaches;
- S_a = 85th-percentile speed on the approach curve (km/h); and
- N_a = number of lanes on the approach.

Accident Model for Entering-Circulating Vehicles. This model includes only the entering vehicles from the approach of interest, the right-turn movement (equivalent to the left-turn movement in the US) from the opposite approach, and the through and right-turn movements (equivalent to the through and left-turn movements in the US) from the previous approach in the direction of traffic. The entering vehicles are assumed to be in the inside lane for multilane approaches. Left turns (equivalent to right turns in the US) and U-turn vehicles from the approach of interest are ignored. The model is given in Equation A-5 as follows:

$$A_e = \frac{7.31\times10^{-7} Q_a^{0.47} N_c^{0.9} \left(\sum Q_{ci}\right)^{0.41} S_{ra}^{1.38}}{t_{Ga}^{0.21}} \quad \text{(A-5)}$$

where
- A_e = number of entering-circulating vehicle accidents per year per approach leg;
- Q_a = AADT on the approach;
- N_c = number of circulating lanes;
- $\sum Q_{ci}$ = sum of the circulating vehicle AADTs from the other approaches;
- $S_{ra} = \frac{\sum Q_{ci} S_{ri}}{\sum Q_{ci}}$;
- $T_{Ga} = \frac{\sum Q_{ci} t_{Gi}}{\sum Q_{ci}}$;
- S_{ri} = the various relative 85th-percentile speeds between vehicles on the approach curve and circulating vehicles from each direction (km/h);
- t_{Gi} = the various travel times taken from the give way line of the approach to the intersection point between the entering and circulating vehicles;
- $t_{Gi} = 3.6 d_{Gi} / S_{ci}$;
- d_{Gi} = distance from the give way line of the approach to the intersecting point between entering and circulating vehicles (m); and
- S_{ci} = the various 85th-percentile speeds of the circulating vehicles adjacent to the approach (km/h).

Accident Model for Exiting/Circulating Vehicles. The accidents modeled included only those occurring on multi-lane roundabouts that contained one of the following marking systems:

(1) No lane lines between circulating lanes;
(2) Broken lane lines between circulating lanes marked adjacent to each splitter island;
(3) Broken lane lines between circulating lanes marked fully around the roundabout; or
(4) The vehicle volumes modeled include the exiting vehicles from the inside lane and the circulating vehicles from the outside lane of the approach under consideration and the previous approach in the direction of traffic.

The model is given in Equation A-6 as follows:

$$A_d = 1.33\times10^{-11} \left(\sum Q_{ci}\right)^{0.32} \left(\sum Q_{ei}\right)^{0.68} S_{ra}^{4.13} \quad \text{(A-6)}$$

where
- $\sum Q_{ci}$ = sum of the circulating vehicle AADTs from the other approaches;
- $\sum Q_{ei}$ = sum of the various AADT flows exiting the roundabout at the exit point of the departure leg;
- $S_{ra} = \frac{\sum Q_{ei} S_{ri}}{\sum Q_{ei}}$; and

S_{ri} = the various relative 85th percentile speeds between vehicles exiting the roundabout and circulating vehicles at the particular departure leg.

Accident Model for Sideswipe Vehicles. This model was developed for segments consisting of two lanes. Left-turn (right-turns where vehicles travel on the right side of the road) and u-turn vehicles from the approach of interest are ignored within the roundabout.

The model is separately applied to segments prior to the approach curve, the approach curve, the circulating-through segment, the circulating-right turn segment, the departing-through segment and the departing-right turn segment. The model is given in Equation A-7 as follows:

$$A_{ss} = 6.49 \times 10^{-8} \left(QQ_t\right)^{0.72} \Delta f_l^{0.59} \quad \text{(A-7)}$$

where A_{ss} = number of sideswipe vehicle accidents per leg per vehicle path segment;
Q = AADT for the particular movement on the particular geometric element;
Q_t = total AADT on the particular geometric element; and
Δf_l = difference in potential side friction (km/h^2/m).

Accident Model for Other Vehicles. The other vehicle accident model is simply an accident rate calculated by dividing the total number of accidents not falling into one of the five model categories by the total number of vehicles approaching all of the roundabouts and multiplied by 365. The model is given in Equation A-8 as follows:

$$A_O = 4.29 \times 10^{-6} \sum Q_a \quad \text{(A-8)}$$

where A_O = number of "other" accidents per year; and
Q_a = AADT on approach *a*.

France

A French model *(A4)* for predicting the total number of injury accidents at a roundabout does not contain any geometric variables and applies to roundabouts where the total incoming traffic ranges between 3,200 and 40,000 vehicles per day. The model is given in Equation A-9 as follows (designated in this project as FR-INJ1):

$$\text{Injury accidents/year} = 0.15\left(10^{-5}\right) Q_{TE} F_c \quad \text{(A-9, FR-INJ1)}$$

where Q_{TE} = total daily incoming traffic; and
F_c = adjustment coefficient for the period under consideration.

Sweden

A study in Sweden *(A5)* surveyed roughly 650 roundabouts in 1997, classifying them according to geometric design, speed level and other variables. Accident and vehicle, bicycle and pedestrian volumes were collected for certain subsets of the total database for 1994 to 1997. An analysis of cyclist and pedestrian accident data was undertaken for 72 roundabouts and an

analysis of vehicle accident data for 182 roundabouts. A speed analysis was conducted for 536 roundabouts.

With regards to vehicle speeds the following conclusions were drawn:

- Speeds are higher when the general speed limit is higher than the local limit;
- Speed is, on average, higher at multilane roundabouts than single lane roundabouts;
- Speed is lower if the radius of the central island is 10 to 20 m (33 to 66 ft) than if the radius is smaller or larger;
- Provision of additional travel surface around the central island has no effect on speed;
- Developing the approach to be as perpendicular as possible at the roundabout entry reduces speed into and through the roundabout;

With regards to accidents involving cyclists and pedestrians the following conclusions were drawn:

- Single lane roundabouts are much safer for cyclists than multilane roundabouts
- Fewer cyclist accidents occur when the central island is greater than 10 m (33 ft) and when bicycle crossings are provided
- It is safer for cyclists to bypass a roundabout on a bicycle crossing than to travel on the carriageway
- For pedestrians, roundabouts are no less safe than conventional intersections and single lane roundabouts are more safe than multi-lane roundabouts

For vehicle accidents, 456 accidents occurred at the 182 roundabouts from 1994–1997. Nineteen percent of these resulted in an injury and there were no fatalities. General observations with regards to vehicle accidents include:

- Accident frequency is directly proportional to vehicle speeds.
- Injury accident frequency has a more quadratic relationship with speed.
- A central island radius of 10 to 25 m (33 to 82 ft) results in the lowest accident frequency.

Two variations of a prediction model were developed to predict vehicle accident rates (accidents per million entering vehicles) at roundabouts *(A5)*. The models predict vehicle accident rates (accidents per million entering vehicles) and are based on data from both urban and rural sites. The first of these was designated in this study as SWED-TOT1; both are given in Equations A-10a and A-10b as follows:

$$\text{Predicted accident rate} = 0.1353 \times 0.86^{3leg} \times 1.88^{speed70} \times 1.2^{2lanes} \qquad \text{(A-10a, SWED-TOT1)}$$

where $3leg$ = 1 if 3-legged, 0 if 4-legged;
$speed70$ = 1 if speed limit is 70 km/h (44 mph), 0 if 50 km/h (31 mph); and
$2lanes$ = 1 if there are 2 lanes on roundabout, 0 if there is one.

$$\text{Predicted accident rate} = 0.1130 \times 0.92^{3leg} \times 1.84^{speed70} \times 1.40^{loclow} \times 1.17^{2lanes} \qquad \text{(A-10b)}$$

where $3leg$ = 1 if 3-legged, 0 if 4-legged;
$speed70$ = 1 if speed limit is 70 km/h (44 mph), 0 if 50 km/h (31 mph);
$loclow$ = 1 if general speed limit within 600 m (1970 ft) of roundabout is higher than the local limit; and

2lanes = 1 if there are 2 lanes on roundabout, 0 if there is one.

Due to a low number of injury accidents, injury accident models were developed by fitting observed injury accident rates to a function of the prediction for the total accident rate. Two variations were developed (with the first designated in this study as SWED-INJ1) and are given in Equations A-11a and A-11b as follows:

Predicted injury rate = 0.8178 (Predicted accident rate)$^{1.6871}$ (A-11a, SWED-INJ1)
Predicted injury rate = 0.7215 (Predicted accident rate)$^{1.6119}$ (A-11b)

The authors compared predictions from the roundabout models to previously calibrated models for conventional signalized and unsignalized intersections and concluded that roundabouts are generally slightly safer than conventional intersections, particularly when the local speed limit is assumed to be 50 km/h (31 mph). However, evidence is not provided in the paper to support the notion that the two sets of models indeed make valid comparisons. For example, the data used to develop the conventional intersection models may have come from locations with a much different distribution of traffic volumes, different location types and/or other factors that may impact safety but are not necessarily included in any of the models. Thus, these conclusions on the relative safety of roundabouts compared to other intersection types may not be reliable.

An earlier study also developed injury models for several classes of roundabouts *(A6)*. The *aggregate* models for predicting the number of motor vehicle crashes *with personal injury* per year for *urban* junctions are as follows (designated for this project as SWED-INJ2 and SWED-INJ3):

<u>50 km/h (31 mph)</u>:
Injury Crashes /year = 0.00000308 (Total entering AADT)$^{1.20}$ for 4 legs (A-12a, SWED-INJ2)
Injury Crashes /year = 0.00000232 (Total entering AADT)$^{1.20}$ for 3 legs (A-12b, SWED-INJ2)
<u>70 km/h (44 mph)</u>:
Injury Crashes /year = 0.00000440 (Total entering AADT)$^{1.20}$ for 4 legs (A-12c, SWED-INJ3)
Injury Crashes /year = 0.00000332 (Total entering AADT)$^{1.20}$ for 3 legs (A-12d, SWED-INJ3)

Review of Before-After Safety Studies

Studies on the safety effect of converting conventional intersections to roundabouts were also reviewed. The results are usually reported without reservations. This does not mean that there are not any. For example, the reported safety benefits of roundabout installation may be exaggerated due to regression-to-the-mean in cases where this bias is not accounted for. In most cases, it is difficult to make a determination if this bias exists or, if so, if it was accounted for. Thus, the reader is cautioned to accept the results summarized here in the spirit in which this section is provided – to provide a flavor for the safety benefits of roundabouts. The decision to report these results in spite of possible reservations was based on a belief that, with the very large reductions that were consistently observed, the benefits of roundabouts would remain substantial if regression-to-the-mean effects were removed and any other methodological limitations were to be overcome.

United States

A before-after study of roundabout conversions in the United States used the empirical Bayes methodology to control for regression-to-the-mean and other trends in accident occurrence

(A7). The analyses used data from seven states—Colorado, Florida, Kansas, Maine, Maryland, South Carolina, and Vermont—where a total of 23 intersections were converted to modern roundabouts between 1992 and 1997. Of the 23 intersections studied, 19 were previously controlled by stop signs, and four were controlled by traffic signals. Fourteen of the roundabouts were single-lane circulation designs, and nine, all in Colorado, were multilane. For all of the study intersections the empirical Bayes procedure estimated a highly significant 40-percent reduction for all crash severities combined. Because injury data were not available for the period before construction of the four roundabouts in Vail, overall estimates for changes in injury crashes are based on the other 19 intersections. The empirical Bayes procedure estimated a highly significant 80-percent reduction for injury crashes for these 19 converted intersections.

Because of major operational differences between various roundabout designs and settings, results were analyzed and reported for several groups of conversions for which there were sufficient crash data to provide meaningful results. These include eight urban single-lane roundabouts that prior to construction were stop-controlled, five rural single-lane roundabouts that prior to construction were stop-controlled, six urban multilane roundabouts that prior to construction were stop-controlled, and four urban intersections converted to roundabouts from traffic signal control.

The results are summarized in Table A-4 which is taken directly from the aforementioned study *(A7)*. In summary:

- For the group of eight urban single-lane roundabouts converted from stop control, the empirical Bayes procedure estimated highly significant reductions of 72 percent for all crash severities combined and 88 percent for injury crashes.
- For the group five rural single-lane roundabouts converted from stop control, similar effects were estimated: a 58-percent reduction for all crash severities combined and an 82-percent reduction for injury crashes.
- For the group of six urban multilane roundabouts, however, the estimated effect on all crash severities combined was much smaller: a 5-percent reduction. Because injury data were not available for the period before construction of four of these roundabouts, overall estimates for changes in injury crashes were not computed for this group of intersections.
- For the four roundabouts converted from traffic signal control, estimated reductions were 35 percent for all crash severities combined and 74 percent for injury crashes. Three of these roundabouts had multilane circulation designs.

A recent project undertaken by some members of the NCHRP 3-65 project team for the New York State Department of Transportation (NYSDOT) *(A8)* increased the sample size of the Persaud et al. study *(A7)* with more sites and additional years of data. The preliminary results were generally supportive of those in Persaud et al. *(A7)* as well as those of an earlier and limited effort by Flannery and Elefteriadou *(A9)* who used a number of the same sites in their study. Finer levels of disaggregation than was possible for the Persaud et al. study were, however, not feasible despite the larger sample size.

TABLE A-4: Estimates of Safety Effects for Groups of Conversions

Group Characteristic Before Conversion/Jurisdiction	Count of Crashes During Period After Conversion		Crashes Expected During After Period Without Conversion (Standard Deviation)		Index of Effectiveness (Standard Deviation)		Percent Reduction in Crashes	
	All	Injury	All	Injury	All	Injury	All	Injury
Single Lane, Urban, Stop Controlled								
Bradenton Beach, FL	1	0	9.9 (3.6)	0 (0)				
Fort Walton Beach, FL	4	0	16.9 (3.9)	2.7 (1.1)				
Gorham, ME	4	0	6.8 (1.4)	0.9 (0.4)				
Hilton Head, SC	9	0	42.8 (6.0)	8.2 (1.9)				
Manchester, VT	1	1	1.7 (0.7)	0 (0)				
Manhattan, KS	0	0	4.2 (1.2)	1.2 (0.5)				
Montpelier, VT	1	1	4.3 (1.8)	1.1 (0.6)				
West Boca Raton, FL	7	0	8.1 (3.0)	2.6 (1.3)				
Entire group (8)	27	2	94.6 (9.0)	16.6 (2.6)	0.28 (0.06)	0.12 (0.08)	72%	88%
Single Lane, Rural, Stop Controlled								
Anne Arundel County, MD	14	2	24.6 (4.0)	6.2 (1.7)				
Carroll County, MD	4	1	15.2 (2.6)	3.2 (0.9)				
Cecil County, MD	10	1	14.3 (2.9)	5.6 (1.4)				
Howard County, MD	14	1	36.7 (5.5)	7.7 (2.1)				
Washington County, MD	2	0	14.4 (3.1)	4.2 (1.3)				
Entire group (5)	44	5	105.2 (8.4)	26.9 (3.4)	0.42 (0.07)	0.18 (0.09)	58%	82%
Multilane, Urban, Stop Controlled								
Avon, CO	3	0	19.9 (4.9)	0 (0)				
Avon, CO	17	1	12.2 (3.1)	0 (0)				
Vail, CO	14	—	19.1 (4.4)	—				
Vail, CO	61	—	50.9 (7.6)	—				
Vail, CO	8	—	9.8 (2.1)	—				
Vail, CO	15	—	11.8 (2.3)	—				
Entire group (6)	118		123.7 (11.0)	n/a	0.95 (0.10)	n/a	5%	n/a
Urban, Signalized								
Avon, CO	44	1	49.8 (7.0)	5.4 (1.7)				
Avon, CO	13	0	30.1 (5.7)	2.3 (1.0)				
Avon, CO	18	0	52.1 (7.0)	5.3 (1.7)				
Gainesville, FL	11	3	4.8 (1.5)	1.3 (0.5)				
Entire group (4)	86	4	131.7 (10.9)	15.0 (2.7)	0.65 (0.09)	0.26 (0.14)	35%	74%
All conversions (23)	275	12	454.6 (19.8)	58.5 (5.1)	0.60 (0.04)	0.20 (0.06)	40%	80%

SOURCE: *(A7)*

Non-US Studies

International experience with roundabout conversion was summarized in a report for the Insurance Institute for Highway Safety *(A10)*. A summary of this information is provided here.

A before and after evaluation of 230 sites where roundabouts were built (and 60 control sites) in New South Wales, Australia, found a 41-percent reduction in total crashes, 45-percent reduction in injury crashes, and 63-percent reduction in fatal crashes *(A11)*.

A Danish study found that the reconstruction of urban give-way (yield) intersections into roundabouts leads to a considerable reduction in injury crashes for occupants of cars, in fact, about 85 percent. For bicyclists there was no safety benefit from the reconstruction from give-way intersections to roundabouts. The number of cyclist injury crashes was unchanged (and now make up roughly 70-percent of all injury crashes). The effect on the number of injury crashes at reconstructed rural intersections is approximately the same as that for urban ones *(A12)*. The

study also found that injury crashes became less serious, decreasing from an average of 1.3 to 1.0 injured persons per injury crash for urban junctions and from 2.1 to 1.25 for rural junctions. The injury crashes at the rural roundabouts were mainly bicyclist crashes. This study also looked at the severity of crashes and concluded that small roundabouts do well with respect to this parameter. The percent of serious and fatal crashes was substantially lower at small roundabouts (3.3 percent) than at conventional ones (8.4 percent). The average percent of serious and fatal crashes at roundabouts on dual carriageways was 4.2 percent. At signalized dual carriageway intersections this percentage was 9.2 percent for two-phase signals and 7.8 percent for three-phase signals (separate right-turn phase—left hand driving).

A study of 83 roundabouts in France concluded that conversion to roundabouts reduces injury crashes by 78 percent and fatality crashes by 82 percent *(A13)*.

A German study by Brilon *(A14)* compared the crash experience of 32 newly constructed single-lane roundabouts to their safety prior to reconstruction. Two of the intersections had previously been signalized; the others had had two-way stop control or yield. The total effect was a 40-percent reduction in crash frequency. The effect was particularly impressive for rural intersections, where the number of serious injuries was reduced from 18 to 2, the number of light injuries went from 25 to 3, and the number of crashes causing "heavy" property damage went from 24 to 3. There was a small reduction in the number of pedestrian crashes as a result of the construction of roundabouts, whereas the number of bicycle crashes went up somewhat. This increase took place at roundabouts that had marked bicycle lanes on the outer edge of the circulating roadway (where crash numbers went from one to eight). The number of bicycle crashes was more or less unchanged at locations with mixed traffic as well as at locations with separate bicycle/pedestrian paths.

The Dutch research institute SWOV did a study on the safety of 201 single-lane roundabouts built in 1990 *(A15)*. These all have yield at entry and access roads with radial orientation. This study found that "the substitution of an intersection by a roundabout has a particularly favorable effect on road safety: a reduction of 47 percent in the number of crashes and 71 percent in the number of road crash victims (after trend correction). However, the various categories of road user did not all profit from the change to the same degree: a large reduction in road crash victims was noted amongst occupants of cars and pedestrians (95 percent and 89 percent, respectively) and a slight reduction amongst cyclists ('only' 30 percent)." According to Ourston *(A16)* another study from the Netherlands investigated the effect of conversion of nine traffic signals to roundabouts. They found a 27-percent reduction in crashes and a 33-percent reduction in casualties *(A16)*.

A recent paper by Elvik performed a meta-analysis study on 28 non-U.S. studies evaluating the safety effects of converting conventional intersections to roundabouts *(A17)*. Table A-5 lists the year and origin of publication and the study design used for the studies reviewed. Some of these studies were reviewed in the IIHS report summarized above. The analysis found that roundabouts reduce the number and severity of injury crashes. For all severities of injury the best estimate is a 30- to 50-percent reduction. Fatal crashes are estimated to reduce from 50 to 70 percent. For property-damage-only crashes the effect is uncertain but may in fact increase after roundabout conversion, particularly at 3-legged intersections. There is some evidence that roundabout conversion has a greater effect on injury crashes at 4-legged intersections than 3-legged. A greater effect is apparent at yield-controlled than at signalized intersections.

TABLE A-5: Year and origin of Studies Reviewed by Elvik

Year	Country	Study design
1975	Great Britain	Simple before-and-after
1977	Great Britain	Before-and-after, controlling for general trends
1981	Denmark	Comparative study and before-and-after, controlling for general trends
1983	Sweden	Comparative study of crash rates in various types of intersections
1983	Norway	Before-and-after, data on traffic volume
1985	Sweden	Before-and-after, controlling for trends and regression-to-the-mean
1985	Norway	Comparative study of crash rates in various types of intersections
1988	Great Britain	Comparative study of crash rates in various types of intersections
1988	Norway	Before-and-after, controlling for general trends
1990	Norway	Comparative study of crash rates in various types of intersections
1990	Australia	Before-and-after, controlling for general trends
1990	Netherlands	Simple before-and-after
1991	Denmark	Comparative study and simple before-and-after
1992	Sweden	Comparative study of crash rates in various types of intersections
1992	Switzerland	Simple before-and-after
1992	Germany	Simple before-and-after
1992	Sweden	Simple before-and-after
1992	Denmark	Before-and-after, controlling for general trends
1992	Norway	Before-and-after, controlling for general trends
1992	Germany	Before-and-after, data on traffic volume
1993	Germany	Before-and-after, data on traffic volume
1993	Netherlands	Simple before-and-after
1994	Germany	Comparative study and before-and-after, data on traffic volume
1994	Denmark	Before-and-after, controlling for trends and regression-to-the-mean
1994	Norway	Before-and-after, controlling for general trends
1994	Switzerland	Before-and-after, controlling for general trends
1995	Norway	Before-and-after, controlling for general trends
1997	Norway	Before-and-after, controlling for trends and regression-to-the-mean

SOURCE: *(A17)*

As for the safety effect of specific design features, few studies provided adequate information to reach conclusions. The 1983 Swedish study looked at AADT, proportion of traffic entering from the minor road, number of legs, speed limit and diameter of the central traffic island but found no significant relationship between the diameter of the central traffic island and crash rate. It is unclear if this lack of effect is “true” or due to inadequate sample sizes or data ranges. Most of the roundabouts in the study had a central traffic island with a diameter of more than 40 m (131 ft). The 1992 Swedish study and the 1991 and 1992 Danish studies found an increase in the crash rate with a larger central traffic island. The effects of other design parameters were found to be small. The four factors with the strongest effect on crash rates in roundabouts are cited as total traffic volume, proportion of vehicles entering from the minor road, speed limit, and number of legs. The direction of this relationship is not specified in Elvik's paper.

Summary of the Review on the Safety Effect of Converting Conventional Intersections to Roundabouts

Prior to NCHRP 3-65, the one definitive study of US conversions, and its subsequent update for the NYSDOT, was based on a rather small sample size. As such, only limited disaggregate analysis could be done to try to isolate the geometric factors associated with the greatest safety benefits of roundabout construction. While some of these factors have been isolated in evaluations outside of the US it is not clear that that knowledge is directly transferable. In addition, several of those studies had methodological limitations. The review of the previous studies did provide useful insights for guiding the disaggregated before-after analysis done for this study. Useful lessons were learned from the pitfalls and limitations of many of those studies (e.g., small sample sizes, ignoring regression to the mean, and improperly accounting for traffic volume and secular changes over time). These lessons emphasized the need for, and use to be made of, recent advances in safety estimation methodology aimed at overcoming these limitations.

References

A1. Maycock, G., and R. D. Hall. *Accidents at 4-arm roundabouts.* Report LR 1120. Transport and Road Research Laboratory, Crowthorne, Berkshire, United Kingdom, 1984.

A2. Arndt, O. K. *Relationship Between Roundabout Geometry and Accident Rates.* M. E. thesis. Queensland University of Technology, Brisbane, Queensland, Australia, June 1994.

A3. Arndt, O. K. *Relationship Between Roundabout Geometry and Accident Rates - Final Report*. Infrastructure Design, Transport Technology Division, Department of Main Roads, Brisbane, Queensland, Australia, 1998.

A4. Service d'Etudes Techniques des Routes et Autoroutes (SETRA). Accidents at intersections: the use of models to predict average accidents rates. Memorandum. Bagneux Cedex, France, 1998.

A5. Brüde, U., and J. Larsson. What Roundabout Design Provides the Highest Possible Safety? In *Nordic Road and Transport Research*, No. 2. Swedish National Road and Transport Research Institute, 2000.

A6. Brüde, U., K. Hedman, J. Larsson, and L. Thuresson. *Design of Major Urban Junctions—Comprehensive Report.* VTI EC Research 2, 1998.

A7. Persaud, B. N., R. A. Retting, P. E. Garder, and D. Lord. Observational Before-After Study of the Safety Effect of U.S. Roundabout Conversions Using the Empirical Bayes Method. In *Transportation Research Record: Journal of the Transportation Research Board, No. 1751*. TRB, National Research Council, Washington, DC, 2001, pp. 1–8.

A8. Eisenman, S., J. Josselyn, G. List, B. Persaud, C. Lyon, B. Robinson, M. Blogg, E. Waltman, and R. Troutbeck. *Operational and Safety Performance of Modern*

Roundabouts and Other Intersection Types. Final Report, SPR Project C-01-47. New York State Department of Transportation, Albany, NY, April 7, 2004.

A9. Flannery, A., and L. Elefteriadou. "A Review of Roundabout Safety Performance in the United States." In *Proceedings of the 69th Annual Meeting of the Institute of Transportation Engineers*. Institute of Transportation Engineers, Washington, DC, 1999.

A10. Persaud, B., and P. Garder. *Roundabout Safety in the U.S.—Volume 1: Background Paper on Roundabout Safety*. Draft Final Report. Insurance Institute for Highway Safety, 1999.

A11. Tudge, R. T. Crashes at Roundabouts in New South Wales. *Proc., Part 5 of the 15th AARB Conference*. August 1990, pp. 341–349.

A12. Jørgensen, E., and N. O. Jørgensen. *Trafiksikkerhed i 82 danske rundkørsler—anlagt efter 1985*. Rapport 4. IVTB, DTU, 1994.

A13. Centre D'Etudes Techniques de l'Equipment de l'Ouest. *Evolution de la Securite Sur Les Carrefours Giratoires,* Nantes, France, 1986. As referenced in Jacquemart, G. *NCHRP Synthesis of Highway Practice 264: Modern Roundabout Practice in the United States,* TRB, National Research Council, Washington, DC, 1998.

A14. Brilon, W. *Sicherheit von Kreisverkehrsplätzen.* Ruhr-University Bochum, Bochum, Germany, 1996, p. 3.

A15. Schoon, C., and J. van Minnen. *Ongevallen op rotondes II.* Report No. R-93-16. SWOV, Leidschendam, Netherlands, 1993.

A16. Ourston, L. Comparative Safety of Modern Roundabouts and Signalized Intersections. March 2, 1996.

A17. Elvik, R. Effects on road safety of converting intersections to roundabouts: Review of evidence from non-U.S. studies. *Transportation Research Record: Journal of the Transportation Research Board, No. 1847*. Transportation Research Board of the National Academies, Washington, DC, 2003, pp. 1–10.

APPENDIX B

LITERATURE REVIEW OF OPERATIONAL MODELS

This appendix presents a detailed literature review of the operational models used in this project. A reference list for this appendix is included at the end.

Fundamental Capacity Methods

While the focus of the research is on roundabouts, a number of fundamental methods applicable to two-way-stop-controlled and two-way-yield-controlled intersection capacity analysis serve as a foundation for roundabout operational performance. There are currently two methods that have been used to develop such models:

- Gap acceptance
- Linear or exponential empirical regression

Gap Acceptance Models

In a gap acceptance model, the driver on the minor (entering) stream is required to select an acceptable gap on the major (circulating) stream, to perform the desired maneuver. The "gap" is defined as the headway maintained between two consecutive vehicles in the conflicting stream. The minimum gap that is acceptable to the minor-stream driver is their critical headway, t_c (historically referred to in the literature as critical gap). The critical headway is not a constant and is typically represented by a distribution of values based on the variation of driver behavior. Estimation procedures exist for critical headway that do not require sites with oversaturated conditions. The follow-on time (otherwise known as follow-up time), t_f, is defined as the time headway between two consecutively entering vehicles, utilizing the same gap in the circulating stream. The follow-on time can be directly measured in the field without utilizing complicated mathematical equations.

According to Tanner *(B1)*, from the point of view of the traffic on the minor road, the traffic on the major road forms alternate "blocks" and "gaps". Bunched vehicles, each of which is separated by a minimum gap t_m, form a block. During such a block no vehicles can enter the major stream flow. When the gap after the last vehicle in the block is equal to or greater than the critical headway, vehicles are able to enter the major stream flow. Vehicles can enter the larger gaps with a follow-on time of t_f.

Based on the gap acceptance model, the capacity of the simple two-stream situation can be evaluated by elementary probability theory for the assumptions:

a) constant t_c and t_f values
b) exponential distribution for priority stream gaps
c) constant traffic volumes for each traffic stream

Harders *(B2)* developed one of the first models, which is used in the current *Highway Capacity Manual (B3)*. These idealized assumptions are considered somewhat unrealistic; however, various evaluations have suggested that more realistic headway distributions are not significantly more accurate. Furthermore, the resulting generalized solutions are not easy to apply in practice.

In addition to the concern related to realistic distributions of headways and other gap acceptance parameters, there are a number of other theoretical limitations. These are described below:

- Inconsistent gap acceptance occurs in practice and has not been accounted for in theory. These include (a) rejecting a large gap before accepting a smaller gap, (b) driver on the roundabout giving up the right of way, (c) forced right of way when the traffic is congested, and (d) different vehicle types accepting different gaps.
- Estimation of the critical headway is difficult. Maximum likelihood was found to be one of the most consistent methods *(B4, B5)*; however, the evaluation is quite complicated.
- Geometric factors are not directly taken into account.

In response to concerns related to gap acceptance, Troutbeck and Kako have developed a theory for incorporating a "limited priority" process, in which the major stream vehicle slows down to allow the minor street vehicle to enter the circulating stream *(B6)*.

Linear or exponential empirical regression models are based on traffic volumes at one-minute intervals observed during periods of oversaturation. A linear or exponential regression equation is then fitted to the data, as shown in Figure B-1. Variation in the data is often created by driver behavior and geometric design. A multivariate regression equation can also be developed to include the influence of geometric design. Limitations of this technique include the following:

- Empirical regression models may have poor transferability to other countries or at other times (e.g., inexperienced US drivers versus experienced UK drivers).
- Regression models provide no real understanding of the underlying traffic flow theory of determining and accepting gaps upon entering the intersection.
- The models are typically based on driver behavior in oversaturated conditions, thus requiring sites with continuous queuing.
- Each situation (traffic volume pattern and/or geometric conditions) must be observed in order to develop an appropriate model. This requires a large data collection effort.

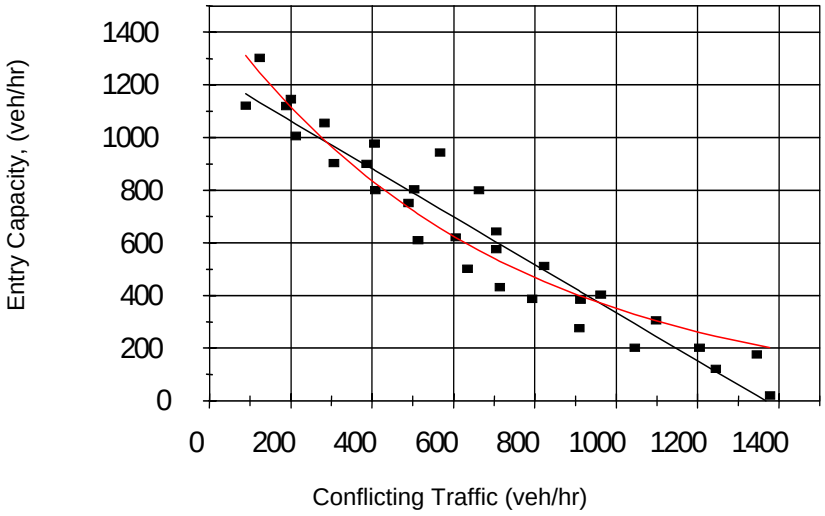

Figure B-1. Exponential and Linear Regression Model.

Regression Capacity Models

Simply capacity models can be developed using linear and exponential regression forms. These are given in Equations B-1a and B-1b as follows:

$$q_{e,\max} = A - B \cdot q_c \quad \text{(B-1a)}$$

$$q_{e,\max} = A \cdot \exp(B \cdot q_c) \quad \text{(B-1b)}$$

where: $q_{e,max}$ = maximum entry flow (veh/hr)
q_c = circulating flow (veh/hr)
A, B = intercept and slope constants

Expression for the constants may also be developed, e.g. as a function of other parameters including the roundabout geometry.

Survey of International Capacity Models

U.S. Capacity Models

There are two major methods currently found in United States literature: 1) the operational method cited in the FHWA Roundabout Guide *(B7)*, and 2) a gap acceptance procedure in the Highway Capacity Manual *(B3)*.

FHWA Method. The FHWA Roundabout Guide *(B7)* presents three capacity formulas for estimating the performance of roundabouts. These were intended for use as provisional formulas until further research could be conducted with US data. The FHWA method for urban compact roundabouts is based on German research *(B8)* and is given as follows:

$$q_{e,\max} = 1218 - 0.74 q_c, \text{ for } 0 \le q_c \le 1646 \quad \text{(B-2)}$$

where: $q_{e,max}$ = maximum entry flow (veh/h)
q_c = traffic flow on the circulatory roadway (veh/h)

The FHWA method for single-lane roundabouts is based on the UK's Kimber equations *(B9)* with assumed default values for each of the geometric parameters. In addition, an upper cap to the entry plus circulating flow of 1800 veh/h was imposed. The resulting equation is given as follows:

$$q_{e,\max} = \min\begin{bmatrix} 1212 - 0.5447 q_c \\ 1800 - q_c \end{bmatrix}, \text{ for } 0 \le q_c \le 1800 \quad \text{(B-3)}$$

where: $q_{e,max}$ = maximum entry flow (veh/h)
q_c = traffic flow on the circulatory roadway (veh/h)

The FHWA method for double-lane roundabouts is also based on the Kimber equations with assumed default values for each of the geometric parameters. The resulting equation is given as follows:

$$q_{e,\max} = 2424 - 0.7159 q_c \text{, for } q_c \geq 0 \quad \text{(B-4)}$$

where: $q_{e,max}$ = maximum entry flow (veh/h)
q_c = traffic flow on the circulatory roadway (veh/h)

HCM 2000 Method. The HCM 2000 method for one-lane roundabouts, first introduced in 1997 with background provided by Troutbeck *(B10)*, is described below:

$$q_{e,\max} = \frac{q_c e^{-q_c t_c/3600}}{1 - e^{-q_c t_f/3600}} \quad \text{(B-5)}$$

where: $q_{e,max}$ = maximum entry flow (veh/h)
q_c = conflicting flow (veh/h)
t_c = critical headway (s)
t_f = follow-up time (s)

The critical headway has an upper and lower bound of 4.1 and 4.6 seconds respectively. The follow-up time has an upper and lower bounds of 2.6 and 3.1 seconds respectively.

UK Capacity Models

Kimber *(B9)* reports the capacity estimation procedure currently used for roundabouts in the UK. The capacity, $q_{e,max}$, has a linear relationship to the circulating flow rate, q_c (see Equation B-1a). The regression parameters depend on geometric details of the entry roadway and roundabout. This method has been incorporated into the software packages ARCADY *(B11)* and RODEL *(B12)*.

The capacity formula used in the UK for roundabout entries is given as follows:

$$q_{e,\max} = k \cdot (F - f_c \cdot q_c) \text{ for } Q_e > 0 \text{ else } Q_e = 0 \quad \text{(B-6)}$$

where: $q_{e,max}$ = maximum entry flow (veh/h)
q_c = circulating flow (veh/h)
F = $303 x_2$ (veh/h)
f_c = $0.21 T_D (1 + 0.2 x_2)$
k = $1 - 0.00347 (\phi - 30) - 0.978(1/r - 0.05)$
T_D = $1 + \dfrac{0.5}{1 + \exp\left(\dfrac{D - 60}{10}\right)}$
x_2 = $v + (e - v)/(1 + 2S)$
S = $(e - v)/l'$
e = entry width (m)
v = approach half-width (m)
l' = effective flare length (m)
r = entry radius (m)
ϕ = entry angle (°)
S = measure of the degree of the flaring
D = inscribed circle diameter (m)

Australian Capacity Models

Detailed capacity expressions have been published in Australia. These are most recently available in Akçelik et. al. *(B13)*, and have been incorporated into the software aaSIDRA *(B14)*. The capacity is calculated lane-by-lane. The Australian capacity formula published by Akçelik et al. *(B13)* and used in this study is as follows:

$$q_{e,\max} = \max(f_{od} q_g , q_m) \quad \text{(B-7a)}$$

$$q_g = \frac{3600}{\beta}\left(1 - \Delta\frac{q_c}{3600} + 0.5\beta\varphi_c\frac{q_c}{3600}\right)\exp(-\lambda(\alpha - \Delta_c)) \quad \text{(B-7b)}$$

$$q_m = \min(q_e, 60 n_m) \quad \text{(B-7c)}$$

$$f_{od} = 1 - f_{qc}(p_{qd} p_{cd}) \quad \text{(B-7d)}$$

where:
- $q_{e,max}$ = maximum entry flow for an entry lane (veh/h)
- q_g = minimum entry flow (veh/h)
- q_c = conflicting flow (veh/h)
- q_e = entry arrival flow (veh/h)
- f_{od} = o-d adjustment factor
- $p_{cd}p_{qd}$ ≈ 0.5 to 0.8 (0.6 used)
- n_m = minimum entry flow (veh/min)
- n_c = number of lanes in conflicting flow
- Δ_c = minimum headway in circulating traffic (s)
  - = 2.0 for $n_c = 1$
  - = 1.2 for $n_c = 2$
- λ = arrival headway distribution factor (veh/s)

$$= \begin{cases} \dfrac{\varphi_c q_c / 3600}{1 - \Delta_c q_c / 3600} & for\ q_c / 3600 \le 0.98 / \Delta_c \\ \dfrac{49\varphi_c}{\Delta_c} & else \end{cases}$$

- φ_c = proportion of unbunched conflicting vehicles
  - = $\exp(-5.0 q_c/3600)$ for $n_c = 1$
  - = $\exp(-3.0 q_c/3600)$ for $n_c = 2$
- β = follow-up headway (s)

For the dominant entry lane (lane at a multi-lane roundabout with the largest entry flow):

$$\beta = \beta_d = \beta'_0 - 3.94 * 10^{-4} q_c \text{, subject to } \beta_{\min} \le \beta'_d \le \beta_{\max} \quad \text{(B-7e)}$$

$$\beta'_0 = 3.37 - 0.0208 D_i + 0.889 * 10^{-4} D_i^2 - 0.395 n_e + 0.388 n_c \text{, subject to } 20 \le D_i \le 80 \quad \text{(B-7f)}$$

where:
- D_i = inscribed diameter (m)
- n_e = number of entry lanes
- $\beta_{\min}$ = 1.2 (s)
- $\beta_{\max}$ = 4.0 (s)

For the subdominant entry lane (lane at a multi-lane roundabout with the smallest entry flow):

$$\beta = \beta_s = 2.149 + (0.5135\beta_d - 0.8735)r_{ds}, \text{ subject to } \beta_d \le \beta_s \le \beta_{\max} \quad \text{(B-7g)}$$

where:

r_{ds} = ratio of dominant and subdominant flow in the entry
= q_d/q_s
α = critical headway (s)
= $\begin{cases} (3.6135 - 3.137 * 10^{-4} q_c - 0.339 w_L - 0.2775 n_c)\beta & for\ q_c \le 1200 \\ (3.2371 - 0.339 w_L - 0.2775 n_c)\beta & else \end{cases}$

subject to
$3.0 \ge \alpha / \beta \ge 1$ and $\alpha_{\min} \le \alpha \le \alpha_{\max}$

$\alpha_{\min}$ = 2.2 (s)
$\alpha_{\max}$ = 8.0 (s)
w_L = average entry width (m)

For n_c = 1
f_{qc} = $0.04 + 0.00015 q_c$ for $q_c < 600$
= $0.0007 q_c - 0.29$ for $600 \le q_c \le 1200$
= 0.55 for $q_c > 1200$

For n_c = 2
f_{qc} = $0.04 + 0.00015 q_c$ for $q_c < 600$
= $0.0035 q_c - 0.29$ for $600 \le q_c \le 1800$
= 0.55 for $q_c > 1800$

German Capacity Models

The Tanner-Wu capacity equation has been introduced officially into the German Highway Capacity Manual *(B15)*. The German capacity formula for roundabout entries is given by Wu *(B16)*:

$$q_{e,\max} = n_e \cdot \frac{3600}{t_f} \cdot \left(1 - \frac{\Delta \cdot \frac{q_c}{3600}}{n_c}\right)^{n_c} \cdot \exp\left[-\frac{q_c}{3600} \cdot \left(t_c - \frac{t_f}{2} - \Delta\right)\right] \quad \text{(B-8)}$$

where: $q_{e.\max}$ = maximum entry flow (pcu/h)
q_c = conflicting flow (pcu/h)
n_c = number of conflicting lanes (1 or 2 with $n_c \le n_e$)
n_e = number of lanes in the entry
t_c = critical headway = 4.1 s

t_f = follow-up time = 2.9 s
Δ = minimum headway of circulating traffic = 2.1 s

More recent re-calibrations show some bias of this equation for two-lane entries. Thus, as a better approximation to German observation data a new set of parameters is presented here for comparison purposes:

$$q_{e,\max} = \frac{n_e^{\,n_F/(n_F+1)}}{t_f} \cdot \left(1 - \frac{\Delta \cdot \frac{q_c}{3600}}{n_c}\right)^{n_c} \cdot \exp\left[-q_c \cdot \left(t_c - \frac{t_f}{2} - \Delta\right)\right] \quad \text{(B-9)}$$

where:
t_c = critical headway = 3.3 s
t_f = follow-up time = 3.1 s
Δ = minimum headway of circulating traffic = 1.8 s
n_F = short lane length = 1.4 veh

French Capacity Models

Three parallel modeling efforts have been reported in France *(B17)*. The model considered most current, employed within the software implementation Girabase, is an exponential regression that takes into account a number of geometric parameters and the influence of exiting flow. The form of the Girabase model published in 1997 and used for this study is as follows:

$$q_{e,\max} = A \cdot \exp(-C_B \cdot q_g) \quad \text{(B-10)}$$

where:
$q_g = q_a \cdot k_a \cdot \left(1 - \frac{q_a}{q_c + q_a}\right) + q_{ci} \cdot k_{ti} + q_{ce} \cdot k_{te}$
$A = \frac{3600}{t_f}\left(\frac{L_e}{3.5}\right)^{0.8}$
$q_{e.max}$ = maximum entry flow (pcu/h)
q_c = total conflicting flow (pcu/h)
q_{ci} = conflicting flow on inner lane (default 0.4*q_k) (pcu/h)
q_{ce} = conflicting flow on outer lane (default 0.6*q_k) (pcu/h)
q_a = exiting flow (pcu/h)
C_B = 3.525 for urban area
= 3.625 for rural area
t_f = follow-up time = 2.05 s
R = radius of the central island (m)
L_e = entry width (m)
L_a = circulating width (m)

L_i = width of the splitter island (m)

$$L_{i,max} = 4.55 \cdot \sqrt{R + \frac{L_a}{2}}$$

$$k_a = \begin{cases} \dfrac{R}{R + LA} - \dfrac{L_i}{L_{i,\max}} & for\ L_i < L_{i,\max} \\ 0 & else \end{cases}$$

$$K_{t,i} = Min\left\{ \dfrac{160}{LA \cdot (R + LA)},\ 1 \right\}$$

$$K_{t,e} = Min\left\{ 1 - \dfrac{(LA - 8)}{LA} \cdot \left(\dfrac{R}{R + LA} \right)^2,\ 1 \right\}$$

Swiss Capacity Models

The Swiss model *(B18)* includes the influence of exiting flow and the width of the splitter island. This capacity model is described below:

$$q_{e,\max} = \left(1500 - \frac{8}{9} \cdot q_b \right) \cdot \beta \qquad \text{(B-11)}$$

where:
q_b = $\gamma \cdot q_k + \alpha \cdot q_a$ (pcu/h)
$q_{e.max}$ = maximum entry flow (pcu/h)
q_k = circulating flow (pcu/h)
q_a = exiting flow (pcu/h)
γ = 0.9 to 1.0 for single circulating lane (default = 1.00)
= 0.6 to 0.8 for double circulating lane (default = 0.66)
= 0.5 to 0.6 for triple circulating lane (default = 0.55)
β = 0.9 to 1.1 for single entry lane (default = 1.00)
= 1.4 to 1.6 for double entry lane (default = 1.50)
= 1.9 to 2.1 for triple entry lane (default = 2.00)
b = taken from Figure B-2 (m)

$$\alpha = \begin{cases} 0.6 & for\ 0 < b \le 9 \\ 0.6 - 0.5/12 * (b-9) & for\ 9 < b \le 21 \\ 0.1 & for\ 21 < b \le 27 \\ 0.1 - 0.1 * (b-27) & for\ 27 < b \le 28 \\ 0 & for\ b > 28 \end{cases}$$

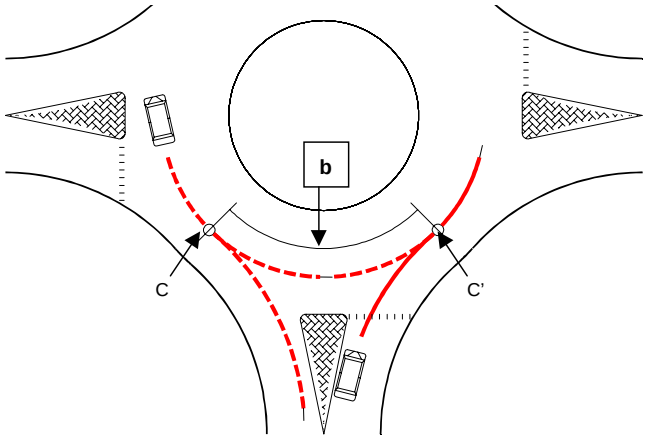

Figure B-2. Swiss Measure of the Parameter 'b'

Operational Performance Measures

In general, the performance of traffic operations at an intersection can be represented by the following measures of effectiveness:

- Degree of saturation (volume/capacity)
- Average delay
- Average queue length
- Distribution of delays
- Distribution of queue lengths (i.e. number of vehicles queuing on the minor road)
- Number of stopped vehicles
- Acceleration or deceleration between stop and normal velocity

Delay

Authors such as Kremser *(B19)*, Brilon *(B20)*, and Yeo *(B21)* have developed average delay equations based on queuing theory. These models are only applicable to undersaturated conditions where the traffic is considered constant over time.

Time-dependant delay solutions (those that consider oversaturated conditions) were developed by Kimber and Hollis *(B22)*. These were later simplified by Akçelik and Troutbeck *(B23)* and are presented in the HCM. The simplified equations do not take into flow rates before or after the analysis period. The Kimber and Hollis method is preferred, though more complicated.

The HCM control delay equation for a given stop-controlled movement is presented below (Equation 17-38, HCM 2000, *B3*):

$$d = \frac{3600}{c} + 900 \cdot T \cdot \left[\frac{v}{c} - 1 + \sqrt{\left(\frac{v}{c} - 1 \right)^2 + \frac{\left(\frac{3600}{c} \right) \cdot \left(\frac{v}{c} \right)}{450 \cdot T}} \right] + 5 \qquad \text{(B-12)}$$

where: d = control delay (s/veh)
T = analysis time period ($T = 0.25$ for a 15-min period) (h)
c = capacity (veh/h)
v = flow rate (veh/h)

The first term in the equation, "3600/c", represents the average service time, or the time spent in the first position in the queue. The last term, "+ 5", represents additional time added to reflect deceleration to and acceleration from a stopped position. In FHWA's *Roundabouts: An Informational Guide* (*B7*), this last term has been dropped from the equation to more accurately reflect a yield condition.

Queue Length

The average queue length is of limited practical value, however, the maximum queue length is useful for design. Maximum queue length (95th-percentile queue length) relationships have been developed by Wu *(B24)* in the form of graphs, and are presented in the HCM 2000. These are illustrated in Figure B-3. The graph is only valid where the volume-to-capacity ratio immediately before and after the study period is no greater than 0.85, such that the queue length is negligible.

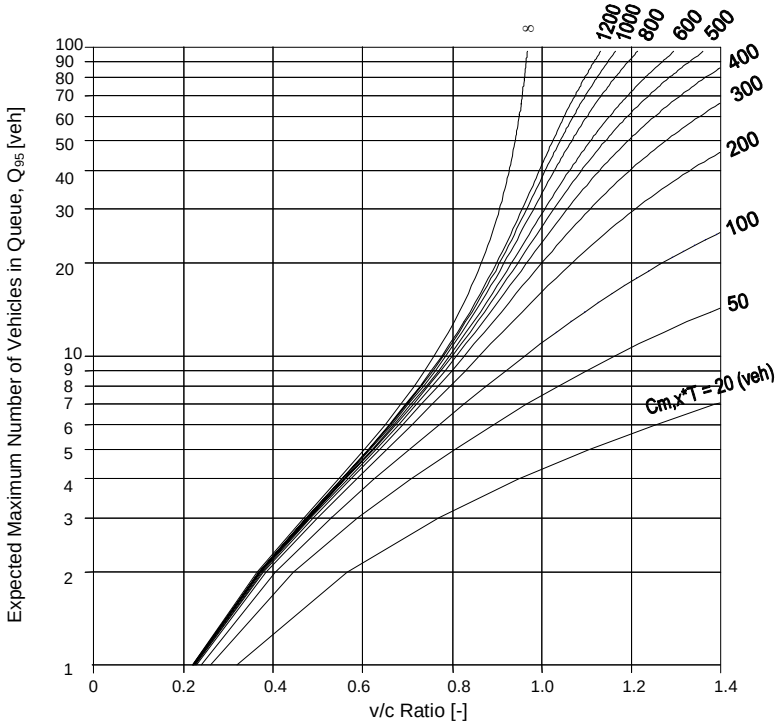

Figure B-3. 95th Percentile Queue Length

Effects of Pedestrians on Entry Capacity

Consideration of the effect of pedestrian modes on entry capacity has been of limited concern in previous research efforts. Stuwe *(B25)* observed three roundabouts with heavy pedestrian flow and developed an empirical entry capacity equation for one-lane and two-lane roundabouts. The method is included in the FHWA Roundabout Guide *(B7)*. Marlow and Maycock *(B26)* also developed entry capacity models with pedestrian considerations, based on queuing theory. The capacity of roundabout exits with significant pedestrian flows has not been investigated to date.

In most states in the United States, pedestrians have the right-of-way at intersections whenever they are in or about to enter a crosswalk. This legal priority for pedestrians is not universally observed in the United States, nor is it the rule of the road throughout the world. In German law, for example, pedestrians have priority over vehicles leaving the roundabout, because this situation is handled like leaving a main road into a side street. These regulations take place even if there is no Zebra crossing. However, the pedestrian does not have priority over the vehicles that are entering the roundabout. Pedestrians only have priority at entries if there is a Zebra crossing.

If pedestrians have priority, they can cause a capacity reduction for vehicular traffic at the entries and exits of a roundabout. The extent to which the pedestrians may affect the capacity depends on the volume of pedestrians. To take this into account, there are three methods, which will be briefly explained later. All these methods are only valid if pedestrians have right of way.

However, in reality the traffic doesn't exactly follow the rules. The awareness of these rules and their specific application to roundabouts doesn't seem to be common. For example, the following behavior can be observed in Germany:

- **Zebra crossings:** If there are Zebra crossings, they are normally situated at both entry and exit of a roundabout. Generally, under these conditions pedestrians assume the right-of-way. There are sites where pedestrians totally bring down the traffic flow.
- **Roundabouts without Zebra crossings:** Pedestrians and vehicles arrange themselves. Pedestrians cross the road with care, and vehicles can use this to their advantage to gain priority. On the other hand vehicles, even with the legal right-of-way, sometimes give the pedestrians right-of-way. This behavior cannot be described by theoretical mathematical methods. The traffic engineer should therefore be careful with his calculations. As a result, in Germany it is advisable to use this calculation method of the influence of pedestrians, although there is no Zebra-striped crosswalk.

The following calculation methods were all developed for the case that pedestrians on crosswalks have unrestricted right of way. The following two calculations lead to completely different results. The method by Marlow and Maycock *(B26)* was developed from purely theoretical methodology of the queuing theory; the method by Stuwe *(B25)*, recommended for use in Germany, was developed from interpretation of observed traffic. It considers, contrary to the Marlow-Maycock method, that even when a queue reaches across the Zebra-striped crosswalk it can still be used by pedestrians without having negative effect on the traffic.

Consideration of Pedestrians at the Entry of Roundabouts

Using video cameras, Stuwe *(B25)* has observed a total of twelve entries at three German roundabouts with heavy pedestrian traffic (one in Münster and two in Lübeck). At all entries there were Zebra-striped crosswalks installed. The study analyzed the number of pedestrians, the number of vehicles entering the roundabout, and the number of vehicles circulating inside the

roundabout during continuous queuing. All values were transformed into passenger car units using German definitions. Here an influence by the pedestrians on the capacity of the entry could be observed. This influence was described more clearly by Brilon, Stuwe, and Drews *(B27)* with a formula that was based on the same set of data. The analysis of these relations by statistical methods led to the following equations.

Using this method, the capacity $q_{e,max}$ of the entry is calculated without consideration of pedestrians. Then, capacity of the entry is reduced by a factor M to account for the influence of pedestrians on the capacity of the entry. Thus, the capacity considering pedestrians is:

$$q_{e,\max,Fg} = q_{e,\max} * M \tag{B-13}$$

For M the following regression equations are valid:

One-lane entry: $$M = \frac{1119.5 - 0.715 \cdot q_k - 0.644 \cdot q_{Fg} + 0.00073 \cdot q_k \cdot q_{Fg}}{1069 - 0.65 \cdot q_k} \tag{B-14}$$

Two-lane entry: $$M = \frac{1260.6 - 0.329 \cdot q_k - 0.381 \cdot q_{Fg}}{1380 - 0.50 \cdot q_k} \tag{B-15}$$

where: M = entry capacity reduction factor
q_k = volume of circulating vehicles in front of the subject entry (pcu/h)
q_{Fg} = volume of pedestrians (ped/h)

This method is therefore a valid application of the empirical regression method on the problem of pedestrians at Zebra-striped crosswalks in the case of roundabouts. The reduction factor M is dependent on the volume of traffic on the roundabout and the volume of pedestrians, shown in Figure B-4 (two-lane entry) and Figure B-5 (one-lane entry), where q_k is the traffic volume in the roundabout (in pcu/h). The volume of pedestrians q_{Fg} is shown in some curves. Interim values can be interpolated. It can be seen that the more traffic on the roundabout, the less are pedestrians influencing the traffic flow. Pedestrians do not have any more influence on the capacity of the entry, if the circulating traffic is 900 pcu/h or higher at one-lane entries (or 1600 pcu/h at two-lane entries). The result seems to be logical, because when there is a queue the pedestrians can use the crosswalk without interfering with traffic. This calculation is recommended for German circumstances and for others as well. The Marlow-Maycock Method (two mostly independent operating queuing-systems) does, however, not consider the before-stated case of pedestrians when there is a queue.

The number of observations supporting the work by Stuwe and by Brilon, Stuwe, and Drews is limited. Besides, it is possible that the situation measured did not exactly reflect all possible parameters (e.g., traffic volume, lane width, and speed). Further comparable measurements are unlikely to be done in the near future due to the costs. Therefore, this method will remain the most meaningful calculation method for the near future.

The formulas in Equations B-13 to B-15 lead, in boundary areas (in which they are not supported by data), to implausible results. For example, it is possible, at one-lane roundabouts and low pedestrians volume (< 100 ped/h), that with a marginal rising volume of pedestrians q_{Fg} the capacity would rise too. This does not question the formula as it is, but it demands careful application.

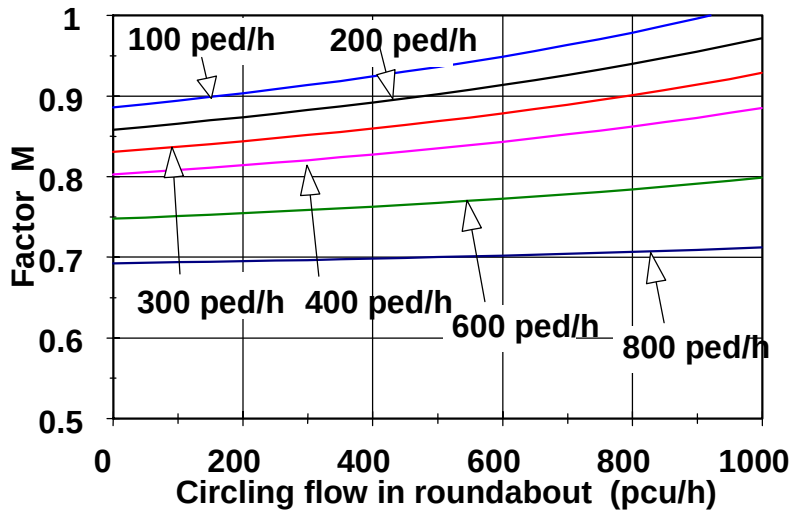

Figure B-4: Reduction Factor M for the Consideration of Pedestrians on the Entry at Two-Lane Roundabout Entries.

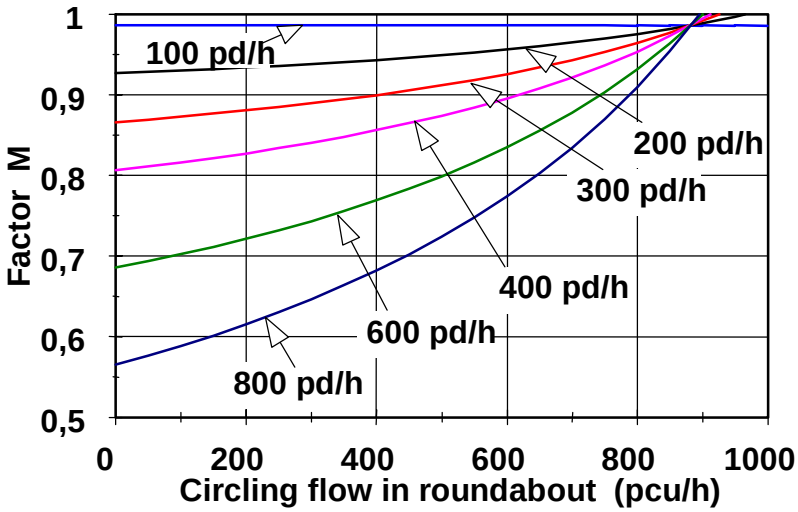

Figure B-5. Reduction Factor M for the Consideration of Pedestrians on the Entry at One-Lane Roundabout Entries.

Marlow and Maycock *(B26)* investigated the effects of pedestrians, who cross the entry to a roundabout, by using mathematical methods from the queuing theory. They treat the crosswalk and the roundabout entry as two queuing systems in secession. First of all, the capacity of the two queuing systems (crosswalk and entry) is calculated. Following that the calculation of the total capacity is calculated.

Under the condition that pedestrians have priority, the capacity of the crosswalk is calculated based on the formula by Griffiths *(B28)*:

$$c_{FG\ddot{U}} = \frac{\mu}{\mu \cdot \beta + \left(e^{\mu \cdot \alpha} - 1\right) \cdot (1 - e^{-\mu \cdot \beta})} \cdot 3600 \quad \text{(B-16)}$$

where:
$c_{FG\ddot{U}}$ = capacity of the crosswalk for vehicles (veh/h)
μ = volume of pedestrians = q_{Fg} / 3600 (ped/s)
β = minimum time gap between two vehicles (s) when driving across the crosswalk.
= $\frac{1}{c_0}$
c_0 = capacity of one lane of the entry, at an otherwise empty roundabout (veh/s)
α = time needed to cross the crosswalk by the pedestrians (s)
= B / v_{FG}
B = width of road at crosswalk (m)
v_{FG} = walking speed of pedestrians at the crosswalk (m/s)

The speed v_{FG} is about 0.5 to 2.0 m/s. If no further information is available, a value of 1.4 m/s should be used.

The parameter B is set for every entry individually. This value has to be set according to the given situation in every single entry, when using the Marlow-Maycock formula. The parameter β is set to the capacity (c_0) for one lane of the entry at an otherwise empty roundabout. For the total capacity of the crosswalk-entry system, the relation of R is very significant.

$$R = \frac{c_{FG\ddot{U}}}{q_{e,\max}} \quad \text{(B-17)}$$

where:
$c_{FG\ddot{U}}$ = capacity of the crosswalk for vehicles (veh/h)
$q_{e,max}$ = capacity of the entry neglecting pedestrian-traffic (veh/h)

The total-capacity $q_{e,max,\,Fg}$ of the crosswalk-entry system is the according to Marlow and Maycock *(B26)*:

$$q_{e,\max,Fg} = q_{e,\max} * M \quad \text{(B-18)}$$

where:
M = $\frac{R^{N+2} - R}{R^{N+2} - 1}$
$q_{e,max}$ = Capacity of the entry neglecting pedestrian traffic (veh/h)
N = Number of vehicles that can queue between the area between crosswalk and entry

The parameter N is to be set for every single entry. It is the number of queue spaces for cars that fit into the area between the crosswalk and the boundary of the roundabout (queue spaces). The value can be taken from a map. For the car length the value of 5 to 6 m can be taken. The queue spaces for cars have to be added up for all lanes of the entry (e.g., 2 lanes and a

5 m gap between crosswalk and the edge of the roundabout: $N = 2$). This value, when using the Marlow-Maycock formula, has to be set according to the given situation.

Consideration of Pedestrians at the Exit of Roundabouts

Exits of roundabouts have a limited capacity, too. However, this has not been investigated to date (at least there are no relevant publications known). Observations in Germany show that a capacity of, for example, 1800 veh/h cannot be reached. The absolute limit seems to be somewhere near c_A = 1200 to 1400 pcu /h (per lane). Note that many European countries choose not to build two-lane exits for safety reasons.

Heavy pedestrian traffic that crosses the exit can also reduce the capacity. The effects of this can be calculated by the Marlow-Maycock method *(B26)* with usage of Equation B-18. The length of the crosswalk is considered in Equation B-16; the longer the crosswalk, the less the capacity. The variable c_A (see above) is replaced by $q_{e,\,max}$ in Equation B-17. However, recent research has shown that the influence of pedestrians on the capacity of the exit is overestimated in these equations.

Because of the general lack of scientifically valid results, a different calculation method, which seems more realistic, can be used as follows. The capacity of the exit is calculated using the formula by Griffiths (Equation B-16); this assumes that pedestrians have always priority when using the crosswalk at the exit. The queue length can be calculated by the method described in the previous paragraph (Little-M/M/1). This method is the best for the given task. However, caution is still advised in the use of these methods, as further research is needed to validate the methods.

Use of a Gap Acceptance Approach Versus a Regression Approach to Estimating Capacity

This section, prepared by Rod Troutbeck, documents the process used in Australia to adopt a gap-acceptance approach in the development of their capacity models. This discussion is relevant to the present study, as the US faces a similar dilemma in the development of its capacity models.

Background

The analysis of roundabouts in Australia has been developed from the gap acceptance approach in the late 1970's *(B29, B30)*. In the early 1980's, a national body for standards and practices, then known as the National Association of Australian State Road Authorities (NAASRA), commissioned the Australian Road Research Board to develop relationships between the geometry of the roundabout and its performance. There was a natural tendency for Australia to continue to use the gap acceptance approach as this technique was currently in use. The author reviewed the practices worldwide before making a final decision.

This report describes the thinking and the process around the adoption of the gap-acceptance approach and some of the history of the empirical approach from the UK. It also describes the history of the Australian method in some detail.

Discussion with TRL Staff on the Use of the Linear Regression Equations

In August 1993, Troutbeck went to England, Scotland, and Europe to discuss the analysis of roundabouts with different research organizations and staff. The comments and conversations have been recorded by Troutbeck *(B31)*. Extracts from this report have been reproduced in this section and shown in italics. Other relevant and recent comments are also given here.

In 1983, Troutbeck reported the following major conclusions.

'The British have spent a considerable amount of effort studying the capacity of roundabouts. The TRRL [Transport Research Road Laboratory] has produced equations for the prediction of capacity on roundabouts and these have been included in the current Department of Transport practices. ... Other researchers, particularly at universities, have also attempted to develop predictive equations for roundabout capacity, but have based these on gap-acceptance techniques. However, since the publication of the TRRL formula, their efforts have been reduced. Ashworth and Laurence (B32) have shown that the capacity of the smaller roundabouts [is] better modeled by gap acceptance theory. There seems to be no reason for ARRB not to continue to develop capacity formula based on the gap-acceptance approach.'

'After reviewing the research on the capacity of roundabouts and talking with the researchers, I consider that the dominant variables will be the number of entry lanes, the number of circulatory lanes, and aspects of the circulation flow. It is, however, the last aspect [that] I believe has not been well handled in the UK. TRRL studies at a roundabout with light and heavy circulation flows, as observed in track experiments, have been considered together, when in fact the flow conditions are quite different. At high circulation flows, the speed of the circulating vehicles is low and the gap-acceptance characteristics of the entering drivers are likely to be quite different to their characteristics when the flow is low. I now consider the speed of the circulating vehicles to be an important parameter in determining the research of a roundabout.'

These conclusions were developed from a detailed discussion with a number of researchers. The major issues are discussed in the following sub-sections.

Gap Acceptance or Linear Regression Approach? Troutbeck *(B31)* reported that on the 18th August, the author met with Mike Grimmer, the head of the Traffic Systems Division; Mike Taylor, who was head of the traffic capacity and delay group; and Marie Semmens, who was involved in the early roundabout work and developed ARCADY2 *(B33)*. Troutbeck *(B31)* reports:

'When I questioned Marie on the use of a linear rather than a gap-acceptance model, she pointed to the fact that the circulating drivers tend to adjust their speed to allow the entering drivers to merge. Marie considered this adjustment to be contrary to gap-acceptance models. However, it can be handled by gap-acceptance techniques if the critical gap is made circulation flow dependent or, more promisingly, speed dependent. Marie considered that since the gap-acceptance models tend to give a second order relationship between entry capacity and circulation flow, the significance of this second order term will indicate whether the gap-acceptance approach is reasonable. TRRL examined the significance of this second order term for all their data sets, and in general, found that it was not significant. ... However, recent work by myself indicates that the gap-acceptance formulae can give almost linear relationship within the workable limits of the data and I was not surprised that the second order term was not significant.'

It has since been found that the limited priority merging system allows for the gap acceptance approach to give results that are even closer to a linear line.

John Wardrop, University College London who developed the weaving equation for roundabouts was Golias' supervisor. He also gave an insight into the TRL approach.

> *He believed that it may be unprofitable to use a complicated model when a simple linear equation might be quite satisfactory. I agreed that no practicing engineer would be interested in using complicated models or equations if a more simplified one gave 'reasonable' estimates. However, I believe that the process of finding suitable simplications requires knowledge of the effect of many parameters and the behaviour of more complicated (and more realistic) models.*

John Tanner, from TRRL, developed the formulae for delays (and hence capacity) of uncontrolled intersections also offered advice on the TRL approach. His equations have been included in the 1979 NAASRA *(B34)* guide to urban intersection design and the updated 1982 roundabout guide *(B35)*.

> *'John was also defensive of the TRRL approach. He reiterated many times that this formulation was largely an academic exercise and that the more empirical model of Kimber was more appropriate for estimating capacity.'*

Vitz and de Wijngaert *(B36)* compared the gap-acceptance technique with the TRRL method of estimating capacity. They concluded that PICADY significantly overestimated capacity.

At the University of Sheffield, Troutbeck met Robert Ashworth and Chris Laurence who have been researching the capacity of roundabouts since the early 70's. Much of their work has been summarized in Troutbeck *(B37)*. Troutbeck *(B31)* reports:

> *'I asked Robert why he thought TRRL adopted the linear regression approach. His answer was that he thought that exponentials were too clumsy to incorporate into a design formula. Pocket calculators were not in general use at that time and the simpler linear approach was favoured.'*

> *'A third report by Ashworth and Laurence (B32) documented the final stages of the study sponsored by TRRL. In the third stage data were collected at 21 other large (conventional); roundabouts to assess the accuracy and predictive ability of equations developed in phase II. They concluded that the exponential equation given above was the best predictor. The original aim of the third phase was to identify the principal factors [that] cause a small island roundabout to have increased capacity over the larger ones. Time precluded a detailed analysis and all that could be done was to determine the effective number of lanes. Ashworth and Laurence concluded that the doubling of the number of entry lanes increased capacity by up to 34 per cent. They felt that insufficient length for splayed lanes and drivers' reluctance to use them gave rise to the small increase in capacity. Intuitively, a similar conclusion would be expected from Australian data. They were not able to shed any more light on the effect of geometric parameters. '*

> *'Robert Ashworth and Chris Laurence also gave me reprints of a number of published papers on the prediction of roundabout capacity (B38, B39, B40) In*

> *these papers the predictive ability of the formulae given by TRRL, the University of Southampton and the University of Sheffield, were examined. Ashworth and Laurence concluded that 'no single formula was the best predictor for conventional, small or conventional with flared entry roundabouts' .The TRRL equations predicted the capacity of larger roundabouts better than the gap-acceptance equations However, the gap-acceptance equations performed better for the smaller roundabouts and the roundabouts with flared entries.'*

These statements indicate that the linear approach adopted by TRRL was not universally accepted and the gap acceptance approach still had some credence in the UK.

At the University of Glasgow, Troutbeck met Roy Hewitt who was the supervisor of Khayer whose doctoral thesis was 'Capacity and delays at roundabouts'. Troutbeck *(B31)* reports:

> *Khayer, as did Robert Ashworth in Sheffield, found that the critical gap was dependent upon flows. Khayer introduced two lag times. The first is the time a driver needs to follow another minor stream vehicle through the intersection. The second is the time required for a driver to enter without stopping. The second time is similar to the critical gap and was timed the critical lag. Khayer found that the critical lag was [slightly] shorter than the critical gap.*

This finding causes the gap acceptance equations to have a more linear alignment.

Accuracy of Models. At Southampton, Troutbeck met with Nick Hounsel and Richard Hall. Troutbeck *(B31)* reports that the research by Mike McDonald *(B41)* had found that:

> *Data from Hounsdown roundabout Figure 11 [Figure B-6 here] indicated that observed capacities could be more than 30 per cent greater than the values predicted by Kimber (B9). Figure 11 also indicates that the gap-acceptance curves (solid line) [provide] a reasonable estimate of capacity. At the Redbridge roundabout, Mike McDonald found [that] entering capacities were about 50 per cent greater than those predicted by Kimber's equations for low circulating flows. This evidence suggests that estimates within 20 per cent should be considered to be satisfactory. Moreover, there would seem to be little point of including parameters [that] produce effects of less than 10 per cent.*

Effect of Exiting Vehicles at the Preceding Leg. TRRL has developed procedures that ignore the impact of exiting vehicles. This has been an issue that other researchers have considered important. When TRL was questioned about this the result was:

> *'Marie said that the exiting flows did not affect the capacity implying that entering drivers can perceive the intentions of the exiters. Hence, the conflicting, circulation flow is that measured across the entrance and not mid-way between the previous exit. Kimber and Semmens (B42) found that the proportion of vehicles leaving at the previous exit, the proportion of entering vehicles turning left, and the proportion of circulating vehicles leaving at the next exit did not have a discernable effect on entry capacity'. I find it difficult to accept that the effect of the exiting vehicles is likely to be insignificant at all sites.'*

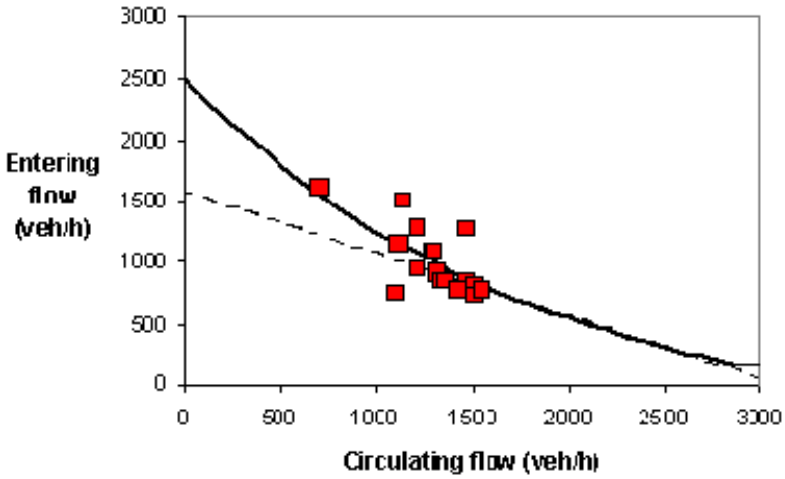

SOURCE: (B41)

Figure B-6. Entry Capacity from the Hounsdown Roundabout.

Effect of Platooning. The effect of platooning in a priority stream does affect the capacity to some extent. Although extreme levels of platooning are not common. Troutbeck *(B31)* reports that TRRL considered that:

> *'Kimber and Semmens (B42) experimented with the circulating traffic interrupted and released with a 20 s cycle time. Under these extreme conditions they found that the entry capacity was increased by 10 per cent for circulation flows of about 800 to 1000 veh/h (my estimate). Kimber and Semmens dismiss the level of platooning as a parameter which is likely to affect capacity.'*

Effect of Circulating Vehicle Speeds. It has been identified that speed of traffic through a roundabout does affect the performance of the roundabout at the higher flows. TRRL reported that:

> *'Marie Semmens had no idea of circulating vehicle speeds in track experiments. If these speeds were lower than on public roads then we have some idea of whether the drivers would be accommodating. To travel around a roundabout at a lower speed is in itself accommodating. Although speeds were used to determine geometric delays, they were not used in the evaluation of capacity or queuing delay. Marie said that TRRL have only made limited speed measurements and it was concluded (but not reported) that the effect of speed was marginal. See comments in Semmens (B43).'*

Delays at Roundabouts. The TRRL method of calculating delays is based on a queuing process with random arrivals and random service times. In 1983, Troutbeck asked Marie Semmens if they have experimental data to support the assumed arrival times and service times. The response was that:

'She said that they did not have any data although the measured delays are not unlike the experimental delays. The random service time [function] seems to be intuitively unreasonable and I find it hard to accept. Mike McDonald of the University of Southampton has a similar opinion. It [may be], however, that random arrivals/random service time gives good estimates in spite of the seemingly irrational basis.'

Track Studies. Track experiments were an important part of the TRRL approach. These experiments provided data that were not available from the public road system. TRRL reported that:

'Since TRRL [has] relied on the track experiments to measure capacity, I questioned whether these experiments were representative. The fact that drivers are participating in an experiment generally results in a change of behaviour from the Hawthorne Effect. The drivers in the track experiment were asked to drive normally, and are paid according to the distance driven. This should cause drivers not to wait for excessively large gaps. On the other hand, the drivers were using their own cars and would not be too impatient. TRRL used a 'control' intersection to determine if drivers' behaviour had changed throughout the day and the week. Since, the control intersection capacity varied by less than 6 per cent throughout the week, Rod Kimber was satisfied that the drivers were behaving normally and consistently. He argued that if they were not driving normally they would not be as consistent. This conclusion would seem to be justified and the track experiments produced reasonable results in the usable range of flows.'

Further, TRRL reported that:

'The track experiments taxed the resources of the group. About 35 researchers and technical staff members were required to control about 200 subject drivers.'

The Transport Research Group in Southampton found the TRRL test track experiments to be of considerable value to their study. The data from the test track experiments proved to be more consistent than the results from public roads, although not statistically significantly different.

Concluding Remarks. Given the comments form researchers overseas, there are good arguments for the use of linear equations to describe the relationship between the circulating flow and entry capacity. There was not a strong statement for adopting either the linear model or the gap acceptance approach. The author has also sought to have approaches that explained the relationship so that any extrapolation could be useful. Secondly, there were insufficient sites in Australia that had continual queuing and were available for a linear regression approach. Consequently, it was reasonable that Australia adopted the gap-acceptance approach.

The value of the empirical model was tested using a congested site *(B44, B45)*. The results indicated that the gap acceptance technique tended to overestimate slightly, but this was not considered to be excessive.

It should be pointed out that the linear regression approach has been considerably enhanced with the test track experiments. In fact, if only public road data was used it, is unlikely that all the geometric terms used in the TRRL model would have been statistically significant.

Development of the Gap Acceptance Terms in the ARRB Procedure

The ARRB procedure *(B46)* formed the basis of the Austroads guide *(B47)*. The development of the ARRB procedures is described in this section. Much of this section is a direct quote from Troutbeck *(B46)*.

Site Selection. Roundabout entries which had significant, but not necessarily continuous, queuing during the peak period were selected for this study. The behavior of motorists at these entries was monitored using a video camera mounted on a mast attached to a small trailer *(B48)*. The trailer was positioned off the road, without obscuring the view of motorists. Data were recorded at roundabouts in Melbourne, Sydney, Canberra and Brisbane during 1985–1986.

Geometric Terms Considered. The UK terms *(B9)* to describe the entry geometry were considered and the following list was chosen for the study *(B46)*:

- Inscribed Diameter (D): the largest arc that can be drawn inside the curb line of the roundabout.
- Conflict angle (ϕ): represents the change in direction a driver would need to make to be tangential to the central island after entry.
- Entry radius (r_e): measured at the 'Give Way' (yield) line. A more useful term is the curvature of the entry, $1 / r_e$.
- Entry width (e): the width available to the entering drivers.
- Approach width: the road width for this direction of travel upstream of the entry.
- Circulatory roadway width (cw): the clear distance between the central island and the inscribed diameter measure.
- Extra circulatory roadway width (ecw): extra width results from a slip lane (left turn in Australia, right turn in US).
- Maximum circulatory roadway width: the sum of the circulatory lane width and the extra circulatory lane width.

These parameters were based on those used in the UK study. Figure B-7 illustrates these measures.

Gap Acceptance Parameters for the Different Lanes of an Approach

The ARRB study found that drivers in different lanes of an approach behaved differently. For instance, when reviewing the follow-on times for the different lanes, the lane with the largest flow had the shorter follow-on time. This was captured in the ARRB procedure by labeling the lane with the largest flow as the ‘Dominant’ stream as the drivers tended to ‘take control’ at that entry. The other stream was termed the ‘Sub-Dominant stream’. Figure B-8 indicates that the follow-on time for the dominant stream is usually less than the follow-on time for the sub-dominant stream. The mean ratio between the follow-on time for sub-dominant streams to the dominant stream is 1.2. The behavior in these two types of entry lanes is analyzed separately.

Dominant Stream Follow-On Time. The follow-on time for this dominant entry stream was evaluated with additional transformed geometric parameters as follows.

The number of entry lanes, n_e, is a broad classification of the entry width. The value of n_e is 1 for entry widths less than 6 m, 2 for entry widths between 6 m and 10 m, and 3 for entry widths between 10 m and 15 m.

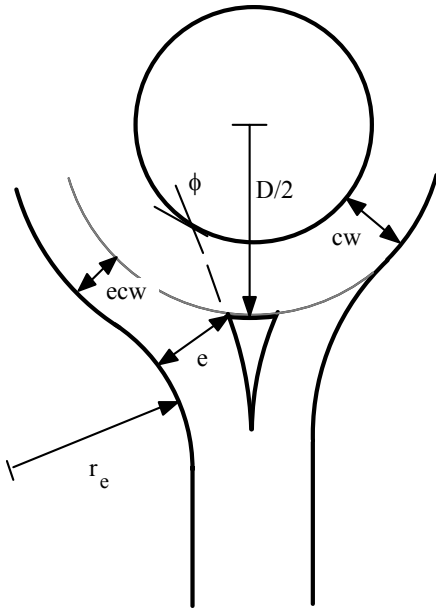

Figure B-7. Description of the Roundabout Entry Terms

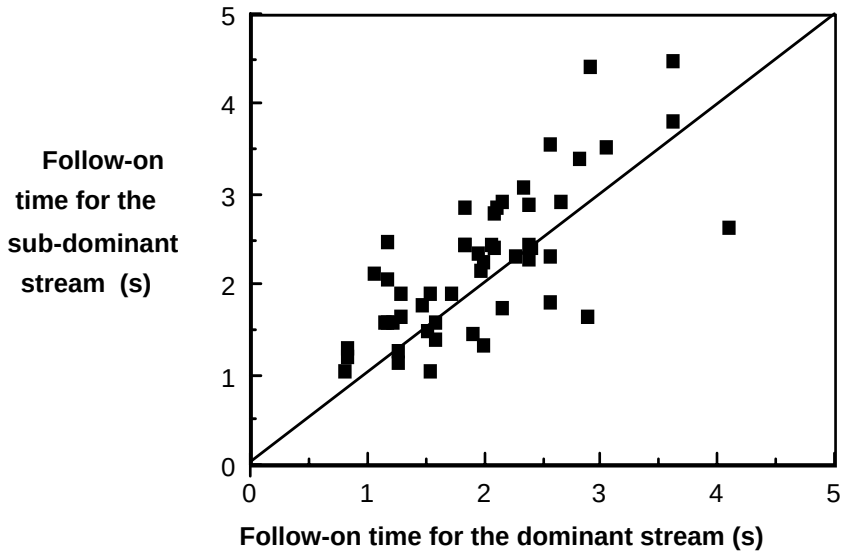

Figure B-8. Relationship between the Follow-On Times for the Dominant and Sub-Dominant Streams

The number of circulatory lanes n_c is again a broad classification of circulatory road width. The value of n_c is 1 for entry widths less than 10 m, 2 for entry widths between 10 m and 15 m, and 3 for entry widths between 15 m and 20 m.

The follow-on times had a significant correlation with the entry width (r = –0.682), the number of entry lanes (r = –0.658), the circulating road width (r = –0.492), the number of circulating lanes (r = –0.488), the entry curvature (r = +0.345), and the circulating flow (r = –0.505). A quadratic function of the diameter of the roundabout also had a significant effect on the dominant stream follow-on time.

Troutbeck *(B46)* states:

> *'A linear function of the entry widths implies that an increase in width from 3 to 4 m or from 5 to 6 m produces the same net result. In the first case the lane remains a single lane whereas in the second case the result enables the entry to change from a one lane to a two lane operation. A linear function of width would also encourage designers to use the relationships for quite detailed geometric design and to assume that the relationships offer a degree of accuracy above that recorded.'*

The equation developed used the number of lanes and not the total road width.

The equation for the dominant stream follow-up time was

$$t_{fdom} = 3.37 - 0.000394Q_c - 0.0208D + 0.0000889D^2 - 0.395n_e + 0.388n_c \quad \text{(B-19)}$$

where:
- Q_c = is the circulatory flow
- D = the inscribed diameter
- n_e = the number of entry lanes.
- n_c = the number of circulatory lanes.

This equation explained 64.5 percent of the sum of squares and the equation and its regression coefficients were significant at the five percent level. The standard error was 0.40 s.

For all practical purposes, the coefficients for the number of entry lanes and for the number of circulating lanes are equal. Sites with an increased circulating flow have a shorter follow-on time. Similarly, roundabouts with a small inscribed diameter have a longer follow-on time than moderately sized roundabouts. Exceptionally large roundabouts may be expected to have a longer follow-on time because of the higher circulating vehicle speeds.

Sub-Dominant Stream Follow-On Time. The drivers in the sub-dominant stream, generally have longer follow-on times than the drivers in the dominant stream as shown in Figure B-8.

The follow-on time for the sub-dominate stream was significantly affected by the dominate stream follow-on time and by the ratio of dominant stream flow to the sub-dominate stream flow. The selected equation was

$$t_{f,sub} = 21.49 + 0.5135t_{f,dom}\frac{Q_{dom}}{Q_{sub}} - 0.8735\frac{Q_{dom}}{Q_{sub}} \quad \text{(B-20)}$$

where:
- Q_{dom} = the dominant entry lane flow
- Q_{sub} = the sub dominant entry lane flow
- t_{fdom} = the calculated dominant stream follow-on time

This equation explained 40 percent of the variance. All coefficients were significant at the 5 percent level and the standard error was 0.58 s. Equation B-20 demonstrates that the follow-on time of the sub-dominant stream increases as the follow-on time of the dominant stream increases and generally as the ratio of flows of the approach lanes increases.

Critical Acceptance Gap. The critical gap for a driver is assumed to be such that all gaps greater than his critical gap are acceptable whereas the gaps less than his critical gap are unacceptable. For the population of drivers, it has been frequently assumed that the critical gaps have a log-normal distribution *(B4, B46, B49, B50, B51)*.

The 'critical acceptance gap' is the mean of drivers' critical gaps and is used to quantify the overall performance of the driving population. These terms are used in the equations for capacity and delay.

For the ARRB study, the maximum likelihood technique was used to estimate the distribution of critical gaps *(B37)*. Most other methods of evaluating the mean critical gap have considerable bias.

Kimber's equations *(B9)* imply an almost constant ratio between the critical acceptance gap (or the mean critical gap) and the follow-on time. As a consequence the measured mean critical gap was related to the estimated follow-on time. It would be logical to think of the critical acceptance gap as being the primary term with the follow-on time being related to it. The follow-on time is a simple term to measure reasonably accurately. The critical acceptance gap is far more difficult to estimate and considered better to relate its measure to the follow-on time.

The mean critical gap was found to have a significant correlation (at the five per cent level) with the expected follow-on time, the circulating flow, entry width and the number of entry lanes. The circulatory width and the number of circulatory lanes were significantly correlated with the mean critical gap at the 10 percent level. Figure B-9 is a plot of the mean critical acceptance gap divided by the follow-on time as a function of the circulating flow. Apart from four points towards the higher circulating flows, there is a general downward trend.

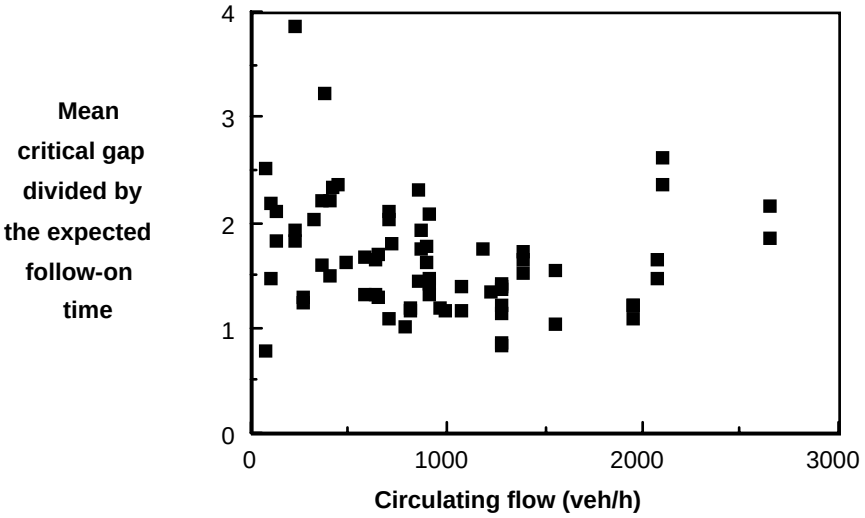

Figure B-9. The Mean Critical Gap Divided by the Expected Follow-On Time

The chosen equation identified was

$$t_c = (3.6135 - 0.0003137 Q_c - 0.3390 \bar{e} - 0.2775 n_c) \cdot t_f \quad \text{(B-21)}$$

where: t_f = expected follow-on time
$\bar{e}$ = average entry lane width (m)

This equation explained 44.2 percent of the variance. The equation is significant at the 5 percent level, and the standard error is 1.09 s.

Equation B-21 is essentially a ratio of t_c / t_f, which is related to the gradient in Kimber's equation *(B9)* and hence the ratio can also be considered to be the relative influence of an additional circulating vehicle. Equation B-21 implies that this influence reduces as circulating flow increases, as the number of circulating lanes increase and the average entry lane width increases. The effect of the average entry lane width can be expected if it is accepted that wider entry lanes put less demands on the driver.

The ratio of t_c / t_f given in Equation B-21 is less than 1.0 for high circulating flows. If this ratio is less than 1, then the capacity equation would not give a monotonic decreasing function for capacity against circulating flow. This is intuitively unacceptable. The gap acceptance assumptions would also be suspect under these conditions. Accordingly the ratio should be restrained to be not less than 1.1. The field results (Figure B-9) indicate the mean critical gap to follow-on time ratio does decrease with flow, and the ratio was typically greater than 1.0 although there were a few exceptions.

Using equations B-19 to B-21, both the follow-on times and the mean critical gap decrease with circulating flow. While the data in this paper cannot describe detailed driver behavior, the study does indicate that at sites with a low circulating flow, the gap acceptance parameters are larger. This could result from drivers being prepared to reject the smaller gaps in the knowledge that a larger gap will be available shortly. This more relaxed behavior is evident at some roundabouts in provincial towns. At high circulating flows the entering drivers cannot yield right of way all the time without incurring long delays.

Troutbeck *(B46)* wrote,

> *"At sites with high circulating flows, the entering drivers 'share' their priority with the circulating drivers. Troutbeck (B52) demonstrated that the total average delay due would be reduced with priority sharing without involving a significant delay to the 'major' stream. When the entering drivers 'share' priority, they accept shorter gaps and cause the circulating drivers to slow. It is a mutual arrangement; the entering drivers accept shorter gaps and the circulating drivers allow these drivers to enter."*

This priority sharing phenomena has been identified in Troutbeck *(B46)*, but it has only been more recently that a process has been developed for evaluating a limited priority system that includes priority sharing *(B53, B54)*.

Shorter gap acceptance parameters, recorded at sites with larger circulating flows, can be expected from slower circulating vehicle speeds.

Characteristics of the Circulating Streams. In Troutbeck *(B55)*, it was concluded that the entering drivers gave way to all circulating drivers. As a consequence, a single lane Cowan

M3 model was used to represent the headways in all circulating streams. Cowan's model assumes that $(1 - \alpha)$ vehicles are in bunches with a consistent intra-bunch headway of τ. The remaining vehicles have an exponential headway. The cumulative probability equation for Cowan's headway model is as follows (shown graphically in Figure B-10):

$$F(t) = 1 - \alpha \cdot \exp\left[-\lambda(t-\tau)\right] \qquad t \geq \tau,$$
$$F(t) = 0 \qquad \textit{otherwise} \tag{B-22}$$

where:
- t = time
- α = proportion of free vehicles (those not in bunches)
- τ = intra-bunch headway (the same for all vehicles in bunches)
- λ = decay rate which is related to the flow, q, by the equation

$$\lambda = \frac{\alpha q}{1 - \tau q} \tag{B-23}$$

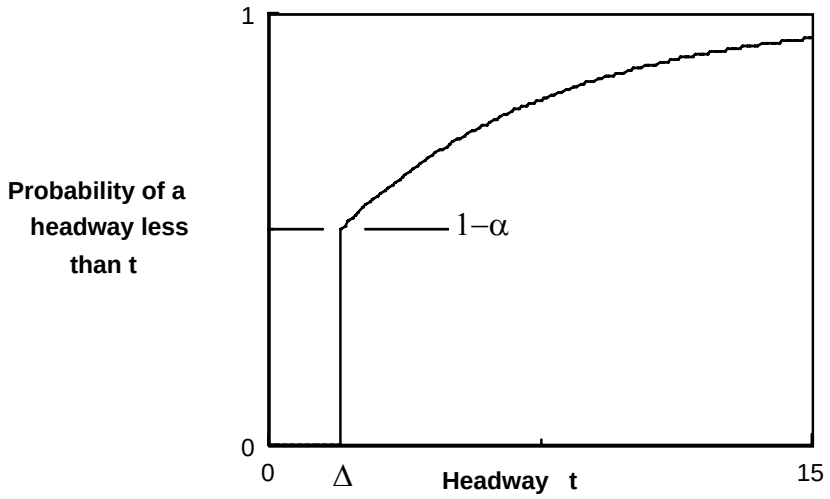

Figure B-10. Cowan's Headway Model

The characteristics of the circulating streams headways at the Australian roundabouts were quantified using a technique to estimate the parameters (α, τ and λ) for Cowan's M3 model *(B56)*. This technique, described in Troutbeck *(B45)*, minimized the deviation between the predicted and recorded cumulative distributions and provided satisfactory estimates of the cumulative probability functions for gaps greater than 4 s, say, but did not necessarily provide satisfactory estimates for the short headways. This is not considered to be important, as these headways are unacceptable and would be rejected. A Kolmogorov-Smirnov goodness-of-fit test was used to compare the fitted distribution to the data.

Intra-Bunch Headway. The minimum headway between vehicles in bunches is likely to be dependent on flow. If traffic arrivals were regular then the minimum headway τ would be inversely proportional to flow. Increase the flow and τ would decrease. The proportion of free vehicles, α, is dependent on the proximity of the roundabout to signalized intersections or to other traffic devices that establish platoons. The parameter α is expected to be more significantly affected by the nearby road infrastructure than by the geometry of the roundabout. As the flow in the circulating lanes increases so the proportion of free vehicles decreases. The parameter λ is not independent as it related to q, α and τ by Equation B-23. The α and τ terms must be considered jointly. It is not important to accurately describe the distribution of small headways and these two terms can be used to locate the 'knee' in the curve shown in Figure B-10. It is then preferable for one of these terms to be chosen and the other related to the geometry and the flows.

The headway between vehicles in bunches could be related to flow by a hyperbolic function (Figure B-11). However, this figure also indicates that values of about 1 and 2 predominate and it could be convenient to set τ to 1.0 or to 2.0 s. Note that the choice of these values for τ as arbitrary, and are roughly the same as values of 2.2 and 1.1 used by Avent and Taylor *(B30)*.

Single-lane roundabouts with wider circulatory lanes (8 to 10 m) and higher flows (greater than about 1000 veh/h) could also be considered to have two effective lanes and intra-bunch headways of 1 s. This occurs because drivers are prepared to adopt a staggered orientation as shown in Figure B-12, forming in effect two lanes with small intra-bunch headways.

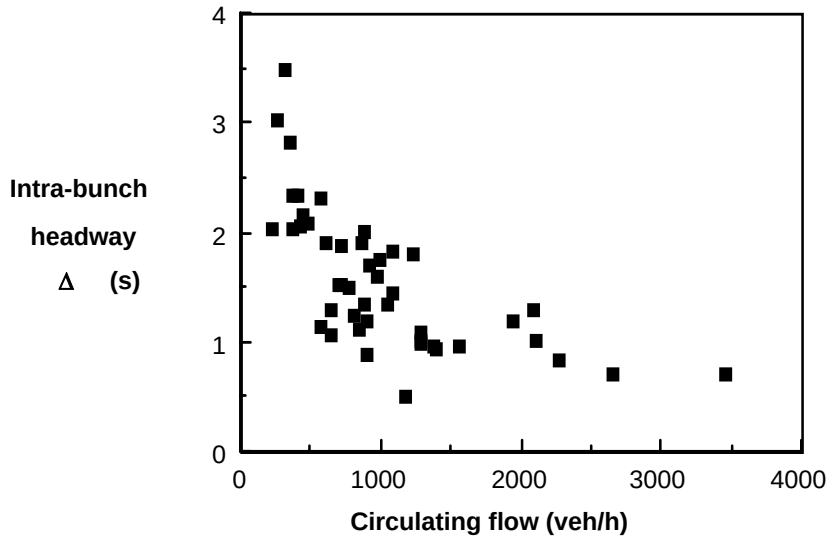

Figure B-11. The Influence of the Circulating Flow on the Calculated Intra-Bunch Headway

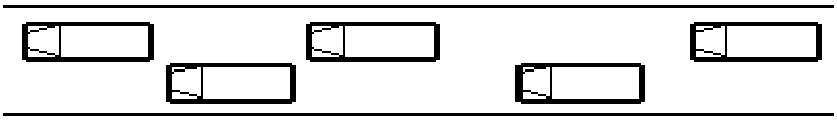

Figure B-12. Staggered Vehicles in a Single Wide Lane

Proportion of Free Vehicles. Considering the case of roundabouts with a single circulating lane, the proportion of free vehicles decreases with flow as shown in Figure B-13. The regression equation is as follows:

$$\alpha = 0.723 - 0.000386Q \quad \text{(B-24)}$$

where: α = proportion of free vehicles
Q = flow (veh/h).

This equation explains 47 percent of the variance, and with 13 data points the coefficient is significant at the one percent level. No geometric term had a significant correlation with α (at the 1 percent level).

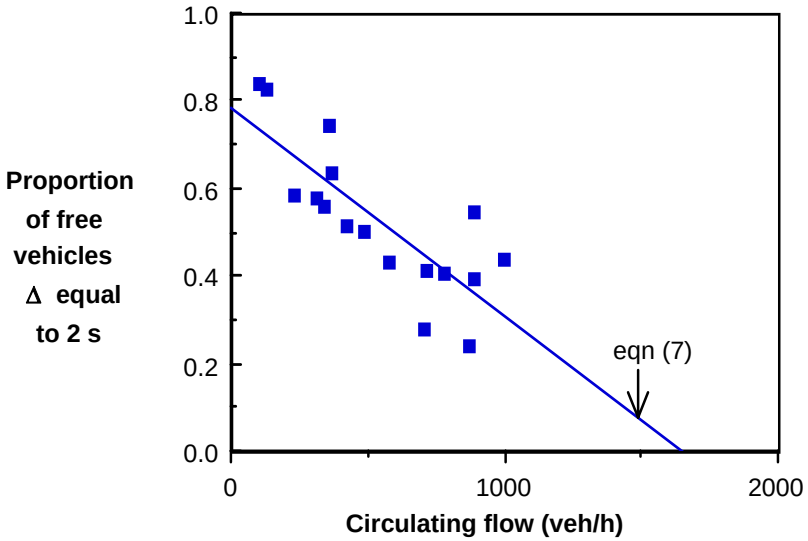

Figure B-13. Relationship Between the Proportion of Free Vehicles and the Circulating Flow for Single Circulating Lane Roundabouts

For the multiple circulating lane roundabouts, a similar finding was obtained. The proportion of free vehicles was related to flow by

$$\alpha = 0.754 - 0.000241Q \quad \text{(B-25)}$$

This equation explains 50 percent of the variance and the coefficient was significant at the one percent level. Refer to Figure B-14. Again no geometric parameters were found to be significant at the one percent level.

These expressions were be approximated to

$$\alpha = 0.8 - 0.0005Q \quad \text{(B-26)}$$

for roundabouts with single circulating lanes and

$$\alpha = 0.8 - 0.00025Q \quad \text{(B-27)}$$

for roundabouts with multiple circulating lanes.

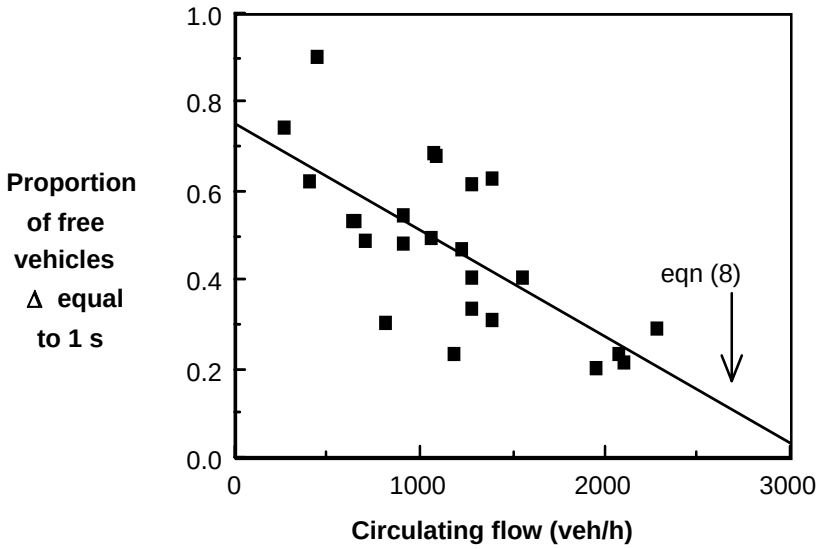

Figure B-14. Relationship Between the Proportion of Free Vehicles and the Circulating Flow for Multiple Circulating Lane Roundabouts

Estimating Capacity Using the ARRB Method

The maximum entry capacity is estimated using the equation from Troutbeck *(B57)*, as follows:

$$q_{e\max} = \frac{\alpha q \cdot \exp\left[-\lambda(t_c - \tau)\right]}{1 - \exp(-\lambda t_f)} \quad \text{(B-28)}$$

where: α = the proportion of free vehicles in the circulating streams

q = the flow of vehicles in the circulating streams
t_c = the critical acceptance gap
t_f = the follow-on time
τ = the minimum headway in the circulating streams, and these are related by Equation B-23, given above

Single-Lane Roundabouts. For a roundabout with a single entry and a single circulating lane the maximum entry capacity is significantly less than the results from the 1986 NAASRA *(B58)* guide for low circulating flows (Figure B-15). For higher flows, the values are comparable with those from NAASRA *(B58)*. Comparisons were made with the NAASRA approach, as this was the accepted standard of the time. Roundabouts with a larger inscribed diameter have a greater capacity, although the increase is not large. Similarly, roundabouts with a wider entry width have a greater capacity.

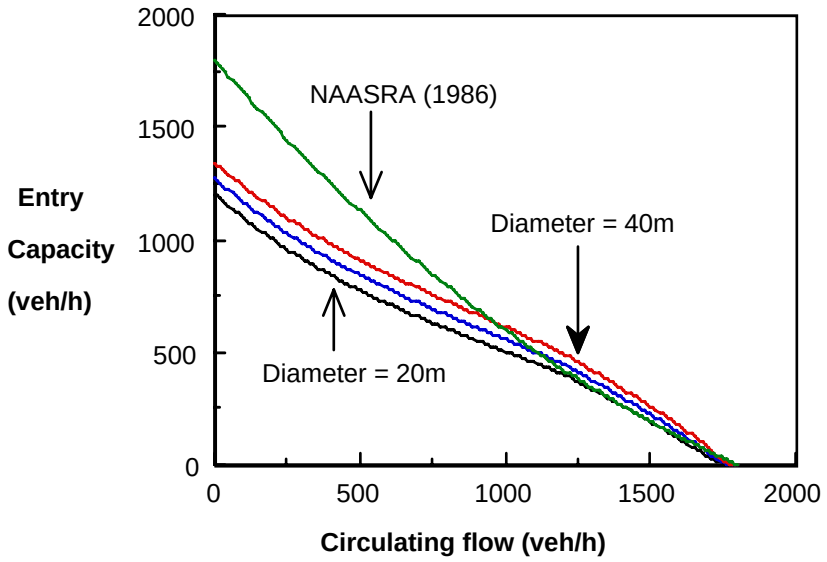

Figure B-15. Effect of the Inscribed Diameter of a Single Lane Roundabout

Multilane Roundabouts. When analyzing roundabout legs with more than one entry lane, each entry lane is considered separately. The potential capacity of the entry is then approximately the sum of the capacity for each lane. The capacity for each lane is different, with the dominant stream having the greater capacity. Doubling the number of entry lanes does not give double the total entry capacity.

As for single-lane roundabouts, the performance of multiple lane roundabouts will be improved if the inscribed diameter is increased (Figure B-16), and if the average entry lane width is increased (Figure B-17). This is because the drivers' gap acceptance parameters are reduced. The curves for different average entry width are co-incident at larger circulating flows because of the restraint that the critical gap be greater than the follow-on time. As discussed above, driver behavior is expected to be different at higher circulating flows where priority sharing occurs. The

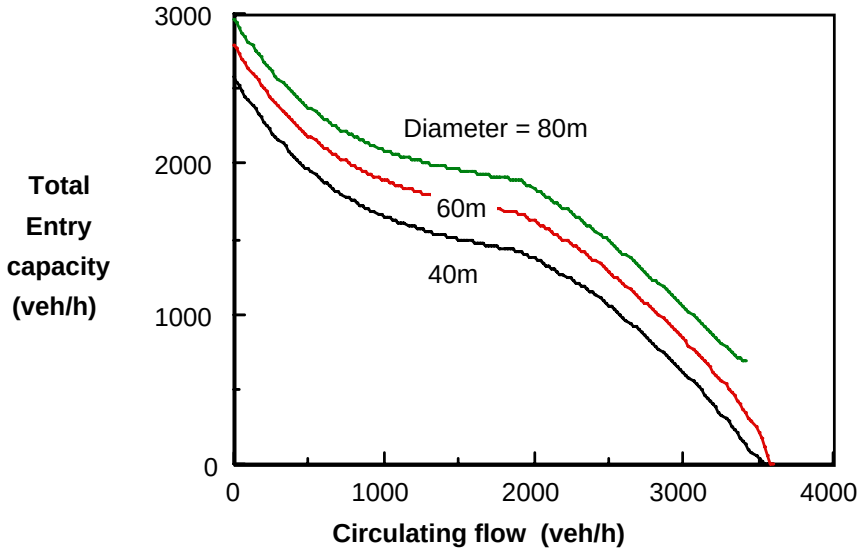

Figure B-16. The Effect of the Inscribed Diameter on the Total Entry Capacity for a Roundabout with Two Entry Lanes

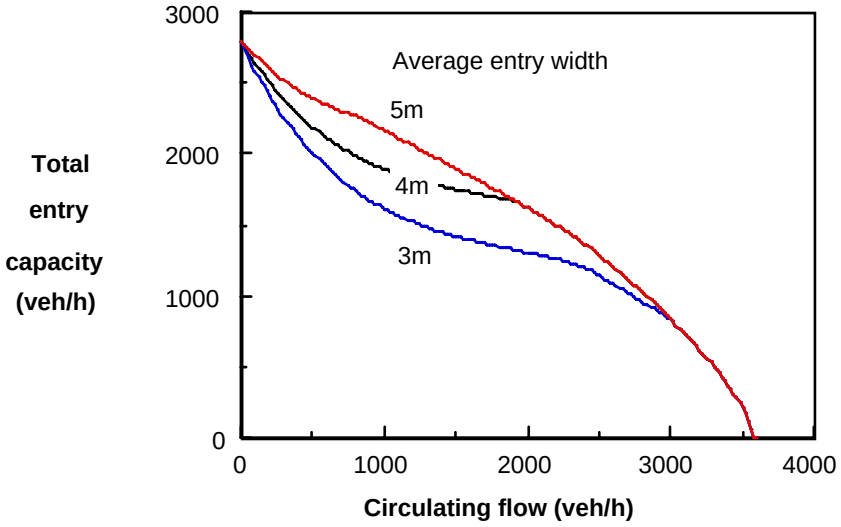

Figure B-17. The Effect of the Average Entry Lane Width on the Total Entry Capacity

speed of the circulating vehicles is likely to be low and it is reasonable for the entering drivers to be less affected by the entry width. Most drivers will be stopped before entering the roundabout and the difficulty of driving in a narrow lane will be decreased. The results in Figure B-16 are thus considered to be reasonable.

The discontinuity at a circulating flow of about 2000 veh/h is developed from the limiting value of the ratio of the follow-on time to the critical acceptance gap to be greater than 1.1. This discontinuity will be further discussed.

Concluding Remarks. The ARRB research has been based on empirical data and was able to relate driver behavior attributes to the gap-acceptance terms and the geometry of the roundabout. This has provided the basis for techniques that can reflect the behavior of motorists.

SIDRA Development

In the early editions of SIDRA, there was a faithful representation of the ARRB research. SIDRA 4.1 introduced the effect of origin and destination and SIDRA 5 introduced the alternative approaches to the analysis and the prediction of headway characteristics. These changes have influenced the outcome and they will be discussed in this section. In order to identify the effect of changes from the ARRB procedure, each change will be identified using results for both single-lane roundabouts with an inscribed diameter of 20 m to 40 m and double lane roundabouts with an inscribed diameter of 40 m to 60 m.

Gap Acceptance Parameters Adjusted for Low Circulating Flows and High Entry Flows. In the ARRB study, it was identified that the critical gap parameters were affected at sites were there has a high degree of saturation and when the circulating flows are low. The effect was small, and it was not considered necessary to include this effect, as it would have made the approach iterative and more complex than necessary. Nevertheless the phenomenon still exists. SIDRA 5 has included this effect, but without detailed research on the outcomes. On the other hand, the effect in SIDRA 5 is in the right direction.

The SIDRA approach is to reduce the follow-on time if the circulating flow is less than a specified limit (currently 900 pcu/h). The reduction is proportional to the ratio of the entry flow to the circulating flow. This ratio has a limit of 3. The reduction is also proportional to the ratio of the circulating flow to the specified limiting circulating flow.

The effect of this change only on the ARRB *(B46)* formulation is shown in Figure B-18. The SIDRA curves relate to conditions where the entry flow is three times the circulating lane flow. The average queue length is a function of the degree of saturation and the effect is only likely for degrees of saturation above 0.8. The SIDRA effect is significant below circulating flows of 900 veh/h. This effect is more than is expected from the ARRB data collection. There is no evidence to support the SIDRA level of this effect.

Limits on the Gap Acceptance Parameters. SIDRA limits the critical gap parameters to avoid extreme values. The limits used are as shown in Table B-1.

The effect of these is shown in Figure B-19. These limits did not affect the single-lane roundabouts and had only a marginal effect on the multilane roundabouts. Again these limits were arbitrary and are designed to decrease the capacity at higher circulating flows.

Revised Circulating Flow Characteristics. The most significant effect has been the changes to the circulating flow characteristics for two-lane roundabouts. These changes were again arbitrary and were not done with the appreciation of the interconnectedness of the terms used to define the headway distributions.

The effect of the change in means to determine the proportion of bunched vehicles is marginal for single-lane roundabouts, as the minimum headway was not changed. This is shown in Figure B-20.

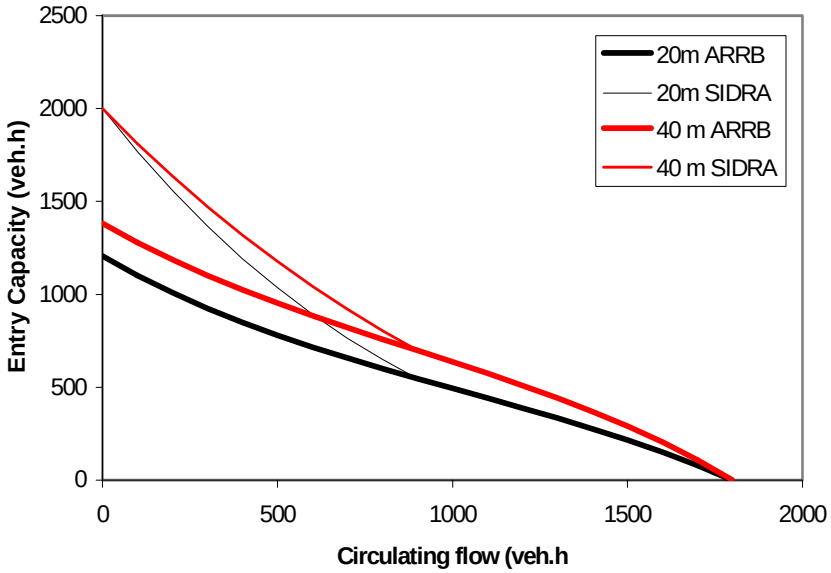

Figure B-18. Effect of the High Entry Flows at Low Circulating Flows Using the Sidra Routines for Single Lane Roundabouts.

TABLE B-1. Limits Employed within SIDRA on Gap Acceptance Parameters

	Minimum	Maximum
t_c	1.2	4.0
t_f	4.0	8.0
t_c/t_f	1.1	3.0

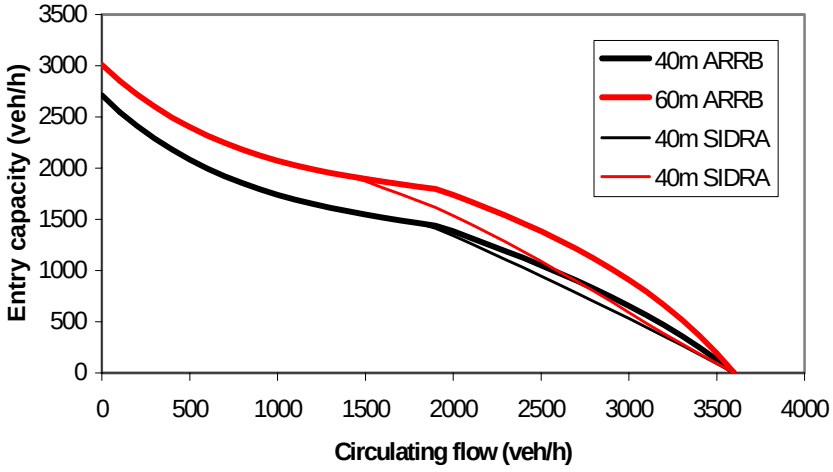

Figure B-19. Effect of the Change to the Critical Gap Parameter Limits at Two-Lane Roundabouts.

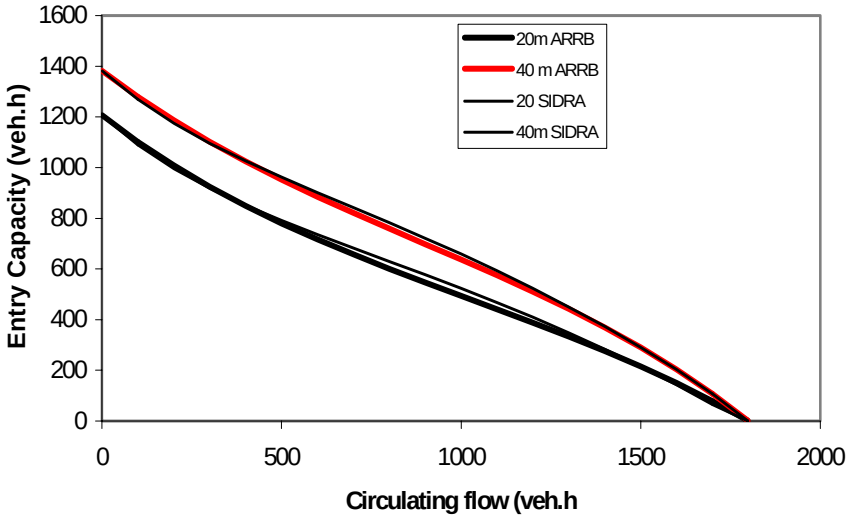

Figure B-20. Effect of the Change to the Circulating Flow Characteristics.

For the multilane case there are two effects. The first is change in the proportion of bunched vehicles, and the second is the change in the minimum headway. This latter change had the effect of significantly reducing the capacities at the higher flows, as shown in Figure B-21. The minimum headway variable should not be changed without good reason, as the small change in the headway distribution significantly affects the distribution of headways. For instance, for a flow of 2200 veh/h, the distribution of headways assumed from the different analysis techniques is shown in Figure B-22. The process developed by Troutbeck *(B59)* and reviewed by Luttinen *(B60)* sought the best fit to the empirical headway. The transformation used in SIDRA has significantly altered the relationship.

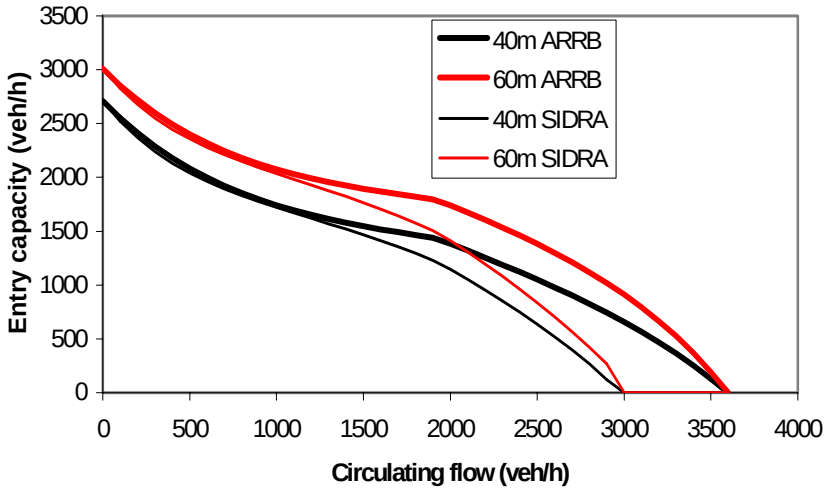

Figure B-21. Effect of the Change to the Circulating Flow Characteristics for Two Lane Roundabouts.

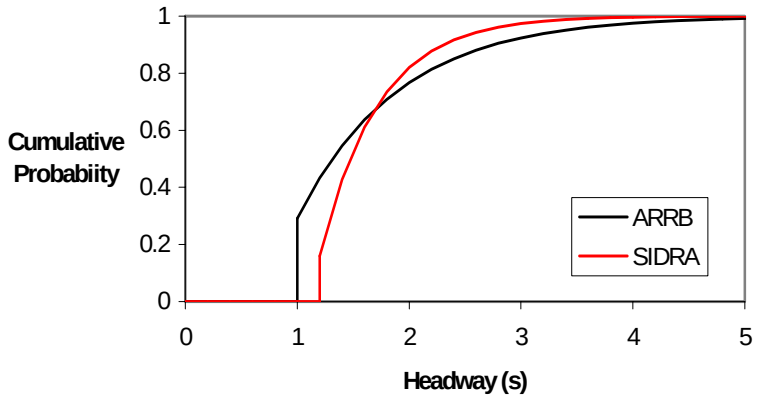

Figure B-22. Effect of Changing the Circulating Flow Characteristics for Two Lane Roundabouts with a Diameter of 60m.

Use of an Origin-Destination Pattern. SIDRA has recognized that the origin-destination (O-D) pattern may have an effect. O-Ds certainly influence the characteristics of the circulating stream as it passes the entry. A number of left turners will cause traffic in the circulating lane to be in a single lane. SIDRA uses relationships for the reduction of capacity, developed from the output of a simulation model. The reduction factor, f_{od}, is in turn a function of the proportion of the total circulating stream flow that originated from the 'dominant' approach. The 'dominant' approach contributes the highest proportion of queued traffic to the circulating flow. The reduction factor is also a function the proportion queued for that part of the circulating stream that originated from the 'dominant' approach.

In the extreme, both the parameters for the proportion of traffic from the dominant approach and the proportion queued from that approach, could be equal to 1.0. Under these conditions, the reduction in capacity is shown in Figure B-23 and Figure B-24. The maximum effect ranges from 4 to 55 percent. Hence the effect is significant.

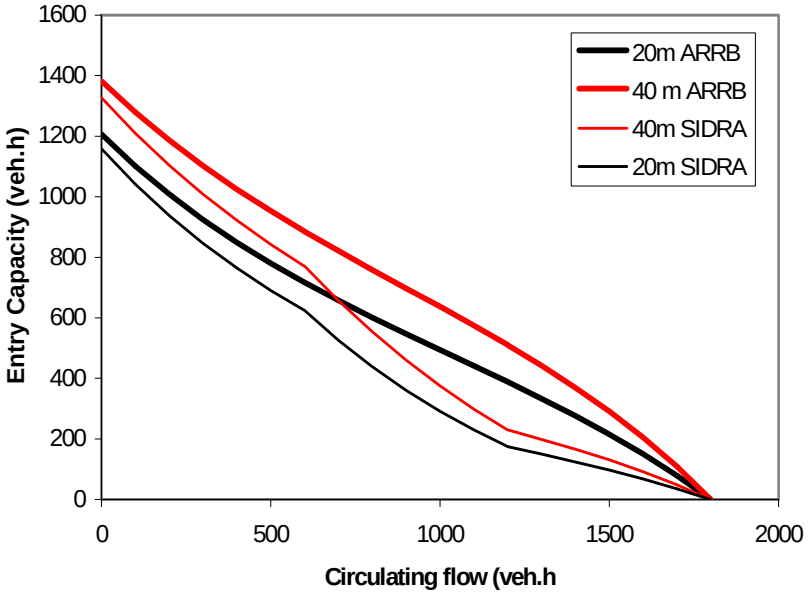

Figure B-23. Maximum Effect of the Origin Destination Procedure in SIDRA for One Lane Roundabouts.

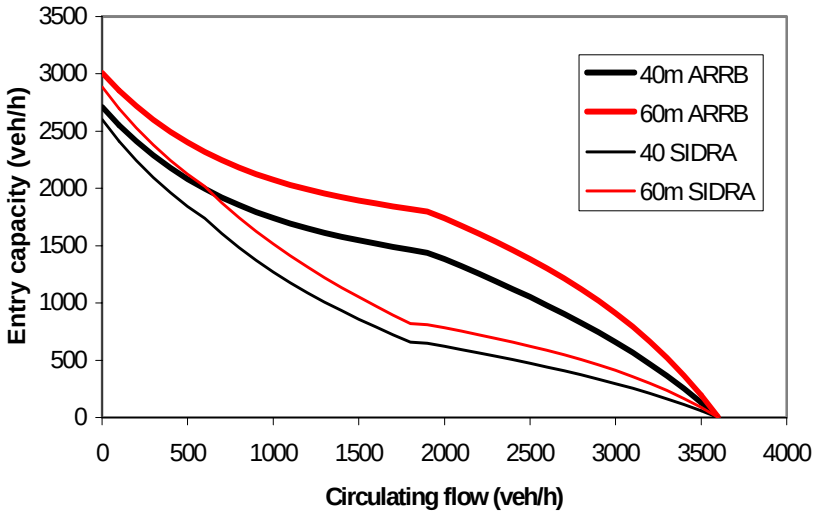

Figure B-24. Maximum Effect of the Origin Destination Procedure in SIDRA for Multi-Lane Roundabouts.

The Combined Effect of Changes. The combined effect of all aspects can be developed. However, the reader needs to check the outcomes with output from SIDRA, as other minor effects can influence the results. The analysis presented here is a combination of all effects listed above and does not account for the smaller effects in SIDRA.

Figure B-25 describes the combined effect for single lane roundabouts and assuming that there are high entry flows at low circulating flows. Figure B-26 illustrates the same effect for two-lane roundabouts. These figures illustrate only the broad combined effect of the parts presented earlier. Both of these figures indicate the widely different answers for capacity based on the proportion of traffic from the dominant approach and the proportion queued from that approach. For the upper-bound cases both parameters were set to 0.0 and for lower-bound cases these parameters were set to 1.0. Both conditions are extreme.

The conclusion reached is that the SIDRA changes were to decrease the capacity of the higher flows where the ARRB technique has been found to be lacking (also refer to *B13*).

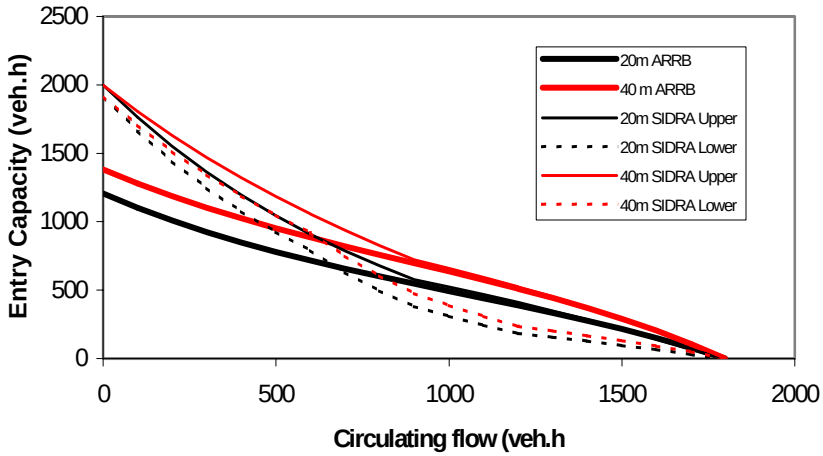

Figure B-25. Combined Effect of Changes in SIDRA for Single-Lane Roundabouts

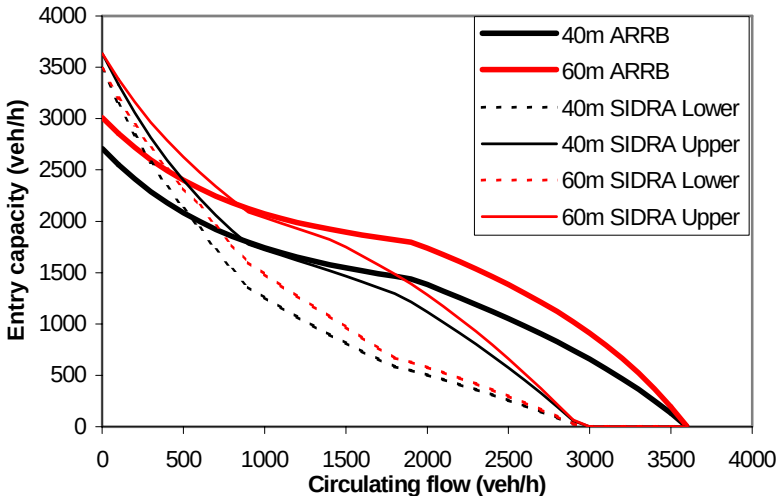

Figure B-26. Combined Effect of Changes in SIDRA for Double-Lane Roundabouts

The Limited Priority Process

The limited priority process has been found to improve the capacity estimates significantly. This section describes the limited priority approach.

Assumptions. Troutbeck *(B54)* states the assumptions of the limited priority process are as follows.

- The opportunity for minor-stream drivers is defined as the time the last major-stream vehicle departed until the next major-stream vehicle is expected to arrive.
- The minor-stream drivers will accept an opportunity that is greater than the critical gap, t_c.
- A number of minor-stream drivers will accept an opportunity if it is long. The headway between these minor-stream vehicles is the follow-up time, t_f.
- The minor-stream drivers are assumed to be both consistent and homogeneous.
- After the merge, each minor-stream vehicle will have a headway of t_f to the vehicle in front. Similarly, each major-stream vehicle will have a headway of τ to a minor-stream vehicle in front.
- If an opportunity is not acceptable, less than t_a, then the headway between the major-stream vehicles will be at least ψ.
- The major-stream drivers will have a headway distribution, upstream of the merge, given by Cowan's M3 headway distribution *(B56)*.
- Major-stream headways will maintain a minimum headway specified by Cowan's M3 distribution.
- The critical gap, t_c, is less than the $t_f + \tau$.

Using these assumptions a generalized equation for the capacity is developed.

Description of the Process. A minor-stream driver contemplating entering the intersection will review the opportunity to enter. This will require drivers looking upstream at the expected arrival time of the next major-stream vehicle and comparing this time with the departure time of the last major-stream vehicle. Figure B-27 illustrates the time of passage of major-stream vehicles upstream. This time and expected speeds enable the minor-stream vehicles to predict the arrival times of the major-stream vehicles. This is shown as the oblique arrows on

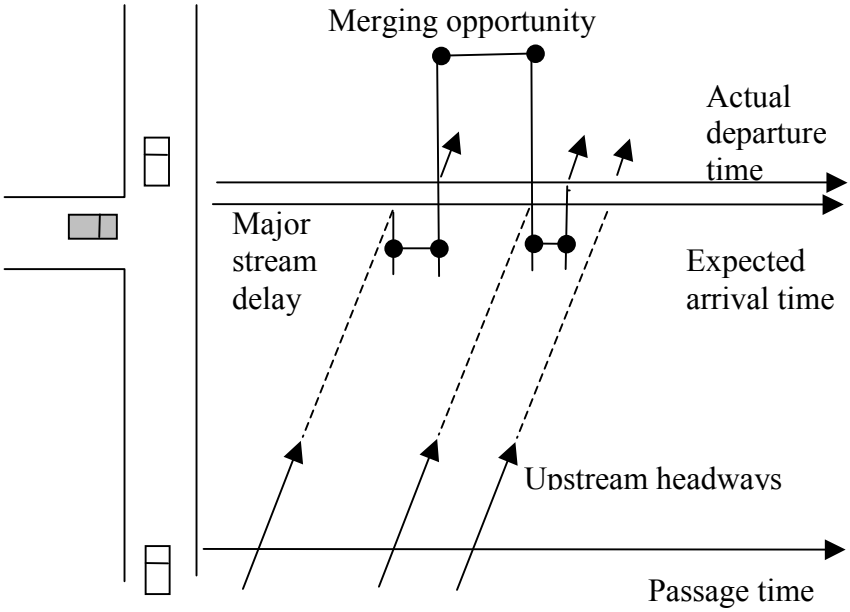

Figure B-27. Definition of the "Merging Opportunity"

the lower part of the figure. However, in fact the driver is delayed slightly by either major stream vehicles ahead or by minor-stream drivers entering. The opportunity for merging is the difference between expected time of arrival of the major-stream vehicle and the departure of the previous major-stream vehicle.

The delay to the next major-stream is dependent on the duration of the merging opportunity, whether the opportunity allows a minor-stream vehicle to merge and the relative headway between the major-stream vehicles. Troutbeck *(B53, B54)* has provided the following equations for the delay to the major-stream vehicles and the capacity of the merge.

This approach gives the following equation for capacity as:

$$\text{Capacity} = \frac{\alpha q C \cdot \exp\left[-\lambda(t_c - \psi)\right]}{1 - \exp(-\lambda t_f)} \qquad \text{(B-29)}$$

where:

$$C = \frac{\exp(\lambda t_f) - 1}{\lambda\beta \cdot \exp\left[\lambda(\beta - \tau + \psi)\right] + \exp(\lambda t_f) - 1 + \exp\left[\lambda(\psi - \tau)\right] - \exp\left[\lambda(\beta - \tau + \psi)\right]}$$

β = $t_f + \tau - t_c$

ψ = the minimum headway between the major-stream vehicles upstream.

α = the proportion of non-bunched vehicles in the major-stream upstream

t_c = the critical gap

t_f = the follow-up time or headway and the headway in front of the minor-stream vehicles after the merge.

τ = the headway in-front of the major-stream vehicles after the merge.

q = the circulating flow

λ = given by Equation B-23

The average delay to major-stream vehicles when the merge is at capacity is:

$$d_{1,1} = \frac{0.5\ \lambda\beta^2 \cdot \exp[\lambda(\beta-\tau+\psi)]}{\lambda\beta \cdot \exp[\lambda(\beta-\tau+\psi)] + \exp(\lambda t_f) - 1 + \exp[\lambda(\psi-\tau)] - \exp[\lambda(\beta-\tau+\psi)]} \quad \text{(B-30)}$$

When Does Limited Priority Occur? Limited priority merging occurs when the relative speeds between vehicles are slow and drivers are confident that the consequences of drivers not slowing are insignificant. Troutbeck and Kako *(B6)* have reported the limited priority effect at roundabouts in Australia. They collected headway data for circulating vehicles just before and just after the merge area and found that the opportunities in which a minor-stream vehicle had entered had generally increased in size. This found that the circulating drivers were prepared to slow and to accommodate a minor-stream vehicle. Figure B-28 from Kako and Troutbeck illustrates this point. The statistics of the distribution of the differences between the passage times of major stream vehicles are shown in Table B-2 and demonstrate that the means are significantly different from zero.

Troutbeck *(B61)* investigated the critical gaps used by heavy vehicles and those used by cars. The result was that the drivers of cars and trucks had longer average critical gaps when accepting a gap terminated by a truck rather than a car (Table B-3). The drivers were less inclined to assume that the truck drivers in the major stream would slow. This behavior is consistent with the limited priority behavior. Troutbeck *(B61)* recorded the behavior at a roundabout.

Roundabout studies and their discussion (for instance *B27*, *B46*) have identified a unique issue with heavily trafficked roundabouts. Drivers' critical acceptance gaps are only marginally greater than their follow-up times. This again is a demonstration of limited priority behavior.

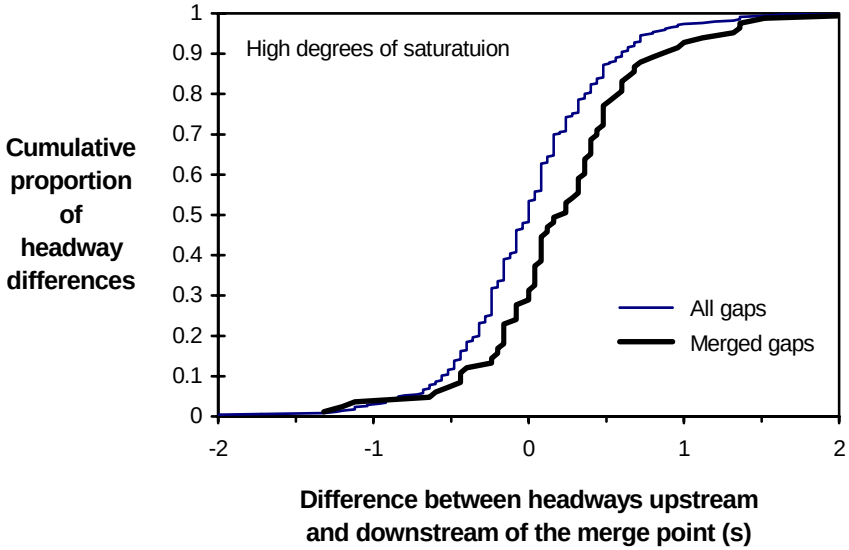

SOURCE: *(B63)*

Figure B-28. Cumulative Difference Between the Times of Passage of Major Stream Vehicles at a Roundabout

TABLE B-2. Statistics of the Differences Between Major Stream Vehicles Before and After the Merge (Downstream - Upstream)

Data-set		Sample size	Mean [s]	Standard deviation [s]	t-value
Low saturation period	Site A	67	- 0.02	0.56	- 0.29
	Site B	63	- 0.08	0.39	- 1.63
	Site C	63	- 0.01	0.62	- 0.13
High saturation period	Site A	76	0.24	0.59	3.55
	Site B	66	0.17	0.48	2.88
	Site C	83	0.23	0.58	3.61

SOURCE: (B54)

TABLE B-3. Critical Acceptance Gaps

Entering vehicle type	Cars	Heavy vehicles
Accepted gaps terminated by a car	5.37	5.37
Accepted gaps terminated by a heavy vehicle	6.60	7.36

SOURCE: (B61)

What Are the Implications? The implication of the limited priority process is that the delays are reduced. The merge system is more efficient with more vehicles using the merge area more effectively. Looking at Equation B-29, it would appear that the capacity is reduced, as the *C* term is less than 1. However, this must be read with the fact that the critical acceptance gap is also reduced. If short critical gap values were used in the more traditional absolute priority system, then the headways after the merge would be similarly short and unrealistic.

If the limited priority process is applied to the results from Austroads *(B47)* then for a 60 m diameter roundabout with 4 m entry lanes, the capacity – circulating flow relationship is very similar to other relationships worldwide. The Austroads approach was based on absolute priority and did not include the limited priority process. The SIDRA 5 *(B62)* curve uses absolute priority relationships but adjusts the variables in the model to provide the relationship shown here. The parameter values used in SIDRA 5 have been chosen arbitrarily and this work provides an increased understanding and demonstrates that the parameters need not be altered to achieve the same end. The effect of the limited priority process is shown in Figure B-29. The average delays to the circulating stream were modest.

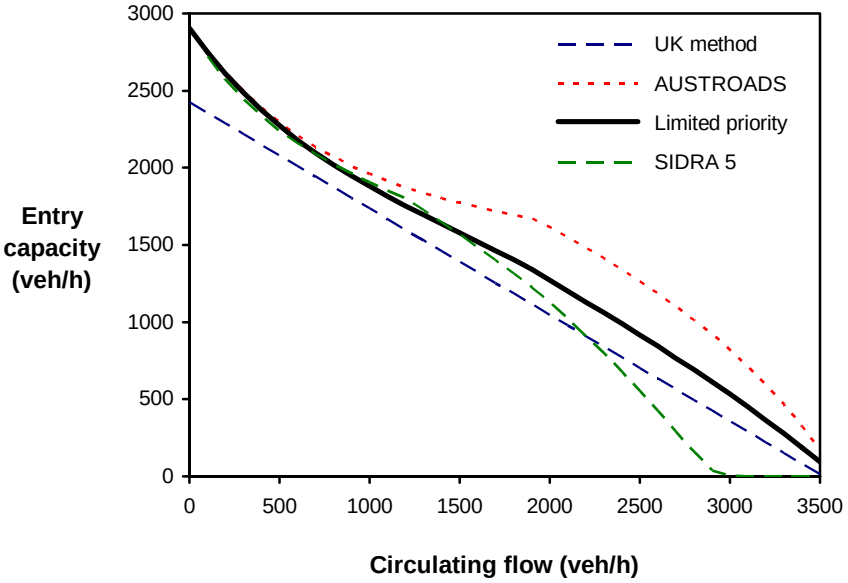

Figure B-29. Entry Capacity Against the Circulating Flow for a 60-m Diameter Roundabout with Two 4-m Entry Lanes and Two Circulatory Lanes

The implications of the merge are complicated. In using the approach given here, it is assumed that the headway between the major-stream vehicles can be shortened to ψ if the major-stream vehicles are delayed. The headways after the merge between the major-stream vehicles may not be able to close to ψ as assumed. An estimate of changing the value of ψ to ψ' and by keeping all other attributes the same can be found by using an assumed distribution as specified in Troutbeck and Kako *(B63)*. Here the minimum headway has been changed and the proportion of free vehicles adjusted to compensate. The relationship between the assumed proportion of free vehicles, α', and the recorded proportion of free vehicles α is given by the equation:

$$\alpha' = \alpha \cdot \exp\left[\lambda(\psi' - \psi)\right] \tag{B-31}$$

The capacity is then given by:

$$\text{Capacity} = \frac{\alpha' q\, C \cdot \exp\left[-\lambda(t_c - \psi')\right]}{1 - \exp(-\lambda t_f)} \tag{B-32}$$

$$\text{where: } C = \frac{\exp(\lambda t_f) - 1}{\lambda\beta \cdot \exp\left[\lambda(\beta - \tau + \psi')\right] + \exp(\lambda t_f) - 1 + \exp\left[\lambda(\psi' - \tau)\right] - \exp\left[\lambda(\beta - \tau + \psi')\right]} \tag{B-33}$$

and β has the same definition as before. If Equations B-31 and B-32 are used with the condition that ψ' is equal to τ, then this will give an estimate of the maximum average delay to the major

stream vehicles. Figure B-30 illustrates the effect and indicates that this approximation gives a similar curve shape but with slightly lower capacities.

Concluding Remarks. The limited priority process has been demonstrated to exist at roundabouts. The consequences of the process are larger capacities and reduced delays. Using the limited priority assumption, the equations for the capacity and the average delay to the circulating stream vehicles have been developed for a range of generalized conditions. The headways of major-stream vehicles approaching the merge are assumed to have a Cowan distribution. The minor-stream drivers are assumed to accept any gap greater than the critical gap and to enter into the larger merging opportunities with headways equal to the follow-on time. The headway between a major-stream vehicle and a merging vehicle is assumed to be τ. These conditions will cause the major-stream vehicles to be delayed up to $t_f + \tau - t_c$, with the average delay to the major-stream vehicles being considerably less.

Conclusions

Australia has had a long history of use gap acceptance techniques. When the Austroads Guide for roundabouts was produced it is understandable that a gap acceptance approach was favored. This paper describes the processes and discussion used to identify if there were any issues in using a gap acceptance approach rather than the regression approach before the roundabout study was conducted. The outcome was that the there were no significant issues to preclude the use of the gap acceptance technique.

The ARRB study was founded on empirical evidence. The data have been shown here in a graphical form. The ARRB study was not as extensive as the UK study, but there were few options to either increase the size of the study or to use more heavily congested roundabouts.

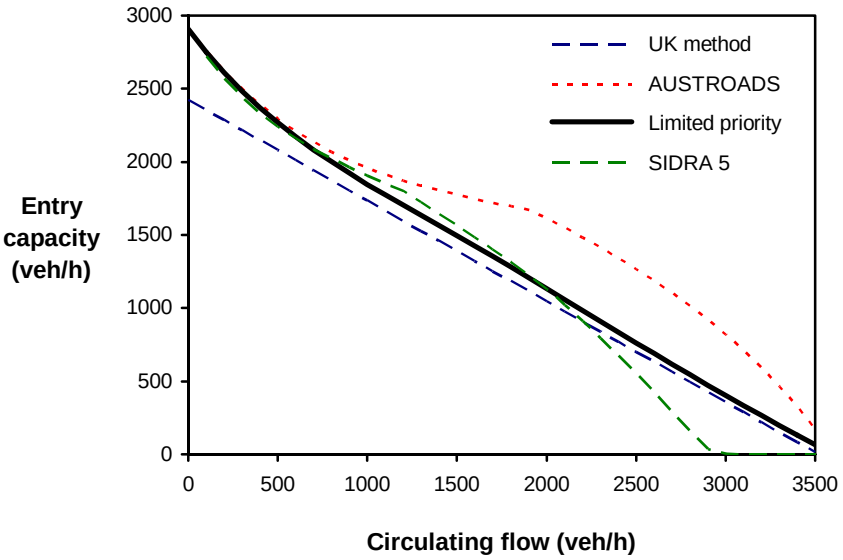

SOURCE: *(B63)*

Figure B-30. Entry Capacity against the Circulating Flow for a 60-m Diameter Roundabout with Two 4-m Entry Lanes and Two Circulatory Lanes and Using an Assumed Headway Distribution with ψ' equal to τ

The ARRB study used only absolute priority queuing systems. For higher circulating flows the critical gap is not much larger that the follow-on time and the use of these absolute priority models is not appropriate as it causes an overestimation of capacity.

SIDRA has a strong use and reputation in Australia and uses the ARRB roundabout study for the fundamentals of roundabout analysis. However, SIDRA has had a number of changes to account for the overestimation of capacity. The changes to the model were developed from a simulation model and with professional judgment by Akçelik. The consequences of the changes have been discussed here. Finally, the concept of a limited priority process has been discussed and shown to produce an improvement in the estimation of the capacity, particularly at the higher circulating flows.

References

B1. Tanner, J. C. A theoretical analysis of delays at an uncontrolled intersection. In *Biometrica*, No. 49, 1962, pp. 163–170.

B2. Harders, J. Die Leistungsfaehigkeit nicht signalgeregelter staedtischer Verkehrsknoten (The capacity of unsignalized urban intersections). *Schriftenreihe Strassenbau und Strassenverkehrstechnik*, Vol. 76, 1968.

B3. *Highway Capacity Manual*. TRB, National Research Council, Washington, DC, 2000.

B4. Kyte, M.; Z. Tian, Z. Mir, Z. Hameedmansoor, W. Kittelson, M. Vandehey, B. Robinson, W. Brilon, L. Bondzio, N. Wu, and R. J. Troutbeck. *NCHRP Web Document 5: Capacity and Level of Service at Unsignalized Intersections: Final Report Volume 1: Two-Way Stop Controlled Intersections.* TRB, National Research Council, Washington, DC, 1996.

B5. Brilon, W., R. Koenig, and R. J. Troutbeck. Useful Estimation Procedures for Critical Gaps. *Proc., Third International Symposium on Intersections Without Traffic Signals,* Portland, Oregon, TRB, National Research Council, Washington DC, July 1997, pp. 71–87.

B6. Troutbeck, R. J., and S. Kako. Limited Priority Merge at Unsignalized Intersections. *Proc., Third International Symposium on Intersections Without Traffic Signals* (M. Kyte, ed.), Portland, Oregon, TRB, National Research Council, Washington DC, July 1997.

B7. Robinson, B. W., L. Rodegerdts, W. Scarbrough, W. Kittelson, R. Troutbeck, W. Brilon, L. Bondzio, K. Courage, M. Kyte, J. Mason, A. Flannery, E. Myers, J. Bunker, and G. Jacquemart. *Roundabouts: An Informational Guide*. Report FHWA-RD-00-067. FHWA, U. S. Department of Transportation, June 2000.

B8. Brilon, W., N. Wu, and L. Bondzio. Unsignalized Intersections in Germany—a State of the Art 1997. *Proc., Third International Symposium on Intersections Without Traffic Signals* (M. Kyte, ed.), Portland, Oregon, TRB, National Research Council, Washington DC, July 1997.

B9. Kimber, R. M. *The Traffic Capacity of Roundabouts*. Laboratory Report LR 942. Transport and Road Research Laboratory, Crowthorne, Berkshire, United Kingdom, 1980.

B10. Troutbeck, R. J. Background for HCM Section on Analysis of Performance of Roundabouts. *Transportation Research Record 1646*, Transportation Research Board, National Research Council, Washington, DC, 1998, pp. 54–62.

B11. Binning, J. C. *ARCADY 5 (International) User Guide.* Application Guide AG 37. TRL Limited, Crowthorne, Berkshire, United Kingdom, 2000.

B12. Rodel Software Ltd and Staffordshire County Council. *RODEL*. Staffordshire County Council, Cheadle, Stoke-on-Trent, United Kingdom, 2002.

B13. Akçelik, R., E. Chung, and M. Besley. *Roundabouts: Capacity and Performance Analysis*. Research Report ARR No. 321, 2nd ed. ARRB Transport Research Ltd, Australia, 1999.

B14. Akcelik and Associates Pty Ltd. *aaSIDRA*. Greythorn, Victoria, Australia, 1999–2004.

B15. FGSV. *Handbuch für die Bemessung von Straßenverkehrsanlagen (German Highway Capacity Manual).* Forschungsgesellschaft für Straßen- und Verkehrswesen (Hrsg.), No. 299. FGSV Verlag GmbH, Köln, Germany (2001).

B16. Wu. N. A Universal Procedure for Capacity Determination at Unsignalized (priority-controlled) Intersections. *Transportation Research B*, No. 35, Issue 3. Elsevier Science Ltd., New York, Tokyo, Oxford, 2001.

B17. Louah, G. Panorama Critique des Modeles Francais de Capacite des Carrefours Giratoires. *Proc., Roundabouts 92,* Nantes, France, October 1992. SETRA, Bagneux, France, February 1993.

B18. Bovy, H., K. Dietrich, and A. Harmann. *Guide Suisse des Giratoires.* Lausanne, Switzerland, February 1991, p. 75 (cf. summary: *Straße und Verkehr (Road and traffic)* No. 3, p. 137–139, March 1991).

B19. Kremser, H. Wartezeiten und Warteschlangen bei Einfaedelung eines Poissonprozesses in einen anderen solchen Prozess (Delays and queues with one poisson process merging into another one). *Oesterreichisches Ingenieur-Archiv*, Vol. 18, 1964.

B20. Brilon, W. Recent developments in calculation methods for unsignalized intersections in West Germany. *Intersections without Traffic Signals* (W. Brilon, ed.), Springer-Verlag, Berlin, Germany, 1988.

B21. Yeo, G. F. Single-server queues with modified service mechanisms. *Journal Australia Mathematics Society,* Vol. 2, 1962, pp. 499–502.

B22. Kimber, R. M., and E. M. Hollis. Traffic queues and delays at road junctions. Laboratory Report LR 909. Transport and Road Research Laboratory, Crowthorne, Berkshire, United Kingdom, 1979.

B23. Akçelik, R., and R. J. Troutbeck. Implementation of the Australian roundabout analysis method in SIDRA. *Highway Capacity and Level of Service: Proceedings of the International Symposium on Highway Capacity* (U. Brannolte, ed.), Karlsruhe, Germany, 1991, Balkema Publisher, Rotterdam, Netherlands, 1991, pp. 17–34.

B24. Wu, N. An Approximation for the Distribution of Queue Lengths at Unsignalized Intersections. *Proc., 2nd International Symposium on Highway Capacity* (R. Akçelik, ed.), Vol. 2, Sydney, Australia, Vol. 2, Australian Road Research Board, 1994.

B25. Stuwe, B. (formerly Hartz, B.) Untersuchung der Leistungsfähigkeit und Verkehrssicherheit an deutschen Kreisverkehrsplätzen. Schriftenreihe des lehrstuhls für Verkehrswesen der Ruhr-universität Bochum, Heft 10, Ruhr-University Bochum, Bochum, Germany, 1992.

B26. Marlow, M., and G. Maycock. *The effect of zebra crossing on junction entry capacities*. Special Report SR 724. Transport and Road Research Laboratory, Crowthorne, Berkshire, United Kingdom, 1982.

B27. Brilon, W., B. Stuwe, and O. Drews. *Sicherheit und Leistungsfaehigkeit von Kreisverkehrsplaetzen (Safety and capacity of roundabouts)*. Research Report. Ruhr-University Bochum, Bochum, Germany, 1993.

B28. Griffiths, J. D. A mathematical model of a non signalized pedestrian crossing. *Transportation Science*, Vol. 15, No. 3, Sept. 1981, pp. 223–232.

B29. Horman, C. H., and H. H. Turnbull. Design and analysis of roundabouts. *Proc., 7th ARRB Conf.*, 7(4), 1974, pp. 58–82.

B30. Avent, A. D., and R. A. Taylor. Roundabouts—Aspects of their design and operations. Institution of Eng. Aust. (Qld Div. tech. papers), Vol. 20(7), July 1979.

B31. Troutbeck, R. J. Overseas Trip Report—August, September 1983. Internal Report AIR 393-3, Australian Road Research Board, December 1983.

B32. Ashworth, R., and C. J. D. Laurence. *Capacity of rotary intersections phase III and IV*. Department of Civil and Structural Engineering, University of Sheffield, United Kingdom, 1977.

B33. Semmens, M. C. *ARCADY2: An enhanced program to model capacities, queues and delays at roundabouts*. Research Report 35. Transport and Road Research Laboratory, Crowthorne, Berkshire, United Kingdom, 1985.

B34. National Association of Australian State Road Authorities (NAASRA). *Interim guide for the design of intersections at grade*. NAASRA, Sydney, Australia, 1979.

B35. National Association of Australian State Road Authorities (NAASRA). *Roundabouts – A guide to application and design*. NAASRA, Sydney, Australia, 1982.

B36. Vits, A., and J. de Wijngaert. Comparison of some results obtained by using different methods to evaluate the capacity of priority junctions. PTRC meeting, 1983.

B37. Troutbeck, R. J. Capacity and Delays at roundabouts—A Literature Review. Australian Road Research Board 14(4), Dec. 1984, pp. 205–216.

B38. Ashworth, R., and C. J. D. Laurence. A new procedure for capacity calculations at conventional roundabouts. *Proc., Institute of Civil Engineers*, Part 2, Vol. 65, March 1978, pp. 1–16.

B39. Ashworth, R., and C. J. D. Laurence. Methods of estimating capacity at offside priority roundabouts. *Proc., Symposium on Identification and Control of Road Traffic*, Technical University of Krakow, Poland, Sept. 13–15, 1979.

B40. Laurence, C. J. D., and R. Ashworth. Roundabout capacity prediction—a review of recent developments. Presented at PTRC Summer Annual Meeting, Seminar J, July 11, 1979.

B41. McDonald, M. *Analytical methods of traffic at road junctions and on inter-urban transport networks*. Unpublished PhD thesis, University of Southampton, United Kingdom, 1981.

B42. Kimber, R., and M. Semmens. A track experiment on the entry capacities of offside priority roundabouts. Supplementary Report SR334. Transport and Road Research Laboratory, Crowthorne, Berkshire, United Kingdom, 1977.

B43. Semmens, M. The capacity of some grade separated roundabout entries. Supplementary Report SR721. Transport and Road Research Laboratory, Crowthorne, Berkshire, United Kingdom, 1982.

B44. Troutbeck, R. J. Does gap acceptance theory adequately predict the capacity of a roundabout? *Proc., 12th ARRB Conf.*, 12(4), 1984, pp. 62–75.

B45. Troutbeck, R. J. The use of different approaches to predict the capacity of a single lane roundabout. Internal Report AIR 393-5. Australian Road Research Board, 1984.

B46. Troutbeck, R. J. Evaluating the performance of a roundabout. *Special Report 45*, Australian Road Research Board, 1989.

B47. AustRoads. *Guide to Traffic Engineering Practice Part 6—Roundabouts*. AustRoads, Sydney, Australia, 1993.

B48. Troutbeck, R. J., and J. S. Dods. Collecting Traffic Data Using the ARRB Video Analysis Data Acquisition System. *Proc., 13th ARRB/5THREAAA Conf.*, July 13, 1986, pp. 183–195.

B49. Miller, A. J. and R. L. Pretty. Overtaking on two-lane rural roads. *Proc., 4th ARRB Conf.*, 4(1), 1968, pp. 583–594.

B50. Troutbeck, R. J., N. Szwed, and A. J. Miller. Overtaking sight distances on a two-lane rural road. *Proc., 6th ARRB Conf.*, Australian Road Research Board, 6(3), 1972, pp. 286–301.

B51. Troutbeck, R. J. Overtaking behaviour on Australian two lane rural highways. Special Report SR 20. Australian Road Research Board, 1981.

B52. Troutbeck, R. J. Current and future Australian practices for the design of unsignalised intersections. *Intersections without Traffic Signals* (W. Brilon, ed.), Springer-Verlag, Berlin, Germany, 1988, pp. 1–19.

B53. Troutbeck, R. J. The Capacity of a Limited Priority Merge. *Transportation Research Record: Journal of the Transportation Research Board, No. 1678,* TRB, National Research Council, Washington, DC, 1999, pp 269–276.

B54. Troutbeck, R. J. The performance of uncontrolled merges using a limited priority process. *Transportation and Traffic Theory in the 21st Century: Proceedings of the Fifteenth International Symposium on Transportation and Traffic Theory* (Pergamon M Taylor, ed.), Adelaide, Japan, 2002, pp. 463–482.

B55. Troutbeck, R. J. Intersections, roundabouts and minis. *Proc., 26th ARRB Regional Symposium*, Bunbury, Australia, March 1988, pp. 45–65.

B56. Cowan, R. J. Useful headway models. *Transportation Research,* Vol. 9, No. 6, 1975, pp. 371–375.

B57. Troutbeck, R. J. Average Delay at an unsignalised intersection with two major streams each having a dichotomised headway distribution. *Transportation Science*, Vol. 20, No. 4, 1986, pp. 272–286.

B58. National Association of Australian State Road Authorities (NAASRA). *Roundabouts—A Design Guide*. NAASRA, Sydney, New South Wales, Australia, 1986.

B59. Troutbeck, R. J. A review of the process to estimate the Cowan M3 Headway distribution parameters. *Traffic Engineering and Control*, Vol. 38, No. 11, Nov. 1997, pp. 600–603.

B60. Luttinen. R. T. Properties of Cowan's M3 Headway Distribution. *Transportation Research Record: Journal of the Transportation Research Board, No. 1768.* TRB, National Research Council, Washington, DC, 1999, pp. 189–196.

B61. Troutbeck, R. J. The capacity and design of roundabouts in Australia. *Transportation Research Record 1398.* TRB, National Research Council, Washington, DC, 1993.

B62. Akcelik, R., and M. Besley. *SIDRA 5: User Guide*. ARRB Transport Research, Vermont South, Victoria, Australia, 1996.

B63. Troutbeck, R. J., and S. Kako. Limited priority merge at unsignalised intersections. *Transportation Research A*, Vol. 33A (3/4), 1999, pp 291–304.

APPENDIX C
SITE INVENTORY

TABLE C-1. Master Site Inventory

Site ID	State	City	County/ Borough	Intersection	Setting	No. of Legs	No. of Lanes
AK01	AK	Anchorage	Anchorage	Southport Dr/Maritime Loop/Washington Ave	Urban	4	1
AR01	AR	Little Rock	Pulaski	36th St/Romine Road/West Road	Urban	4	1
AZ01	AZ	Phoenix	Maricopa	I-17 NB Ramps/Happy Valley Road	Suburban	4	2
AZ02	AZ	Phoenix	Maricopa	I-17 SB Ramps/Happy Valley Road	Suburban	4	2
CA01	CA	Arcata	Humboldt	Samoa Blvd/Buttermilk Ln	Urban	4	1
CA02	CA	Arcata	Humboldt	Samoa Blvd/Union St	Urban	4	1
CA03	CA	Arcata	Humboldt	West End Rd/Spear Ave/St. Louis Rd	Urban	3	1
CA04	CA	Calabasas	Los Angeles	Parkway Calabasas/Camino Portal	Suburban	4	1
CA05	CA	Davis	Yolo	5th St/Cantrill Dr	Urban	3	1
CA06	CA	Davis	Yolo	Anderson Rd/Alvarado Ave	Urban	4	1
CA07	CA	Davis	Yolo	Moore Blvd/Rockwell Dr	Urban	3	1
CA08	CA	Davis	Yolo	Moore Blvd/Wright Blvd	Urban	3	1
CA09	CA	Davis	Yolo	Shasta Dr./Olympic Pl.	Urban	3	1
CA10	CA	Long Beach	Los Angeles	Hwy 1/Hwy 19/Los Coyotes Diagonal	Urban	4	3
CA11	CA	Modesto	Stanislaus	La Loma/James St./G St.	Urban	5	1
CA12	CA	Modesto	Stanislaus	Chandon Dr./Calero Dr.	Suburban	4	1
CA13	CA	Modesto	Stanislaus	Bowen Ave./Fremont Ave.	Suburban	4	1
CA14	CA	Modesto	Stanislaus	Bowen Ave./Phelps Ave.	Suburban	3	1
CA15	CA	Modesto	Stanislaus	Lifescapes Dr./Grecian Ave.	Suburban	3	1
CA16	CA	Santa Barbara	Santa Barbara	Alameda/Montecito/Salinas/Syc Cyn (5 pts Intx)	Urban	5	1
CA17	CA	Santa Barbara	Santa Barbara	Milpas St/US 101 NB Ramps/Carpinteria St	Urban	5	2
CA18	CA	Truckee	Nevada	Donner Pass Rd/ I-80 Ramps	Urban	3	1
CA19	CA	Woodland	Yolo	Gum Ave/Bourn Dr	Urban	4	1
CA20	CA	Sacramento	Sacramento	San Juan Rd/Azevedo Dr	Suburban	4	1
CA21	CA	Modesto	Stanislaus	Sylvan Ave/Roselle Ave	Suburban	4	1
CA22	CA	Modesto	Stanislaus	E Orangeburg Ave/Rose Ave	Suburban	4	1
CA23	CA	Modesto	Stanislaus	W Rumble Rd/Carver Rd	Urban	4	1
CO01	CO	Eagle	Eagle	SH-6/I-70 spur/Eby Creek Rd	Rural	4	1
CO02	CO	Golden	Jefferson	South Golden Road/Johnson Rd/16th Street	Urban	4	2
CO03	CO	Golden	Jefferson	South Golden Road/Utah St.	Urban	4	2
CO04	CO	Aspen	Pitkin	SH 82/Maroon Crk/Castle Crk	Suburban	4	2
CO05	CO	Aurora	Arapahoe	Lowry Blvd/Fremont Dr./Rampart Way	Suburban	4	2
CO06	CO	Avon	Eagle	Avon Rd./Beaver Creek Blvd.	Urban	4	3
CO07	CO	Avon	Eagle	Avon Rd./Benchmark Road	Urban	4	2
CO08	CO	Avon	Eagle	Avon Rd./I-70 Eastbound Ramp	Urban	4	2
CO09	CO	Avon	Eagle	Avon Rd./I-70 Westbound Ramp	Urban	4	2
CO10	CO	Avon	Eagle	Avon Rd./U.S. Hwy 6	Urban	4	2
CO11	CO	Bayfield	La Plata	CR 501/Bayfield Center Dr	Suburban	3	1
CO12	CO	Boulder	Boulder	Arapahoe Ave/4th St	Suburban	3	1
CO13	CO	Boulder	Boulder	Arapahoe Ave/5th St	Suburban	3	1
CO14	CO	Boulder	Boulder	Balsam Ave/14th St	Urban	4	1
CO15	CO	Boulder	Boulder	Balsam Ave/15th St	Urban	4	1
CO16	CO	Boulder	Boulder	Evergreen Ave/9th St	Urban	4	1

Site ID	State	City	County/ Borough	Intersection	Setting	No. of Legs	No. of Lanes
CO17	CO	Boulder	Boulder	Kings Ridge Blvd/Edison Ave	Urban	3	1
CO18	CO	Boulder	Boulder	Kings Ridge Blvd/Franklin Drive	Urban	4	1
CO19	CO	Boulder	Boulder	Maxwell Ave/6th St	Urban	4	1
CO20	CO	Boulder	Boulder	Pearl Street/4th St	Suburban	4	1
CO21	CO	Boulder	Boulder	Pearl Street/Mid-Block	Suburban	2	1
CO22	CO	Boulder	Boulder	Pine St/15th St	Suburban	4	1
CO23	CO	Boulder	Boulder	Pine St/17th St	Suburban	4	1
CO24	CO	Boulder	Boulder	St Johns Ave/New Haven Ct, Hamton Circle	Suburban	4	1
CO25	CO	Colorado Springs	El Paso	Beech Ave/1st St	Suburban	4	1
CO26	CO	Colorado Springs	El Paso	Chapel Hills Dr./Divot Trl	Suburban	3	2
CO27	CO	Colorado Springs	El Paso	Chapel Hills Dr./Graycroft	Suburban	4	2
CO28	CO	Colorado Springs	El Paso	E.Cheyanne Mountain Blvd/Springmeadow Dr	Suburban	4	
CO29	CO	Colorado Springs	El Paso	Lake Avenue/Lake Circle	Suburban	4	1
CO30	CO	Colorado Springs	El Paso	Lake Avenue/Berthie Circle	Suburban	4	1
CO31	CO	Colorado Springs	El Paso	Lake Avenue/Old Broadmoor Rd.	Suburban	4	1
CO32	CO	Denver	Denver	Lowry Blvd/Unita Way	Urban	3	1
CO33	CO	Denver	Denver	Lowry Blvd/Yosemite St	Suburban	3	2
CO34	CO	Denver	Denver	Unita Way/6th Ave.		3	1
CO35	CO	Frisco	Summit	I-70 Ramps N/SH 9	Suburban	5	1
CO36	CO	Golden	Jefferson	Jefferson County Parkway/Civic Center	Urban	4	1
CO37	CO	Golden	Jefferson	South Golden Road/ Lunnanhaus	Urban	4	2
CO38	CO	Golden	Jefferson	South Golden Road/ Ulysses St.	Urban	4	1
CO39	CO	Grand Junction	Mesa	Horizon Drive/12th	Suburban	4	1
CO40	CO	Lakewood	Jefferson	Allison Parkway/Civic Center	Urban	5	1
CO41	CO	Lakewood	Jefferson	S. Allison Parkway/W. Virginia Ave.	Urban	5	1
CO42	CO	Loveland	Larimer	Rocky Mountain Ave/Fox Trail	Urban	4	2
CO43	CO	Loveland	Larimer	Rocky Mountain Ave/McWinney	Urban	4	2
CO44	CO	Nederland	Boulder	SH 72/ SH-119, SH 72, 2nd, Bridge	Urban	5	1
CO45	CO	New Castle	Garfield	Castle Valley Blvd/Pyramid St.	Suburban	3	1
CO46	CO	New Castle	Garfield	Castle Valley Blvd/TBD	Suburban	2	1
CO47	CO	Northglenn	Adams	Melody/Kennedy	Suburban	4	2
CO48	CO	Superior	Boulder	5th Ave./Center Drive	Suburban	4	2
CO49	CO	Vail	Eagle	Chamonix Rd/I-70 EB Ramps/South Frontage Rd	Suburban	6	2
CO50	CO	Vail	Eagle	Chamonix Rd/I-70 WB Ramps/North Frontage Rd	Suburban	5	2
CO51	CO	Vail	Eagle	Vail Rd/I-70 EB Ramps/South Frontage Rd	Suburban	6	3
CO52	CO	Vail	Eagle	Vail Rd/I-70 WB Ramps/North Frontage Rd/Spraddle Cr. Rd	Suburban	5	2
CO53	CO	Westminster	Adams	Promenade Dr South/Mid-Block	Suburban	2	1
CT01	CT	Killingworth	Middlesex	Rte 80/Rte 81	Rural	4	1
CT02	CT	New London	New London	Pequot Ave/Willets Ave/Shaw St/Howard St	Urban	4	1
CT03	CT	Willimantic	Tolland	Eastern Rd/unnamed driveway (ECSU campus)	Suburban	3	1
CT04	CT	North Stonington	New London	Rte 2/Rte 184	Urban	4	1
FL01	FL	Amelia Island	Nassau	SR AIA/Amelia Island Plantation	Suburban	4	1
FL02	FL	Boca Raton	Palm Beach	Cain Blvd/Boca Raton Dr	Suburban	4	1

Site ID	State	City	County/ Borough	Intersection	Setting	No. of Legs	No. of Lanes
FL03	FL	Boca Raton	Palm Beach	SW 12th Ave/SW 18th St	Urban	4	1
FL04	FL	Boynton Beach	Palm Beach	Hagen Ranch Rd/Charleston Shores Blvd	Suburban	4	1
FL05	FL	Boynton Beach	Palm Beach	Hagen Ranch Rd/Gateway Blvd	Suburban	4	2
FL06	FL	Boynton Beach	Palm Beach	Hagen Ranch Rd/Le Chalet Blvd	Suburban	4	1
FL07	FL	Boynton Beach	Palm Beach	Lake Ida Rd/Via Flora Dr	Suburban	4	1
FL08	FL	Boynton Beach	Palm Beach	Hagen Ranch Rd/Livomo St.	Suburban	4	1
FL09	FL	Bradenton Beach	Manatee	SR 789/Bridge St	Suburban	3	1
FL10	FL	Clearwater Beach	Pinellas	Acacia/Mandalay Ave.	Urban	4	1
FL11	FL	Clearwater Beach	Pinellas	SR 60 (Memorial Causeway)/Coronado Dr (SR 699)/Mandalay Ave/Poinsettia Ave (Gateway Roundabout)	Urban	5	2
FL12	FL	Coral Gables	Miami-Dade	Sunset Dr (SW 72nd St)/Lejune Rd (SW 42nd Ave)/Cocoplum Rd	Urban	4	1
FL13	FL	Fort Pierce	St. Lucie	Ave. A/N. Indian River Dr.	Urban	4	1
FL14	FL	Ft. Walton Beach	Okaloosa	Hollywood Blvd/Doolittle Blvd	Urban	3	1
FL15	FL	Gainesville	Alachua	SE 7th Street/SE 4th Avenue	Urban	4	1
FL16	FL	Lake Worth	Palm Beach	Lakeworth Ave (SR 802)/South A Street	Urban	4	2
FL17	FL	Naples	Collier	7th St N/11th Ave N	Urban	4	1
FL18	FL	Naples	Collier	7th St N/12th Ave N	Urban	4	1
FL19	FL	Naples	Collier	7th St N/3rd Ave N	Urban	4	1
FL20	FL	Naples	Collier	7th St N/7th Ave N	Urban	4	1
FL21	FL	Naples	Collier	8th St S/12th Ave S	Urban	4	1
FL22	FL	Port St. Lucie	St. Lucie	SE Pine Valley St./SE Westmoreland	Suburban	4	1
FL23	FL	Stuart	Martin	Federal Hwy(US 1)/SR 76/SR A1A	Urban	4	1
FL24	FL	Stuart	Martin	N. Colorado Ave/E. Osceola St	Urban	4	1
FL25	FL	Tallahassee	Leon	Killarney Way/Shamrock Dr	Suburban	3	1
FL26	FL	Tallahassee	Leon	Sutor Rd/Old Sutor Rd	Suburban	3	1
FL27	FL	Tampa	Hillsborough	North Blvd/Country Club	Urban	4	1
FL28	FL	Tavares	Lake	Main St/Disston Ave/Lake Dora Dr/ Railroad Tracks	Urban	4	1
FL29	FL	Ybor City	Hillsborough	13th St/4th Ave	Urban	3	1
IN01	IN	Bloomington	Monroe	High St/Winslow Rd/Rogers Rd		4	1
IN02	IN	Carmel	Hamilton	Hazel Dell/126th St.	Urban	4	1
IN03	IN	Carmel	Hamilton	Hazel Dell/131st St.	Urban	4	1
IN04	IN	Fort Wayne	Allen	Adams Center/Marion Center Rd	Suburban	5	1
IN05	IN	Indianapolis	Marion	Monument Cir. (Market/Meridian)	Urban	4	2
KS01	KS	Olathe	Johnson	Sheridan St./Rogers Rd	Urban	4	2
KS02	KS	Hutchinson	Reno	23rd Ave./Severence St.	Urban	4	1
KS03	KS	Lawrence	Douglas	24th Place/Crossgate Dr	Suburban	3	1
KS04	KS	Lawrence	Douglas	24th Place/Inverness Dr	Suburban	4	1
KS05	KS	Lawrence	Douglas	Monterey Way/Harvard Rd	Suburban	3	1
KS06	KS	Lawrence	Douglas	Sunflower Park Pl./Inverness Dr.	Suburban	3	1
KS07	KS	Lawrence	Douglas	West Campus Rd/Jayhawk Blvd/Cresent Rd	Suburban	3	1
KS08	KS	Lenexa	Johnson	Montecello Rd/Prairie Star Parkway	Suburban	4	2
KS09	KS	Manhattan	Riley	Candlewood Dr/Gary Avenue	Suburban	4	1
KS10	KS	Manhattan	Riley	Kimball Ave/Grand Mere Parkway	Suburban	3	1
KS11	KS	Newton	Harvey	I-135 Ramps/Broadway St.	Suburban	4	1
KS12	KS	Newton	Harvey	I-135 Ramps/First St.	Suburban	4	1

Site ID	State	City	County/ Borough	Intersection	Setting	No. of Legs	No. of Lanes
KS13	KS	Olathe	Johnson	Sheridan St./Clairborne Rd.	Urban	4	1
KS14	KS	Olathe	Johnson	Sheridan St./Ridgeview Rd	Urban	4	1
KS15	KS	Overland Park	Johnson	110th St./Lamar Ave.	Suburban	4	2
KS16	KS	Paola	Miami	K-68/Old Kansas City Rd/Hedge Lane	Rural	5	1
KS17	KS	Topeka	Shawnee	I-70 EB Ramps/Rice Rd/Cyprus Dr	Urban	4	2
KS18	KS	Topeka	Shawnee	I-70 WB Ramps/Rice Rd/Sycamore Dr	Urban	4	2
KS19	KS	Topeka	Shawnee	SW 29th St/Urish Rd	Suburban	4	1
KS20	KS	Overland Park	Johnson	W 141st St/Bluejacket St	Suburban	4	1
MA01	MA	Duxbury	Plymouth	Lincoln St./Congress St.	Suburban	4	1
MD01	MD	Bel Air	Harford	Tollgate Rd./Marketplace Dr.	Suburban	3	1
MD02	MD	Leeds	Cecil	MD 213/Leeds Rd/Elk Mills Rd (Lanzi Circle)	Rural	4	1
MD03	MD	Jarrettsville (North Harford)	Harford	MD 24/MD 165	Rural	4	1
MD04	MD	(unincorporated)	Baltimore	MD 139 (Charles St.)/Bellona Ave	Urban	4	2
MD05	MD	Towson	Baltimore	MD 45/MD 146/Joppa Rd	Urban	5	2
MD06	MD	Lothian	Anne Arundel	MD 2/MD 408/MD 422	Rural	4	1
MD07	MD	Taneytown	Carroll	MD 140/MD 832/Antrim Blvd	Suburban	4	1
MD08	MD	Annapolis	Anne Arundel	MD 450/Spa Rd./Taylor Ave (Annapolis Gateway)	Urban	4	2
MD09	MD	Hanover	Anne Arundel	MD 295 NB Ramps/Arundel Mills Blvd	Suburban	4	
MD10	MD	Hanover	Anne Arundel	MD 295 SB Ramps/Arundel Mills Blvd	Suburban	3	
MD11	MD	(unincorporated)	Baltimore	MD 372/Hilltop Circle (UMBC)	Urban	4	1
MD12	MD	Bel Air	Harford	MD 7/Holly Oaks Drive	Suburban	3	1
MD13	MD	Brunswick	Frederick	MD 17/A St/B St/Maryland Ave	Urban	5	1
MD14	MD	Cearfoss (Hagerstown)	Washington	MD 63/MD 58/Cearfoss Pike	Rural	4	1
MD15	MD	Ellicott City	Howard	MD 100 EB Ramps/MD 103	Suburban	4	1
MD16	MD	Ellicott City	Howard	MD 100 WB Ramps/MD 103	Suburban	4	1
MD17	MD	Ellicott City	Howard	MD 100 WB Ramps/MD 104	Suburban	4	2
MD18	MD	Ellicott City	Howard	MD 100 WB Ramps/Snowden River Pkwy	Suburban	4	1
MD19	MD	Federalsburg	Caroline	MD 307/MD 313/MD 318	Rural	4	1
MD20	MD	Jessup	Howard	MD 32 Ramps/Guilford Road	Suburban	3	1
MD21	MD	Fort Washington	Prince Georges	Ft. Washington Rd.	Suburban	4	1
MD22	MD	Frederick	Frederick	MD 80/Sugarloaf Pkwy	Rural	4	2
MD23	MD	Gaithersburg	Montgomery	Longdraft Rd./Kentlands	Suburban	4	2
MD24	MD	Greenbelt	Prince Georges	Hanover Pkwy/Schrom Hills Park	Suburban	4	1
MD25	MD	Lisbon	Howard	MD 94/MD144	Rural	4	1
MD26	MD	Lisbon	Howard	MD 94/Old Frederick Rd	Rural	4	1
MD27	MD	Millington	Kent	US 301 NB Ramps/MD 291	Rural	4	1
MD28	MD	Millington	Kent	US 301 SB Ramps/MD 291	Rural	4	1
MD29	MD	Mount Aetna	Washington	MD 66 (Mapleville Rd)/Mount Aetna Rd	Suburban	4	1
MD30	MD	Mount Rainier	Prince Georges	US 1/Perry St/34th St	Urban	6	2
MD31	MD	Oak Grove (Kettering)	Prince Georges	MD 193/Oak Grove Rd	Urban	3	1
MD32	MD	Rising Sun	Cecil	MD 273/MD 276	Rural	4	1
MD33	MD	Rosemont	Frederick	MD 17/MD 180	Rural	4	1
MD34	MD	Scaggsville	Howard	US 29 NB Ramps/MD 216	Suburban	4	2
MD35	MD	Scaggsville	Howard	US 29 SB Ramps/MD 216	Suburban	4	2
MD36	MD	Scaggsville	Howard	US 29 NB Ramps/Hopkins-Gorman Road	Suburban	4	2

Site ID	State	City	County/ Borough	Intersection	Setting	No. of Legs	No. of Lanes
MD37	MD	Scaggsville	Howard	US 29 SB Ramps/Hopkins-Gorman Road	Suburban	4	2
MD38	MD	Stevensville (Castle Marina)	Queen Annes	MD 18/Castle Marina Rd	Suburban	4	1
MD39	MD	Temple Hills	Prince Georges	MD 637/Good Hope Ave.	Suburban	4	1
MD40	MD	Temple Hills	Prince Georges	MD 637/Oxon Run Dr.	Suburban	4	1
ME01	ME	Gorham	Cumberland	US 202/State Route 237	Urban	4	1
MI01	MI	Okemos	Ingham	Hamilton Rd/Marsh Rd	Suburban	3	2
MI02	MI	Dimondale	Eaton	East Rd/Creyts Rd (mini-roundabout)	Suburban	3	1
MI03	MI	East Lansing	Ingham	Bogue Street/Shaw Lane	Urban	4	2
MI04	MI	Rochester Hills	Oakland	Tienken Rd/Sheldon Rd	Suburban	4	1
MI05	MI	Rochester	Oakland	Tienken Rd/Runyon Rd/Washington Rd	Suburban	4	1
MN01	MN	Medford	Steele	I-35/CR 12	Suburban	4	2
MO01	MO	Columbia	Boone	Business Loop/I-70	Suburban	5	1
MO02	MO	Parkville	Platte	MO 45 (Tom Watson Pkwy)/National Dr	Suburban	4	1
MO03	MO	Town & Country	St. Louis	MO 141 Ramps/Woods Mill Rd	Suburban	3	1
MS01	MS	Jackson	Rankin	MS 475/Airport Rd/Old Brandon Rd	Suburban	4	1
NC01	NC	Advance	Davie	I-40 EB Ramps/Hwy 801	Suburban	3	1
NC02	NC	Clemmons	Forsyth	Fraternity Church Rd/Hope Church Rd	Suburban	3	1
NC03	NC	Clemmons	Forsyth	Styers Ferry Rd./Utility Dr (River Ridge Roundabout)	Suburban	4	1
NC04	NC	Lewisville	Forsyth	US 421 SB Ramp/Williams Rd	Suburban	3	1
NE01	NE	Seward	Seward	7th St, 6th Av, 8th Av.	Suburban	3	1
NE02	NE	Blair	Washington	NE 133/US 30		3	1
NH01	NH	Nashua	Hillsborough	Coburn Ave./Chuck Drudging Dr.		4	1
NJ01	NJ	Belmar	Monmouth	10th Ave/B St	Suburban	4	1
NJ02	NJ	Belmar	Monmouth	10th Ave/D St	Suburban	4	1
NJ03	NJ	Maplewood	Essex	Midland Blvd/Highland Blvd	Suburban	4	1
NJ04	NJ	Maplewood	Essex	Midland Blvd/Norfolk Ave	Suburban	4	1
NJ05	NJ	Princeton	Mercer	Faculty Rd/Elm Dr	Urban	3	1
NJ06	NJ	Rutherford	Bergen	Park Ave/Erie Ave	Suburban	3	1
NJ07	NJ	Southampton	Burlington	Red Lion Circle	Suburban	4	1
NJ08	NJ	Summit	Union	Union Place/Beechwood Rd	Suburban	3	1
NJ09	NJ	Westfield	Union	NJ 28/East Broad St. (Westfield Circle)	Urban	3	2
NV01	NV	Las Vegas	Clark	Hills Center Dr./Village Center Cir./Meadow Hills Dr.	Suburban	4	2
NV02	NV	Las Vegas	Clark	Town Cen. Dr/Hualapai Way/Far Hills Ave.	Suburban	4	3
NV03	NV	Las Vegas	Clark	Town Center Dr./Village Center Cir./Library Hills Dr.	Suburban	4	2
NV04	NV	Las Vegas	Clark	Town Cen./Canyon Run Dr/Banburry Cross Dr	Suburban	4	3
NV05	NV	Carson City	Carson City	5th St/Edmonds	Rural	4	1
NV06	NV	Carson City	Carson City	US 395 NB Ramp/Arrowhead/Imus	Suburban	4	1
NV07	NV	Carson City	Carson City	US 395 SB Ramp/Arrowhead	Suburban	3	1
NV08	NV	Las Vegas	Clark	Carey Ave/Belmont St	Urban	4	1
NV09	NV	Las Vegas	Clark	Carey Ave/Hamilton St	Urban	4	2
NV10	NV	Las Vegas	Clark	Carey Ave/Revere St	Urban	4	2
NV11	NV	Las Vegas	Clark	Desert Primrose Ln/Desert Marigold Ln/Blue Willow	Suburban	4	2
NV12	NV	Las Vegas	Clark	Desert Primrose Ln/Spotted Leaf Ln/Pavillion Cen. Dr	Suburban	3	2

Site ID	State	City	County/ Borough	Intersection	Setting	No. of Legs	No. of Lanes
NV13	NV	Las Vegas	Clark	Gate/Longspur	Suburban	4	2
NV14	NV	Las Vegas	Clark	Havenwood Ave/Desert Marigold Ln/Navajo Willow Ln	Suburban	4	2
NV15	NV	Las Vegas	Clark	Havenwood Ave/Spotted Leaf Ln/Golden Willow	Suburban	4	1
NV16	NV	Las Vegas	Clark	Lake South/Crystal Water Way	Suburban	4	1
NV17	NV	Las Vegas	Clark	Thornbury/Enclave	Suburban	3	1
NV18	NV	Las Vegas	Clark	Hills Drive/Longspur	Suburban	3	2
NY01	NY	Erwin (Painted Post)	Stueben	Robert Dann/Science Center	Suburban	4	2
NY02	NY	Kingston	Ulster	I-587/Rt 28/I-87/Washington Ave	Rural	4	2
NY03	NY	North Haven	Suffolk	Tyndall Road/Route 114	Suburban	4	1
NY04	NY	Greenwich	Washington	Rte 29/Rte 40	Suburban	3	
NY05	NY	Guilderland	Albany	Rte 155/Rte 85A/Rte 20	Suburban	3	
OR01	OR	Bend	Deschutes	Colorado Ave/Simpson Dr	Urban	4	1
OR02	OR	Astoria	Clastop	Hwy 101/Hwy 202 (Nehalem Hwy)	Urban	3	2
OR03	OR	Bend	Deschutes	8th St/Franklin Ave/9th St.	Urban	4	1
OR04	OR	Bend	Deschutes	Century Dr/Colorado Ave/Chandler Ave	Urban	4	1
OR05	OR	Bend	Deschutes	Century Dr/Mt. Washington Dr./Reed Market Rd.	Suburban	4	1
OR06	OR	Bend	Deschutes	Mt. Washington Dr/NW Crossing Dr	Suburban	4	1
OR07	OR	Bend	Deschutes	Mt. Washington Dr/Shevlin Park Rd.	Suburban	4	1
OR08	OR	Bend	Deschutes	Reed Market Rd./Mt Bachelor Dr	Suburban	4	1
OR09	OR	Bend	Deschutes	Century Dr./14th St./Simpson Ave.	Urban	4	1
OR10	OR	Bend	Deschutes	14th St./Galveston Ave.	Urban	4	1
OR11	OR	Bend	Deschutes	Awbrey Rd./Sonora Dr.	Suburban	3	1
OR12	OR	Bend	Deschutes	Bond St./Reed Market Rd.	Suburban	3	1
OR13	OR	Bend	Deschutes	Industrial Way/Wall St.	Urban	3	1
OR14	OR	Bend	Deschutes	Industrial Way/Bond St.	Urban	3	1
OR15	OR	Eugene	Lane	Barger Dr/Green Hill Rd	Suburban	3	1
OR16	OR	Eugene	Lane	N. Terry St/ Roosevelt Blvd	Urban	3	1
OR17	OR	Portland	Multnomah	NE Lombard St/N Perimeter Rd (PDX airport)	Suburban	4	1
OR18	OR	Portland	Multnomah	SW Terwilliger Rd/SW Palater Rd	Suburban	4	1
OR19	OR	Sherwood	Washington	NE Oregon St./SW Murdock Rd.	Suburban	3	1
OR20	OR	Springfield	Lane	Maple Island Rd./Facility Entrance	Suburban	3	1
OR21	OR	Springfield	Lane	Maple Island Rd./International Way	Suburban	4	1
OR22	OR	Springfield	Lane	Maple Island Rd/Game Farm Rd	Suburban	3	1
OR23	OR	Springfield	Lane	Thurston/58th St	Urban	4	1
SC01	SC	Hilton Head	Beaufort	Whooping Crane Way/Main St	Suburban	4	1
TX01	TX	Addison	Dallas	Mildred St./Quorum Dr	Urban	4	2
UT01	UT	Orem	Utah	1200 South/400 West	Urban	4	2
UT02	UT	Orem	Utah	2000 South/Sandhill Rd	Urban	4	2
UT03	UT	Draper	Salt Lake	Vestry Rd/Rocky Mouth Ln	Suburban	4	1
UT04	UT	Draper	Salt Lake	300 East/12200 South	Suburban	3	1
UT05	UT	Orem	Utah	E 850 North/N Palisade Dr	Suburban	3	1
UT06	UT	Orem	Utah	Palisade Drive/Cascade Pkwy		3	1
UT07	UT	Orem	Utah	400 South/Lindon Park Circle (600 West)		4	2
UT08	UT	Orem	Utah	Utah Valley State College	Suburban	4	2
UT09	UT	Park City	Summit	RT 224 (Deer Valley Dr.)/Heber Ave/Marsac Ave	Suburban	4	2
UT10	UT	Provo	Utah	1730 North/1740 West	Suburban	4	1
UT11	UT	Provo	Utah	1720 North/550 West	Urban	4	1
UT12	UT	Provo	Utah	3700 North/300 West	Suburban	3	1
UT13	UT	Provo	Utah	700 East/Center	Urban	4	1

Site ID	State	City	County/ Borough	Intersection	Setting	No. of Legs	No. of Lanes
UT14	UT	Provo	Utah	1700 North/1500 West	Suburban	4	1
UT15	UT	Provo	Utah	300 North/Seven Peaks Blvd	Suburban	4	2
UT16	UT	Provo	Utah	5000 North/Edgewood	Suburban	4	1
UT17	UT	Provo	Utah	920 South/200 West	Suburban	4	1
UT18	UT	Provo	Utah	Veterans Parkway/Edgewood (Shops at Riverwoods)	Suburban	3	1
UT19	UT	Summit	Summit	Powderwood Dr/Factory Outlet Parking	Suburban	3	1
UT20	UT	Summit	Summit	Kilby Road/Factory Outlet Parking	Suburban	3	2
UT21	UT	Draper	Salt Lake	1300 East/Pioneer Rd	Suburban	4	1
VT01	VT	Manchester	Bennington	Rte 7A/Equinox(Grand Union)	Suburban	4	1
VT02	VT	Montpelier	Washington	Main St./Spring St (Keck Circle)	Urban	3	1
VT03	VT	Brattleboro	Windham	RT 9/RT 5	Suburban	4	2
WA01	WA	Gig Harbor	Pierce	SR 16 SB Ramp/Borgen Blvd.	Suburban	4	1
WA02	WA	Gig Harbor	Pierce	Borgen Blvd/51st	Suburban	4	1
WA03	WA	Bainbridge Island	Kitsap	High School Rd/Madison Ave.	Urban	4	1
WA04	WA	Port Orchard	Kitsap	Mile Hill Dr. (Hwy 166)/Bethel Ave	Suburban	3	1
WA05	WA	Sammamish	King	NE Inglewood Hill/216th Ave NE	Suburban	4	1
WA06	WA	Monroe	Snohomish	SR 522 EB Ramps/W. Main St.(164th St SE)/Tester Rd	Suburban	5	2
WA07	WA	Lacey	Thurston	I-5 NB Ramp/Quinault Dr/Galaxy Dr	Suburban	4	1
WA08	WA	Kennewick	Benton	27th Ave/Union St/Union Loop Rd	Urban	4	1
WA09	WA	Gig Harbor	Pierce	SR 16 NB Ramps/Burnham Dr./Borgen Blvd.	Urban	6	2
WA10	WA	Federal Way	King	Weyerhauser Way/33rd Pl./32nd Dr. S.	Suburban	3	2
WA11	WA	Kennewick	Benton	12th Ave./Irving St.	Urban	4	1
WA12	WA	Kennewick	Benton	Columbia Park Dr. #1	Suburban	3	1
WA13	WA	Kennewick	Benton	Columbia Park Dr. #2	Suburban	3	1
WA14	WA	Kent	King	S.216th St/42nd Ave S/40th Place S	Suburban	4	1
WA15	WA	Lacey	Thurston	Marvin Rd/Britton Pkwy./Willamette Drive	Suburban	4	2
WA16	WA	Lacey	Thurston	College St. SE/45th Ave. SE	Suburban	4	2
WA17	WA	Lacey	Thurston	Marvin Rd./Hawk Prairie Rd.	Suburban	4	1
WA18	WA	Moses Lake	Grant	Yonezawa Blvd./Division St./Belmont Ave.	Suburban	4	1
WA19	WA	Moses Lake	Grant	Yonezawa Blvd./Monroe St. (future)	Suburban	4	1
WA20	WA	Moses Lake	Grant	Yonezawa Blvd./Clover Dr.	Suburban	4	1
WA21	WA	Sammamish	King	W. Lake Sammamish Parkway SE/Lakemont Blvd SE	Urban	4	1
WA22	WA	University Place	Pierce	Grandview Dr/56th St W	Suburban	3	1
WA23	WA	University Place	Pierce	Grandview Dr/62nd Court W/Park Entrance	Suburban	4	1
WA24	WA	University Place	Pierce	Grandview Dr/Bristonwood Dr/48th St W	Suburban	4	1
WA25	WA	University Place	Pierce	Grandview Dr/Cirque Dr	Suburban	3	1
WA26	WA	University Place	Pierce	Grandview Dr/Olympic Blvd	Suburban	4	1
WA27	WA	University Place	Pierce	56th Ave./Alameda Ave. W/Cirque Dr.	Suburban	4	1
WA28	WA	Lacey	Thurston	Marvin Rd./TBD Commercial Access	Suburban	2	2
WA29	WA	Bellevue	King	SR 90/West Lake Sammamish	Suburban	4	1
WI01	WI	Howard	Brown	Lineville Rd (CTH M)/Cardinal Ln	Suburban	4	1
WI02	WI	Howard	Brown	Lineville Rd (CTHM)/Rockwell Rd	Suburban	3	1
WI03	WI	Milwaukee	Milwaukee	S 6th St/W Virginia St	Urban	4	1

Site Summary

The following tables and figures show the fields of view for a sample of sites from which video was collected. Each site included in the following sample has an overhead view (designated with a "V") and several views of each leg (designated by general direction, e.g., "E", "W", "N", "S"). An arrow indicating the designated north direction (which may not necessarily correspond to true north) has been placed on each overhead view.

CO01: SH-6/I-70 spur, Eagle, Colorado

CO01-E1

CO01-N1

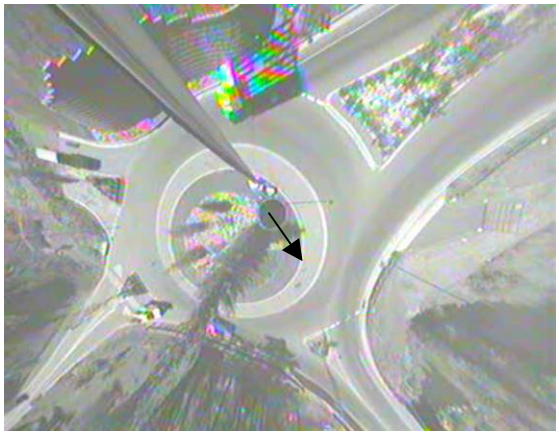

CO01-V1

CO01-W1

CO02: South Golden Road/Johnson Rd/16th Street, Golden, Colorado

CO02-E1

CO02-S1

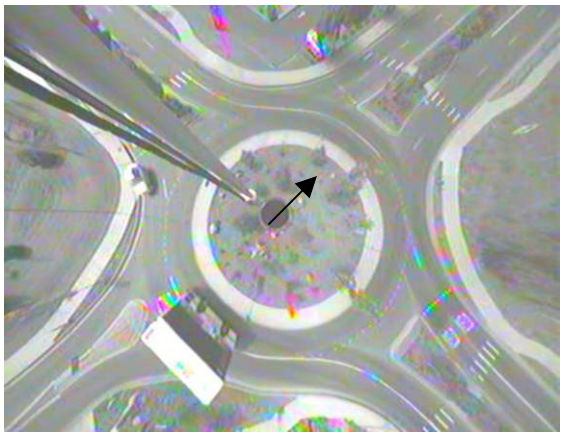

CO02-V1

CO02-W1

CO03: South Golden Road/Utah St., Golden, Colorado

CO03-E1

CO03-N1

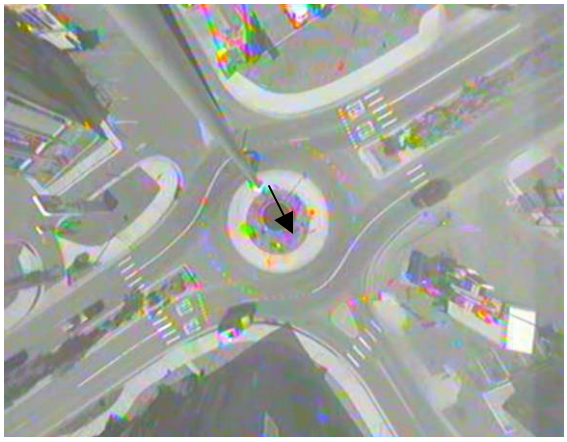

CO03-V1

MD01: Tollgate Rd./Marketplace Dr., Bel Air, Maryland

MD01-E1

MD01-N1

MD01-S1

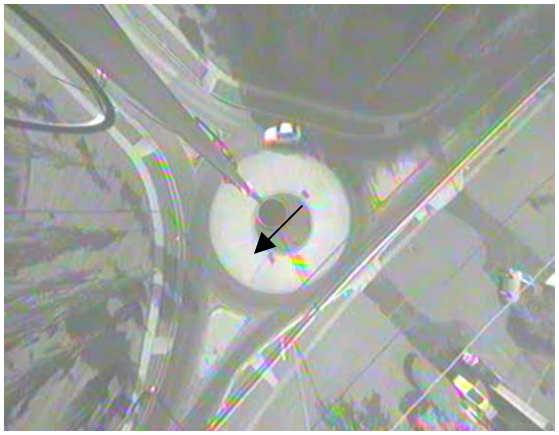

MD01-V1

MD02: MD213/Leeds Rd/Elk Mills Rd. (Lanzi Circle), Leeds, Maryland

MD02-N1

MD02-S1

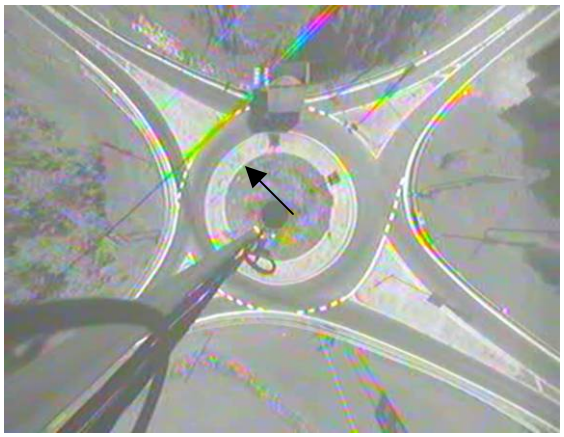

MD02-V1

MD02-W1

MD03: MD24/MD165, Jarrettsville (North Harford), Maryland

MD03-E1

MD03-N1

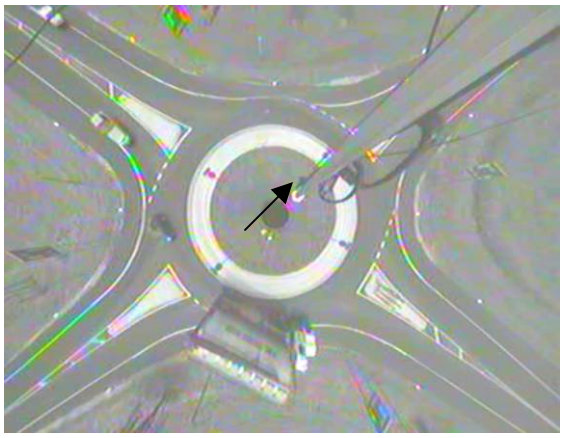

MD03-V1

MD03-W1

MD04: MD 139 (Charles St.)/Bellona Ave., Baltimore County, Maryland

MD04-E1

MD04-S1

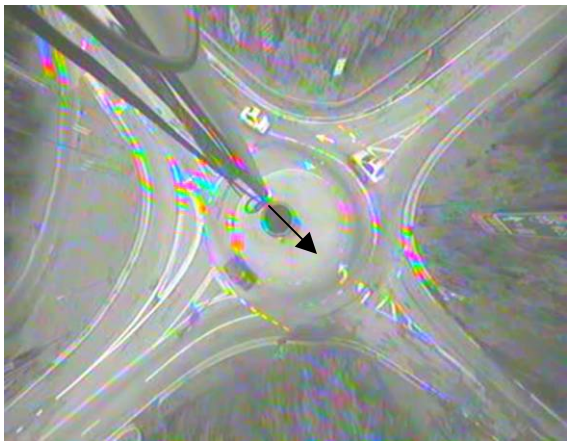

MD04-V1

MD04-W1

MD05: MD45/MD146/Joppa Rd., Towson, Maryland

MD05SW-NW1

MD05SW-S1

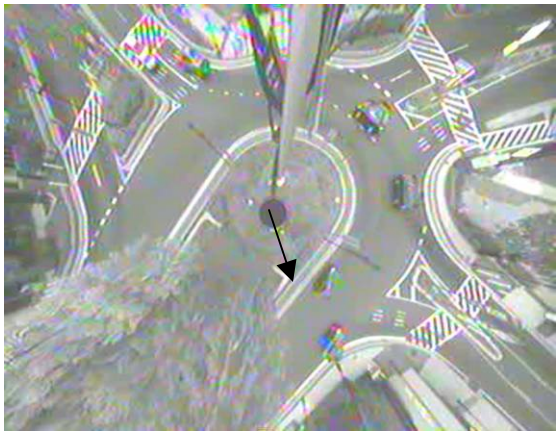

MD05SW-V1

MD05SW-W1

MD06: MD 2/MD 408/MD 422, Lothian, Maryland

MD06-E1

MD06-N1

MD06-S1

MD06-V1

MD07: MD 140/MD 832/Antrim Blvd, Taneytown, Maryland

MD07-E1

MD07-N1

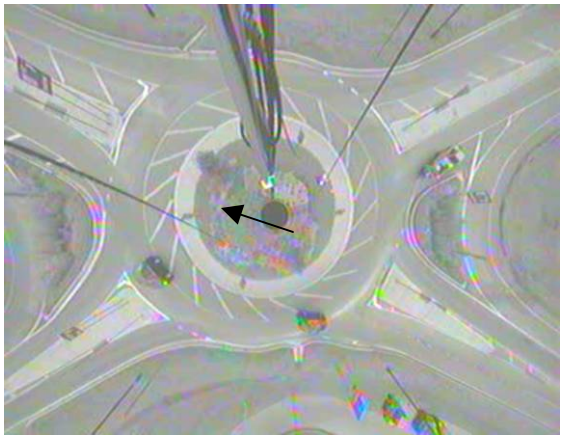

MD07-V1

MD07-W1

ME01: US 202/State Route 237, Gorham, Maine

ME01-E1

ME01-N1

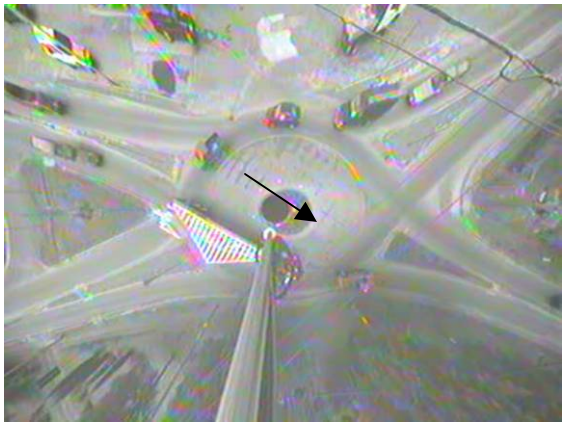

ME01-V1

ME01-S1

MI01: Hamilton Rd/Marsh Rd, Okemos, Michigan

MI01-E1

MI01-N1

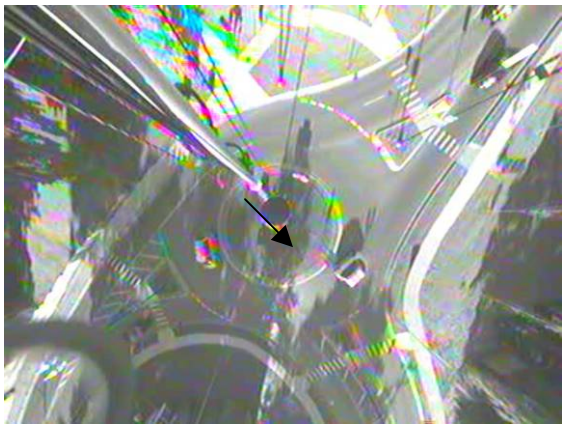

MI01-V1

MI01-W1

NV01: Hill Center Drive/Village Center Circle/Meadow Hills Drive, Las Vegas, Nevada

NV01-N1

NV01-E1

NV01-W1

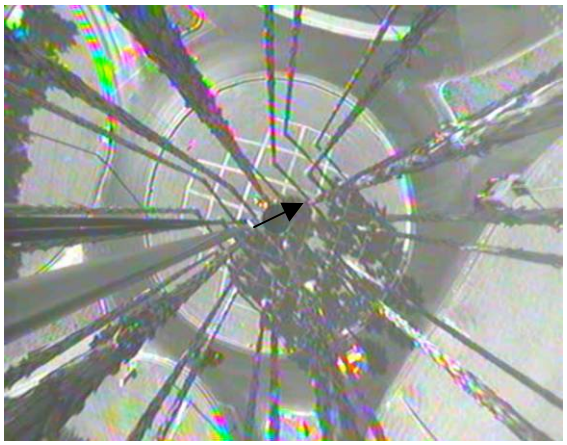

NV01-V1

NV02: Town Center Drive/Hualapi Way/Far Hills Drive, Las Vegas, Nevada

NV02-E1

NV02-S1

NV02-W1

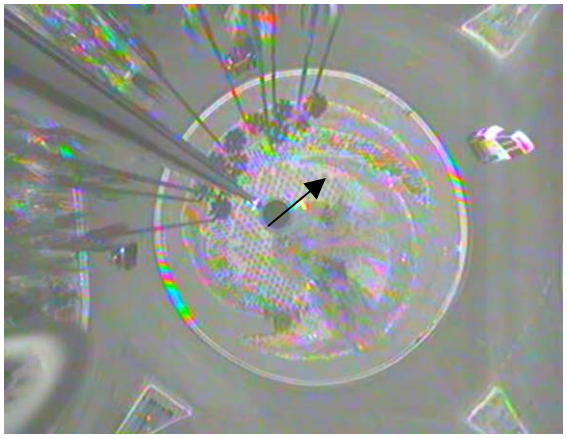

NV02-V1

NV03: Town Center Drive/Village Center Circle/Library Hills Drive, Las Vegas, Nevada

NV03-N1

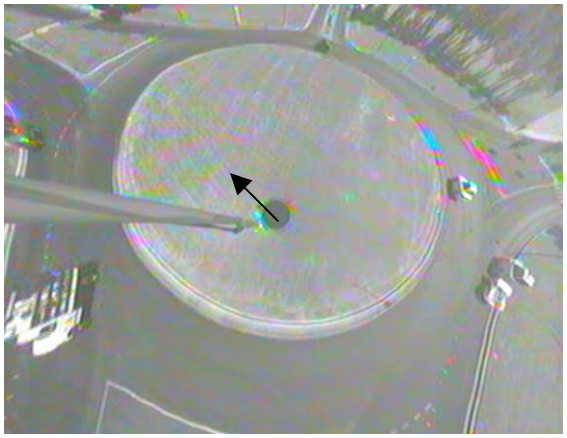

NV03-V1

NV03-S1

NV03-W1

NV04: Town Center Drive/Banburry Cross Drive/Canyon Run Drive, Las Vegas, Nevada

NV04-E1

NV04-V1

NV04-S1

NV04-W1

OR01: Colorado/Simpson, Bend, Oregon

OR01-N1

OR01-W1

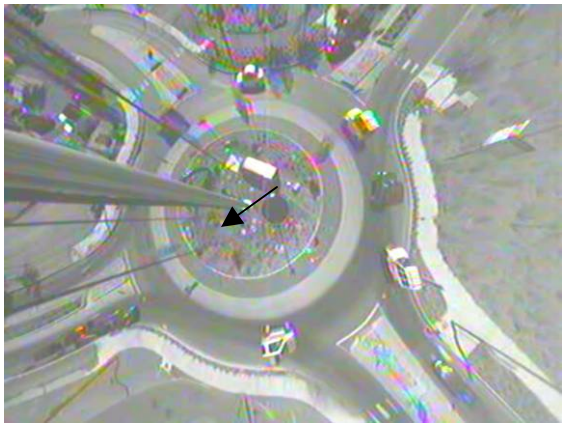

OR01-V1

OR01-S1

VT03: Rte. 9/Rte. 5, Brattleboro, Vermont

VT03-W1

VT03-N1

VT03-S1

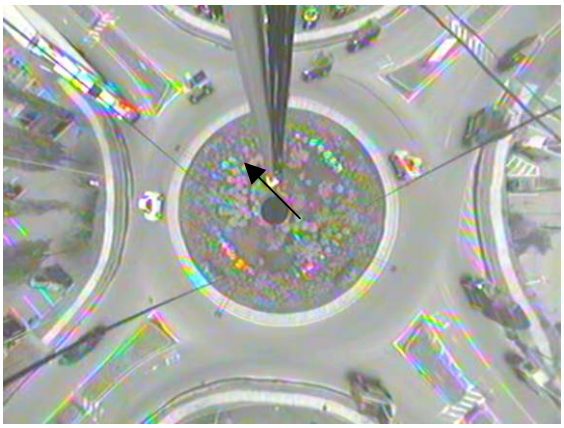

VT03-V1

WA01: SR 16 SB Ramp Terminal, Gig Harbor, Washington

WA01-E1

WA01-N1

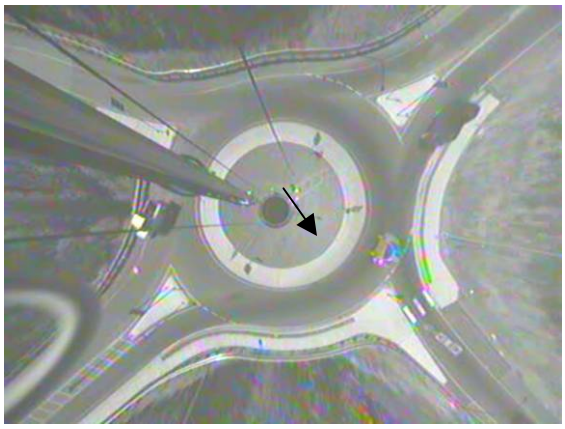

WA01-V1

WA01-W1

WA03: High School Rd/Madison Ave, Bainbridge Island, Washington

WA03-E1

WA03-N1

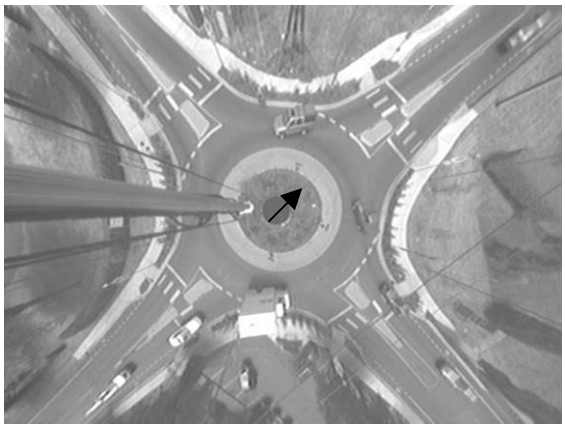

WA03-V1

WA03-S1

WA04: Mile Hill Dr. (Hwy 166)/Bethel Ave, Port Orchard, Washington

WA04-E1

WA04-N1

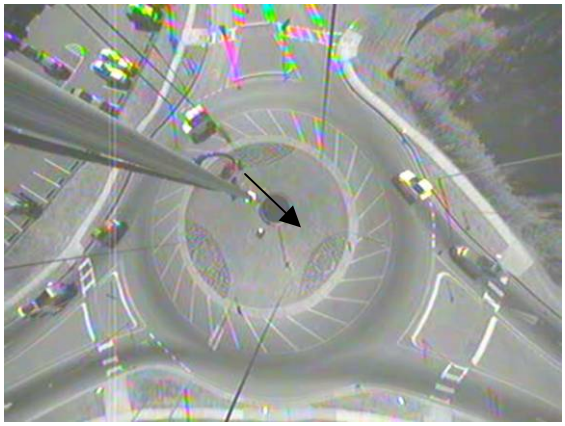

WA04-V1

WA04-S1

WA05 NE Inglewood Hill/216th Ave NE, Sammamish, Washington

WA05-E1

WA05-N1

WA05-V1

WA05-W1

WA07: I-5 off-ramp/Quinault Dr/Galaxy Dr, Lacey, Washington

WA07-E1

WA07-N1

WA07-V1

WA07-S1

Details on Pedestrian-Bicycle Study Sites

CA06: Anderson Road/Alvarado Avenue, Davis, California

- Roundabout is located in an urban area and includes 4 approaches and 1 circulatory lane. - The inscribed circle diameter and central island diameter are 98 ft and 44 ft, respectively. There is also a 10-ft wide truck apron. - Bicyclist data were collected for 89 observations on one approach. - The crosswalk traverses one lane on the entry leg, a raised splitter island, and one lane on the exit leg. The splitter island is 15 ft wide. The curb-to-curb travel distance is 50 ft.	

CA17: Milpas Street/US 101 NB ramps/Carpinteria Street, Santa Barbara, California

- Roundabout is located in an urban area and includes 4 approaches and 1 circulatory lane. - Bicyclist data were collected for 57 observations on one of the surface street approaches. - The crosswalk traverses one lane on the entry leg, a raised splitter island, and one lane on the exit leg. The splitter island is approximately 12 ft wide. The estimated curb-to-curb travel distance is estimated to be 48 ft.	

FL11-E: SR 60/Gulf Boulevard (SR 699), Clearwater Beach, Florida

- Roundabout is located in an urban area and includes 6 approaches and 2 circulatory lanes. The roundabout has a generally elliptical shape. - The inscribed circle diameter and central island diameter are approximately 200 to 220 ft and 171 to 191 ft, respectively. There is also a 2.5-ft wide truck apron. - Data were collected for 135 pedestrian crossing events on the east approach (Causeway). Bicyclist data were collected for 19 observations on the same approach. - The crosswalk traverses two lanes on the entry leg, a raised splitter island, and two lanes on the exit leg. The splitter island is approximately 14 ft wide. The estimated curb-to-curb travel distance is 62 ft.	

MD05-SW-W: MD 45/MD 146/Allegheny Avenue/Joppa Road, Towson, Maryland

- Roundabout is located in an urban area and includes 5 approaches and 2 circulatory lanes. - The oval-shaped roundabout has an average inscribed circle diameter of 140 ft. The central island measures 60 ft wide by 190 ft long. There is also a 5-ft wide truck apron. - Data were collected for 65 pedestrian crossings on the west approach (Allegheny Avenue). - The crosswalk traverses two lanes on the entry leg, a raised splitter island, and one lane on the exit leg. The splitter island is 6 ft wide. The curb-to-curb travel distance is 52 ft.	

MD05-SW/NW: MD 45/MD 146/Allegheny Avenue/Joppa Road, Towson, Maryland

- Roundabout is located in an urban area and includes 5 approaches and 2 circulatory lanes. - The oval-shaped roundabout has an average inscribed circle diameter of 140 ft. The central island measures 60 ft wide by 190 ft long. There is also a 5-ft wide truck apron. - Data were collected for 38 pedestrian crossings on the northwest approach (York Road). - The crosswalk traverses one lane on the entry leg, a raised splitter island, and one lane on the exit leg. The splitter island is approximately 8 ft wide. The curb-to-curb travel distance is 40 ft.	

MD05-SW/S: MD 45/MD 146/Allegheny Avenue/Joppa Road, Towson, Maryland

- Roundabout is located in an urban area and includes 5 approaches and 2 circulatory lanes. - The oval-shaped roundabout has an average inscribed circle diameter of 140 ft. The central island measures 60 ft wide by 190 ft long. There is also a 5-ft wide truck apron. - Data were collected for 89 pedestrian crossings on the south approach (York Road). - The crosswalk traverses two lanes on the entry leg, a raised splitter island, and two lanes on the exit leg. The splitter island is approximately 15 ft wide. The curb-to-curb travel distance is estimated to be 65 ft.	

NV03-S: Town Center Drive/Village Center Circle/Library Hills Drive, Las Vegas, Nevada

- Roundabout is located in an urban area and includes 4 approaches and 2 circulatory lanes. - The inscribed circle diameter and central island diameter are 300 ft and 214 ft, respectively. There is also a 5-ft wide truck apron. - Data were collected for 22 pedestrian crossings on the south approach (Town Center Drive). - The crosswalk traverses two lanes on the entry leg, a raised splitter island, and two lanes on the exit leg. The splitter island is approximately 20 ft wide. The curb-to-curb travel distance is estimated to be 80 ft.	

OR01-N: Colorado Avenue/Simpson Drive, Bend, Oregon

- Roundabout is located in an urban area and includes 4 approaches and 1 circulatory lane. - The inscribed circle diameter and central island diameter are 158 ft and 78 ft, respectively. There is also a 20-ft wide truck apron. - Bicyclist data were collected for 59 observations on the north approach. - The crosswalk traverses one lane on the entry leg, a raised splitter island, and one lane on the exit leg. The splitter island is 18 ft wide. The curb-to-curb travel distance is 48 ft.	

OR01-S: Colorado Avenue/Simpson Drive, Bend, Oregon

- Roundabout is located in an urban area and includes 4 approaches and 1 circulatory lane. - The inscribed circle diameter and central island diameter are 158 ft and 78 ft, respectively. There is also a 20-ft wide truck apron. - Bicyclist data were collected for 27 observations on the south approach. - The crosswalk traverses one lane on the entry leg, a raised splitter island, and one lane on the exit leg. The splitter island is 18 ft wide. The curb-to-curb travel distance is 48 ft.	

OR01-W: Colorado Avenue/Simpson Drive, Bend, Oregon

- Roundabout is located in an urban area and includes 4 approaches and 1 circulatory lane. - The inscribed circle diameter and central island diameter are 158 ft and 78 ft, respectively. There is also a 20-ft wide truck apron. - Bicyclist data were collected for 26 observations on the south approach. - The crosswalk traverses one lane on the entry leg, a raised splitter island, and one lane on the exit leg. The splitter island is 16 ft wide. The curb-to-curb travel distance is 48 ft.	

UT02-E: 2000 South/Sandhill Road, Orem, Utah

- Roundabout includes 4 approaches and 2 circulatory lanes. - Data were collected for 131 pedestrian crossings on the east approach. - The crosswalk is located at the very end of the splitter island and traverses one lane on the entry leg, the raised splitter island, and one lane on the exit leg. The splitter island at this point is approximately 4 ft wide. The curb-to-curb travel distance is estimated to be 60 ft.	

UT02-W: 2000 South/Sandhill Road, Orem, Utah

- Roundabout includes 4 approaches and 2 circulatory lanes. - Data were collected for 35 pedestrian crossings on the east approach. - The crossing is located upstream of the splitter island and traverses one lane on the entry leg, a narrow painted median, and one lane on the exit leg. The painted median at this point is approximately 3 ft wide. The curb-to-curb travel distance is estimated to be 30 ft.	

VT01-N: Main Street (Route 7A)/Grand Union, Manchester, Vermont

- Roundabout is located in an urban area and includes 4 approaches and 1 circulatory lane. - The inscribed circle diameter and central island diameter are 100 ft and 22 ft, respectively. There is also a 21-ft wide truck apron. - Data were collected for 95 pedestrian crossings on the north approach (Main Street). - The crosswalk traverses one lane on the entry leg, a raised splitter island, and one lane on the exit leg. The splitter island is 4 ft wide. The curb-to-curb travel distance is 41ft.	

VT02-N: Main Street/Spring Street, Montpelier, Vermont

- Roundabout is located in an urban area and includes 3 approaches and 1 circulatory lane. - The inscribed circle diameter and central island diameter are 110 ft and 35 ft, respectively. There is also a 17 to 20-ft wide truck apron. - Bicyclist data were collected for 39 observations on the north approach. - The crosswalk traverses one lane on the entry leg, a raised splitter island, and one lane on the exit leg. The splitter island is approximately 6 ft wide. The curb-to-curb travel distance is estimated to be 42 ft.	

VT02-S: Main Street/Spring Street, Montpelier, Vermont

- Roundabout is located in an urban area and includes 3 approaches and 1 circulatory lane. - The inscribed circle diameter and central island diameter are 110 ft and 35 ft, respectively. There is also a 17 to 20-ft wide truck apron. - Bicyclist data were collected for 58 observations on the south approach. - The crosswalk traverses one lane on the entry leg, a raised splitter island, and one lane on the exit leg. The splitter island is approximately 15 ft wide. The curb-to-curb travel distance is 50 ft.	

VT02-W: Main Street/Spring Street, Montpelier, Vermont

- Roundabout is located in an urban area and includes 3 approaches and 1 circulatory lane. - The inscribed circle diameter and central island diameter are 110 ft and 35 ft, respectively. There is also a 17 to 20-ft wide truck apron. - Bicyclist data were collected for 49 observations on the west approach. - The crosswalk traverses one lane on the entry leg, a raised splitter island, and one lane on the exit leg. The splitter island is 10 ft wide. The curb-to-curb travel distance is estimated to be 46 ft.	

WA02-E: Borgen Boulevard/51st Avenue, Gig Harbor, Washington

- Roundabout is located in a suburban area and includes 4 approaches and 1 circulatory lane. - The inscribed circle diameter and central island diameter are 148 ft and 72 ft, respectively. There is also a 7-ft wide truck apron. - Data were collected for 24 pedestrian crossings on the east approach (Borgen Boulevard). - The crosswalk traverses one lane on the entry leg, a raised splitter island, and one lane on the exit leg. The splitter island is 12 ft wide. The curb-to-curb travel distance is estimated to be 55 ft.	

WA03-S: High School Road/Madison Avenue, Bainbridge Island, Washington

- Roundabout is located in a suburban area and includes 4 approaches and 1 circulatory lane. - The inscribed circle diameter and central island diameter are 104 ft and 44 ft, respectively. There is also a 10-ft wide truck apron. - Data were collected for 136 pedestrian crossings on the south approach (Madison Avenue). Bicyclist data were collected for 112 observations on the approach. - The crosswalk traverses one lane on the entry leg, a raised splitter island, and one lane on the exit leg. The splitter island is 7 ft wide. The curb-to-curb travel distance is 38 ft.	

WA03-E: High School Road/Madison Avenue, Bainbridge Island, Washington

- Roundabout is located in a suburban area and includes 4 approaches and 1 circulatory lane. - The inscribed circle diameter and central island diameter are 104 ft and 44 ft, respectively. There is also a 10-ft wide truck apron. - Bicyclist data were collected for 84 observations from the east approach (High School Road). - The crosswalk traverses one lane on the entry leg, a raised splitter island, and one lane on the exit leg. The splitter island is 7 ft wide. The curb-to-curb travel distance is 40 ft.	

WA03-W: High School Road/Madison Avenue, Bainbridge Island, Washington

- Roundabout is located in a suburban area and includes 4 approaches and 1 circulatory lane. - The inscribed circle diameter and central island diameter are 104 ft and 44 ft, respectively. There is also a 10-ft wide truck apron. - Bicyclist data were collected for 30 observations from the east approach (High School Road). - The crosswalk traverses one lane on the entry leg, a raised splitter island, and one lane on the exit leg. The splitter island is 6 ft wide. The curb-to-curb travel distance is 38 ft.	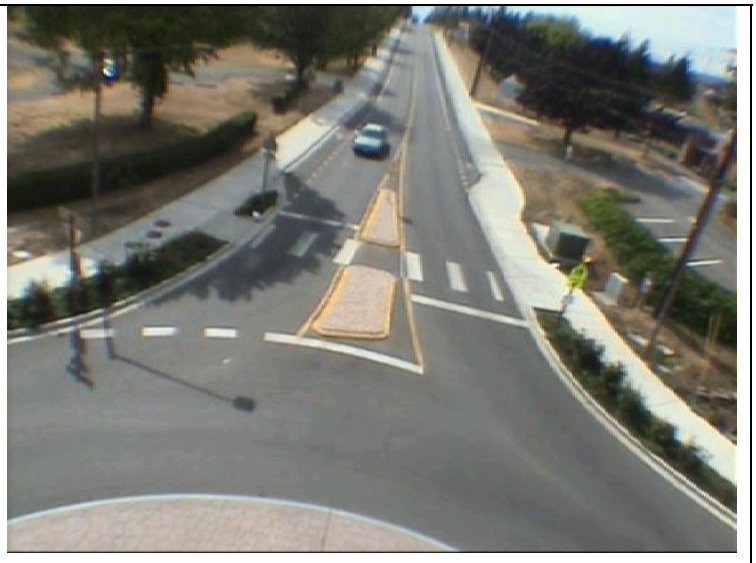

WA03-N: High School Road/Madison Avenue, Bainbridge Island, Washington

- Roundabout is located in a suburban area and includes 4 approaches and 1 circulatory lane. - The inscribed circle diameter and central island diameter are 104 ft and 44 ft, respectively. There is also a 10-ft wide truck apron. - Bicyclist data were collected for 29 observations from the east approach (Madison Avenue). - The crosswalk traverses one lane on the entry leg, a raised splitter island, and one lane on the exit leg. The splitter island is 6 ft wide. The curb-to-curb travel distance is 39 ft.	

APPENDIX D
PEDESTRIAN AND BICYCLE ANALYSIS DETAILS

TABLE D-1. Pedestrian data variables.

Recorded Variables
Event Number = unique identifier for each crossing event
Ped Number = number of pedestrians crossing during event
Age (adult or youth)
Start Location
1 - Entry Leg - within CW extended
2 - Entry Leg - outside CW extended
3 - Exit Leg - within CW extended
4 - Exit Leg - outside CW extended
5 - Other location (e.g., on circle to cross central island)
Crossing Type
1 - Crossed entry and exit legs on painted crosswalk
2 - Crossed entry leg on painted crosswalk, exit leg off painted crosswalk
3 - Crossed exit leg on painted crosswalk, entry leg off painted crosswalk
4 - Did not cross on painted crosswalk at all
4A - Did not cross on crosswalk at all AND used center turn lane as splitter island / crossing refuge (only for
Arrival Time = time at which the pedestrian arrived at the curb
Start Time = time at which the pedestrian initiated the crossing
Splitter Arrival = time at which the pedestrian arrived at the splitter island (after crossing first leg)
Splitter Departure = time at which the pedestrian left the splitter island (to cross second leg)
End Time = time at which pedestrian reached the far curb
The following variables were recorded for each crossing leg (entry and exit).
Rejected Gaps (time in seconds of each gap rejected upon arrival) - time between point of arrrival and the next vehicle reaching the crosswalk AND time between each subsequent pair of vehicles until the pedestrian crosses.
Accepted Gap (time in seconds of the gap accepted, with max value of 30 sec) - time between point of arrival and when the next vehicle reaches the crosswalk after the pedestrian crosses OR time between rejected gap and the

TABLE D-1. Pedestrian data variables (continued).

Recorded Variables
Motorist Behavior
0 - not applicable (no vehicle in vicinity at time of crossing)
1 - vehicle yielded - slowed for ped in transit (not necessarily in crosswalk)
2 - vehicle yielded - stopped for ped in transit (not necessarily in crosswalk)
3 - vehicle yielded - slowed for ped waiting on curb or on splitter island
4 - vehicle yielded - stopped for ped waiting on curb or on splitter island
5 - vehicle did not yield - ped in transit
6 - vehicle did not yield - ped waiting on curb or on splitter island
7 - vehicle already stopped for other reason (applies to accepted and rejected gaps)
Pedestrian Behavior
0 - not applicable (no vehicle in vicinity or vehicle yields)
1 - ped hesitated on curb or splitter island due to approaching vehicle (only applied to accepted gaps)
2 - ped hesitated after stepping into CW due to approaching vehicle
3 - ped stopped after stepping into CW due to approaching vehicle
4 - ped retreated to curb after stepping into CW due to approaching vehicle
5 - ped ran due to approaching vehicle
Conflict
0 - none
1 - motorist swerved or abruptly stopped to avoid striking pedestrian
2 - pedestrian abruptly stopsped or moved to avoid being struck
3 - 1 and 2 both occurred
4 - collision occurred
Notes (e.g., crossing to central island, peds with special needs, pedestrian age, etc.)
Derived Variables
Initial Wait Time = Start Time - Arrival Time
Crossing Time (Leg 1) = Splitter Arrival - Start Time
Splitter Wait/Crossing Time = Splitter Departure - Splitter Arrival
Crossing Time (Leg 2) = End Time - Splitter Departure
Total Crossing Time = End Time - Start Time

TABLE D-2. Bicyclist data variables.

Recorded Variables
Event Number = unique identifier for each bicylist event
Event Type
1 - Bicyclist approaching/entering roundabout
2 - Bicyclist exiting roundabout
3 - Bicyclist circling roundabout
4 - Bicyclist crossing approach leg (like a pedestrian)
Bicyclist Position (at entry and exit)
1 - righthand side of vehicle lane
2 - center of vehicle lane
3 - lefthand side of vehicle lane
4 - bike lane/paved shoulder
5 - sidewalk
Motor Vehicle Presence (at entry and exit)
1 - passing bicyclist
2 - trailing bicyclist
3 - leading bicyclist
4 - no vehicle present
Bicyclist Behavior (for approaching/entering bicyclists)
1 - entered with a safe gap (no yield necessary)
2 - entered with a safe gap (yielded to motor vehicle)
3 - entered with an unsafe gap (did not yield)
4 - entered with an unsafe gap (yielded, then entered)
5 - not applicable (e.g., used sidewalk)
Bicyclist Behaviors (for exiting bicyclists)
1 - exited and remained to the right in the vehicle lane
2 - exited and remained in the center of the vehicle lane
3 - exited and moved to the bike lane/paved shoulder
4 - exited and moved to sidewalk
5 - not applicable (exited from the sidewalk)
Start Location for Bicyclists Crossing Approach Leg
1 - Entry Leg - within CW extended
2 - Entry Leg - outside CW extended
3 - Exit Leg - within CW extended
4 - Exit Leg - outside CW extended
5 - Other location (e.g., on circle to cross central island)
Crossing Type for Bicyclists Crossing Approach Leg
1 - Crossed entry and exit legs on painted crosswalk
2 - Crossed entry leg on painted crosswalk, exit leg off painted crosswalk
3 - Crossed exit leg on painted crosswalk, entry leg off painted crosswalk
4 - Did not cross on painted crosswalk at all
4A - Did not cross on crosswalk at all AND used center turn lane as splitter island / crossing refuge (only for MD05-SW/NW1)
Other Behaviors (e.g., wrong-way riding, conflicts with motor vehicles)

APPENDIX E
SUMMARY OF GOODNESS-OF-FIT MEASURES AND STATISTICAL TERMS

Mean Prediction Bias (MPB)

The mean prediction bias (MPB) is the sum of predicted accident frequencies minus observed accident frequencies in the validation data set, divided by the number of validation data points. This statistic provides a measure of the magnitude and direction of the average model bias. The smaller the average prediction bias, the better the model is at predicting observed data. The MPB can be positive or negative, and is given by:

$$MPB = \frac{\sum_{i=1}^{n}\left(\hat{Y}_i - Y_i\right)}{n}$$

where n = validation data sample size, $\hat{Y}$ = the predicted value, Y_i = observation

A positive MPB suggests that on average the model overpredicts the observed validation data. Conversely, a negative value suggests systematic underprediction. The magnitude of MPB provides the magnitude of the average bias.

Mean Absolute Deviation (MAD)

The mean absolute deviation (MAD) is the sum of the absolute value of the predicted value minus the observed observations, divided by the number of observations. It differs from mean prediction bias in that positive and negative prediction errors will not cancel each other out. Unlike MPB, MAD can only be positive.

$$MAD = \frac{\sum_{i=1}^{n}\left|\hat{Y}_i - Y_i\right|}{n}$$

where n = validation data sample size

The MAD gives a measure of the average magnitude of variability of prediction. Smaller values are preferred to larger values.

Mean Squared Prediction Error (MSPE) and Mean Squared Error (MSE)

The mean squared prediction error (MSPE) is the sum of squared differences between observed and predicted crash frequencies, divided by sample size. MSPE is typically used to assess error associated with a validation or external data set. Smaller values are preferred to larger values.

$$\text{MSPE} = \frac{\sum_{i=1}^{n}\left(Y_i - \hat{Y}_i\right)^2}{n_2}$$

where n_2 = data sample size

To normalize the GOF measures to compensate for the different numbers of years associated with different data sets, GOF measures can be computed on a per year basis. For MPB and MAD per year, MPB and MAD are divided by number of years. However, since MSPE is the mean values of the squared errors, MSPE is divided by the square of number of years to calculate MSPE per year, resulting in a fair comparison of predictions based on different numbers of years.

Other Parameters

Wald's 95% Confidence Limits – Parameter estimates are not estimated exactly. Each has a point estimate and a standard error. The 95% confidence limits give a range of values for which it can be said that the true value lies within that range with 95% certainty. In other words, there is a 5% chance that the true value of the parameter lies outside of this range.

Chi Squared Statistic – Calculated by squaring the ratio of the parameter estimate to its standard error.

Pr > ChiSq – Is the probability that the chi-squared statistic could exceed the calculated value if the true value of the parameter estimate was zero. This statistic is often referred to as the p-value. Thus a value of less that 0.05 would indicate significance at the 5% level.

Dispersion Parameter – This calibrated dispersion parameter of the negative binomial distribution and relates the mean to the variance of the model prediction such that the smaller the value is the better the fit is. A perfect model would have a dispersion parameter close to zero.

Correlation Coefficients - Correlation coefficients contain information on both the strength and direction of a linear relationship between two numeric random variables. If one variable x is an exact linear function of another variable y, a positive relationship exists when the correlation is 1 and an inverse relationship exists when the correlation is -1. If there is no linear predictability between the two variables, the correlation is 0. If the variables are normal and correlation is 0, the two variables are independent. However, correlation does not imply causality because, in some cases, an underlying causal relationship may exist.

APPENDIX F
STATISTICAL TESTING OF INTERSECTION-LEVEL SAFETY MODELS

Total Collision SPF

Definitions Of Independent Variables
logaadt – log of the total entering AADT
noappr 1 – 3 approaches
2 – 4 approaches
3 – 5 approaches
nolanes 1 – 1 circulating lane
2 – 2 circulating lanes
3 – 3 or 4 circulating lanes

Model 1

Observations Used 89

Parameter	DF	Estimate	Standard Error	Wald 95% Confidence Limits		Chi-Square	Pr > ChiSq
Intercept	1	-3.6786	1.3235	-6.2726	-1.0845	7.72	0.0054
logaadt	1	0.5531	0.1394	0.2798	0.8264	15.74	<.0001
Dispersion	1	1.4986	0.2314	1.1073	2.0283		

Model 2

Observations Used 87

Parameter		DF	Estimate	Standard Error	Wald 95% Confidence Limits		Chi-Square	Pr > ChiSq
Intercept		1	-3.7075	2.3496	-8.3127	0.8976	2.49	0.1146
logaadt		1	0.7490	0.2197	0.3183	1.1797	11.62	0.0007
noappr	1	1	-1.4305	0.4750	-2.3614	-0.4997	9.07	0.0026
noappr	2	1	-0.6645	0.4033	-1.4550	0.1261	2.71	0.0995
noappr	3	0	0.0000	0.0000	0.0000	0.0000	.	.
nolanes	1	1	-1.6992	0.6054	-2.8859	-0.5126	7.88	0.0050
nolanes	2	1	-1.2070	0.6013	-2.3855	-0.0284	4.03	0.0447
nolanes	3	0	0.0000	0.0000	0.0000	0.0000	.	.
Dispersion		1	0.8986	0.1644	0.6278	1.2862		

Model 3

Observations Used 52

Parameter		DF	Estimate	Standard Error	Wald 95% Confidence Limits		Chi-Square	Pr > ChiSq
Intercept		1	-0.9397	3.1715	-7.1558	5.2764	0.09	0.7670
logaadt		1	0.5532	0.3007	-0.0362	1.1426	3.38	0.0658
noappr	1	1	-1.9545	0.6847	-3.2965	-0.6125	8.15	0.0043
noappr	2	1	-1.1971	0.6083	-2.3894	-0.0048	3.87	0.0491
noappr	3	0	0.0000	0.0000	0.0000	0.0000	.	.
nolanes	1	1	-2.3303	0.9895	-4.2696	-0.3910	5.55	0.0185
nolanes	2	1	-1.6670	0.9502	-3.5294	0.1954	3.08	0.0794
nolanes	3	0	0.0000	0.0000	0.0000	0.0000	.	.
newvar		1	0.1203	0.2768	-0.4222	0.6627	0.19	0.6639
Dispersion		1	0.8348	0.1965	0.5262	1.3242		

Model 4

Observations Used 58

Parameter		DF	Estimate	Standard Error	Wald 95% Confidence Limits		Chi-Square	Pr > ChiSq
Intercept		1	0.1321	2.7914	-5.3390	5.6032	0.00	0.9623
logaadt		1	0.4162	0.2612	-0.0956	0.9281	2.54	0.1110
noappr	1	1	-1.7609	0.5917	-2.9207	-0.6012	8.86	0.0029
noappr	2	1	-1.0325	0.5037	-2.0198	-0.0452	4.20	0.0404
noappr	3	0	0.0000	0.0000	0.0000	0.0000	.	.
nolanes	1	1	-2.0821	0.8054	-3.6607	-0.5035	6.68	0.0097
nolanes	2	1	-1.3508	0.7954	-2.9097	0.2081	2.88	0.0894
nolanes	3	0	0.0000	0.0000	0.0000	0.0000	.	.
Inscribed_Diameter__		1	0.0002	0.0021	-0.0039	0.0044	0.01	0.9147
Dispersion		1	0.7792	0.1746	0.5022	1.2088		

Model 5

Observations Used 52

Parameter		DF	Estimate	Standard Error	Wald 95% Confidence Limits		Chi-Square	Pr > ChiSq
Intercept		1	-0.7417	3.2568	-7.1249	5.6415	0.05	0.8199
logaadt		1	0.5597	0.3019	-0.0321	1.1515	3.44	0.0638
noappr	1	1	-1.9170	0.7194	-3.3269	-0.5071	7.10	0.0077
noappr	2	1	-1.1587	0.6228	-2.3794	0.0619	3.46	0.0628
noappr	3	0	0.0000	0.0000	0.0000	0.0000	.	.
nolanes	1	1	-2.3142	1.0454	-4.3632	-0.2652	4.90	0.0269
nolanes	2	1	-1.6943	0.9972	-3.6488	0.2602	2.89	0.0893
nolanes	3	0	0.0000	0.0000	0.0000	0.0000	.	.
Central_island_diame		1	-0.0006	0.0036	-0.0077	0.0065	0.03	0.8632
Dispersion		1	0.8408	0.1970	0.5311	1.3309		

Total Intersection - Fatal+Injury SPF

Definitions Of Variables
logaadt – log of the total entering AADT
noappr 1 – 3 approaches
2 – 4 approaches
3 – 5 approaches
nolanes 1 – 1 or 2 circulating lanes
3 – 3 or 4 circulating lanes

Model 1

Observations Used 88

Analysis Of Parameter Estimates

Parameter	DF	Estimate	Standard Error	Wald 95% Confidence Limits		Chi-Square	Pr > ChiSq
Intercept	1	-7.8638	1.7497	-11.2931	-4.4345	20.20	<.0001
logaadt	1	0.7656	0.1825	0.4078	1.1233	17.59	<.0001
Dispersion	1	1.7262	0.4306	1.0587	2.8146		

Model 2

Observations Used 86

Parameter		DF	Estimate	Standard Error	Wald 95% Confidence Limits		Chi-Square	Pr > ChiSq
Intercept		1	-3.6232	2.8333	-9.1764	1.9299	1.64	0.2010
logaadt		1	0.5923	0.2531	0.0962	1.0885	5.48	0.0193
noappr	1	1	-1.2499	0.6354	-2.4953	-0.0044	3.87	0.0492
noappr	2	1	-0.8064	0.4739	-1.7352	0.1224	2.90	0.0888
noappr	3	0	0.0000	0.0000	0.0000	0.0000	.	.
nolanes	1	1	-2.2167	0.6467	-3.4843	-0.9491	11.75	0.0006
nolanes	3	0	0.0000	0.0000	0.0000	0.0000	.	.
Dispersion		1	0.9459	0.3294	0.4780	1.8718		

Model 3

Observations Used 52

Parameter		DF	Estimate	Standard Error	Wald 95% Confidence Limits		Chi-Square	Pr > ChiSq
Intercept		1	-0.4654	4.0732	-8.4487	7.5179	0.01	0.9090
logaadt		1	0.3637	0.3728	-0.3670	1.0943	0.95	0.3293
noappr	1	1	-2.0996	0.9457	-3.9532	-0.2460	4.93	0.0264
noappr	2	1	-1.5722	0.7938	-3.1279	-0.0164	3.92	0.0476
noappr	3	0	0.0000	0.0000	0.0000	0.0000	.	.
nolanes	1	1	-2.8410	1.0195	-4.8391	-0.8429	7.77	0.0053
nolanes	3	0	0.0000	0.0000	0.0000	0.0000	.	.
newvar		1	0.1249	0.3954	-0.6501	0.9000	0.10	0.7520
Dispersion		1	0.8714	0.4393	0.3244	2.3408		

Model 4

Observations Used 58

Parameter		DF	Estimate	Standard Error	Wald 95% Confidence Limits		Chi-Square	Pr > ChiSq
Intercept		1	-1.5264	3.3073	-8.0086	4.9559	0.21	0.6444
logaadt		1	0.3971	0.3086	-0.2078	1.0020	1.66	0.1982
noappr	1	1	-1.6696	0.7076	-3.0564	-0.2828	5.57	0.0183
noappr	2	1	-1.4571	0.5681	-2.5705	-0.3437	6.58	0.0103
noappr	3	0	0.0000	0.0000	0.0000	0.0000	.	.
nolanes	1	1	-2.1759	0.9231	-3.9852	-0.3666	5.56	0.0184
nolanes	3	0	0.0000	0.0000	0.0000	0.0000	.	.
Inscribed_Diameter__		1	0.0023	0.0031	-0.0038	0.0083	0.53	0.4663
Dispersion		1	0.6891	0.3561	0.2503	1.8975		

Model 5

Observations Used 52

Parameter		DF	Estimate	Standard Error	Wald 95% Confidence Limits		Chi-Square	Pr > ChiSq
Intercept		1	0.0335	3.9708	-7.7491	7.8161	0.00	0.9933
logaadt		1	0.3976	0.3854	-0.3578	1.1530	1.06	0.3023
noappr	1	1	-2.1836	0.9806	-4.1056	-0.2616	4.96	0.0260
noappr	2	1	-1.6783	0.8607	-3.3652	0.0087	3.80	0.0512
noappr	3	0	0.0000	0.0000	0.0000	0.0000	.	.
nolanes	1	1	-3.0939	1.1842	-5.4150	-0.7728	6.83	0.0090
nolanes	3	0	0.0000	0.0000	0.0000	0.0000	.	.
Central_island_diame		1	-0.0032	0.0065	-0.0160	0.0095	0.25	0.6205
Dispersion		1	0.8894	0.4447	0.3338	2.3697		

APPENDIX G
DEFINITIONS FOR ESTIMATING FASTEST VEHICLE PATHS

The following outlines the general approach used in this study for sketching the fastest paths and predicting the speeds through a roundabout. The method is generally consistent with that described in the FHWA Roundabout Guide *(G1)*.

1. The vehicle was assumed to be 1.8 m (6 ft) wide.
2. The path was drawn with the following offsets to the particular geometric elements (except where a larger offset will create a faster path) acting as outer limits of the path:
    a. 1.5 m (5 ft) from concrete curbing and splitter islands,
    b. 1.5 m (5 ft) from a roadway centerline (marking the boundary with traffic traveling in the opposite direction), and
    c. 1.0 m (3 ft) from a painted edge line (marking the boundary with either a painted median or traffic in the same direction).
3. The vehicle path was constructed beginning at a point not less than 50 m (164 ft) upstream of the yield line, per the British method.
4. The vehicle path was drawn by hand to allow natural transitions between tangents and curves.

Several radii at various points along the vehicle paths are of interest. These are based in principle on the five measurements as shown in the FHWA guide *(G1)*. For analysis purposes, the entry path radii and exit path radii have been differentiated between left-turn and through movements, and right-turn path radii have been separated into entry and exit path radii. The complete list is as follows and is diagrammed in Figure G-1.

- R_0: Approach path radius – measured along the path at a point upstream of the entry yield line for the through movement.
- R_1: Through movement entry path radius – measured along the path prior to the entry yield line for the through movement.
- R_2: Through movement circulating path radius – measured around the central island in the circulatory roadway.
- R_3: Through movement exit path radius – measured on the exit for the through movement.
- R_{1L}: Left-turn movement entry path radius – measured along the path prior to the entry yield line for the left turn movement. In practice, this is often very similar to R_1.
- R_4: Left-turn movement circulating path radius – measured on the circulatory roadway upstream of the conflict point with the opposing through movement.
- R_6: Left-turn movement exit path radius – measured on the exit for the left turn movement. In practice, this is often very similar to R_3.
- R_5: Right-turning entry path radius – measured along the path prior to the entry yield line for the right-turn movement.
- R_{5x}: Right-turning exit path radius – measured on the exit for the right-turn movement. In practice, this is often identical to R_5.

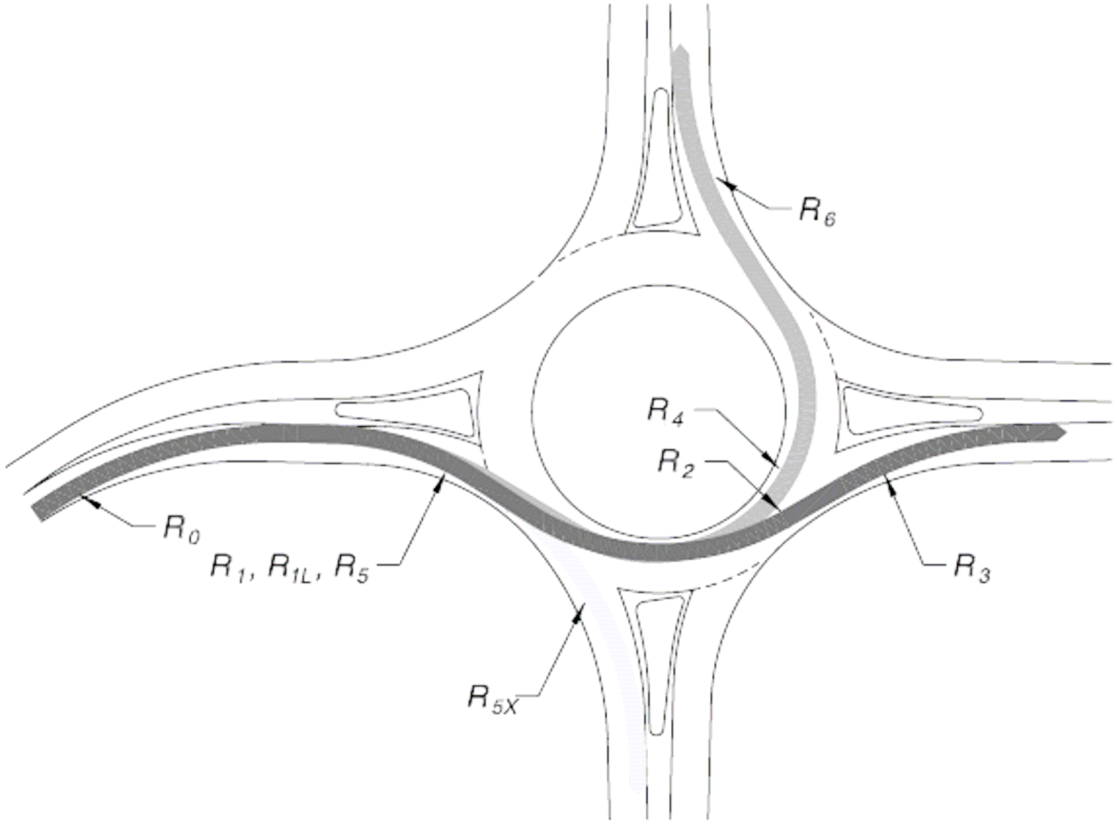

Figure G-1. Definition of Vehicle Path Radii.

The research team estimated predicted speeds for each roundabout using the FHWA methodology as described previously. For each site selected for the analysis, the team plotted plans to a scale of 1 inch = 50 ft and sketched fastest paths for each movement through the roundabout. For each path radius, the team estimated a speed by using the basic speed-curve relationships as defined in the AASHTO *Policy on Geometric Design of Streets and Roadways (G2).* When predicting the speeds at roundabouts, unless otherwise known, the assumed superelevation was –2 percent for the circulatory roadway in a roundabout and +2 percent for the entry and exit legs, consistent with the methodology used in the FHWA Roundabout Guide. The side friction factor was based on the curve radii as defined by the AASHTO Policy and plotted in the FHWA Roundabout Guide.

For multilane roundabouts, the fastest paths were assumed to occur irrespective of the presence of any striping on the approach, circulatory roadway, or departure. This deviates from the practice suggested in the FHWA Roundabout Guide but is consistent with the UK practice for estimating entry path curvature. This distinction was made to enable data extraction with the parameters used in the UK safety equations. In practice, the estimated difference in speeds between the two methods for estimating multilane paths is usually quite minor (1 to 3 mph).

References

G1. Robinson, B. W., L. Rodegerdts, W. Scarbrough, W. Kittelson, R. Troutbeck, W. Brilon, L. Bondzio, K. Courage, M. Kyte, J. Mason, A. Flannery, E. Myers, J. Bunker, and G. Jacquemart. *Roundabouts: An Informational Guide*. Report FHWA-RD-00-067. FHWA, U. S. Department of Transportation, June 2000.

G2. American Association of State Highway and Transportation Officials. *A Policy on Geometric Design of Highways and Streets*. AASHTO, Washington, DC, 2005.

APPENDIX H
STATISTICAL TESTING OF APPROACH-LEVEL SAFETY MODELS

Entering/Circulating Collisions

Model 1

Dependent Variable: entercirc
Observations Used: 100

Parameter	DF	Estimate	Standard Error	Wald 95% Confidence Limits		Chi-Square	Pr > ChiSq
Intercept	1	-13.2495	2.8978	-18.9291	-7.5699	20.91	<.0001
logaadt	1	1.0585	0.3096	0.4517	1.6652	11.69	0.0006
logcircaadt	1	0.3672	0.2283	-0.0803	0.8146	2.59	0.1078
Dispersion	1	1.6650	0.6546	0.7704	3.5982		

Model 2

Dependent Variable: entercirc
Observations Used: 97

Parameter	DF	Estimate	Standard Error	Wald 95% Confidence Limits		Chi-Square	Pr > ChiSq
Intercept	1	-13.0434	3.1036	-19.1263	-6.9605	17.66	<.0001
logaadt	1	0.9771	0.3342	0.3221	1.6321	8.55	0.0035
logcircaadt	1	0.3088	0.2469	-0.1752	0.7928	1.56	0.2112
Entry_radius	1	0.0099	0.0044	0.0013	0.0185	5.09	0.0241
Dispersion	1	1.6635	0.6865	0.7409	3.7350		

Notes:
1) Dispersion is same as AADT only model.
2) Larger entry radii associated with more accidents.

Model 3

Dependent Variable: entercirc
Observations Used: 100

Parameter	DF	Estimate	Standard Error	Wald 95% Confidence Limits		Chi-Square	Pr > ChiSq
Intercept	1	-12.2601	2.8528	-17.8514	-6.6687	18.47	<.0001
logaadt	1	0.9217	0.3117	0.3108	1.5327	8.74	0.0031
logcircaadt	1	0.2900	0.2268	-0.1545	0.7345	1.63	0.2010
Central_island_diame	1	-0.0076	0.0056	-0.0187	0.0034	1.84	0.1749
Entry_width	1	0.0582	0.0348	-0.0100	0.1263	2.80	0.0942
Dispersion	1	1.4949	0.6077	0.6738	3.3164		

Notes:
1) Dispersion is lower than AADT only model.
2) Larger entry radii associated with more accidents, t-stat 1.67.
3) Larger central island diameter associated with fewer accidents, t-stat 1.36.

Model 4

Dependent Variable: entercirc
Observations Used: 97

Parameter	DF	Estimate	Standard Error	Wald 95% Confidence Limits		Chi-Square	Pr > ChiSq
Intercept	1	-13.0579	3.0605	-19.0564	-7.0595	18.20	<.0001
logaadt	1	1.0048	0.3306	0.3568	1.6528	9.24	0.0024
logcircaadt	1	0.3142	0.2414	-0.1590	0.7874	1.69	0.1932
Entry_radius	1	0.0103	0.0043	0.0018	0.0188	5.64	0.0175
Central_island_diame	1	-0.0046	0.0053	-0.0149	0.0057	0.78	0.3782
Dispersion	1	1.5136	0.6591	0.6447	3.5536		

Notes:
1) Dispersion is similar to central island diameter and entry radius model.
2) Larger entry radii associated with more accidents, t-stat 2.40.
3) Larger central island diameter associated with fewer accidents, t-stat 0.87.

Model 5

Dependent Variable: entercirc
Observations Used: 93

Parameter	DF	Estimate	Standard Error	Wald 95% Confidence Limits		Chi-Square	Pr > ChiSq
Intercept	1	-8.7613	3.3624	-15.3515	-2.1710	6.79	0.0092
logaadt	1	0.9499	0.3374	0.2886	1.6113	7.93	0.0049
logcircaadt	1	0.2687	0.2516	-0.2243	0.7618	1.14	0.2854
Angle_to_next_leg	1	-0.0425	0.0171	-0.0760	-0.0089	6.16	0.0131
Entry_radius	1	0.0105	0.0042	0.0022	0.0188	6.16	0.0131
Dispersion	1	1.3016	0.6807	0.4670	3.6280		

Model 6

Dependent Variable: entercirc
Observations Used: 96

Parameter	DF	Estimate	Standard Error	Wald 95% Confidence Limits		Chi-Square	Pr > ChiSq
Intercept	1	-7.2158	3.0908	-13.2736	-1.1579	5.45	0.0196
logaadt	1	0.7018	0.3000	0.1138	1.2898	5.47	0.0193
logcircaadt	1	0.1321	0.2246	-0.3082	0.5724	0.35	0.5564
Angle_to_next_leg	1	-0.0276	0.0120	-0.0512	-0.0040	5.24	0.0220
Entry_width	1	0.0511	0.0263	-0.0004	0.1027	3.78	0.0518
Dispersion	1	1.0797	0.6333	0.3420	3.4085		

NOTE: The negative binomial dispersion parameter was estimated by maximum likelihood.

Dependent Variable: entercirc
Observations Used: 86

Analysis Of Parameter Estimates

Parameter	DF	Estimate	Standard Error	Wald 95% Confidence Limits		Chi-Square	Pr > ChiSq
Intercept	1	-8.9686	3.4834	-15.7959	-2.1412	6.63	0.0100
logaadt	1	0.8322	0.3639	0.1190	1.5455	5.23	0.0222
logcircaadt	1	0.1370	0.2692	-0.3906	0.6646	0.26	0.6108
var1	1	-138.096	67.1671	-269.741	-6.4505	4.23	0.0398
Dispersion	1	2.0324	0.9133	0.8423	4.9037		

Var1=1/entry path radius

Exiting/Circulating Collisions

Notes:
1) Exiting and circulating AADT terms are in right direction but are never significant.
2) Larger circulating widths, inscribed diameter and central island diameters associated with more accidents. 2 models were done, one with circulating width and inscribed diameter, the other with circulating width and central island diameter.

Model 1

Dependent Variable: circexit
Observations Used: 100

Parameter	DF	Estimate	Standard Error	Wald 95% Confidence Limits		Chi-Square	Pr > ChiSq
Intercept	1	-7.7145	3.8748	-15.3090	-0.1199	3.96	0.0465
logexit	1	0.3413	0.2591	-0.1664	0.8491	1.74	0.1876
logcircaadt	1	0.5172	0.3777	-0.2231	1.2575	1.88	0.1709
Dispersion	1	6.1315	1.5910	3.6872	10.1962		

Model 2

Dependent Variable: circexit
Observations Used: 100

Parameter	DF	Estimate	Standard Error	Wald 95% Confidence Limits		Chi-Square	Pr > ChiSq
Intercept	1	-11.6805	3.6262	-18.7879	-4.5732	10.38	0.0013
logexit	1	0.2801	0.2929	-0.2939	0.8541	0.91	0.3389
logcircaadt	1	0.2530	0.3247	-0.3834	0.8894	0.61	0.4359
Inscribed_circle_dia	1	0.0222	0.0071	0.0083	0.0361	9.81	0.0017
Circulating_width	1	0.1107	0.0470	0.0185	0.2028	5.54	0.0186
Dispersion	1	2.7694	0.8379	1.5305	5.0110		

Model 3

Dependent Variable: circexit
Observations Used: 100

Parameter	DF	Estimate	Standard Error	Wald 95% Confidence Limits		Chi-Square	Pr > ChiSq
Intercept	1	-11.2447	3.7745	-18.6426	-3.8469	8.88	0.0029
logexit	1	0.3227	0.3085	-0.2820	0.9275	1.09	0.2956
logcircaadt	1	0.3242	0.3393	-0.3409	0.9893	0.91	0.3394
Central_island_diame	1	0.0137	0.0066	0.0006	0.0267	4.23	0.0397
Circulating_width	1	0.1458	0.0510	0.0458	0.2459	8.17	0.0043
Dispersion	1	3.0519	0.9588	1.6488	5.6490		

Dependent Variable: circexit
Observations Used: 87

Analysis Of Parameter Estimates

Parameter	DF	Estimate	Standard Error	Wald 95% Confidence Limits		Chi-Square	Pr > ChiSq
Intercept	1	-3.8095	4.1461	-11.9357	4.3167	0.84	0.3582
logexit	1	0.2413	0.2889	-0.3249	0.8076	0.70	0.4035
logcircaadt	1	0.5626	0.3788	-0.1798	1.3051	2.21	0.1375
var2	1	372.8710	85.0465	206.1830	539.5590	19.22	<.0001
Dispersion	1	3.3171	0.9706	1.8694	5.8860		

Var2=1/circulating path radius

Dependent Variable circexit
Observations Used 87

Analysis Of Parameter Estimates

Parameter	DF	Estimate	Standard Error	Wald 95% Confidence Limits		Chi-Square	Pr > ChiSq
Intercept	1	-9.8334	4.3100	-18.2808	-1.3860	5.21	0.0225
logexit	1	0.6005	0.3025	0.0076	1.1934	3.94	0.0471
logcircaadt	1	0.7471	0.3860	-0.0093	1.5036	3.75	0.0529
var3	1	-387.729	121.1334	-625.146	-150.311	10.25	0.0014
Dispersion	1	4.4295	1.2473	2.5507	7.6922		

Var3=1/exit path radius

Approaching Collisions (includes rear-ends and loss of control on the approach)

1) Adding approach half width improves the fit marginally.
2) No other variables worked.

Model 1

Dependent Variable APP
Observations Used 139

Parameter	DF	Estimate	Standard Error	Wald 95% Confidence Limits		Chi-Square	Pr > ChiSq
Intercept	1	-5.6561	1.2119	-8.0313	-3.2808	21.78	<.0001
logaadt	1	0.6036	0.1463	0.3168	0.8903	17.02	<.0001
Dispersion	1	1.3297	0.2870	0.8710	2.0300		

Model 2

Dependent Variable APP
Observations Used 132

Parameter	DF	Estimate	Standard Error	Wald 95% Confidence Limits		Chi-Square	Pr > ChiSq
Intercept	1	-5.1527	1.2429	-7.5886	-2.7167	17.19	<.0001
logaadt	1	0.4613	0.1598	0.1481	0.7744	8.33	0.0039
Approach_half_width	1	0.0301	0.0136	0.0035	0.0567	4.93	0.0265
Dispersion	1	1.2895	0.3022	0.8146	2.0414		

APPENDIX I
STATISTICAL TESTING OF SPEED-BASED SAFETY MODELS

Model 1

Dependent Variable				APP		
Observations Used				36		
Parameter	DF	Estimate	Standard Error	Wald 95% Confidence Limits		Chi-Square	Pr > ChiSq
Intercept	1	-9.0059	3.7301	-16.3167	-1.6951	5.83	0.0158
logaadt	1	0.8255	0.4295	-0.0164	1.6674	3.69	0.0546
Speed_Differential_A	1	0.0622	0.0342	-0.0048	0.1291	3.31	0.0688
Dispersion	1	1.3683	0.6667	0.5265	3.5557		

Model 2

Dependent Variable				APP		
Observations Used				36		
Parameter	DF	Estimate	Standard Error	Wald 95% Confidence Limits		Chi-Square	Pr > ChiSq
Intercept	1	-9.9951	3.9006	-17.6402	-2.3499	6.57	0.0104
logaadt	1	0.8609	0.4307	0.0167	1.7050	3.99	0.0456
Approach_Speed__mph	1	0.0521	0.0286	-0.0040	0.1082	3.32	0.0686
Dispersion	1	1.3346	0.6678	0.5006	3.5586		

APPENDIX J
OPERATIONS APPENDIX

This appendix supports the operational analysis presented in Chapter 4 and provides detail on the specific operational data used for this project.

Operational Data Characteristics

Time Periods of Interest

Extraction of data from video recordings is a time-consuming and costly process. The limited project budget required that a strategy be developed to focus only on those time periods that would provide data to meet requirements established by the project team. One of the major requirements was to identify periods during which queues were present, so that measurements of capacity could be made. To identify these periods, each of the 166 DVDs recorded for individual approaches was reviewed, and the beginning and ending periods of each queue were noted.

This review identified that queues were present during 61 hours and 24 minutes, or 13 percent of the total of 474 hours of video recording. The maximum continuous queue recorded was 31 minutes and 39 seconds. However, most queues were much shorter, often one or two minutes in duration.

The selection of the time periods for which data would be extracted was based on the following criteria:

- The maximum queue duration, the mean queue duration, and the total queue duration were computed for each of the approaches. The approaches were then ranked according to each of these three factors.
- Time plots of the queues were reviewed to visually identify periods of queuing. For example, Figure J-1 shows periods for which vehicles are continuously present at the yield line for MD07-E (Taneytown, Maryland) during a thirty-minute period (the upper lines in the figure). The figure and its associated data show one queue that was present for a period of nine minutes and 37 seconds, from 1:50:29 through 2:00:06. By contrast, there was no queue present from 2:01:14 through 2:09:10, a period of nearly eight minutes. For the three hours of video available on the MD07-E1 DVD, the maximum queue duration was nearly eleven and a half minutes while the mean queue duration was one minute and 43 seconds. A queue was present 55 percent of the time, or one hour and 40 minutes.

Using these data and criteria, a total of 34 hours and 24 minutes of operations (at 13 sites) was identified for data extraction. This includes four two-lane sites (nine individual approaches) with a total of 18 hours and 30 minutes of continuous queuing and nine one-lane sites (15 individual approaches) with a total of 15 hours and 53 minutes of continuous queuing. This represents only seven percent of the total field video recording time, and demonstrates the extent of field recording that must be made to secure a useful amount of data.

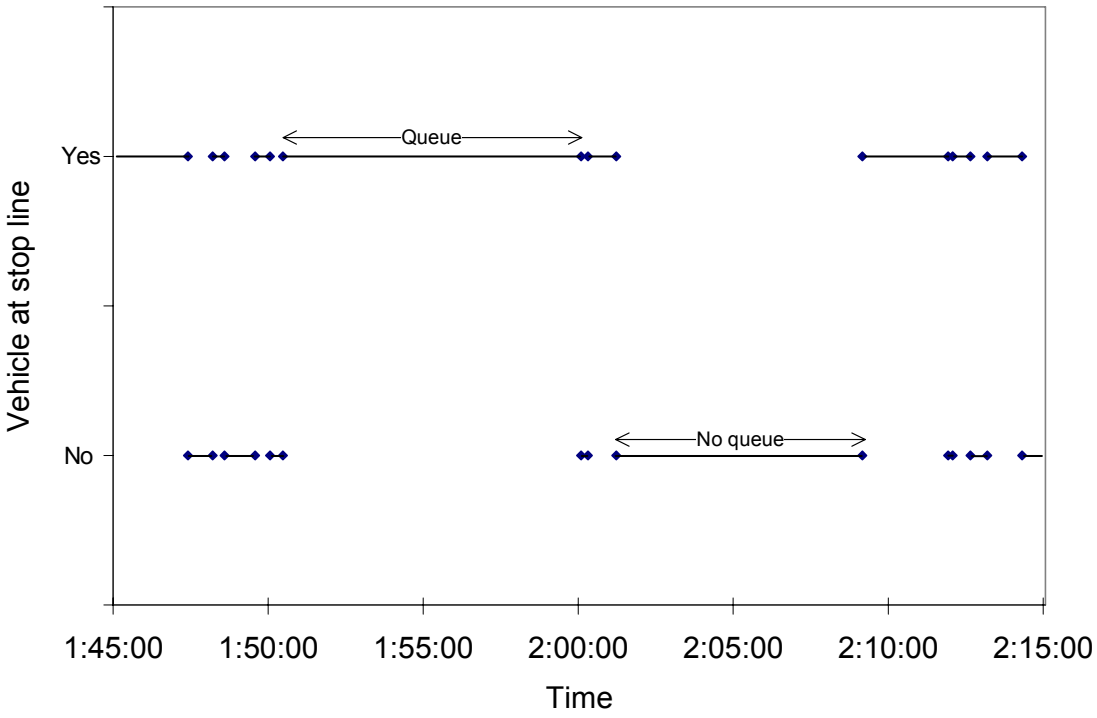

Figure J-1. Presence of Vehicle at Stop Line, MD07-E1.

Data Extraction Process

The data extraction process consisted of five steps, including (1) an initial review of the DVD to identify periods of queuing, (2) the extraction of the raw or event data using event recording software, (3) error checking, (4) data set merging, and (5) preparation of final data sets that included one-minute summaries and computation of selected parameters such as flow rates, delays, and critical gaps. Table J-1 summarizes the steps included in the data extraction process. The parameters and events listed in this table (entry time, for example) are defined in the following sections.

Primary Event Data. Five events were extracted from the DVDs using software that records keystrokes. When any of these five events occurred, the proper key was pressed and a time stamp was generated in a computer file. These events are listed in Table J-2 and illustrated in Figure J-2 for ME01-E (Gorham, Maine). For example, when a vehicle arrived at the yield line, the *"1"* event was recorded; when a vehicle entered the circulating roadway, the *"2"* event was recorded.

TABLE J-1. Data Extraction Process

Activity	Purpose	Description
Step 1. Initial DVD review	To identify periods of continuous queuing and pedestrian/bicycle activity	• Each DVD is reviewed for quality of field of view (can all points of interest be clearly observed?). • Each Sony camera DVD is reviewed for periods of continuous queuing. The begin and end times for queuing activity are noted. • Each time period is reviewed for pedestrian and bicycle activity.
Step 2. Raw data (event) extraction	To record the time stamps for all events of interest during periods of continuous queuing	Flow rate data. The following events are extracted for selected DVDs recorded with the omni-directional camera: • Entry time • Entry approach • Exit time • Exit approach • Vehicle type (passenger car or other)
		Gap data. The following events are extracted for selected DVDs recorded with the Sony camera: • First-in-queue time • Entry time • Conflict time • Exit time
		Delay data. The following events are extracted for selected DVDs recorded with the Sony camera: • Upstream time • First-in-queue time • Entry time
		Pedestrian/bicycle data. The following events are extracted for selected DVDs recorded with the Sony camera: • Pedestrian first-in-queue time • Pedestrian entry time • Vehicle yield • Pedestrian exit time • Pedestrian type • Pedestrian conflict time
Step 3. Error checking and time corrections	To identify keystroke (event recording) errors and to account for differences in DVD starting times	• Common events (Entry time, first in queue time, exit time) from the three data sets (flow rate data, gap data, delay data) are compared for consistency. Problems are reviewed and corrected. • Common vehicle events are identified for each DVD covering the same time periods. Time correction factors are computed based on the observation of these common vehicle events. Time stamps are adjusted based on this time correction factor. • One minute summaries are prepared for the common events to further verify the accuracy of the event data sets.

TABLE J-1 (cont.). Data Extraction Process

Activity	Purpose	Description
Step 4. Merge event data sets	To merge data sets for each roundabout approach	Data from the three data sets (flow rate data, gap data, delay data) for each approach and time period are merged. The following time/events are included for each vehicle: • Upstream time • First-in-queue time • Entry time • Exit time • Exit approach • Vehicle type The following data (time/events) are also recorded for the circulating vehicles affecting the subject approach: • Conflict time • Exit time
Step 5. Prepare data summaries and compute parameters of interest	To prepare one-minute summaries for each data set and to compute selected parameters	The following data are computed based on the merged data sets prepared in step 4. • Turning movement flow rates, 1-minute summaries • Delays, 1-minute summaries • Follow up times • Critical gaps • Entry and circulating flows during periods of continuous queuing, 1-minute summaries

TABLE J-2. Operational Events of Interest

Event	Keystroke	Description
Entry time	2	The entry of a vehicle into the roundabout from the approach. The time was recorded when the vehicle crossed the yield line; the lane placement of the vehicle (either left lane or right lane) was recorded for two lane roundabouts. The vehicle type was also recorded.
First-in-queue time	1	The arrival of a vehicle into the server or first-in-line position on the approach. The time was recorded when the vehicle was about to enter the roundabout (if it did not stop) or the time that it stopped at or near the yield line waiting to enter the roundabout.
Upstream time	z	The passage of a vehicle past a point upstream of where a queue will form on the approach.
Conflict time	s	The passage of a vehicle through the conflict point on the roundabout, a point that is adjacent to the point of entry for a minor street vehicle.
Exit time	a	The exiting of a vehicle from the roundabout.

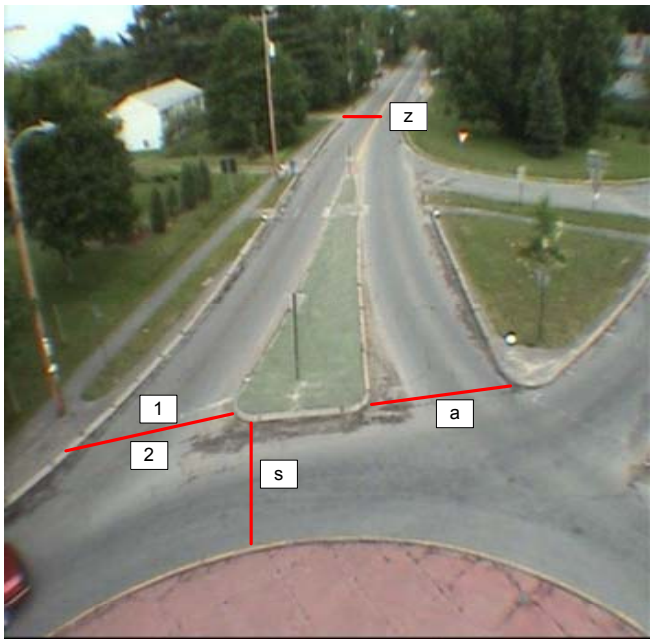

Note: Numbers and letters in figure are defined in Table J-2.

Figure J-2. Location of Events of Interest on Roundabout Approach (ME01-E).

Secondary Derived Data. The event data were used to compute a set of secondary, or derived, data. For example, the number of events that occur during a specified time interval is the flow rate past the point at which the event was recorded. Similarly, the time difference between the passing of two vehicles at a given point is the headway between these two vehicles. A complete list of the secondary data is given below:

- The *flow rate* is the number of vehicles passing by a given point during a specified time interval. Flow rates were computed for entry flows, circulating flows, and exit flows. Events *"2"*, *"s"*, and *"a"* described previously were used to compute these flow rates.
- *Delay* is the time spent traveling from the *"z"* line to the yield line (the *"2"* event) on a given approach that is in excess of the free flow time for this same path. The free flow time was measured for each approach, considering a sample of vehicles moving unobstructed from the *"z"* line to the *"2"* (yield) line. The actual travel time for each vehicle was computed for this same pair of events. The difference between these two travel times is the delay for a given vehicle.
- The *turning movement proportion* is the proportion of vehicles entering from one approach and traveling to each of the possible exit points on the roundabout. The *"2"* and *"a"* events were used to compute the turning movement data.
- The gaps between vehicles on the circulating roadway that were accepted or rejected by vehicles on the minor approach were recorded. A gap sequence is the sequence of events that includes the first circulating vehicle (events *"s"* or *"a"*), any intervening entry vehicles (event *"2"*), and the second circulating vehicle (events *"s"* or *"a"*).

For multi-lane roundabouts, the lane position of vehicles on the circulating roadway must be considered in this gap sequence.

- The service time is the time difference for a minor approach vehicle between the *"1"* event and the *"2"* event. This is the time that a vehicle spends in the server.
- The move up time is the time difference between the entry of one vehicle into the roundabout (the *"2"* event) and the arrival of the following vehicle at the yield line (the *"1"* event).
- The travel time on the roundabout is the elapsed time from the entry of a vehicle into the roundabout (the *"2"* event) and the exit of the vehicle from the roundabout (the *"a"* event).
- The proportion of time that a queue exists on an approach for each minute (referred to later in this paper as *proportion time queued*) is the sum of the service times plus the move-up times for all vehicles that entered the roundabout during that minute, divided by sixty seconds.

One-minute summaries were prepared for the following secondary data:

- Entry flow
- Conflicting flow
- Exit flow
- Average delay
- Proportion time queued

The following gap data were computed for each vehicle entering the roundabout:

- The duration of the accepted or rejected lag, defined as the time from the arrival of the minor vehicle at the server (the *"1"* event) to the arrival of the next conflicting vehicle (the *"s"* event).
- The durations of all gaps that are rejected by the minor vehicle, defined as the times between subsequent vehicles on the circulating roadway (*"s"* events).
- The duration of the gap that is accepted by the minor vehicle, defined as the time between the two consecutive conflicting vehicles on the circulating roadway (*"s"* events).

The following terms are used in the subsequent analysis of the gap data.

- The lag is defined as the time between the arrival of the vehicle in the first in queue position (the *"1"* event) and the passage of the next conflicting vehicle (the *"s"* event).
- The gap is defined as the time between consecutive passages of two conflicting vehicles (the *"s"* event).

Turning Movement Data

Turning movement flow rates were determined using the entry flow rate and the turning movement proportions. The entry flow rate was based on the *"2"* event data, described earlier. Turning movement proportions were estimated by tracking randomly selected vehicles through the roundabout, where the turning movement proportion of the sample was assumed to be similar to that of the population. Vehicle samples were chosen randomly, by following the steps below, while viewing the omni-directional video:

- Step 1. Select a vehicle to sample

- Step 2. Track the selected vehicle to its exit leg
- Step 3. Record the turning movement and times for entry and exit for each vehicle
- Step 4. Repeat steps 1 through 3.

The turning movement proportions were then calculated from the sampled data. Finally, the turning movement flow rate was determined by multiplying the entry flow rate by the turning movement proportion.

Summary of the Operational Database

The operational database assembled for this project represents a rich resource for roundabout operations, not only for this project but also for future research efforts. The database for one-lane sites includes fifteen unique approaches and a total video time of 15:53:16. The database for two-lane sites includes nine unique approaches and a total video time of 18:30:18. In addition, additional video provided by others was used to supplement the video collected and extracted using the methods described above.

Table J-3 shows some of the highlights of the data sets that were produced based on the 34 hours and 24 minutes of traffic operations. The database for the one-lane sites includes 884 one-minute time intervals. The maximum entry flow rate is 24 vehicles per minute, while the maximum conflicting flow rate is 18 vehicles per minute. The maximum one-minute average delay is 47.1 seconds per vehicle. The mean one-minute proportion time queued for all one-minute data points is 0.78.

The database for the two-lane sites includes 923 one-minute time intervals. The maximum entry flow rate per lane is 19 vehicles per minute, while the maximum conflicting flow rate per lane is 48 vehicles per minute. The maximum one-minute average delay is 121.7 seconds per vehicle. The mean one-minute proportion time queued data is 0.55 for the left lane data and 0.65 for the right lane data.

A gap sequence consists of all gaps that must be considered by an entering vehicle. For the one-lane sites, 10,751 gap sequences were measured. Of these:

- The entry vehicle accepted the lag 77 percent of the time (8,282 gap sequences),
- The entry vehicle rejected the lag but then accepted the first gap 12 percent of the time (1,318 gap sequences), and
- The entry vehicle rejected the lag, rejected the first gap, but then accepted a subsequent gap 11 percent of the time (1,151 gap sequences).

For the two-lane sites, 13,530 gap sequences were measured. Of these:

- The entry vehicle accepted the lag 39 percent of the time (5,295 gap sequences),
- The entry vehicle rejected the lag but then accepted the first gap 8 percent of the time (1,067 gap sequences), and
- The entry vehicle rejected the lag, rejected the first gap, but then accepted a subsequent gap 53 percent of the time (7,168 gap sequences).

The mean travel time (from the entry to the exit of the roundabout) for one lane sites ranged from 3.1 seconds for right turning vehicles to 10.8 seconds for left turning vehicles. For two lane sites, the range was 2.7 seconds for right turning vehicles to 11.9 seconds for left turning vehicles.

TABLE J-3. Operational Data Set Highlights

Parameter	One-lane sites	Two-lane sites
Summary		
• Number of sites	9	4
• Number of unique approaches	15	9
• Total video time for extracted data	15:53:16	18:30:18
Number of one-minute data points		
• Total	884	923
• Number in which proportion time queued exceeded 0.90	344	135 (left lane) 218 (right lane)
Ranges, one minute measurements		
• Entry flow per lane, veh/min	2 – 24	0 – 19
• Conflicting flow per lane, veh/min	0 – 18	0 – 48
• Delay, sec/veh	0.0 – 47.1	0 – 121.7
Mean proportion time queued for all one-minute data points	0.78	0.55 (left lane) 0.65 (right lane)
Gap sequences		
• Total	10,751	13,530
• Number involving an accepted lag	8,282	5,295
• Number involving a rejected lag followed by an accepted gap	1,318	1,067
• Number involving a rejected lag, followed by one or more rejected gaps, followed by an accepted gap	1,151	7,168
Turning movement proportions, means for sites		
• Left turns	0.29	0.35*
• Through movements	0.46	0.35
• Right turns	0.31	0.29
Travel time through roundabout (sec)		
• Left turns	10.8	11.8
• Through movements	6.6	7.4
• Right turns	3.1	2.7
• U-turns	16.2	18.8
* Turning movement proportion data were not available for all multi-lane roundabouts. The data shown here are averaged over all four approaches for two different roundabouts (MD04 and VT03), a total of eight approaches.		

Capacity and Delay Data

For capacity analysis, the data described above were extracted in one-minute intervals during periods of persistent queuing. Persistent queuing was identified at eighteen one-lane approaches (from a total of eleven one-lane sites) and seven two-lane approaches (from a total of four multilane sites). A total of 320 and 400 minutes of data during visually verified queuing was extracted at the single-lane and multilane sites respectively. The delay observations are not dependant on periods of persistent queuing, and hence a much larger data based is available for the analysis. Respectively, 849 and 1,012 minutes of delay data were extracted at the single- and multilane sites.

The strength and duration of queuing, the entry capacity flow relationships, and the approach delay and variation are described in subsequent sections.

Single-Lane Approach Summary

A summary of the general operational characteristics of the eighteen single-lane approach data is illustrated in Table J-4. A maximum of 85 queued minutes were observed at WA04-N (Port Orchard, Washington). As noted, the total minutes of queuing are not sequential, and in the case of WA04-N the data were collected over two days. Ten of the eighteen approaches have less than 10 minutes of full minutes of queuing. The maximum observed entry flow is 24 vehicles per minute, or 1440 vehicles per hour, observed at MD06-N (Lothian, Maryland). The maximum conflicting flow is 18 vehicles per minute, or 1080 vehicles per hour, observed at WA01-W (Gig Harbor, Washington). The maximum delay is 47 seconds per vehicle.

The duration of the queue (sequential minutes of queuing), and queue characteristics, are illustrated in Table J-5. While the maximum number of minutes of queuing is observed at WA04-S (Port Orchard, Washington), ME01-E (Gorham, Maine) had a sustained queue for 32 minutes, followed by MD07-E (Taneytown, Maryland), which had a sustained queue for 12 minutes. Five of the eighteen approaches only have a sustained queue of one minute. The maximum queue length was in excess of 20 vehicles.

Table J-5 also illustrates the total time that the approach queue exceeds the distance *z* upstream of the entry line. This distance varies based on the approach, and is between five and eight vehicles in length. Approximately 10 of the full minutes of queuing observations have a queue length less than *z*. Most queued minute observations have queues that extend beyond *z* for some portion of the minute.

TABLE J-4. Parameter Summary for One-Lane Sites, One-Minute Data

Site	Location	Full minutes of queuing (# mins)	Entry flow (veh/min)		Conflicting flow (veh/min)		Delay (sec/veh)	
			Min	Max	Min	Max	Min	Max
MD06-N	Lothian, MD	14	2	**24**	0	5	0.3	16.0
MD06-S	Lothian, MD	4	3	10	5	15	5.4	35.7
MD07-E	Taneytown, MD	56	2	20	0	11	0.0	44.7
ME01-E	Gorham, ME	42	5	18	1	13	0.2	42.3
ME01-N	Gorham, ME	1	2	9	5	15	3.0	38.0
MI01-E	Okemos, MI	8	4	12	3	13	1.5	**47.0**
OR01-S	Bend, OR	15	2	15	0	15	0.4	44.1
WA01-N	Gig Harbor, WA	3	2	10	3	16	1.1	47.1
WA01-W	Gig Harbor, WA	6	3	11	3	**18**	2.9	43.5
WA03-E	Bainbridge Island, WA	2	5	16	1	7	1.7	14.3
WA03-S	Bainbridge Island, WA	28	2	16	0	12	0.3	25.8
WA04-E	Port Orchard, WA	15	6	22	0	14	2.3	18.9
WA04-N	Port Orchard, WA	**85**	3	23	0	13	0.2	28.6
WA04-S	Port Orchard, WA	4	5	16	3	13	0.6	32.4
WA05-W	Sammamish, WA	6	8	21	0	6	1.3	15.1
WA07-S	Lacey, WA	1	11	18	3	7	4.8	13.2
WA08-N	Kennewick, WA	4	7	17	3	13	0.5	19.9
WA08-S	Kennewick, WA	24	8	23	0	10	0.5	19.7

Note: **Bold** indicated maximum value observed.

TABLE J-5. Intervals and Length of Queuing for One-Lane Sites

Approach	Full minutes of queuing (# mins)	Maximum duration of queuing (mins)	Maximum queue length (vehs)	Total time where queue > *z*
MD06–N	14	2	20+	0:26:34
MD06–S	4	1	7	NA
MD07-E	56	12	22+	0:54:08
ME01-E	42	**32**	20+	0:43:29
ME01-N	1	1	7	0:01:33
MI01-E	8	1	NA	NA
OR01-S	15	4	8	0:15:35
WA01–N	3	4	8	0:03:26
WA01-W	3	2	5	0:02:15
WA03-E	2	1	4	0:02:16
WA03-S	28	5	8	0:34:08
WA04-E	15	5	10+	0:18:18
WA04-N	**85**	8	11+	1:59:53
WA04-S	4	3	8	0:03:41
WA05-W	6	6	12+	0:15:31
WA07-S	1	1	5	0:04:23
WA08-N	4	3	NA	NA
WA08-S	24	15	NA	NA

As shown in Table J-6, a large number of entering vehicles hesitate unnecessarily at the entry line. No conflicting vehicles were observed during these periods; however, the impact of the exiting vehicles on the entering vehicles is significant enough to warrant further investigation.

Single-Lane Entry Flow and Conflicting Flow Data

Figure J-3 illustrates the entry flow as a function of the conflicting flow for queuing and non-queuing minutes. The density of the data is shown for each entry flow-conflicting flow combination. A large number of observations fall between an entry-plus-conflicting flow of 18 vehicles per minute, or 1080 vehicles per hour. The maximum observed entry-plus-conflicting flow was 25 vehicles per minute, or 1500 vehicles per hour.

A potential caution regarding the data is that other roundabout sites may be serving higher volumes (and thus operating at higher capacities) but were not included in the data due to a lack of observed queuing. However, as can be seen in Figure J-4 for the sites for which data were reduced, entry volumes are much lower for the non-queued minutes than for queued minutes. There are very few non-queued data points that fall within the queue data, and there are no non-queued data points that exceed the queued data. This cannot discount the possibility that sites outside of those for which data were collected and reduced may experience higher capacities, but a more extensive data collection and reduction effort was not possible within the scope and budget of this effort.

TABLE J-6. Percent of Vehicles that Hesitate Unnecessarily at One-Lane Sites

Site #	% Entry Vehicles (that yield to non-conflicting vehicles)
MD06-N	26
MD06-S	0
MD07-E	6
ME01-E	5
ME01-S	33
MI01-E	NA
OR01-S	5
WA01-N	8
WA01-W	0
WA03-E	40
WA03-S	13
WA04-E	14
WA04-N	11
WA04-S	4
WA05-W	11
WA07-S	7
WA08-N	NA
WA08-S	NA

The maximum entry flow as a function of the conflicting flow for data measured during period of continuous queuing is illustrated in Figure J-5. When there is no conflicting flow (data along the *y*-axis) the maximum entry flow varies between 15 and 25 vehicles per minute, or 900 and 1500 vehicles per hour. A maximum conflicting flow of approximately 15 vehicles per minute or 900 vehicles per hour was observed. Under this condition the entry capacity varies between 5 and 10 vehicles per minute, or 300 and 600 vehicles per hour.

The maximum entry and conflicting flow for site approaches with 15 or more minutes of queued data are illustrated by site in Figure J-6. For a given conflicting flow, WA04-N (Port Orchard, Washington) and MD07-E (Taneytown, Maryland) have significant variation in the maximum entry flow. Given that the geometry at the approach is fixed, the minute-by-minute variation in the maximum entry flow is dictated by driver behavior, vehicle type, and in some cases the apparent influence of exiting vehicles. The OR01-S site (Bend, Oregon) has high conflicting flows with maximum entering flows that are typical when compared with observations at other sites. The WA08-S site (Kennewick, Washington) has typically high maximum entry flows; these are likely the result of a large proportion of high school drivers due to the site's proximity to a high school.

Entry flow (veh/min) \ Conflicting flow (veh/min)	0	1	2	3	4	5	6	7	8	9	10	11	12	13	14	15	16	17	18	19	20	21	22	23	24	25
25																										
24		1																								
23		1																								
22	1		1																							
21	1	1																								
20	2	1	2																							
19	3	3	2	4																						
18	5	4	9	4	3	2	1																			
17	2	3	7	7	7	1	2																			
16	2	5	6	10	5	4	1			1																
15	2	6	9	15	6	7	4	4	2	1	1															
14	4	8	6	20	17	9	8	5	2																	
13	1	3	9	10	7	16	13	2	3		1	1														
12	3	3	5	9	16	12	16	8	7	3																
11	4	5	6	7	6	11	12	5	7	9	3	2	2													
10	1	3	5	8	8	8	7	9	11	6	7	3														
9	1	4	5	5	9	5	6	7	6	4	6	2	4													
8	2	1	4	4	7	5	9	8	5	3	4	1	2	2	4	2										
7	1	1	2	4		7	2	8	2	3	5	1	4	2	1	2										
6	1	5	1	2	2	6	8	2	4	1	3	1	3		3		1									
5		2		2	1	1	2	1	1	2	5	2	2	2	2	2			1							
4	1				1	2	1	5	2	2	1	5	1	2												
3			3	3		2	1	1		1		1	1		2	2										
2	1	2	2	1	1	1					1		2			1										
1																										

Figure J-3. Entry Flow vs. Conflicting Flow, Number of Observations for Each Entry Flow/Conflicting Flow Cell, One-Lane Sites

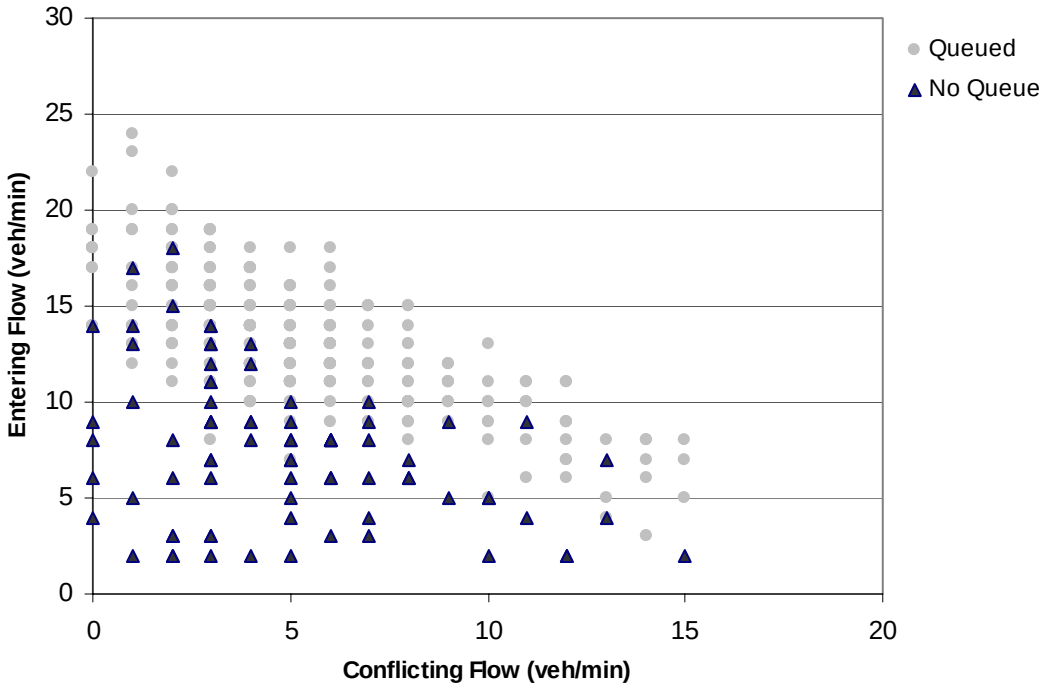

Figure J-4. Entry and Conflicting Flow for Queued and Non-Queued Minutes

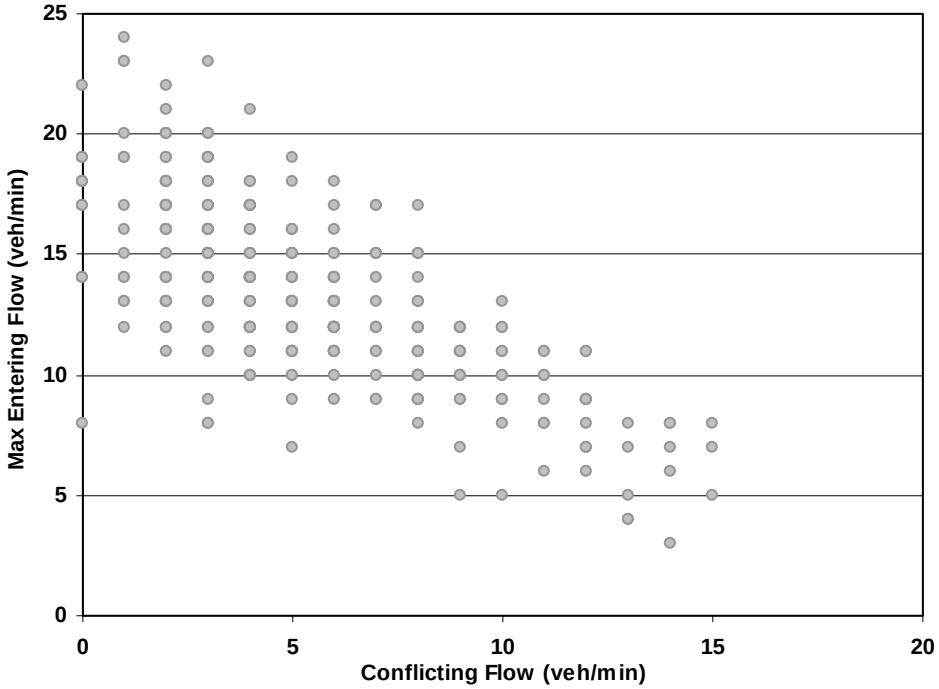

Figure J-5. Maximum Entry Flow as a Function of Conflicting Flow, One-Minute Data

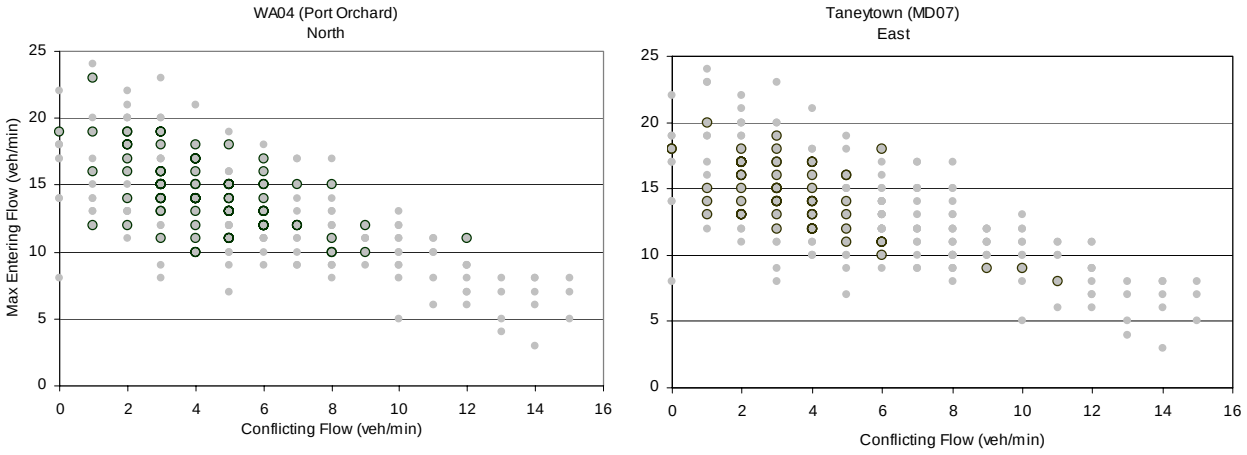

Figure J-6. Maximum Entry Flow as a Function of Conflicting Flow – Sites with Greater Than 15 or More Full Minutes of Queuing

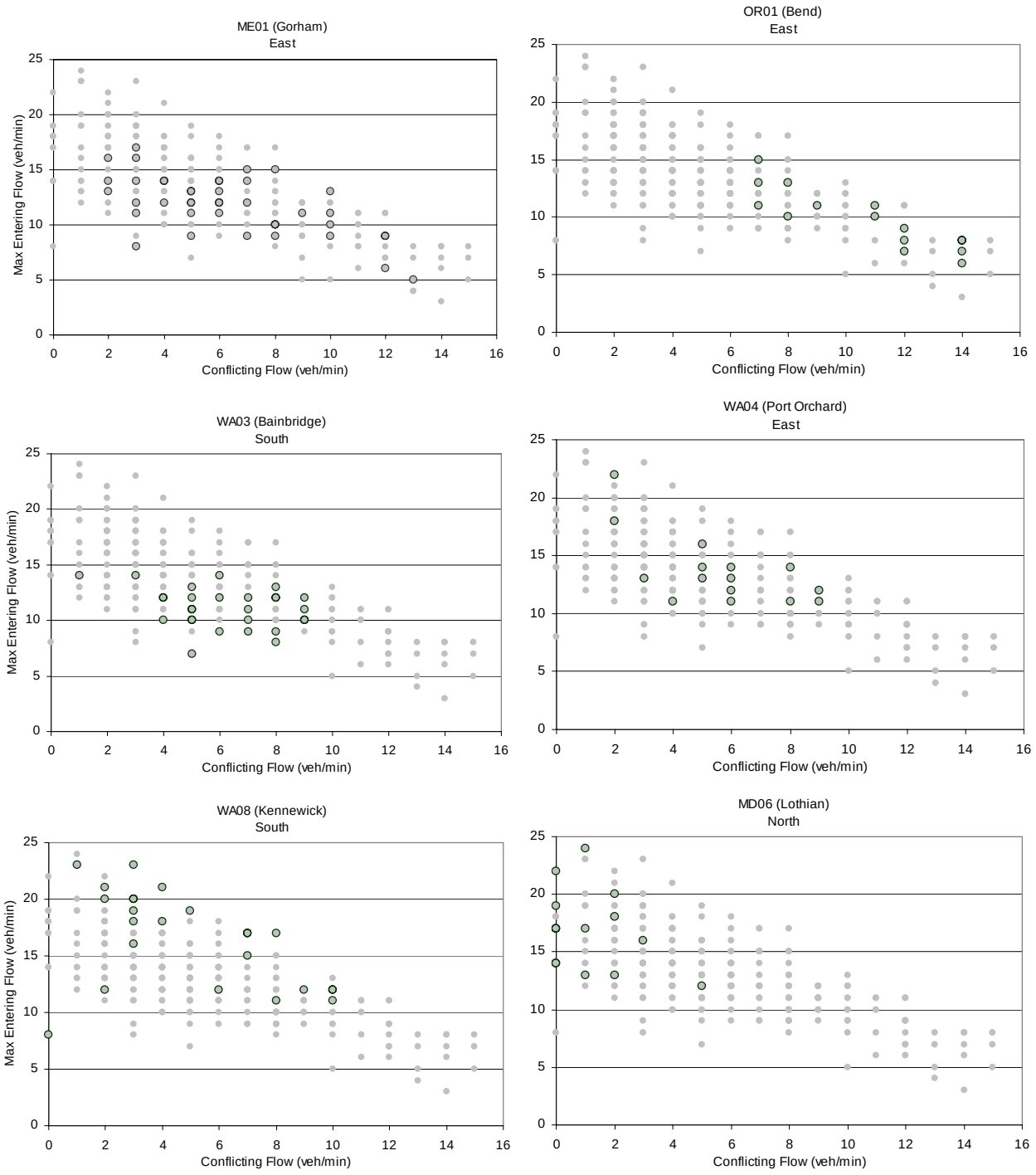

Figure J-6 (cont). Maximum Entry Flow as a Function of Conflicting Flow – Sites with Greater Than 15 or More Full Minutes of Queuing

Single-Lane Delay Data

The measured delay is based on the difference between the free flow and measured travel time of a travel trip between *z* (an arbitrary distance upstream of the entry line) and the entry line. By definition, *control delay* at a roundabout includes the initial deceleration delay, queue move-up time and stopped delay caused by the traffic control device and the right-of-way rules it establishes. If the queue is greater than z, the deceleration delay and some of the queue move-up time is excluded. As noted in Table J-5, most of the data collected during a full minute of queuing are also observations where the queue exceeds z. Furthermore, the deceleration delay is also excluded for observation where the queue is just less than z. Because this behavior has not been identified on a minute-by-minute basis, only preliminary delay comparisons can be made.

Figure J-7 illustrates the frequency of delay observations for the one-lane approaches, using five-second bins from zero seconds to 50 seconds. The mean delay is 9.9 seconds. Most of the delay measurements are less than 15 seconds per vehicle.

Figure J-8 illustrates a plot of the mean delay for each entry flow/conflicting flow pair. As expected, delays increase as the combination of entry and conflicting flows increase.

Multilane Approach Summary

Table J-7 summarizes the multilane approach characteristics. Of the eight approaches, four different lane configurations:

- Two entry and two conflicting lanes (5 approaches),
- Two entry and one conflicting lane (1 approach),
- One entry and two conflicting lanes (1 approach), and
- Two entry lanes (one short lane) and two conflicting lanes (1 approach).

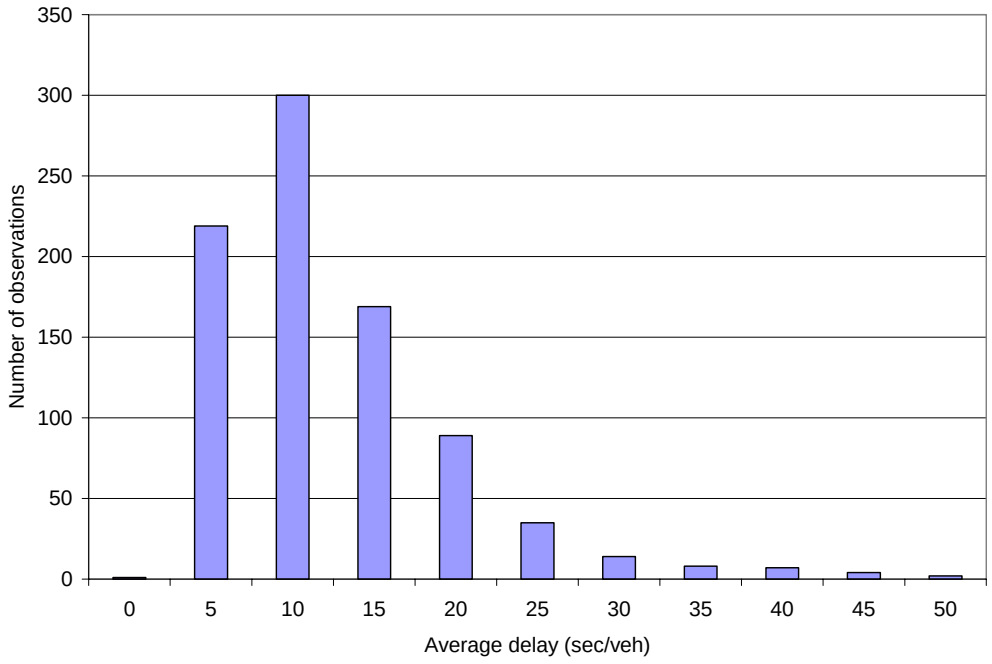

Figure J-7. Number of One-Minute Observations, Average Delay, One-Lane Sites

Entry flow (veh/min)	Conflicting flow (veh/min)																								
	0	1	2	3	4	5	6	7	8	9	10	11	12	13	14	15	16	17	18	19	20	21	22	23	24	25
25																										
24		2.8																								
23		2.6																								
22	3.9		6.9																							
21	5.0	5.0																								
20	4.1	11.7	5.1																							
19	4.1	4.4	2.6	7.7																						
18	6.5	5.3	6.0	5.7	6.0	6.3	11.9																			
17	4.1	4.3	13.1	9.1	9.1	5.1	8.6																			
16	4.3	6.4	9.2	9.0	7.4	9.5	10.0			7.3																
15	9.9	8.5	6.5	8.7	8.8	9.2	8.3	11.9	15.4	12.5	10.2															
14	5.4	7.5	14.7	8.0	9.9	8.5	10.6	8.7	9.9																	
13	1.0	10.4	15.1	8.3	10.6	12.3	11.0	7.5	12.9		9.5	6.5														
12	5.6	11.5	7.2	6.8	9.3	10.7	10.9	12.5	11.1	17.4																
11	5.2	4.7	8.7	6.6	7.4	16.6	14.1	9.9	10.6	13.0	16.7	18.2	25.2													
10	4.9	6.3	9.2	6.1	10.9	9.2	10.9	12.9	14.9	13.8	14.7	19.0														
9	1.7	4.0	4.5	4.4	7.3	9.6	7.9	8.3	13.2	12.0	18.6	7.8	21.5													
8	2.6	3.6	6.2	10.6	7.5	3.8	4.2	8.4	14.6	11.6	16.1	31.8	12.6	30.2	19.2	18.4										
7	18.7	3.0	10.3	5.3		10.4	8.7	9.2	5.7	12.5	10.2	7.8	21.0	10.3	44.1	20.9										
6	0.6	6.1	0.8	6.7	3.2	5.5	5.6	5.3	8.6	21.0	6.1	43.5	21.5		18.3		25.9									
5		6.9		5.7	2.1	2.2	9.3	4.9	3.8	4.9	11.7	20.2	15.6	19.1	25.2	29.2			20.6							
4	3.6				4.1	5.8	3.8	5.9	14.5	5.2	6.6	11.2	38.0	26.3												
3			1.2	2.3		11.6	2.8	1.2		15.0		6.8	4.6		21.5	14.0										
2	1.9	0.9	1.6	5.8	1.4	0.3					3.0		5.6			3.5										
1																										

Figure J-8. Entry Flow vs. Conflicting Flow, One-Minute Data, Delay for One-Lane Sites

TABLE J-7. Multilane Site Characteristics

Site	Location	Lane description	Year Open	Entry Lane Utilization (R/L)	Turning Proportion				Notes
					Left	Thru	Right	U-Turn	
CO51-E	Vail, CO	2L entry 2L circulating	1995	60/40	N/A	N/A	N/A	N/A	
FL11-E	Clearwater, FL	2L entry 2L circulating	1999	55/45	N/A	N/A	N/A	N/A	
FL11-W	Clearwater, FL	2L entry 2L circulating	1999	55/45	N/A	N/A	N/A	N/A	
MD04-E	Baltimore, MD	2L entry, 1L circulating	1999	35/65	**72%**	28%	1%	0%	20% of lefts in right lane
MD05-NW	Towson, MD	1L entry, 2L circulating - unstriped	1996	N/A (1L)	N/A	N/A	N/A	N/A	
MD05-W	Towson, MD	2L entry 2L circulating- unstriped	1996	65/35	N/A	N/A	N/A	N/A	Short right lane
VT03-W	Brattleboro, VT	2L entry, 2L circulating	2000	75/25	30%	49%	21%	0%	50% of lefts in right lane; 15% of throughs in left lane
VT03-E	Brattleboro, VT	2L entry, 2L circulating- unstriped	1999	60/40	28%	39%	31%	3%	
VT03-S	Brattleboro, VT	2L entry (at times 3L), 2L circulating- unstriped	1999	75/25	19%	32%	46%	4%	
WA09-E	Gig Harbor, WA	2L entry, 2L circulating	2001	90/10	9%	**86%**	5%	1%	10% of throughs in left lane

The two-lane southern approach at VT03-S (Brattleboro, Vermont) behaves as three lanes at times (it was previously a three-lane entry before being re-striped as a two-lane entry with no changes to the curb locations).

A utilization of 90 percent in the right lane and 10 percent in the left lane was observed on the east approach of WA09-E (Gig Harbor, Washington). The heavy demand for the right lane is due to the two single-lane downstream exits. MD04-E (Baltimore County, Maryland) is the only site with heavy use of the left lane. Despite markings that allow left turns in both lanes, only 20 percent of left turn vehicles queue in the right lane. The VT03 (Brattleboro, Vermont) site has heavy use of the right lane; however, 50 percent of the left turn movements are performed from the right lane, and only 15 percent of the through movements are performed from the left lane. In this case, drivers do not appear to find the left lane desirable.

A summary of the general operational characteristics of the multilane approach data is illustrated in Table J-8. A maximum of 194 queued minutes were observed at WA09-E (Gig Harbor, Washington). The total minutes of queuing are not sequential, and in the case of WA09-E the data were collected over two days. The maximum observed entry flow in the right lane is 21 vehicles per minute, or 1260 vehicles per hour, observed at WA09-E. The maximum observed entry flow in the left lane is 15 vehicles per minute, or 900 vehicles per hour, observed at MD04-E (Baltimore County, Maryland). The maximum conflicting flow is 42 vehicles per minute, or 2520 vehicles per hour, observed at MD05-NW (Towson, Maryland). The maximum delay in the left and right lanes, respectively, is 55 seconds per vehicle (MD04-E) and 121 seconds per vehicle (MD05-NW).

The duration of the queue (sequential minutes of queuing), and queue characteristics, are illustrated in Table J-9. While the maximum number of minutes of queuing is observed at WA09-E (Gig Harbor, Washington), the MD04-E (Baltimore County, Maryland) has the longest sustained queue of 21 minutes. Two of the eight approaches only have a sustained queue for two minutes.

TABLE J-8. Summary of Multilane Sites, One-Minute Data

Site	Location	Left entry flow (veh/min)		Right entry flow (veh/min)		Total conflicting flow (veh/min)		Left entry delay (sec/veh)		Right entry delay (sec/veh)	
		Min	Max	Min	Max	Min	Max	Min	Max	Min	Max
CO51-E	Vail, CO	3	10	5	14	N/A	N/A	13	25	N/A	N/A
FL11-E	Clearwater, FL	N/A	N/A	N/A	N/A	N/A	N/A	N/A	N/A	N/A	N/A
FL11-W	Clearwater, FL	N/A	N/A	N/A	N/A	N/A	N/A	N/A	N/A	N/A	N/A
MD04-E	Baltimore, MD	**4**	**15**	1	14	2	16	**10**	**55**	1	33
MD05-NW	Towson, MD	N/A	N/A	1	16	**8**	**42**	N/A	N/A	**16**	**121**
MD05-W	Towson, MD	0	4	2	5	20	28	19	36	25	40
VT03-W	Brattleboro, VT	0	9	4	16	3	23	4	33	0	26
VT03-E	Brattleboro, VT	0	10	1	11	11	20	6	40	9	40
VT03-S	Brattleboro, VT	1	10	8	15	7	14	5	22	1	22
WA09-E	Gig Harbor, WA	0	16	**3**	**21**	3	18	0	36	4	76

TABLE J-9. Summary of Multilane Site Operational Characteristics

Site #	Location	Full queued minutes (Left or Right)	Duration of queue (mins)
CO51-E	Vail, CO	16	14
FL11-E	Clearwater, FL	N/A	N/A
FL11-W	Clearwater, FL	N/A	N/A
MD04-E	Baltimore, MD	36	**21**
MD05-NW	Towson, MD	33	14
MD05-W	Towson, MD	16	2
VT03-W	Brattleboro, VT	16	5
VT03-E	Brattleboro, VT	20	5
VT03-S	Brattleboro, VT	83	2
WA09-E	Gig Harbor, WA	**194**	17

Multilane Entry Flow and Conflicting Flow Data

Figure J-9 illustrates the right-lane and left-lane entry flow as a function of the conflicting flow for queuing and non-queuing minutes. The density of the data is shown for each entry-conflicting flow combination. In the right-lane, a large number of entry plus conflicting flow observations are around 20 to 22 vehicles per minute. In contrast, the left-lane observations are much lower, around 13 to 15 vehicles per minute. The maximum entry plus conflicting flow is 29 vehicles per minute or 1740 vehicles per hour.

Figure J-10 illustrates the data for visually observed minutes of queuing identified in either the left or right-lane. The data are broken into observations for the different lane configurations. The two-entry/two-conflicting lane data are dominated by observations at WA09-E (Gig Harbor, Washington). As noted, WA09-E has high right-lane utilization, and there are a number of zero entry flow observations in the left lane. The MD04-E (Baltimore County, Maryland) has two entry lanes, one conflicting lane, and high utilization of the left lane. As a result, the right-lane data is typically low. MD05-NW (Towson, Maryland) has one entry lane and, as shown, some of the highest conflicting flows observed at the multilane sites.

Capacity of the approach is defined as the sum of the maximum entry flow in each lane. Problematic to the investigation of capacity of the approach is the lack of queuing in each lane within the same minute.

The two-entry/two-conflicting right-lane data is illustrated in Figure J-11. For a given conflicting flow, the WA09-E (Gig Harbor, Washington) and VT03-W (Brattleboro, Vermont) sites have significant variation in the maximum entering flow. Given that the geometry at the approach is fixed, the minute-by-minute variation in the maximum entry flow is dictated by driver behavior, vehicle type, and in cases the influence of exiting vehicles.

Entry Flow, RL (veh/min)	0	1	2	3	4	5	6	7	8	9	10	11	12	13	14	15	16	17	18	19	20	21	22	23	24	25	26	27	28	29	30	31	32	33
0			1					1			1					1		1					1						2					1
1	3			3			1		2		2	2	2	1	1		1	1										2	3			1	1	
2			2	1	1	2	1	2	4	1	1	3		2	2	1	1		2	2	2	3		3				1	1	2	1	1		
3	1	1	2	3	3	4	8	4	7	7	1	2	5	2	2	5	1	2	3	3		1	1		1					1	2	4	3	2
4	1		1	1	1	9	1	5	7	5	4	8	7	5	5	5	2	3	5	1	1	1	2			1	1			1	2			1
5	3	1	2	1	6	2	3	8	7	8	2	7	6	8	5	2	1	2	1	3	3		1	1			1	2	1	2	2			
6	1	3		3	3	7	6	8	6	6	2	3	7	1	6	3	2	3	1	1	1			1	1					1				
7			5	3	4	3	6	3	7	8	7	9	9		6	3	2	3	1	2	1	1			1									
8	1	1	3	3	5	2	2	7	5	2	4	12	10	6	7	2	5	2		3	1	1						1						
9				1	4	2	4	4	10	7	7	5	4	3	8	2	1	1			1													
10				2	3	2	2	1	9	4	4	5	8	4	3	2	3	1																
11	1	1	1	1	3		3	7	6	4	6	5	4	2	4	3	1																	
12				1	1	1	5	1	3	3	12	8	3	1	5	2	1																	
13	1			1	1	4	5	6	4	8	4	1	4	1																				
14	1	1			1	4	3	2	2	3	1	3	2	2																				
15		1			2		1	1	2	1		1																						
16				2		1	3	1	1					1																				
17						1		1																										
18									1																									
19				1																														
20																																		
21																																		
22																																		
23																																		
24																																		
25																																		

Entry flow, LL (veh/min)	0	1	2	3	4	5	6	7	8	9	10	11	12	13	14	15	16	17	18	19	20	21	22	23	24	25	26	27	28	29	30	31	32	33
0	2					1	3	4	3	4	2	2	1		4	2	1		1	1	1		1				1		2						
1	1	1		2	3	2	4	7	9	8	4	7	9	1	7	4	4	2	1	1		1		1				2						
2				1	1	1	6	6	6	8	7	12	13	4	6	3	1	2		2	3	1	2	1				1	1					
3		1		2	3	3	7	5	9	3	7	5	13	8	7	6	3	1	3	1		1		1										
4	2		1		1	4	3	5	5	8	9	3	3	8	5	1	3	3		2	3	1							1					
5		1	1	1	3	4	2	5	4	5	7	7	5	2	6	4	3	3	1	1				1						1		1		
6			1	1	5	1		1	5	5	5	6	7	3	2	4	2	2	2					1					1			1		
7			2	3	3	2	4	4	13	4	5	7	2	4	2		2	1																
8				3	3	7	1	5	5	2	1	2	3		5	5	1	1											1		1			
9	2	2	1	1	1	4	2	5	3	3	5	7	5	1	1			2																
10	2	1	6	3	4	3	7		6	6	1	4	1	2														1					
11				3	1		6	5	2		1	2																						
12	1		2	4		2	3	1	3	1	3																					1		
13	2	1	2		1	5		2		2			1		1																			
14			1	1	2		2	2	1																									
15					1				1	1																								
16					2	1																												
17				1	1																													
18							1																											
19	1																																	
20																																		
21																																		
22																																		
23																																		
24																																		
25																																		

Figure J-9. Right and Left Entry Flow vs. Conflicting Flow

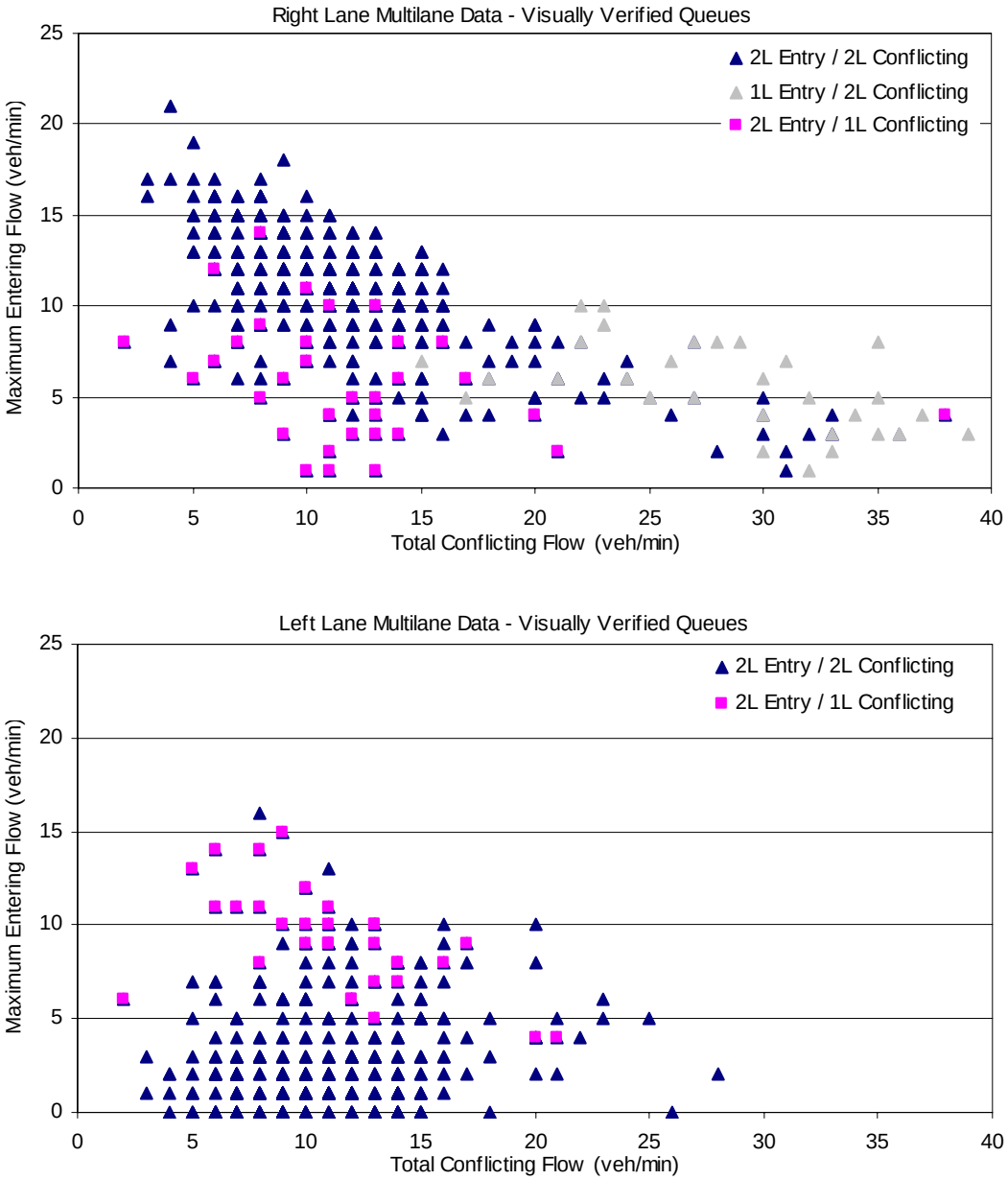

Figure J-10. Right and Left Entry Flow vs. Conflicting Flow

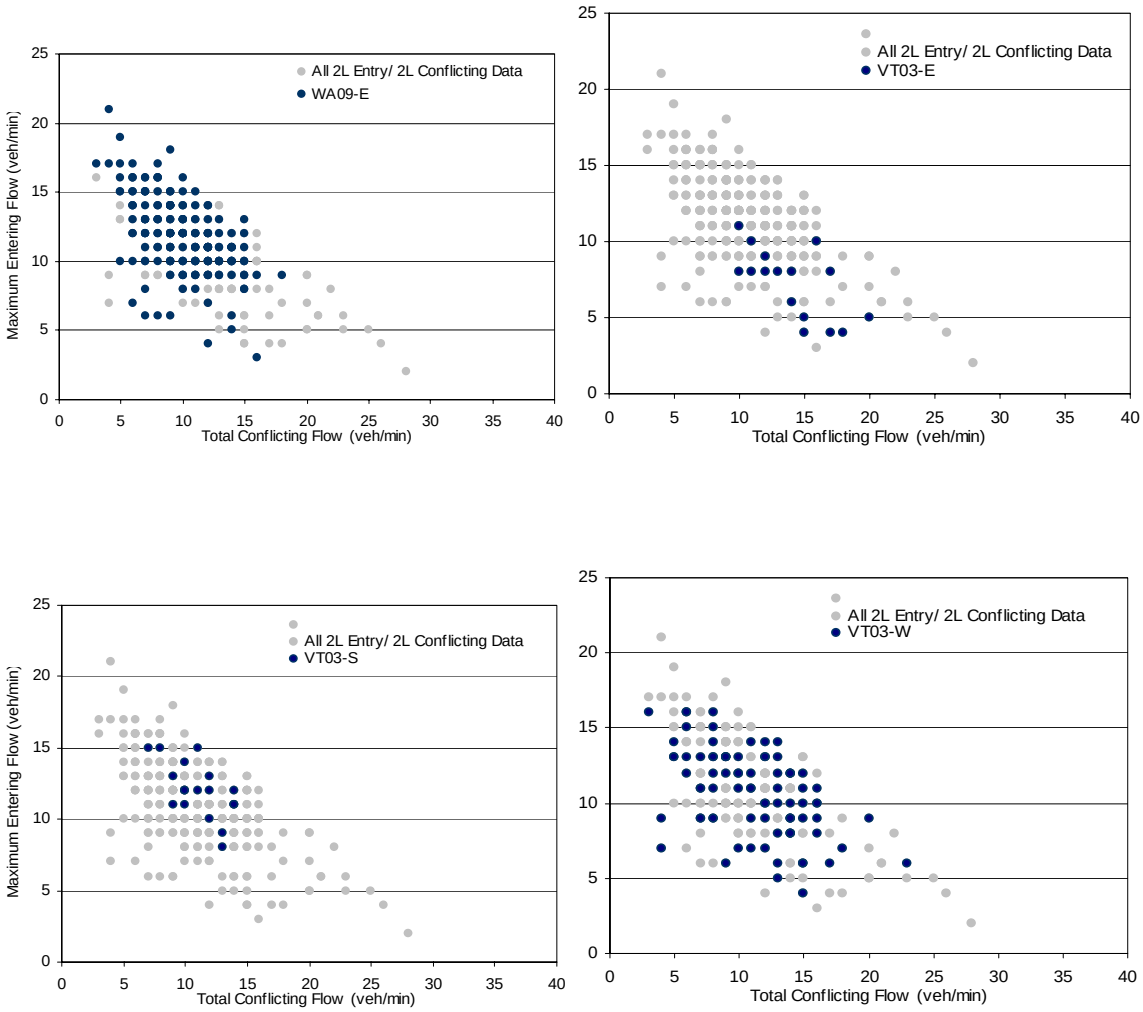

Figure J-11. Right Maximum Entry Flow vs. Conflicting Flow for Two Conflicting Lane Approaches

Comparison of Single-and Multilane Entry and Conflicting Flow Data

The single-lane data have a conflicting flow range of approximately 0 to 15 vehicles per minute, while the multilane data vary between 5 and 40 vehicles per minute. For a conflicting flow of 5 vehicles per minute, the maximum entry flow for the single and multilane sites is approximately 19 vehicles per minute. For a conflicting flow of 15 vehicles per minute the maximum entry flow for the single and multilane sites is approximately 8 and 15 vehicles per minute respectively. Two factors are at play. Firstly, there are fewer observations for the single-lane sites at higher conflicting flows. Secondly, the maximum flow at the multilane sites are typically observed in the right lane and the total conflicting flow does not necessarily represent the actual conflicting flow negotiated by vehicles in the right entry lane.

Multilane Delay Data

Figure J-12 illustrates the frequency of the delay observations for all multilane sites, using five-second bins from zero seconds to 95 seconds. The mean delay is 10.7 seconds per vehicle. Most of the delay measurements are less than 20 seconds per vehicle.

Figure J-13 shows plots of the mean delay for each entry flow/conflicting flow pair. As expected, delays increase as the combination of entry and conflicting flows increase.

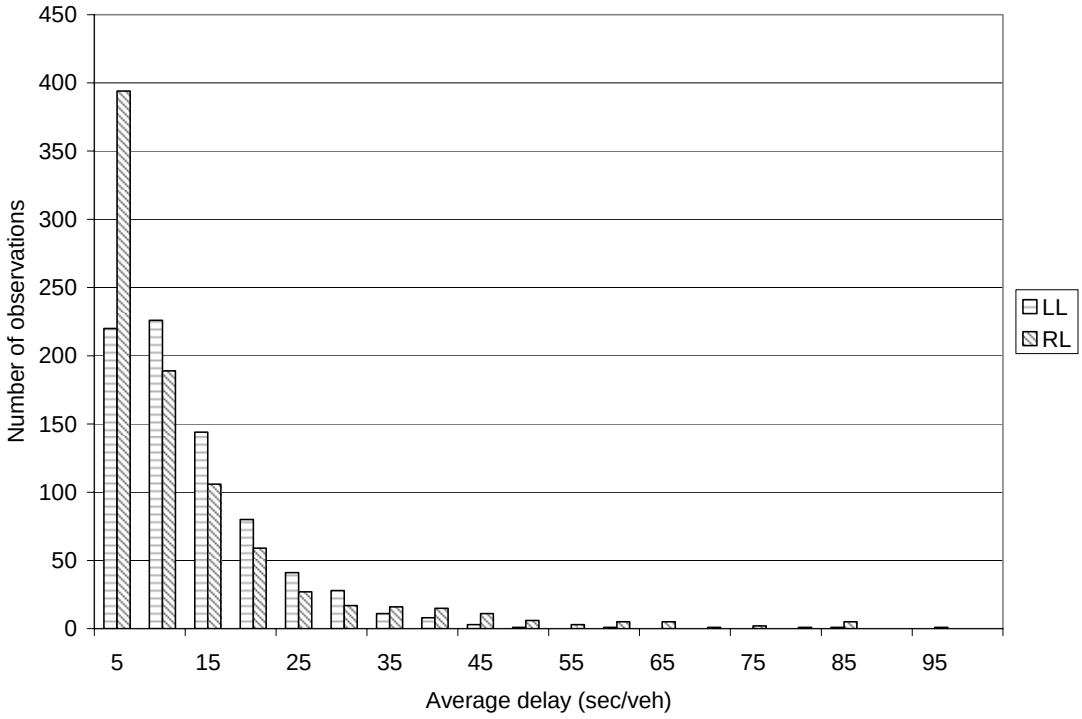

Figure J-12. Number of One-Minute Observations, Average Delay, Two-Lane Sites

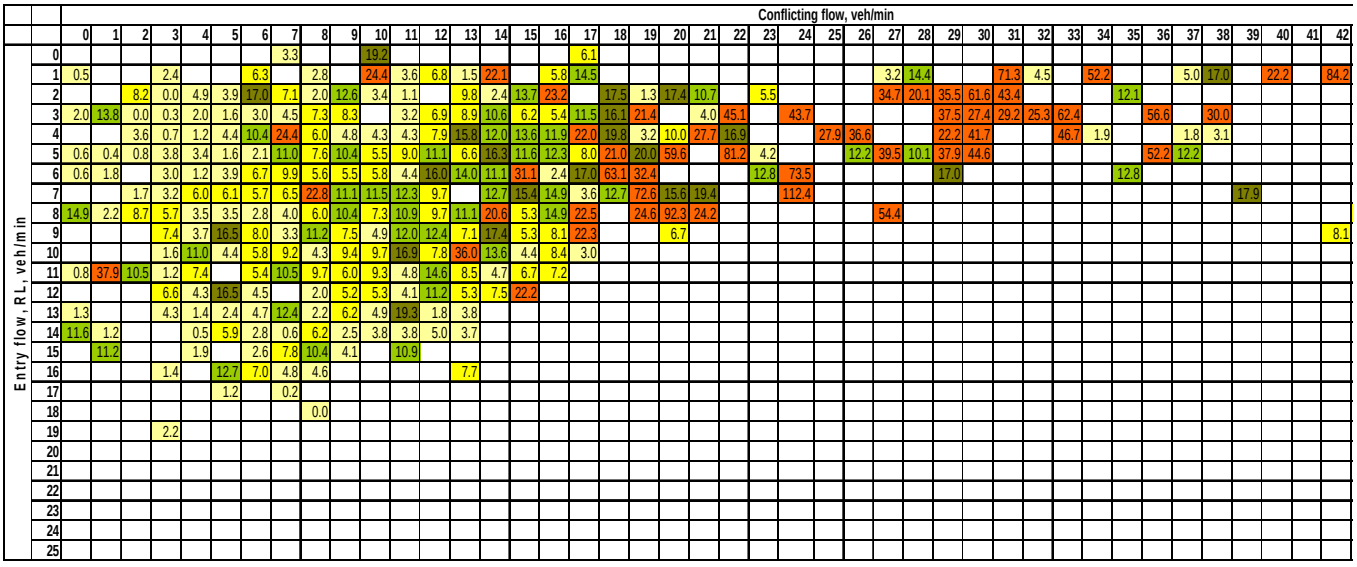

Figure J-13. Right-Lane Entry Flow vs. Conflicting Flow, One-Minute Data, Right-Lane Delay for Two-Lane Sites

Required Sample Size for Capacity Regression

The required sample size for each predefined increment of conflicting flow (otherwise known as a class width) is given by the following expression:

$$n_x = \left(\frac{z_\alpha}{d}\right)^2 \cdot \sigma^2 \qquad \text{(J-1)}$$

where: n_x = Required sample size for a confidence level P
z_α = standard normal variable = 1.96 for $P = 0.95$ (2.58 for $P = 0.99$)
d = allowed deviation of the class mean
σ^2 = variance of date in the class ($\approx s^2$)

Figure J-14 illustrates the one-minute capacity data, class mean and standard deviation for single-lane sites. The standard deviation varies between 2 and 3 vehicles per minute. The standard deviation of the sample has been used to approximate the standard deviation of the population, σ.

In Figure J-15, the actual sample size, n, the confidence level for a deviation $P_d = 0.5$ veh/min, and the required sample size, n_x, for a confidence level of $P = 0.95$ is illustrated. The observed sample size n is much smaller than the required size n_x. An average sample size of 100 per class width is needed to ensure an accuracy of 0.5 veh/min (30 veh/hr) and a confidence level of 0.95.

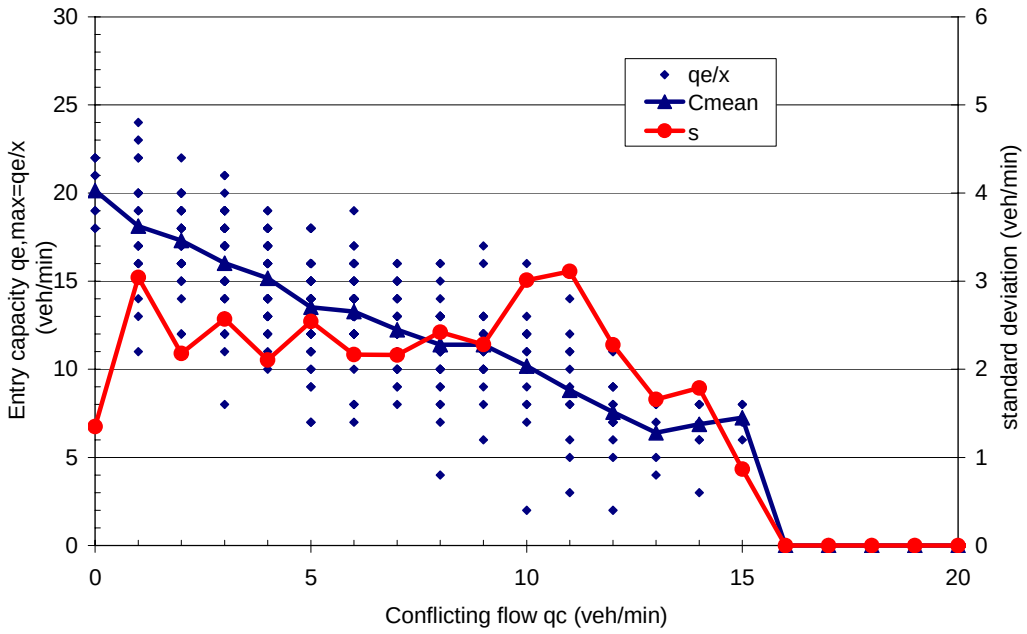

Figure J-14. Class Mean (C_{mean}) and Standard Deviation (s) of the Single-Lane Entry Data

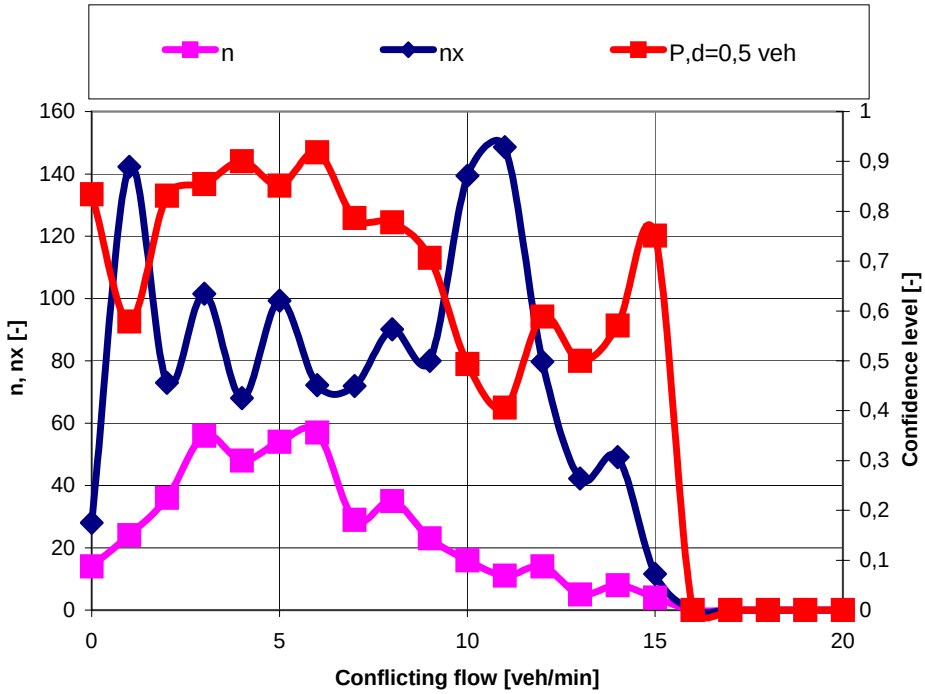

Figure J-15. Sample Size n of the Data Classes (Class Width = veh/min), Confidence Level P with d=0.5 veh/min, and the Required Sample Size n_x for P=0.95 and d=0.5 veh/min (1-Lane Entry Data)

In Figure J-16, the actual sample size, *n*, the confidence level for a deviation of 1.0 vehicles per minute, and the required sample size, n_x, for a confidence level of $P = 0.95$ is illustrated. The confidence level for the actual sample size is between $P = 0.7$ to 1.0. An average sample size of 25 per class width is needed to ensure an accuracy of 1 vehicle per minute for a confidence level of 0.95. For the whole data range (class width = 1 veh/min) a sample size of 320 is required. This compares well with the actual available sample.

These reliability considerations treat each integer value on the horizontal axis (conflicting flow) as independent from its neighbors. There is, however, correlation between the conflicting and maximum entering flow. A more useful reliability analysis would also take the correlations between all points into account to come to a higher degree of estimated statistical precision. The confidence interval of the linear regression function can be used for this determination. A simple linear regression model has been defined. The confidence interval of the regression function can be calculated as follows:

$$y_{\alpha} = y \pm d_{\alpha} \qquad \text{(J-2)}$$

where: y = entry capacity $q_{e.\max}$
x = conflicting flow q_c
y_α = α-percentile of y

$$d_\alpha = \text{deviation}$$

$$= t_{\alpha,n-2}\sigma_{xy}\sqrt{\frac{1}{n}+\frac{(x-\bar{x})^2}{\sigma_x^{\,2}(n-1)}}$$

σ_x^2 = variance of x ($\approx s_x^2$)
σ_{xy}^2 = covariance between y and x ($\approx s_{xy}^2$)
n = sample size
$t_{\alpha,n-2}$ = t-variable for a confidence level $P = \alpha$ with freedom (n-2)
$\bar{x}$ = mean of x

For the single-lane sites, the confidence interval with $P = 0.95$ is presented in Figure J-17.

The required sample size for a predefined confidence level P is obtained by inversing Equation J-2.

In Table J-10, the required sample size for a deviation of 0.5 and 1.0 veh/min and a P = 0.95 and 0.99 is presented for changing values of conflicting flow. The empty cells of the table could not be obtained ($n_x \rightarrow \infty$). For a confidence level $P = 0.95$ and a deviation of 1.0 vehicles per minutes for the y-intercept yields a required sample size $n_x = 288$. The total sample required is greater than the actual sample size. Because the actual sample size is small, it may be unreasonable to interpret the individual approach data.

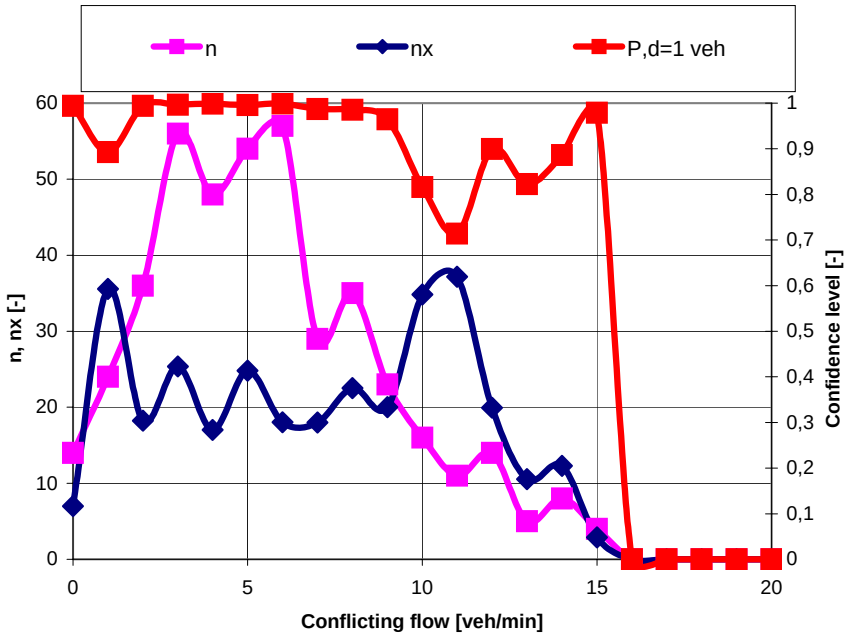

Figure J-16. Sample Size n of the Data Classes (class width = veh/min), Confidence Level P with d=1 veh/min and the Required Sample Size n_x for P=0.95 and d=1 veh/min (1-Lane Entry Data)

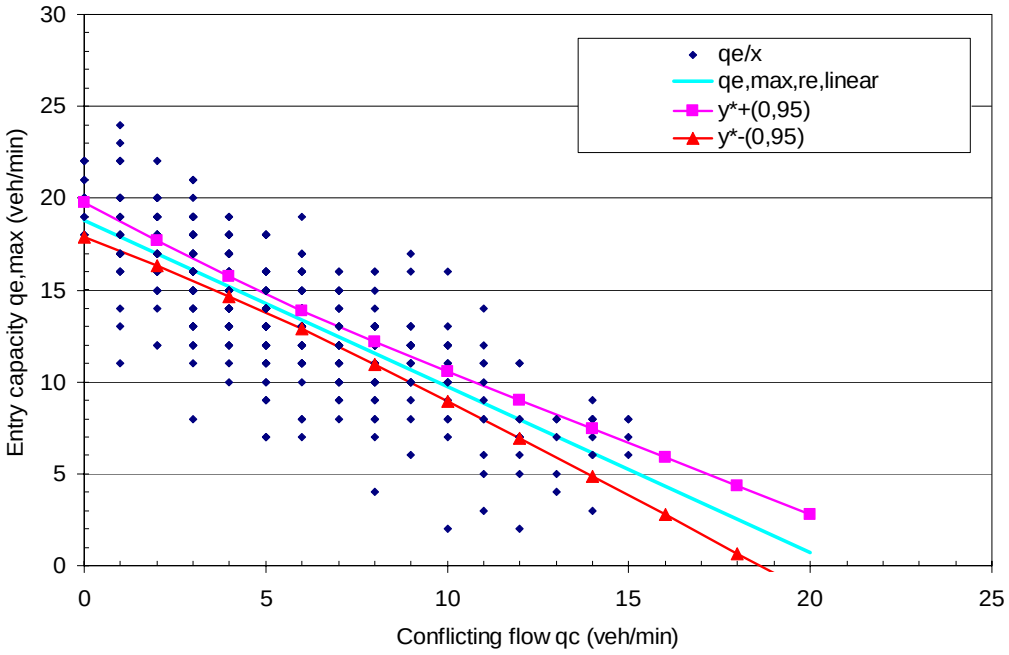

Figure J-17. Confidence Interval of the Regression Function for the Single-Lane Entries with P=0.95.

TABLE J-10. Required Sample Size n_x According to the Confidence Interval of the Regression Function

Conflicting Flow	P=0.95		P=0.99	
	Deviation=1 veh/min	Deviation=0.5 veh/min	Deviation=1 veh/min	Deviation=0.5 veh/min
veh/min	Sample Size	Sample Size	Sample Size	Sample Size
0	288	—	—	—
2	137	—	327	—
4	106	512	191	—
6	100	405	174	707
8	113	743	217	3461
10	165	—	542	—
12	603	—	—	—
14	—	—	—	—
16	—	—	—	—
18	—	—	—	—
20	—	—	—	—

Validity of Regression Models

Using a customized simulation program, the validity of regression has been demonstrated. A number of assumptions have been made within the simulation program including the following:

1. The observed conflicting and maximum entering flows can be regarded as random variables. To simulate these observations, a Monte-Carlo method can be employed.
2. The inter-arrival times both between the circulating vehicles as well as between the entering vehicles can be generated according to a Borel-Tanner distribution (i.e. an exponential distribution). Because the theoretical distribution can generate very small values of the inter-arrival headway, all times are capped at the minimum acceptable headway, Δ.
3. All other parameters, such as critical headway t_c and the follow-up headway t_f, are generated according to a shifted Erlang distribution.
4. The driver's behavior is assumed to be homogeneous and consistent.

One-minute entry and conflicting flows were generated using an average $t_c = 6.0$ s and $t_f = 3.0$ s, and a minimum headway, $\Delta = 2.0$ s. The results are shown in Figure J-18 and include:

- simulated data points (500 1-min-intervals);
- class means (the mean entry for each 1 min/veh of conflicting data);
- regression function (German exponential) representing the simulated data;
- regression function (German exponential) representing the class mean data; and
- standard deviation of the simulated data.

The standard deviation has a tendency towards zero as the conflicting flow approaches zero (capacity approaching its maximum possible value), and as the conflicting flow approaches its maximum value. The standard deviation for this artificial system is always below 2 vehicles per minute. For real systems the deviation is between 2 and 3 vehicles.

The German regression (both of the simulated and the class mean estimates) is very similar to the class means of the simulated data. The class means are regarded as the most reliable estimation since the form of the regression function does not manipulate the results. While the parameters within the German regression do not precisely correspond with the parameters used to define the simulation data, the differences between the class mean average of the simulated data and the regression estimates are small (0.1 s).

To ensure that the class mean is a reasonable, a certain sample size of the simulation of one-minute capacity data for a given confidence level is needed. Using Equation J-1 presented previously, the required sample size for deviations of 0.3, 0.5 and 1.0 veh/min, and a confidence level $P = 0.95$, is presented in Figure J-19. As shown the smaller the allowed deviation, the larger the required sample size. If a predefined deviation of 0.5 veh/min is used, a sample of 40 simulated entry data per class width is needed. This results in a total sample size of 40 * 30 = 1200 simulated entry data per minute for the range of conflicting flow. For a deviation of 0.3 and 1.0 veh/min, the required sample size is approximately 450 and 3000 simulated entry data, respectively. For practical applications, a deviation of 1 veh/min (i.e., 60 veh/h) and a confidence level $P = 0.95$ is sufficient. Hence, each class width should have an observed sample size of about 15 one-minute data points—a total of 450. The simulated sample of 500 data points is therefore acceptable.

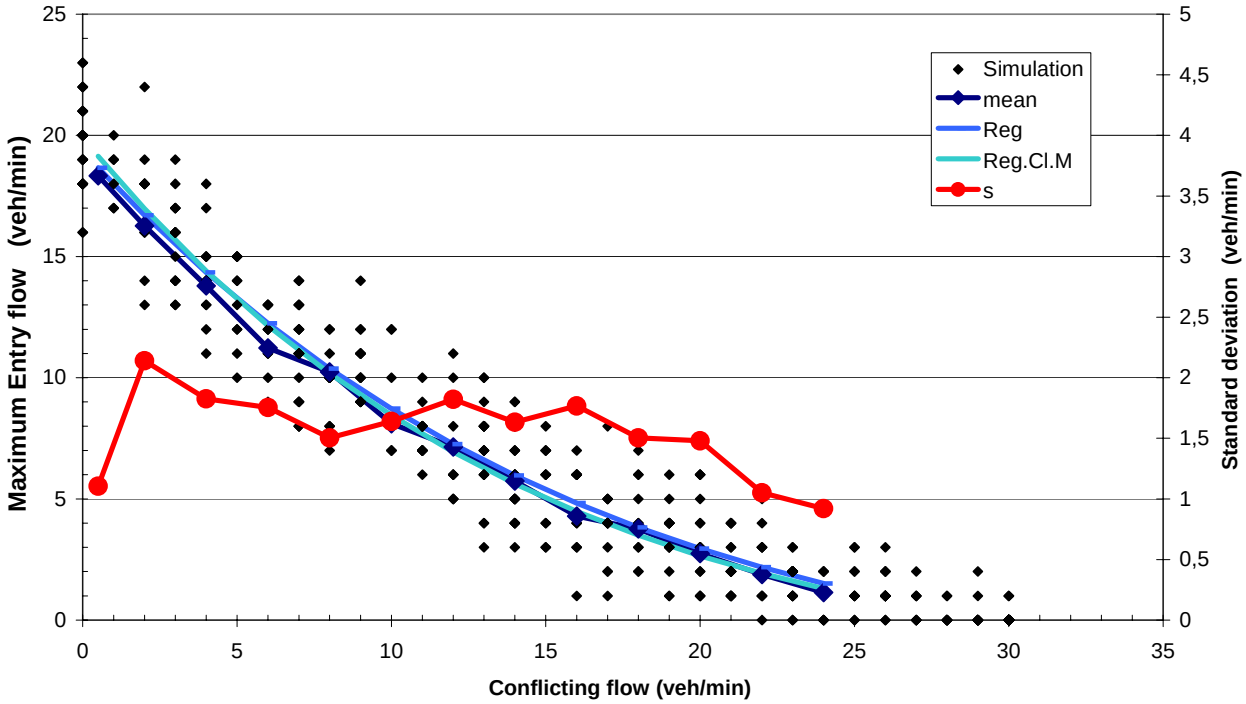

Legend:

- Simulation = results of the simulation (500 data points in 1-min-intervals with given $t_c = 6.0$s, $t_f = 3.0$s, and $\Delta = 2.0$s)
- Mean = class mean.
- Reg = regression (with $t_c = 5.9$s, $t_f = 3.1$s, and $\Delta = 2.0$s)
- Reg.Cl.M = regression for the class mean (yields $t_c = 6.2$s, $t_f = 3.0$s, and $\Delta = 2.0$s)
- s = standard deviation

Figure J-18. Simulation Results for Demonstrating the Stochastic Nature of Capacities.

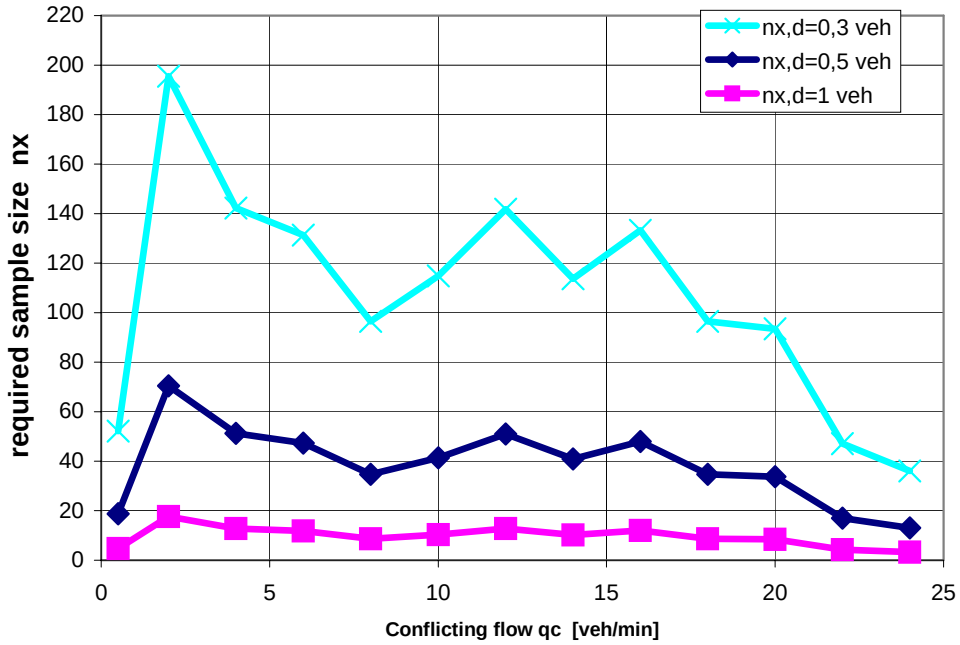

Figure J-19. Required Sample Size for a Confidence Level P=0.95 and the Allowed Deviation d=0.3, 0.5, and 1 veh/min

APPENDIX K
PEDESTRIAN ANALYSIS TABLES

This appendix contains a series of pedestrian analysis tables that show site-by-site results for several variables. The specific tables included are as follows:

TABLE K-1. Percentage of Pedestrian Crossings Requiring Interaction with a Motor Vehicle

Percentage of Crossings with Pedestrian-Vehicle Interaction							
		% Peds Interacting w/Vehicles - Entry Leg			% Peds Interacting w/Vehicles - Exit Leg		
Site	No. of Lanes	Entry Leg Start	Exit Leg Start	Either Leg	Entry Leg Start	Exit Leg Start	Either Leg
MD05-SW/NW1	1	14	46	30	31	19	25
UT02-W1	1	7	5	6	7	0	4
VT01-N1/N2	1	58	16	37	19	36	28
WA02-E1	1	33	25	29	58	27	43
WA03-S1/S2/S3	1	45	16	31	17	46	32
1-Lane Averages		**32**	**22**	**27**	**27**	**26**	**26**
FL11-E1	2	40	21	30	29	41	35
MD05-SW/S1	2	55	43	49	58	80	69
MD05-SW/W1	2	4	22	13	33	26	29
NV03-S1	2	11	8	9	33	53	43
UT02-E1	2	19	14	17	12	26	19
2-Lane Averages		**26**	**22**	**24**	**33**	**45**	**39**
Overall Average		**29**	**22**	**25**	**30**	**35**	**33**

TABLE K-2. Pedestrian Behavior Percentages for Crossings that Began from the Entry Leg Curb

Pedestrian Behaviors - Entry Leg Start															
		Entry Leg Behavior							Exit Leg Behavior						
Site	No. of Lanes	Total Peds	Normal	Hesitated on Curb/Splitter	Hestitated after Start	Stopped after Start	Retreated	Ran	Total Peds	Normal	Hesitated on Curb/Splitter	Hestitated after Start	Stopped after Start	Retreated	Ran
MD05-SW/NW1	1	6	67	0	0	0	0	33	1	0	0	0	0	0	100
UT02-W1	1	3	100	0	0	0	0	0	4	100	0	0	0	0	0
VT01-N1/N2	1	37	49	49	3	0	0	0	28	75	11	0	0	0	14
WA02-E1	1	6	50	33	0	0	0	17	6	17	17	0	0	0	67
WA03-S1/S2/S3	1	46	50	41	0	0	0	9	25	72	16	0	0	0	12
1-Lane Averages			**63**	**25**	**1**	**0**	**0**	**12**		**53**	**9**	**0**	**0**	**0**	**39**
FL11-E1	2	21	43	52	0	0	0	5	27	67	15	0	0	0	19
MD05-SW/S1	2	28	61	25	4	0	0	11	23	65	22	4	0	0	9
MD05-SW/W1	2	5	100	0	0	0	0	0	5	80	0	0	0	0	20
NV03-S1	2	1	0	100	0	0	0	0	2	50	0	0	0	0	50
UT02-E1	2	16	81	19	0	0	0	0	11	82	18	0	0	0	0
2-Lane Averages			**57**	**39**	**1**	**0**	**0**	**3**		**69**	**11**	**1**	**0**	**0**	**19**
		169													
Overall Average			**60**	**32**	**1**	**0**	**0**	**7**		**61**	**10**	**0**	**0**	**0**	**29**

TABLE K-3. Pedestrian Behavior Percentages for Crossings that Began from the Exit Leg Curb

Pedestrian Behaviors - Exit Leg Start															
		Entry Leg Behavior							Exit Leg Behavior						
Site	No. of Lanes	Total Peds	Normal	Hesitated on Curb/Splitter	Hestitated after Start	Stopped after Start	Retreated	Ran	Total Peds	Normal	Hesitated on Curb/Splitter	Hestitated after Start	Stopped after Start	Retreated	Ran
MD05-SW/NW1	1	8	63	25	0	0	0	13	1	0	100	0	0	0	0
UT02-W1	1	7	100	0	0	0	0	0	2	100	0	0	0	0	0
VT01-N1/N2	1	22	73	23	0	0	0	5	13	46	46	8	0	0	0
WA02-E1	1	3	67	0	0	0	0	33	6	50	33	0	0	0	17
WA03-S1/S2/S3	1	49	80	2	0	0	0	18	23	22	74	0	0	0	4
1-Lane Averages			**76**	**10**	**0**	**0**	**0**	**14**		**44**	**51**	**2**	**0**	**0**	**4**
FL11-E1	2	31	65	26	3	0	0	6	19	37	58	0	5	0	0
MD05-SW/S1	2	9	22	33	22	0	0	22	8	50	38	0	0	0	13
MD05-SW/W1	2	5	20	80	0	0	0	0	1	100	0	0	0	0	0
NV03-S1	2	None													
UT02-E1	2	11	82	18	0	0	0	0	6	67	33	0	0	0	0
2-Lane Averages			**47**	**39**	**6**	**0**	**0**	**7**		**63**	**32**	**0**	**1**	**0**	**3**
		145													
Overall Average			**57**	**21**	**3**	**0**	**0**	**10**		**47**	**38**	**1**	**1**	**0**	**3**

TABLE K-4. Pedestrian Crossing and Wait Times

Pedestrian Crossing and Wait Times										
		Avg Initial Wait Time (sec)			Avg Splitter Xing/Wait Time (sec)			Avg Total Crossing Time (sec)		
Site	No. of Lanes	Entry Leg Start	Exit Leg Start	Either Leg	Entry Leg Start	Exit Leg Start	Either Leg	Entry Leg Start	Exit Leg Start	Either Leg
MD05-SW/NW1	1	0.71	1	0.86	2.13	5.57	3.85	8.67	8.35	8.51
UT02-W1	1	0.36	0.43	0.40	1.64	1.29	1.47	9.5	8.71	9.11
VT01-N1/N2	1	3.54	3.05	3.30	1.23	0.95	1.09	11.03	10.81	10.92
WA02-E1	1	0.33	0.36	0.35	2.42	2.17	2.30	8	8.45	8.23
WA03-S1/S2/S3	1	1.45	1.38	1.42	1.31	1.37	1.34	8.29	7.94	8.12
1-Lane Averages		**1.3**	**1.2**	**1.3**	**1.7**	**2.3**	**2.0**	**9.1**	**8.9**	**9.0**
FL11-E1	2	1.6	1.67	1.64	3.93	4.06	4.00	12.57	14.01	13.29
MD05-SW/S1	2	3.22	6.19	4.71	7.72	7.67	7.70	12.31	11.57	11.94
MD05-SW/W1	2	0.11	1.96	1.04	3	2.48	2.74	10.09	14.43	12.26
NV03-S1	2	0.22	3.69	1.96	7.22	5.77	6.50	18.22	13.79	16.01
UT02-E1	2	1.53	1.1	1.32	2.67	2.6	2.64	18.04	18.7	18.37
2-Lane Averages		**1.3**	**2.9**	**2.1**	**4.9**	**4.5**	**4.7**	**14.2**	**14.5**	**14.4**
Overall Average		**1.3**	**2.1**	**1.7**	**3.3**	**3.4**	**3.4**	**11.7**	**11.7**	**11.7**

TABLE K-5. Motor Vehicle Yield Percentages for Crossings that Began from the Entry Leg Curb

Motor Vehicle Yield Behavior - Ped Entry Leg Start									
		Entry Leg Behavior				Exit Leg Behavior			
Site	No. of Lanes	Opportunities	Active Yield	Passive Yield	Did Not Yield	Opportunities	Active Yield	Passive Yield	Did Not Yield
MD05-SW/NW1	1	6	17	83	0	3	33	0	67
UT02-W1	1	4	75	0	25	4	100	0	0
VT01-N1/N2	1	60	65	0	35	29	97	0	3
WA02-E1	1	6	100	0	0	6	100	0	0
WA03-S1/S2/S3	1	56	71	16	13	28	89	0	4
1-Lane Averages			**66**	**20**	**15**		**84**	**0**	**15**
FL11-E1	2	48	48	2	50	36	69	3	28
MD05-SW/S1	2	80	41	4	55	76	32	1	67
MD05-SW/W1	2	6	50	33	17	16	31	0	69
NV03-S1	2	1	100	0	0	4	50	0	50
UT02-E1	2	29	52	3	45	24	79	8	13
2-Lane Averages			**58**	**9**	**33**		**52**	**2**	**45**
Overall Average			**62**	**14**	**24**		**68**	**1**	**30**

TABLE K-6. Motor Vehicle Yield Percentages for Crossings that Began from the Exit Leg Curb.

Motor Vehicle Yield Behavior - Ped Exit Leg Start									
		Entry Leg Behavior				Exit Leg Behavior			
Site	No. of Lanes	Opportunities	Active Yield	Passive Yield	Did Not Yield	Opportunities	Active Yield	Passive Yield	Did Not Yield
MD05-SW/NW1	1	24	8	42	50	6	17	0	83
UT02-W1	1	7	100	0	0	2	50	50	0
VT01-N1/N2	1	22	100	0	0	27	48	0	52
WA02-E1	1	3	67	33	0	4	100	0	0
WA03-S1/S2/S3	1	49	86	14	0	33	70	18	12
1-Lane Averages			**72**	**18**	**10**		**57**	**14**	**29**
FL11-E1	2	36	69	22	8	19	63	37	0
MD05-SW/S1	2	18	67	6	28	45	16	2	82
MD05-SW/W1	2	9	89	0	11	5	20	0	80
NV03-S1	2	1	0	0	100	10	0	0	100
UT02-E1	2	13	77	8	15	15	47	7	47
2-Lane Averages			**60**	**7**	**33**		**29**	**9**	**62**
Overall Average			**66**	**12**	**21**		**43**	**11**	**46**

APPENDIX L
PEDESTRIAN AND BICYCLE IMAGES

This appendix contains a series of images that were captured from the video and illustrate examples of some of the variables that were recorded. The specific figures included are as follows:

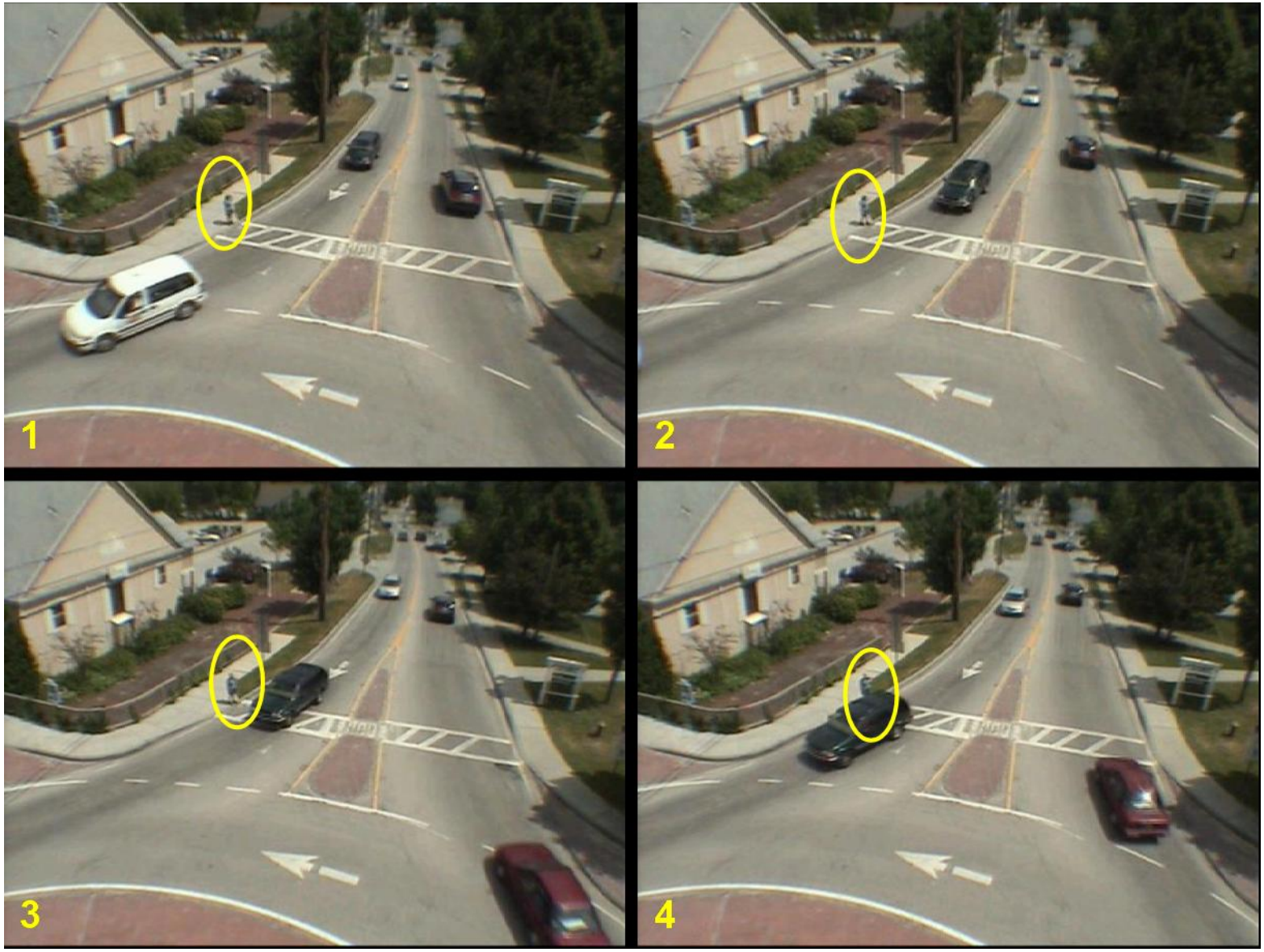

Figure L-1. Motorist that did not yield to pedestrian waiting on the curb.

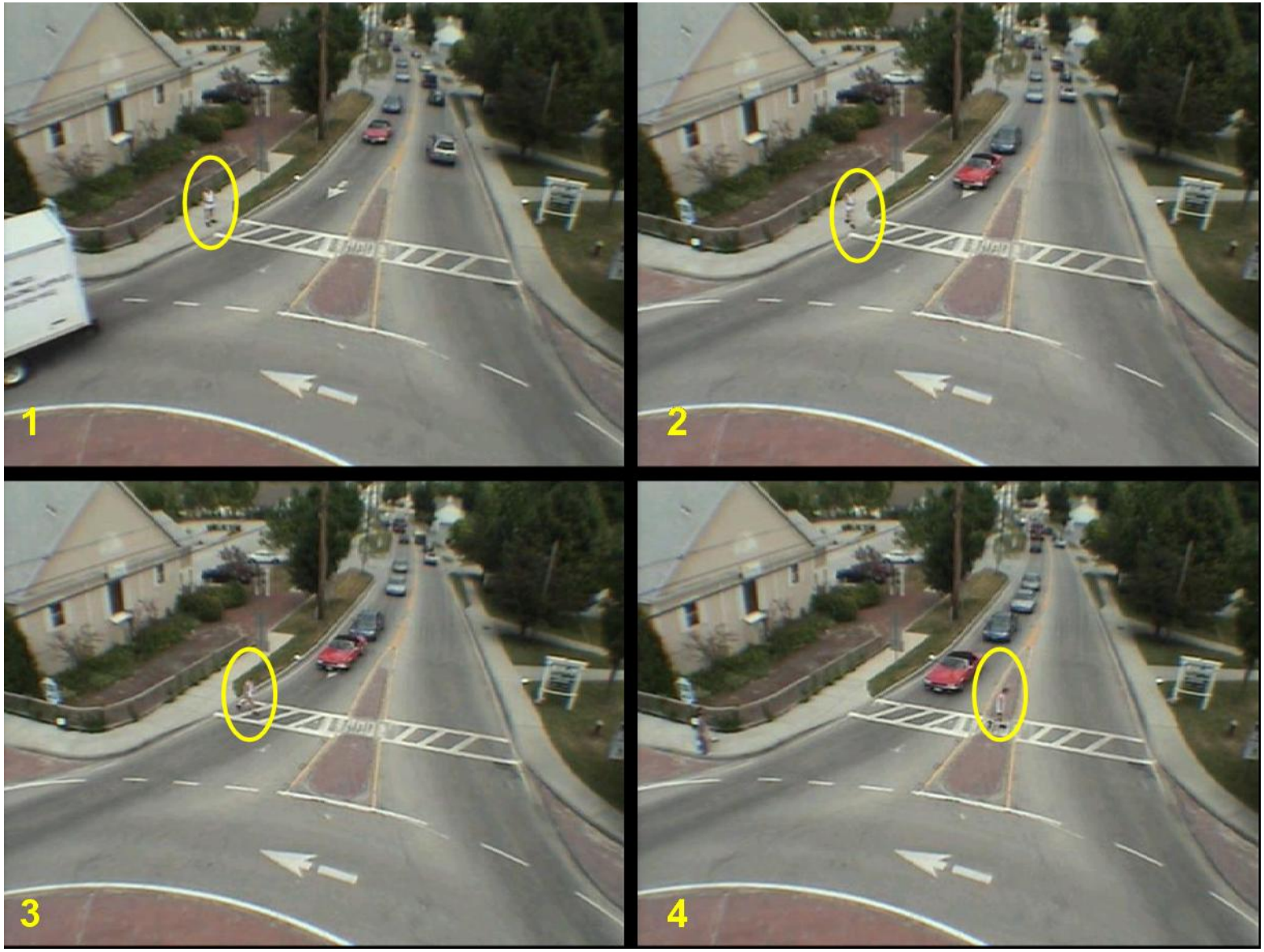

Figure L-2. Motorist that yielded to pedestrian waiting on the curb.

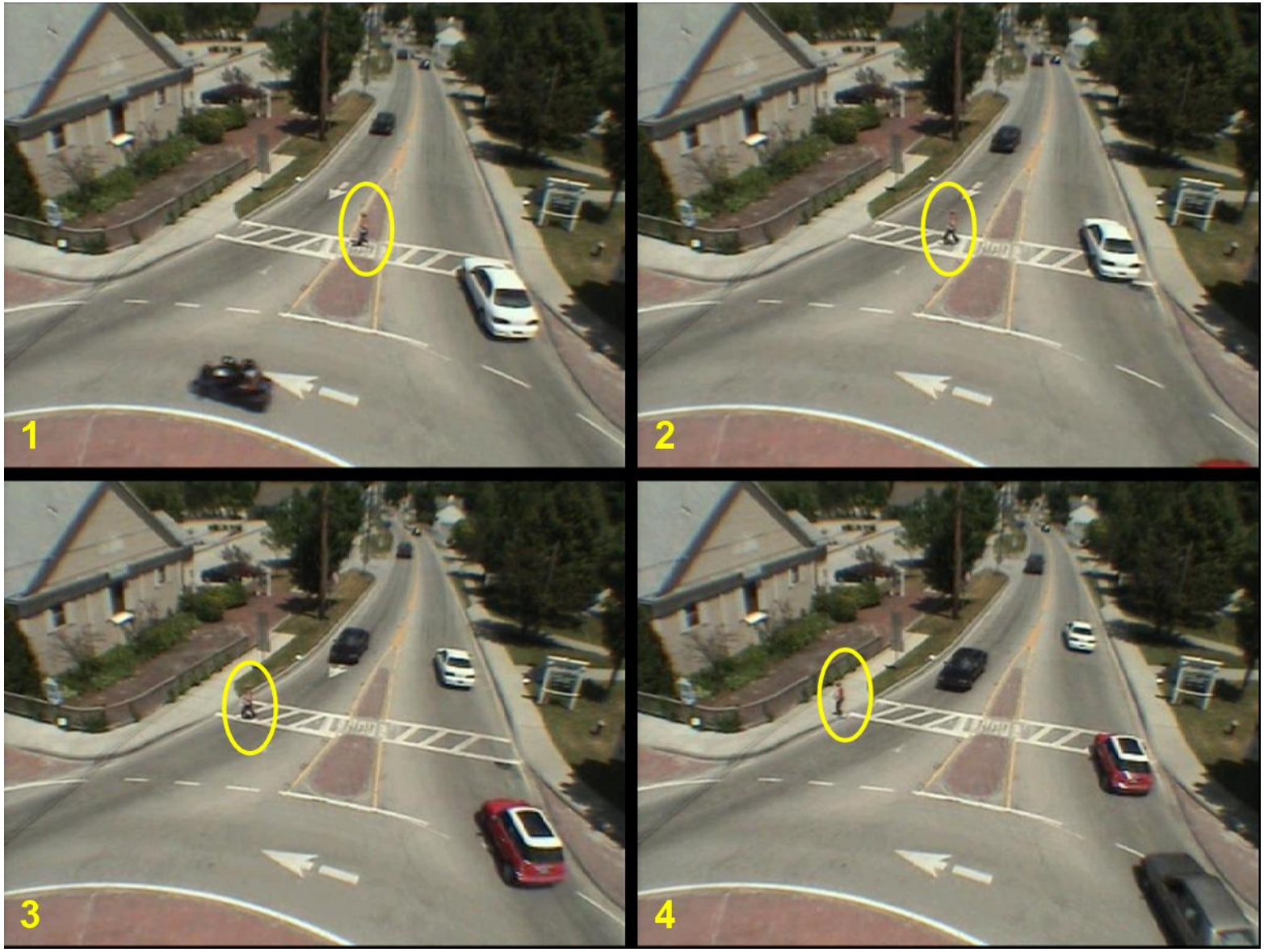

Figure L-3. Motorist that actively yielded to pedestrian in transit.

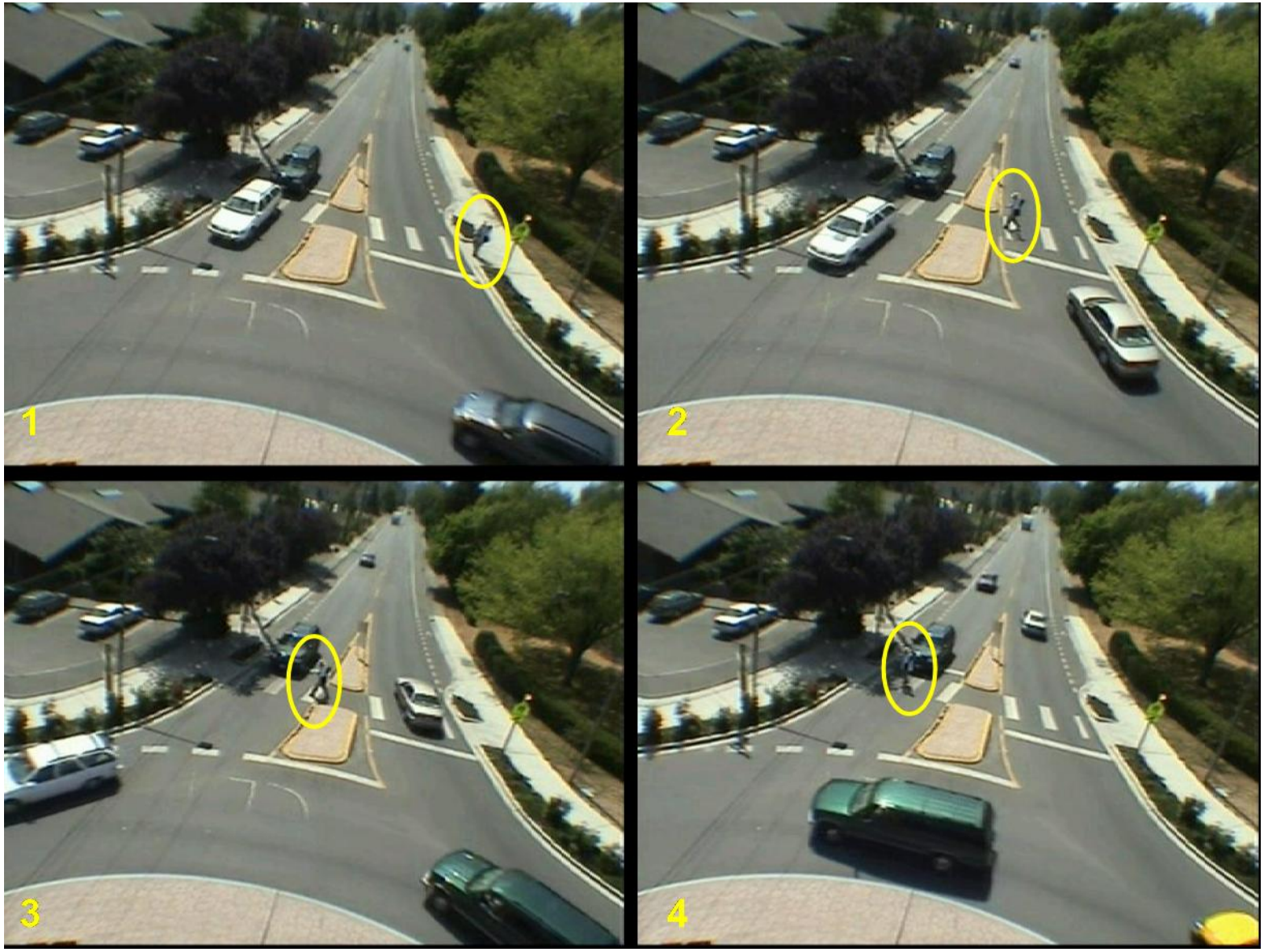

Figure L-4. Motorist that passively yielded to crossing pedestrian (already stopped in vehicle queue).

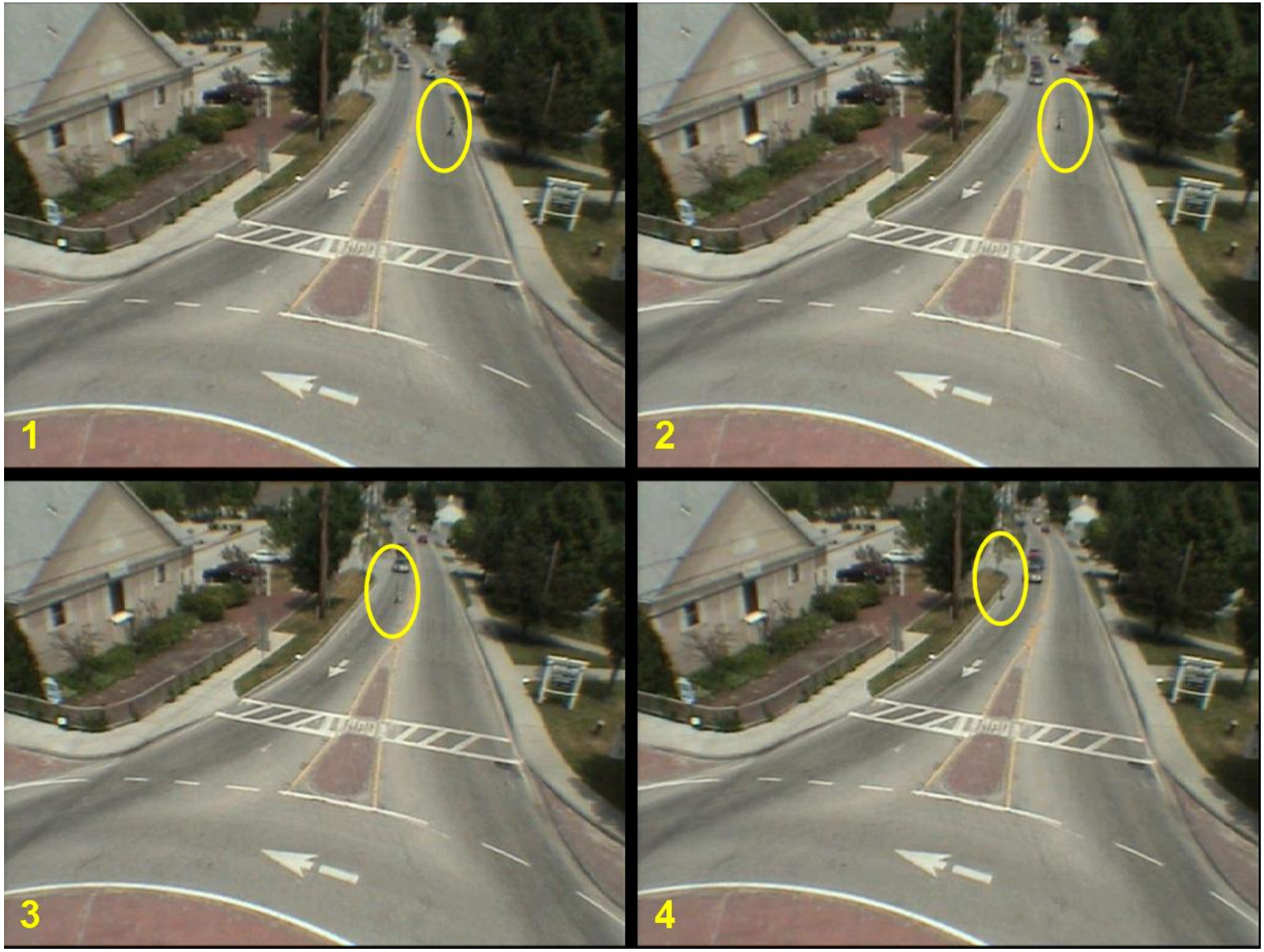

Figure L-5. Pedestrian crossing outside the boundaries of the crosswalk.

Figure L-6. Vehicle leading bicyclist on circulating lane.

Figure L-7. Vehicle trailing bicyclist on approach lane.

Figure L-8. Vehicle passing bicyclist on approach lane.

Figure L-9. Vehicles queued in front and rear of bicyclist on approach lane.

APPENDIX M

DRAFT HIGHWAY CAPACITY MANUAL CHAPTER 17

Note: This version of the HCM procedure is current as of November 2005. This version includes many, but not all, of the elements of interest to the members of the TRB Committee on Highway Capacity and Quality of Service and its Subcommittee on Unsignalized Intersections, with whom project team members have held regular discussions. Among other things, the Committee has requested elements to be added to the procedure that go beyond the scope and/or data of the 3-65 project, such as consideration of geometric delay, effects of short lanes, and so on, as well as further refinement of the mechanics of using the critical lane procedure for multilane roundabouts. As a result, the procedure below is not intended to be complete nor necessarily the latest version under consideration by the Committee, but it reflects a draft implementation of the procedure as completed within the 3-65 project.

I. INTRODUCTION –PART C

In this section of Chapter 17, procedures for the analysis of roundabouts are presented. The unique characteristics of roundabout capacity are introduced along with terminology. For ease of reference, the following terms are defined:

- c_a = approach capacity
- v_e = entry flow rate, and
- v_c = conflicting flow rate.

Roundabouts have been used successfully throughout the world and are being used increasingly in the United States, especially since 1990. A recently completed study provides a comprehensive database of roundabout operations for U.S. conditions based on a study of 31 sites *(1)*. The capacity and level of service analysis procedures that follow were developed in that study. The procedures allow the analyst to assess the operational performance of an existing or planned one-lane or two-lane roundabout given traffic demand levels.

While the database on which these procedures are based is the most comprehensive yet developed for U.S. conditions, it has limitations. It covers typical roundabout facilities quite well, but lacks examples of situations where:

- upstream/downstream signals influence the performance of the facility;
- priority reversal occurs, such as unusual forced entry conditions under extremely high flows;
- a high level of pedestrian or bicycle activity is present;
- the roundabout is in close proximity to one or more other roundabouts; or
- more than two entry lanes are present on one or more approaches.

Both roundabout design practices and the public's use of those roundabouts are still maturing in the U.S. Many of the sites that formed the database for this chapter were less than five years old when the data were collected. Although the available data were insufficient to definitively answer the question of whether capacity increases with driver familiarity, anecdotal observations suggest that this may well be the case. U.S. drivers seem to be displaying more hesitation and

caution in the use of roundabouts than their international counterparts, which in turn has resulted in a lower observed capacity than might be ultimately achievable. It is therefore quite possible that volumes (and capacity) will increase in the years to come as more roundabouts are constructed in the U.S. and as user familiarity grows. Such an increase in capacity over time would be consistent with the historically observed trends in capacity for freeway facilities and signalized intersections, for example.

Intersection analysis models generally fall into two categories. Empirical models rely on field data to develop relationships between geometric features and performance measures such as capacity and delay; these are commonly regression models. Analytical models rely on field measures of driver behavior and an analytic formulation of the relationship between those field measures and performance measures such as capacity and delay. Gap acceptance models are generally the preferable type of analytical model at unsignalized intersections since they capture driver behavior characteristics directly and can be made site-specific by custom-tuning the values that are used for those parameters. However, simple gap acceptance models may not capture all of the observed behavior, and more complex gap acceptance models that account for limited priority or reverse priority are difficult to calibrate. Empirical models are often used in these cases where an understanding of driver behavior characteristics is incomplete. Based on recent analysis of U.S. field data, simple, lane-based, empirical regression models are recommended for both single-lane and double-lane roundabouts.

II. METHODOLOGY – PART C

OVERVIEW OF METHODOLOGY

General

The capacity of a roundabout approach is directly influenced by flow patterns. The three flows of interest, the entering flow, the circulating flow, and the exiting flow, are shown in Exhibit 17-36.

EXHIBIT 17-36. ANALYSIS ON ONE ROUNDABOUT LEG

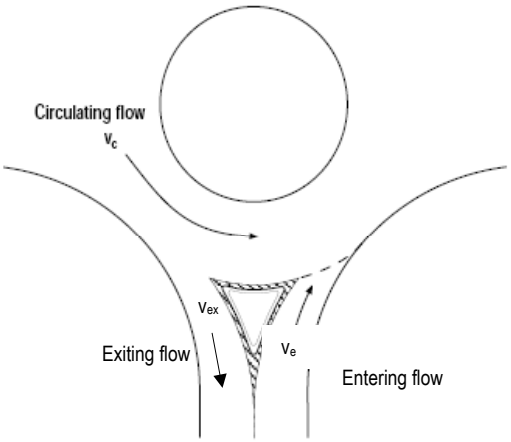

The capacity of an approach decreases as the conflicting flow increases. In general, the primary conflicting flow is the circulating flow that passes directly in front of the subject entry. While the circulating flow directly conflicts with the entry flow, the exiting flow may also affect a driver's decision on when to enter the roundabout. This phenomenon is similar to the effect of the right-turning stream approaching from the left side of a TWSC intersection. Until these drivers complete their exit maneuver or right turn, there may be some uncertainty in the mind of the driver at the yield or stop line about the intentions of the exiting or turning vehicle. However, the inclusion of this effect did not significantly improve the fit of the capacity models to the data and thus is not included herein.

When the conflicting flow approaches zero, the maximum entry flow is given by 3600 divided by the follow-up headway. This condition is similar to the saturation flow rate at an unsignalized intersection. At high levels of conflicting flow, limited priority (where circulating traffic adjusts its headways to allow entering vehicles to enter), priority reversal (where entering traffic forces circulating traffic to yield), and other behaviors may occur, and a simplified gap acceptance model may not give reliable results.

When an approach operates over capacity for a period of time, a condition known as *capacity constraint* may occur. During these conditions, the actual circulating flow downstream of the constrained entry will be less than demand. The reduction in actual circulating flow may therefore increase the capacity of the affected downstream entries during those conditions.

In addition, research has suggested an influence of origin-destination patterns on the capacity of a given entry *(2,3)*. This effect has not been incorporated into the recommended models herein.

One-Lane Roundabouts

The analyst should be aware of the large observed variation in driver behavior at roundabouts. Exhibit 17-37 shows observed combinations of entry flow and conflicting flow during one-minute periods of constant queuing, demonstrating the wide scatter of measured entry flows during capacity conditions. Part of this variation can be explained by the instability of one-minute measurements. The remainder of the variation is attributable primarily to the variation in driver behavior, truck percentage, and exiting vehicles. Since there is no external control device regulating flow interactions at roundabouts, driver interactions govern the operation, and this, by its nature, is highly variable.

Exhibit 17-37. Observed Combinations of Entry Flow and Conflicting Flow During One-Minute Periods of Continuous Queuing at Single-Lane Roundabout Entries

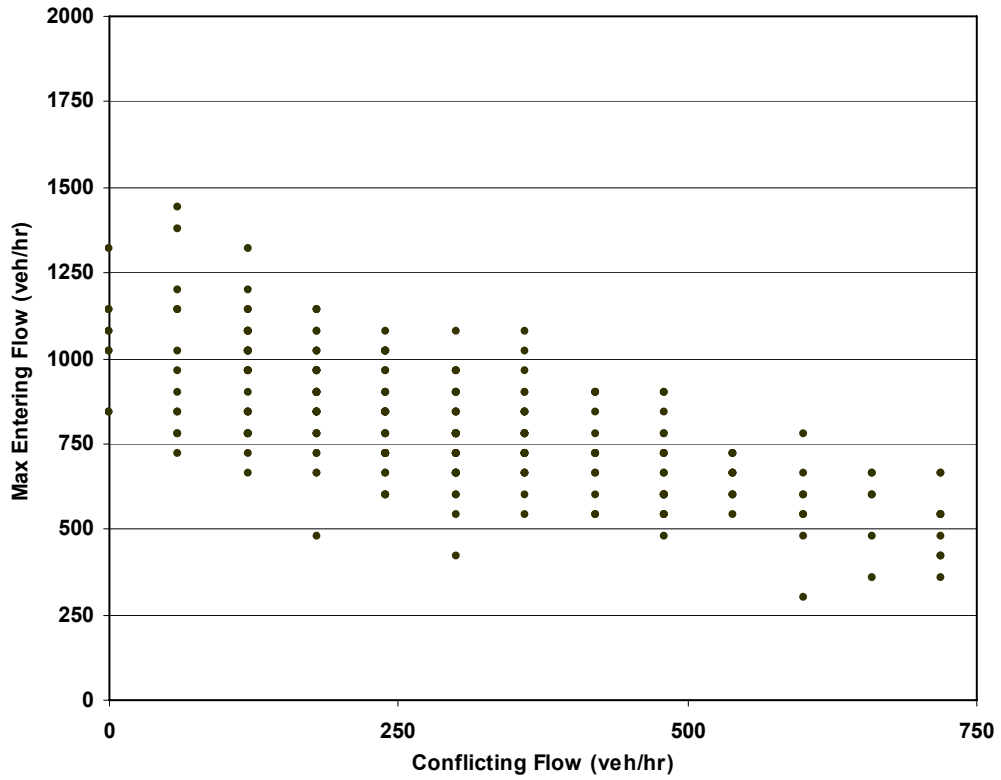

The average critical headway also shows a wide variation between sites. Exhibit 17-38 shows the estimated values of critical headway for sixteen roundabout approaches that were considered in the development of the single-lane models *(1)*. The primary sources for the observed variability appear to be the conflicting volume, the characteristics of the vehicle stream, and variations in driver behavior among sites. The data suggest that the effect of minor changes in geometry appears to have a lesser-order effect.

Exhibit 17-38 – Estimated critical headway values for single-lane approaches

Site (approach)	Sample Size	Mean Critical Headway (seconds)	Standard Deviation of Critical Headway (seconds)
MD 2/MD 408/MD 422, Lothian, MD (north)	32	5.2	1.8
MD 2/MD 408/MD 422, Lothian, MD (south)	38	5.0	1.0
MD 140/MD 832/Antrim Blvd., Taneytown, MD (east)	174	5.4	1.5
US 202/State Route 237, Gorham, ME (east)	198	4.5	1.0
US 202/State Route 237, Gorham, ME (north)	51	5.4	1.2
Colorado Ave./Simpson Dr., Bend, OR (south)	225	4.7	1.2
SR 16 SB Ramp/Borgen Blvd., Gig Harbor, WA (north)	43	4.7	0.7
SR 16 SB Ramp/Borgen Blvd., Gig Harbor, WA (west)	121	4.4	1.0
High School Rd./Madison Ave., Bainbridge Island, WA (south)	332	5.0	1.5
Mile Hill Dr. (Hwy 166)/Bethel Ave., Port Orchard, WA (east)	240	5.3	1.1
Mile Hill Dr. (Hwy 166)/Bethel Ave., Port Orchard, WA (north)	1627	5.2	1.3
Mile Hill Dr. (Hwy 166)/Bethel Ave., Port Orchard, WA (south)	63	4.2	0.8
NE Inglewood Hill/216th Ave. NE, Sammamish, WA (west)	36	5.9	1.6
I-5 NB Ramp/Quinault Dr./Galaxy Dr., Lacey, WA (south)	22	5.0	0.8
27th Ave/Union St./Union Loop Rd., Kennewick, WA (north)	37	5.8	1.1
27th Ave/Union St./Union Loop Rd., Kennewick, WA (south)	60	5.5	1.5
Average	**3299**	**5.1**	**1.2**
Minimum		**4.2**	
Maximum		**5.9**	

The average follow-up headways showed less variation among sites, as shown in Exhibit 17-39, with most sites exhibiting follow-up headways of 1.0 s to 1.2 s.

Exhibit 17-39 – Measured follow-up headways for single-lane approaches

Site (approach)	Sample Size	Mean Follow-up Headway (seconds)	Standard Deviation of Follow-up Headway (seconds)
MD 2/MD 408/MD 422, Lothian, MD (north)	637	3.2	1.1
MD 2/MD 408/MD 422, Lothian, MD (south)	28	3.5	1.3
MD 140/MD 832/Antrim Blvd., Taneytown, MD (east)	1225	3.3	1.1
US 202/State Route 237, Gorham, ME (east)	522	3.4	1.1
US 202/State Route 237, Gorham, ME (north)	39	4.3	1.5
Colorado Ave./Simpson Dr., Bend, OR (south)	262	3.1	1.0
SR 16 SB Ramp/Borgen Blvd., Gig Harbor, WA (north)	33	3.4	1.1
SR 16 SB Ramp/Borgen Blvd., Gig Harbor, WA (west)	86	3.3	1.1
High School Rd./Madison Ave., Bainbridge Island, WA (south)	753	3.6	1.2
Mile Hill Dr. (Hwy 166)/Bethel Ave., Port Orchard, WA (east)	334	3.1	1.4
Mile Hill Dr. (Hwy 166)/Bethel Ave., Port Orchard, WA (north)	2282	3.2	1.2
Mile Hill Dr. (Hwy 166)/Bethel Ave., Port Orchard, WA (south)	120	3.1	1.0
NE Inglewood Hill/216th Ave. NE, Sammamish, WA (west)	453	3.1	1.0
I-5 NB Ramp/Quinault Dr./Galaxy Dr., Lacey, WA (south)	80	2.9	1.1
27th Ave/Union St./Union Loop Rd., Kennewick, WA (north)	400	2.9	1.1
27th Ave/Union St./Union Loop Rd., Kennewick, WA (south)	438	2.6	0.9
Average	**7692**	**3.2**	**1.1**
Minimum		**2.6**	
Maximum		**4.3**	

Multilane Roundabouts

Multilane roundabouts have more than one lane on the circulating roadway and at least one entry. The number of entry, circulating, and exiting lanes may vary throughout the roundabout.

The definition of headways and gaps for multilane facilities is more complicated than it is for single-lane facilities. If the circulating roadway truly functions as a multilane facility, then there are gaps in both the inside and outside lanes that are perceived in some integrated fashion by the motorists on the approach. Many drivers who choose to enter the roundabout via the outside lane will yield to all traffic in the circulatory roadway due to their uncertainty in the path of the circulating vehicles. This uncertainty is more pronounced at roundabouts than other unsignalized intersections due to the curvature of the circulatory roadway. Some drivers, however, will enter next to a vehicle circulating in the inside lane if the circulating vehicle is not perceived to conflict. As a result, the gap acceptance behavior of the outside entry lane, in particular, is imperfect and difficult to quantify with a simple gap acceptance model. This leads to an inclination toward using a regression-based model that implicitly accounts for these factors.

For roundabouts with two circulating lanes, which is the only type of multilane roundabout addressed in this chapter, the entries and exits can be either one or two lanes wide. The conditions represented in the database upon which the multilane model is built are as follows: one one-lane entry with two conflicting lanes, one two-lane entry with a single conflicting lane, one one-lane entry with a short flare in conjunction with two conflicting lanes, and five two-lane entries with two conflicting lanes.

There were few instances in the database used to develop the multilane model in which a steady state queue existed on all lanes of a multilane entry. Most commonly, for the two-lane entries, the outside lane had a sustained queue while the inside lane only had sporadic queuing. In general, several factors contribute to the specific assignment of traffic flow to each lane:

1. The specific assignment of turning movements to each lane (either as exclusive lanes or as shared lanes) directly influences the assignment of traffic volumes to each lane. This is generally accomplished through the use of signs and pavement markings that specifically designate the lane use for each lane. Multilane entries with no lane use signing or pavement markings may be assumed to operate with a shared left-through lane in the left lane and a shared through-right lane in the right lane, although field observations should be made to confirm the lane use pattern of an existing roundabout.
2. Destinations downstream of a roundabout may influence the lane choice at the roundabout entry. A downstream destination such as a freeway on-ramp may increase use of the outer entry lane, for example, even though both lanes could be used.
3. The alignment of the lane relative to the circulatory roadway seems to influence the use of entry lanes where drivers could choose between lanes. Some roundabouts have been designed with a natural alignment of the outer entry lane into the inner lane of the circulatory roadway. Under this design, the inner entry lane is naturally aimed at the central island and thus less comfortable and desirable for drivers. This phenomenon, documented elsewhere *(4)* as vehicle path overlap, may result in poor lane utilization of the inner entry lane. Similarly, poorly aligned multilane exits, where vehicles exiting in the inside lane cross the path of vehicles exiting in the outside lane, may influence lane use on upstream entries. In either case, the effect is most readily measured in the field at existing roundabouts and should be avoided in the design of new roundabouts.

4. Drivers may be uncertain about lane use when using the roundabout, particularly at roundabouts without any designated lane assignments approaching or circulating through the roundabout. This may contribute to use of the outer lane for left turns, for example, due to a perceived or real difficulty in exiting from the inside lane of the circulatory roadway. Proper signing and striping of lane use on the approach and through the roundabout may reduce this uncertainty, although it is likely to always be present to some extent at multilane roundabouts.

Of these items, factors (1) and (2) are common to all intersections and are accounted for in the specific assignment of turning movement patterns to individual lanes. Of the latter two factors, both of which are unique to roundabouts, factor (3) should be addressed through proper alignment of the entry relative to the circulatory roadway and thus may not need to be considered in the analysis of new facilities. However, existing roundabouts may exhibit path overlap resulting in poor lane utilization. Factor (4) can be reduced through proper design, particularly through the effective use of lane use arrows and striping. It is difficult to accurately estimate but may be measured at existing roundabouts.

The lane on a given approach with the highest flow is considered to be the "critical lane," and its performance is used to determine the performance of the approach. This is analogous to the critical movement approach used for TWSC intersections, although the critical lane may serve more than one movement (e.g., left turns and through movements). Consequently, the capacity model focuses first on the performance of the critical entry lane and then expands that result to address the overall capacity and delay for the approach.

The multilane capacity model for the critical lane is based on one-minute observations of continuous queuing in one or more lanes of a multilane roundabout entry.

CAPACITY

The capacity of a given approach is computed using the following process:

1. Adjust flows to account for vehicle stream characteristics.
2. Determine the entry and conflicting flows for each approach. For multilane approaches, evaluate the approach to determine the flow in each lane on an approach and identify the critical lane on the approach.
3. Compute the maximum possible entry flow using the appropriate model (single-lane model or multilane critical lane model).
4. Compute performance measures for each entry lane.

Flow adjustments

The flow rate for each movement may be adjusted to account for vehicle stream characteristics using factors given in Exhibit 17-40.

Exhibit 17-40. Passenger Car Equivalents

Vehicle Type	Passenger Car Equivalent
Passenger Car	1.0
Heavy Vehicle	2.0

The flow rate for each movement may also be adjusted to account for peaking characteristics within the peak hour using a Peak Hour Factor. This concept is discussed in more detail, including assumptions for default values where field measurements are unavailable, in Chapter 10.

Calculation of entry and conflicting flows by lane

In practice, it is necessary to convert the intersection turning movements (volumes v_1 to v_{12} as shown in Exhibit 17-41) into entry and circulating flows. For example, the conflicting traffic for the entry comprising streams 7, 8 and 9 is streams 1, 2, and 10. Thus for the northbound entry ($v_7 + v_8 + v_9$) the conflicting flow would be equal to $v_1 + v_2 + v_{10}$. This methodology can be extended to roundabouts with more or less than four legs. In addition, roundabouts are often used to facilitate U-turns, and these may be readily included in the flow calculations.

Exhibit 17-41. Flow Stream Definitions

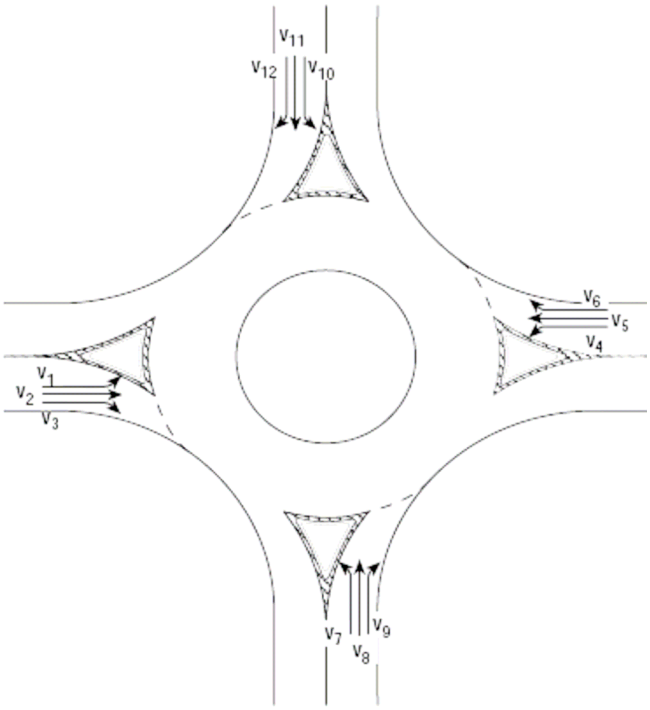

The determination of entry flows for multilane approaches is more complicated and requires the determination of flows on a lane-by-lane basis. To determine the assignment of flows to each roundabout entry lane, the following procedure may be used:

1. If the entry has only one lane, the turning movement flows are combined to determine the entry flow.
2. If only one lane is available for left-turning vehicles, 100% of the left-turn traffic is assigned to that lane.
3. If only one lane is available for right-turning vehicles, 100% of the right-turn traffic is assigned to that lane.

4. The remaining traffic is assumed to be distributed equally across all lanes such that the flow in each lane is equal.[1]
5. If a right-turn bypass lane is provided that does not share the same entrance line with the other entry lanes, the flows that are expected to use the right-turn bypass lane are removed from the calculation of the roundabout entry flows.
6. The critical lane is the lane on the approach with the highest flow rate.

Capacity for Single-Lane Roundabout Entries

The capacity of a one-lane entry to a one-lane roundabout is based on the conflicting flow. The equation for estimating the capacity is given as Equation 17-70.

$$c_{crit} = 1130e^{(-0.0010\,v_c)} \quad (17\text{-}70)$$

where:
c_{crit} = capacity of the critical lane on the approach, veh/h; and
v_c = conflicting flow, veh/h.

The capacity model given above reflects observations made at U.S. roundabouts in 2003. As noted previously, it is expected that capacity at U.S. roundabouts will increase over time with increased driver familiarity. In addition, communities with higher densities of roundabouts may experience a higher degree of driver familiarity and thus potentially higher capacities. Therefore, local calibration of the capacity models is recommended to best reflect local driver behavior.

Substituting variables for the two coefficients in Equation 17-70, it can be shown that the variables can be estimated by field measurements using the expressions in Equations 17-71 through 17-73 as follows:

$$c_{crit} = Ae^{(-B\,v_c)} \quad (17\text{-}71)$$

$$A = \frac{3600}{t_f} \quad (17\text{-}72)$$

$$B = \frac{t_c - t_f/2}{3600} \quad (17\text{-}73)$$

where:
c_{crit} = capacity of the critical lane on the approach, veh/h;
v_c = conflicting flow, veh/h;
t_c = critical headway, s; and
t_f = follow-up headway, s.

[1] This assumption may be overridden by real-world observations, knowledge, or judgment that documents a different lane distribution. For example, lane use may be adjusted based on downstream traffic patterns that would bias a particular traffic movement into one or more lanes. In addition, lane use may be adjusted based on the geometric design of the entry to reflect observed or anticipated lane use deficiencies associated with vehicle path overlap.

Therefore, the proposed capacity model can be calibrated using two parameters: the critical headway, t_c, and the follow-up headway, t_f. For reference, the observed values for these parameters were given previously in Exhibits 17-38 and 17-39, would provide an A value of 1125 and a b value of 0.00097.

Capacity for the Critical Lane of Double-Lane Roundabout Entries

Equation 17-74 gives the capacity of the critical lane of a double-lane roundabout entry as follows:

$$c_{crit} = 1130e^{(-0.0007\, v_c)} \qquad (17\text{-}74)$$

where:
c_{crit} = capacity of the critical lane on the approach, veh/h; and
v_c = conflicting flow, veh/h.

The intercept of this model has been constrained to match the intercept of the single-lane model due to similar follow-up headways measured in the field for each case. Exhibit 17-42 presents a plot showing Equations 17-70 and 17-74. The dashed lines represent portions of the curves that lie outside the range of observed field data.

Exhibit 17-42: Roundabout Entry Capacity for Single-Lane Entries and Critical Lane Roundabout Entry Capacity.

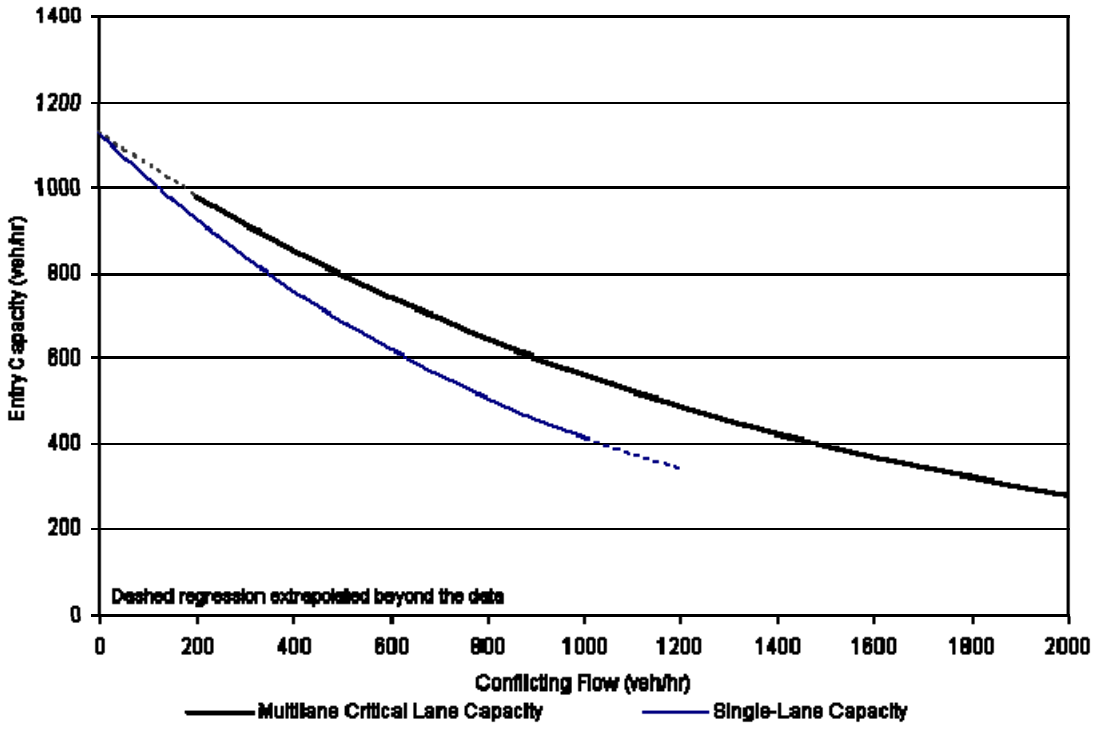

The capacity of the remaining non-critical lanes is assumed to be the same as that of the critical lane. For roundabouts with wide circulatory roadways, this assumption may be conservative, as vehicles in the outer entry lane may more readily enter next to non-conflicting vehicles in the inner circulating lane. The non-critical lane or total approach capacity is not important to the analysis procedure.

As noted previously, the model given above is based on data collected at roundabouts with up to two entry and two circulating lanes. For design purposes, it may be possible to use the same methodology to determine the capacity for entries with more than two lanes that are opposed by two conflicting lanes. However, the analyst is cautioned that in such cases the overall capacity may be underestimated due to a potential increase in the number of vehicles in the outer lanes entering adjacent to non-conflicting vehicles circulating in the inner lanes.

The multilane capacity model, as an empirical regression model, has two parameters that can be calibrated: the coefficient in front of the exponential term (1130), and the coefficient within the exponential term (–0.0007). As noted previously, the coefficient in front of the exponential term is equivalent to 3600 divided by the follow-up headway, which can be readily measured in the field.

Volume-to-Capacity Ratio

The volume-to-capacity ratio for a given approach (for single-lane entries) or critical lane (for multilane entries) can be calculated by dividing the calculated entry capacity into the entry volume for the given approach or lane, respectively.

Right-Turn Bypass Lanes

Two common types of right-turn bypass lanes are used at both single-lane and multilane roundabouts. These are characterized as follows:

- Type 1 (yield bypass lane): A bypass lane that terminates at a high angle, with right-turning traffic yielding to exiting traffic. Right-turn bypass lanes were not explicitly included in the recent national research. However, the capacity of a yield bypass lane may be approximated with the appropriate single-lane or multilane capacity formula given above by treating the exiting flow from the roundabout as the circulatory flow and treating the flow in the right-turn bypass lane as the entry flow.

- Type 2 (non-yielding bypass lane): This is a bypass lane that merges at a low angle with exiting traffic or that forms a new lane adjacent to exiting traffic. The capacity of a merging bypass lane has not been assessed in the United States. Its capacity is expected to be relatively high due to a merging operation between two traffic streams at similar speeds.

Delay, Queues, and Level of Service

Control Delay

Delay data collected for roundabouts in the U.S. suggest that control delays can be predicted in a manner similar to that used for stop-controlled and signal-controlled intersections. Equation 17-

75 shows the model that should be used to estimate average control delay for each lane of an approach of a roundabout.

$$d = \frac{3600}{c} + 900T\left[\frac{v}{c} - 1 + \sqrt{\left(\frac{v}{c} - 1\right)^2 + \frac{\left(\frac{3600}{c}\right)\frac{v}{c}}{450T}}\right] \quad (17\text{-}75)$$

where:
d = average control delay, sec/veh;
v = flow in subject lane, veh/h;
c = capacity of subject lane, veh/h; and
T = time period, h (T=1 for 1-hr analysis, T=0.25 for 15-min analysis).

Equation 17-75 is the same as that for stop-controlled intersections except that it does not include the "+ 5" term. This modification is necessary to account for the yield control on the subject entry, which does not require drivers to come to a complete stop if there is no conflicting traffic.

Average control delay for any particular lane is a function of the capacity of the lane and its degree of saturation. The analytical model used to estimate average control delay (Equation 17-75) assumes that there is no residual queue at the start of the analysis period. If the degree of saturation is greater than about 0.9, average control delay is significantly affected by the length of the analysis period. In most cases, the recommended analysis period is 15 min. If demand exceeds capacity during a 15-min period, the delay results calculated by the procedure may not be accurate due to the likely presence of a queue at the start of the time period. In addition, the conflicting demand for movements downstream of the movement operating over capacity may not be fully realized (in other words, the flow cannot get past the oversaturated entry and thus cannot conflict with a downstream entry). In these cases, an iterative approach that accounts for this effect and the carryover of queues from one time period to the next, such as the Kimber-Hollis formulation documented elsewhere *(5)*, may be used.

Queue Estimation

Queues for a given lane on an approach are calculated using Equation 17-76 as follows:

$$Q_{95} = 900T\left[\frac{v}{c} - 1 + \sqrt{\left(1 - \frac{v}{c}\right)^2 + \frac{\left(\frac{3600}{c}\right)\left(\frac{v}{c}\right)}{150T}}\right]\left(\frac{c}{3600}\right) \quad (17\text{-}76)$$

where:
Q_{95} = 95th-percentile queue, veh;
v = flow in subject lane, veh/h;
c = capacity of subject lane, veh/h; and

T = time period, h (T=1 for 1-hr analysis, T=0.25 for 15-min analysis).

Level of Service

Level of service (LOS) for a roundabout is determined by the computed or measured average control delay and is defined for each lane. LOS is not defined for the intersection as a whole. LOS criteria are given in Exhibit 17-43.

Exhibit 17-43. Level-of-Service Criteria for Roundabouts

Level of Service	Average Control Delay (s/veh)
A	0 – 10
B	> 10 – 15
C	> 15 – 25
D	> 25 – 35
E	> 35 – 50
F	> 50

III. APPLICATIONS – PART C

The steps required to perform a roundabout analysis are identified below. A worksheet is provided to assist the analyst in completing the computations.

The steps are:

1. Enter the volume data (leg-to-leg flow rates) for each entry and compute the total entering flow rate for each lane.
2. For multilane entries, compute the flow for each entry lane.
3. Compute the conflicting flow for each entry.
4. Determine the capacity of each entry using Equation 17-70 for single-lane entries into single-lane roundabouts and Equation 17-74 for the critical lane of multilane entries.
5. Compute the volume-to-capacity ratio for the critical lane on an entry and for a yield-controlled right-turn bypass lane, if present.
6. Compute the average control delay for each entry lane based on Equation 17-75.
7. Determine the Level of Service for each entry lane using Exhibit 17-43.
8. Compute the average control delay for each approach and for the roundabout as a whole.
9. Compute 95th-percentile queues for each lane based on Equation 17-76.

PART D. EXAMPLE PROBLEMS (ROUNDABOUTS)

Buena Vista and El Moro

This sample calculation illustrates the use of the single-lane roundabout capacity analysis procedure.

Description

The intersection of Buena Vista and El Moro is a four-legged roundabout similar to the one depicted in Exhibit 17-R1. The roundabout has two right-turn bypass lanes: a westbound right-turn bypass lane that yields to exiting vehicles, and a southbound right-turn bypass lane that forms its own lane adjacent to exiting vehicles.

Exhibit 17-R1 shows the peak-fifteen-minute turning movement flow rates. Heavy vehicle percentages at the intersection are assumed to be negligible.

Exhibit 17-R1. Geometry and traffic volumes for sample problem 1

(TO BE DEVELOPED).

Exhibit 17-R2 shows the worksheet for the capacity calculations. Lines 1-3 contain the turning movement volumes, and lines 4-6 contain right-turn bypass information. Lines 7-10 contain the entry flow calculations, and lines 11-14 contain the conflicting flow calculations; both show how these flows are derived from the turning movements. Lines 15-18 contain the conflicting flow calculations for a Type 1 right-turn bypass lane.

The calculation for any right-turn bypass lanes depends on the type of right-turn bypass lane. For the westbound approaches with a right-turn bypass lane, the right-turn volume is excluded from the westbound entry volume. In addition, because the westbound right-turn bypass lane yields to the conflicting exiting volume, the conflicting exiting volume must be calculated. In this case, it comprises the northbound through movement and the eastbound left turn movement (210 + 245 = 455). For the southbound right-turn bypass lane, the right-turn volume is excluded from the southbound entry volume, and no further calculations are needed due to the type of bypass lane.

Chapter 17 – Unsignalized Intersections (Roundabouts) (Draft 2005-11-10)

Exhibit 17-R2. Solution to roundabout sample calculation 1, Roundabout Worksheet

Worksheet For Capacity Calculations

Given Volumes		EB	WB	NB	SB
1	LT traffic	$v_1 = 245$	$v_4 = 100$	$v_7 = 145$	$v_{10} = 255$
2	TH traffic	$v_2 = 300$	$v_5 = 395$	$v_8 = 210$	$v_{11} = 95$
3	RT traffic	$v_3 = 105$	$v_6 = 620$	$v_9 = 75$	$v_{12} = 580$

Bypass Lanes		EB	WB	NB	SB
4	Type	0 (none)	1 (yield)	0 (none)	2 (non-yield)
5	RT volume	$v_3 = 105$	$v_6 = 620$	$v_9 = 75$	$v_{12} = 580$
6	RT volume using entry	$v_{3,entry} = 105$	$v_{6,entry} = 0$	$v_{9,entry} = 75$	$v_{12,entry} = 0$

Entry Flow (veh/hr)		Entry Volume, v_e
7	$v_{e,EB} = v_1 + v_2 + v_{3,entry}$	$v_{e,EB} = 245 + 300 + 105 = 650$
8	$v_{e,WB} = v_4 + v_5 + v_{6,entry}$	$v_{e,WB} = 100 + 395 + 0 = 495$
9	$v_{e,NB} = v_7 + v_8 + v_{9,entry}$	$v_{e,NB} = 145 + 210 + 75 = 430$
10	$v_{e,SB} = v_{10} + v_{11} + v_{12,entry}$	$v_{e,SB} = 255 + 95 + 0 = 350$

Conflicting Flow (veh/hr)		Conflicting Flow, v_c
11	$v_{c,EB} = v_4 + v_{10} + v_{11}$	$v_{c,EB} = 100 + 255 + 95 = 450$
12	$v_{c,WB} = v_1 + v_7 + v_8$	$v_{c,WB} = 245 + 145 + 210 = 600$
13	$v_{c,NB} = v_1 + v_2 + v_{10}$	$v_{c,NB} = 245 + 300 + 255 = 800$
14	$v_{c,SB} = v_4 + v_5 + v_7$	$v_{c,SB} = 100 + 395 + 145 = 640$

Type 1 Right-Turn Bypass Lane Conflicting Flow (veh/hr)		Type 1 Right-Turn Bypass Lane Conflicting Volume, v_a
15	$v_{c,EBRT} = v_4 + v_{11}$	N/A
16	$v_{c,WBRT} = v_1 + v_8$	$v_{c,WBRT} = 245 + 210 = 455$
17	$v_{c,NBRT} = v_2 + v_{10}$	N/A
18	$v_{c,SBRT} = v_5 + v_7$	N/A

Lines 19-25 show the results of the capacity, *v/c*, control delay, Level of Service, and 95th-percentile queue calculations.

		EB	WB	WBRT	NB	SB	SBRT
19	Entry volume, veh/hr	650	495	620	430	350	580
20	Capacity, veh/hr (Eq 17-70)	721	620	717	507	596	N/A
21	*v/c* ratio	0.90	0.80	0.86	0.85	0.59	N/A
22	Control delay, sec/veh	33.0	24.8	28.3	35.2	14.3	0.0
23	LOS	D	C	D	E	B	A
24	Approach control delay, sec/veh	33.0	26.7		35.2	5.4	
25	Intersection control delay, sec/veh	22.9					
26	95th-percentile queue, veh	11.8	7.9	10.3	8.8	3.8	N/A

The calculation of capacity for the eastbound entry given in line 20 is illustrated as follows:

$$c_{EB} = 1130e^{(-0.0010)(450)} = 721 \text{ veh/hr}$$

Further, the *v/c* ratio for this approach is 650 / 721 = 0.90.

The control delay for the eastbound entry given in line 22 is illustrated as follows:

$$d_{EB} = \frac{3600}{721} + 900(0.25)\left[\frac{650}{721} - 1 + \sqrt{\left(\frac{650}{721} - 1\right)^2 + \frac{\left(\frac{3600}{721}\right)\frac{650}{721}}{450(0.25)}}\right] = 33.0 \text{ s/veh}$$

Using Exhibit 17-44, the Level of Service for this entry is LOS D.

The approach control delay is the same as the control delay for the entry for those approaches with no right-turn bypass lanes (eastbound and northbound). For the others, the approach control delay is the average for the entry and bypass lane, weighted by volume. Similarly, the intersection control delay is the weighted average of the control delays for every movement at the intersection.

Walnut and Aspen

This sample calculation illustrates the use of the multilane roundabout capacity analysis procedure.

Description

The intersection of Walnut and Aspen is a four-legged roundabout similar to the one depicted in Exhibit 17-R3. The roundabout has two lanes on westbound, eastbound, and southbound approaches and one lane on the northbound approach. The two lanes on the southbound approach are designated as left-through and right; the eastbound and westbound approaches are designated as left-through and through-right.

Exhibit 17-R3 shows the peak-fifteen-minute turning movement flow rates. Heavy vehicle percentages at the intersection are assumed to be negligible.

Exhibit 17-R3. Geometry and traffic volumes for sample problem 2

(TO BE DEVELOPED).

Exhibit 17-R4 shows the worksheet for the capacity calculations. Lines 1-3 contain the turning movement volumes. Lines 4-10 contain the entry flow calculations by lane, and lines 11-14 contain the conflicting flow calculations; both show how these flows are derived from the turning movements.

Exhibit 17-R4. Solution to roundabout sample calculation 2, Roundabout Worksheet

Worksheet For Capacity Calculations

Given Volumes		EB	WB	NB	SB
1	LT traffic	$v_1 = 280$	$v_4 = 450$	$v_7 = 50$	$v_{10} = 240$
2	TH traffic	$v_2 = 620$	$v_5 = 300$	$v_8 = 60$	$v_{11} = 60$
3	RT traffic	$v_3 = 60$	$v_6 = 90$	$v_9 = 120$	$v_{12} = 400$

Entry Flow (veh/hr)		Entry Volume, v_e
4	$v_{e,EB,L} = v_1 + v_{2,L}$	$v_{e,EB,L} = 280 + 200 = 480$
5	$v_{e,EB,R} = v_{2,R} + v_3$	$v_{e,EB,R} = 420 + 60 = 480$
6	$v_{e,WB,L} = v_4 + v_{5,L}$	$v_{e,WB,L} = 450 + 0 = 450$
7	$v_{e,WB,R} = v_{5,R} + v_6$	$v_{e,WB,R} = 300 + 90 = 390$
8	$v_{e,NB} = v_7 + v_8 + v_9$	$v_{e,NB} = 50 + 60 + 120 = 230$
9	$v_{e,SB,L} = v_{10} + v_{11}$	$v_{e,SB,L} = 240 + 60 = 300$
10	$v_{e,SB,R} = v_{12}$	$v_{e,SB,R} = 400$

Conflicting Flow (veh/hr)		Conflicting Flow, v_c
11	$v_{c,EB} = v_4 + v_{10} + v_{11}$	$v_{c,EB} = 450 + 240 + 60 = 750$
12	$v_{c,WB} = v_1 + v_7 + v_8$	$v_{c,WB} = 280 + 50 + 60 = 390$
13	$v_{c,NB} = v_1 + v_2 + v_{10}$	$v_{c,NB} = 280 + 620 + 240 = 1140$
14	$v_{c,SB} = v_4 + v_5 + v_7$	$v_{c,SB} = 450 + 300 + 50 = 800$

The problem presents several scenarios:

- For the eastbound approach, the through volume distributes over the two lanes to balance the flow in each lane.
- For the westbound approach, the left-turn volume, which is restricted to the left lane, is greater than the sum of the through and right-turn volume. Therefore, the left lane acts as a *defacto* left-turn-only lane, with the right lane serving all of the through and right-turn volume.
- For the northbound approach, all of the entering traffic is combined, as it is a single-lane entry.
- For the southbound approach, the left lane is designated as left-through, so only the left-turn and through movements are combined. The right-turning traffic is assigned to the right lane.

Note that no additional lane use adjustments have been made to account for downstream destinations, approach alignment, or observed driver behavior.

Lines 15-24 show the results of the determination of the critical lane and non-critical lane capacities, *v/c*, control delay, Level of Service , and 95th-percentile queue calculations.

		EB Left Lane	EB Right Lane	WB Left Lane	WB Right Lane	NB	SB Left Lane	SB Right Lane
15	Entry volume, veh/hr	480	480	450	390	230	300	400
16	Critical lane?	*	*	*		*		*
17	Critical Lane Capacity, veh/hr (Eq 17-74)	668	668	860		509		645
18	Assumed Non-Critical Lane Capacity, veh/hr				860		645	
19	*v/c* ratio	0.72	0.72	0.52	0.45	0.45	0.47	0.62
20	Control delay, sec/veh	17.9	17.9	8.7	7.6	12.8	10.3	14.2
21	LOS	C	C	A	A	B	B	B
22	Approach control delay, sec/veh	17.9		8.2		12.8	12.5	
23	Intersection control delay, sec/veh	13.1						
24	95th-percentile queue, veh	6.1	6.1	3.1	2.4	2.3	2.5	4.3

The calculation of capacity for the eastbound entry given in line 17 is illustrated as follows:

$$c_{EB} = 1130e^{(-0.0007)(750)} = 668 \text{ veh/hr}$$

Further, the *v*/*c* ratio for this lane is 480 / 668 = 0.72.

The control delay for the eastbound entry given in line 20 is illustrated as follows:

$$d_{EB} = \frac{3600}{668} + 900(0.25)\left[\frac{480}{668} - 1 + \sqrt{\left(\frac{480}{668} - 1\right)^2 + \frac{\left(\frac{3600}{668}\right)\frac{480}{668}}{450(0.25)}}\right] = 17.9 \text{ s/veh}$$

Using Exhibit 17-44, the Level of Service for each lane of this entry is LOS C.

REFERENCES

I. PART C - ROUNDABOUTS

1. Rodegerdts, L., M. Blogg, E. Wemple, M. Kyte, M. Dixon, G. List, A. Flannery, R. Troutbeck, W. Brilon, N. Wu, B. Persaud, C. Lyon, D. Harkey, and D. Carter. *NCHRP Report 572: Roundabouts in the United States*. Transportation Research Board of the National Academies, Washington DC, 2007.
2. Akçelik, R, E. Chung, and M. Besley. "Analysis of Roundabout Performance by Modeling Approach-Flow Interactions." In *Proceedings of the Third International Symposium on Intersections without Traffic Signals*, Portland, Oregon, July 1997, p. 15-25.
3. Krogscheepers, J. C., and C. S. Roebuck. "Unbalanced Traffic Volumes at Roundabouts." In *Transportation Research Circular EC-018: Proceedings of the Fourth International Symposium on Highway Capacity* (Maui, Hawaii), Transportation Research Board, National Research Council, June 27–July 1, 2000, pp. 446-458.
4. Robinson, B.W., L. Rodegerdts, W. Scarbrough, W. Kittelson, R. Troutbeck, W. Brilon, L. Bondzio, K. Courage, M. Kyte, J. Mason, A. Flannery, E. Myers, J. Bunker, and G. Jacquemart. *Roundabouts: An Informational Guide.* Report No. FHWA-RD-00-067. FHWA, U. S. Department of Transportation, June 2000.
5. Kimber, R. M. and E. M. Hollis. *Traffic queues and delays at road junctions.* TRRL Laboratory Report LR 909. Crowthorne, England: Transportation and Road Research Laboratory, 1979.

APPENDIX N
RESEARCH PROBLEM STATEMENT

Refinement of Roundabout Operational Models

A recent NCHRP study (NCHRP 3-65) produced new capacity and safety analysis procedures for modern roundabouts. The procedures were developed based on data collected during a nationwide data collection effort. Despite that extensive effort, it was difficult to find roundabouts that were operating at capacity, with standing queues for extended periods of time. It was also challenging to find roundabouts with widely varying geometric conditions that were operating at capacity. The implication is that more data are needed at a point in time when there are a greater number of roundabouts operating at capacity. This is particularly true for multilane roundabouts, where very few were found to be operating at a capacity condition across all entry lanes of a given approach. This, coupled with the many possible variations of entry and circulating lane assignment, origin-destination patterns, and overall geometry, limited the potential scope of the model developed under the previous NCHRP effort.

In addition, the previous NCHRP effort confirmed that data collection and extraction is an expensive undertaking, particularly when approaching an operational modeling effort that intends to examine both analytical and regression models. In addition, not all of the data collected under 3-65 was dedicated to the development of operational models. Some sites were selected for other purposes, such as speed measurements where free flow conditions are needed. A project dedicated to the development of operational models can optimize site selection to only those sites with queuing, as well as to time periods and seasons where queuing is maximized.

In addition, it is possible that a more efficient data collection and extraction method can be used. The data collection employed in the previous NCHRP effort was primarily restricted to the summer months, which limited the ability to measure higher traffic volumes in other seasons. In addition, the weather during the summer months in much of the country (thunderstorms, windstorms) was found to be frequently incompatible with the free-standing mast used as a camera platform, thus limiting the potential collection of afternoon peak hour data. In addition, even with the elevated platform used in the previous NCHRP effort, it was difficult in some cases to visually observe the back of queue on all approaches, thus limiting the ability to accurately measure delays and queues.

The previous NCHRP effort found that the act of finding appropriate sites to study is not trivial. Although a thorough survey was conducted to find the most useful roundabouts nationwide and most of these were included in the study, it is still unclear whether all of the best sites were found. Since expectations are high that a diverse set of the most “representative” sites will be studied, a way to make sure that that has happened is needed.

Therefore, the key issues are these:

1. Additional sites with queuing are needed. Since most sites in the US are still relatively new, this will likely require additional time to pass for sites to experience traffic volume increases that generate sustained queuing.
2. More multilane sites are needed to produce a more comprehensive model, and additional single-lane sites are needed to validate the current single-lane model. These sites need to have variation in lane configuration, use of striping, truck percentages, and overall

geometric arrangement, plus be operating at capacity. This will require additional time to pass, as few sites existed in 2003 that could meet these criteria (see #1).

3. Innovative data collection strategies are needed to allow the efficient collection and extraction of data during optimal seasons, days of week, and times of day over sites that are widely dispersed geographically.
4. Different techniques are needed to capture backs of queue, particularly for sites where the approach roadway curves or becomes visually obstructed. While the loss of back of queue does not necessarily affect the estimation of entry capacity, it does affect the estimation of delay and queue length.
5. An innovative method is needed to identify the best sites for use in model development.

Hence, this project has three objectives. The first is to find a way to canvas the traffic engineering community to ensure that all the best sites are studied. The second is to find a better way to instrument the facilities so that better data can be collected. The third is to find an efficient procedure to do the data extraction necessary for developing operational models. The objective in this follow-on effort is to build on the work of NCHRP 3-65 and address the outstanding issues that could not be completely addressed with that effort.

To achieve these objectives, the research should produce: a) A definitive way to ensure that the best sites are being studied, b) A method for instrumenting the sites that is simple, straightforward, perhaps do-able by local traffic engineers, and capable of providing the best possible data, and c) A technique for extracting the data that is accurate and cost effective.

The objectives will be met through the following tasks: 1) Review of prior site identification techniques, 2) Refinement of a mechanism to find the best sites, 3) Identification of the best sites to study, 4) Investigation of better instrumentation techniques, 5) Demonstration of the data collection technique, 6) Data collection, 7) Data extraction, 8) Data summary and preliminary analysis, 9) Model refinement, 10) HCM recommendations, and 11) Final report.